WHC-MR-0506

Glass Science Tutorial: Lecture Number 7, Waste Glass Technology for Hanford

Prepared for the U.S. Department of Energy
Office of Environmental Restoration and
Waste Management

Westinghouse
Hanford Company Richland, Washington

Management and Operations Contractor for the
U.S. Department of Energy under Contract DE-AC06-87RL10930

WHC-MR-0506

Glass Science Tutorial: Lecture Number 7; Waste Glass Technology for Hanford

A. A. Kruger
Westinghouse Hanford Company

P. Hrma, Lecturer

Date Published
July 1995

Prepared for the U.S. Department of Energy
Office of Environmental Restoration and
Waste Management

Westinghouse Hanford Company
P.O Box 1970
Richland, Washington

Management and Operations Contractor for the
U.S. Department of Energy under Contract DE-AC06-87RL10930

Available to the U.S. Department of Energy
and its contractors from
Office of Scientific and Technical Information
P.O. Box 62
Oak Ridge, TN 37831
(615) 576-8401

Available to the public from the U.S. Department of Commerce
National Technical Information Service
5285 Port Royal Road
Springfield, VA 22161
(703) 487-4650

Printed in the United States of America

DISCLM-1.CHP (1-91)

Waste Glass Technology for Hanford

P. Hrma, M. Schweiger, G. Piepel,
P. Smith, K. Sundaram, X. Feng,
J. Darab, T. Redgate,
J. Vienna, D. Peeler, Hong Li

27 & 28 June 1995

Tuesday Morning, June 27

Introduction (Pavel Hrma)

Glass properties and their measurement (Michael Schweiger)

Statistical approach to glass development (Greg Piepel)

Feed melting reactions: laboratory investigation of foaming) (Peter Smith)

Processing properties of nuclear waste glasses (Pavel Hrma)

Tuesday Afternoon, June 27

Understanding glass composition effects on glass durability (Xiangdong Feng)

LLW glass structure (John Darab)

Prediction of nuclear waste glass dissolution as a function of composition (Pavel Hrma)

Model comparisons: free energy of hydration (Trish Redgate)

Wednesday Morning, June 28

Introduction (Pavel Hrma)

Glass crystallization (John Vienna)

Effect of crystallization on the chemical durability of nuclear waste glasses (David Peeler)

Amorphous phase separation: theory, prediction, and application (David Peeler)

Corrosion of refractories and electrodes in waste glass melters (Kamakshi Sundaram)

Wednesday Afternoon, June 28

Minor components in nuclear waste glasses (Hong Li)

Effects of experimental parameters on glass durability (Xiangdong Feng)

Glass formulation for maximum waste loading (Pavel Hrma)

Concluding remarks (P. Hrma)

Laboratory Investigations of Foaming

reboil pressure
indirect observation of melt ring heigh
direct observation of foaming

Pacific Northwest Laboratory

Experimental

Samples- Untreated, Formated, Nitrated, Sugar-Added, Oxide/Carbonate

Heat treatments- 3 g of melter feed; heated 10C/min

Temperatures- 1000, 1044, 1200C; immediate quench

Iron redox measured by colorimetric titration

Offgas measured by GC-MS

Volume expansion measured by recorded images using a video camera

Analysis of quenched foam- Microscopy, XRD, bubble composition

Sodium Nitrite/Nitrate Decomposition

$$NaNO_3 \rightarrow NaNO_2 + (1/2)O_2$$

$$2NaNO_2 \rightarrow Na_2O + 2NO + (1/2)O_2$$

$$2NaNO_2 \rightarrow Na_2O + N_2 + (3/2)O_2$$

Abe et al (1983) reacted sodium nitrite with silica
T < 500C, NO observed
T > 600C, NO and O_2 observed

Pacific Northwest Laboratory

Outline

- Introduction
  - Foaming and Iron Redox
  - Temperature Effects
- Experimental
- Results and Discussion
  - Offgas Results from Untreated, Formated, Nit Oxides/ Carbonates and Sugar-added
  - Volume Expansion Measurements and Analys
  - Iron Redox
- Summary

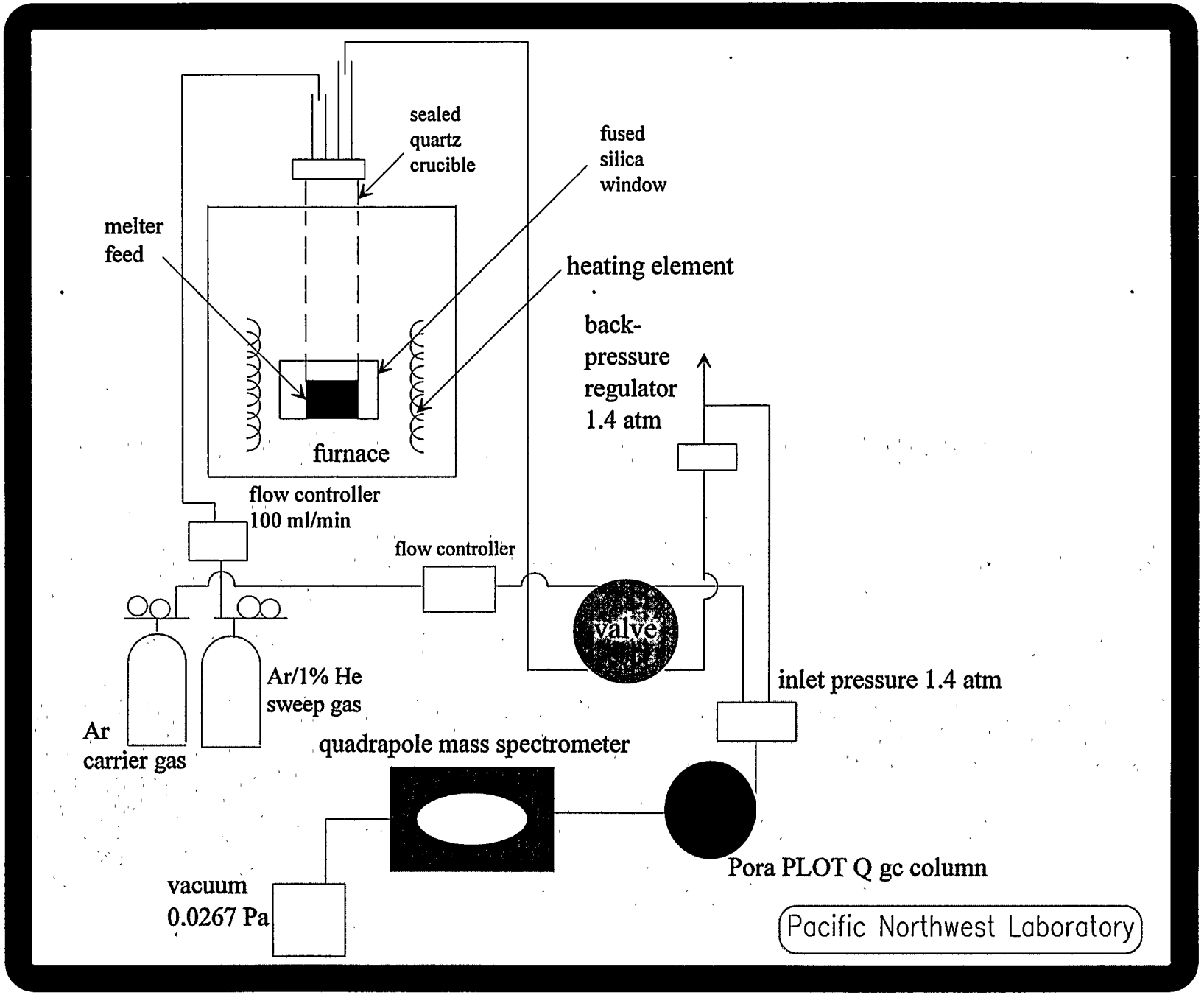
sealed
quartz
crucible
fused
silica
window
melter
feed
heating element
back-
pressure
regulator
1.4 atm
furnace
flow controller
100 ml/min
flow controller
valve
Ar/1% He
sweep gas
Ar
carrier gas
inlet pressure 1.4 atm
quadrapole mass spectrometer
Pora PLOT Q gc column
vacuum
0.0267 Pa
Pacific Northwest Laboratory

Cold Cap Process

Cold cap- region of unreacted feed floating on the melt in a continuous melter
Melting reactions have largest effect in this region

<u>4 zones of gas</u>
unrestrained-gas escape **feed expansion**
bubbly layer **glass melt**

Crucible experiments show max T of decomposition gas free escape

Gas retention affects heat transfer
Feed expansion zone and bubbly layer have low k

Batches prone to expansion- correlated w/ low melting rate?

Differences in nuclear waste vitrification and conventional glass

Raw Materials and their Introduction to the Melter
Conv.- raw material choice, carbonate batches, refining agents matched; powder/pellet
NW- batch contains nitrates and multivalent oxides, redox control via additives; slurry

Frit-
Conv.- cullet and batch are nearly identical in composition
NW- vitrification chemicals are premelted into frit

Foaming and Iron Redox in Simulated Nuclear Waste G a

2 categories of foaming
1) feed expansion (from batch reactions)
2) molten glass foam

$$Fe^{2+} + (1/4)O_2 + (3/2)O^{2-} \rightleftarrows FeO_2^-$$

Typically, reducing agents are used to mitigate foam

Pacific Northwest Laboratory

Summary

For samples (except sugar) prepared under inert atmosphere, the iron redox was not a function of the batch chemistry.

As expected, temperature strongly affected iron redox.

Differences in volume expansion were attributed to reaction paths which resulted from the batch chemistry.

The use of a reductant for foam mitigation may be unneccessary.

Compositional Analysis of Bubbles (wt% of each component)

Sample	N_2	O_2	Ar	CO_2	NO
Formated	17.6	66.0	1.8	1.7	12.9
Untreated	6.1	74.3	1.5	14.6	3.5
Ox/Carbon	25.5	6.9	2.1	65.5	NA
Nitrated	21.2	62.0	2.8	12.7	1.4

Pacific Northwest Laboratory

Stages of Melting

First Stage- Drying, Removing Chemically Bound Water, Hydrothermal Reactions, Crystalline Inversions and Solid State Reactions

Second Stage- Vigorous Reactions, Presence of Molten Salts, Melt Develops, Formation of Intermediate Compounds

Redox/Gas Generating Reactions

Third Stage- Dissolution of Solid Residues, Bubble Removal

Stages of Melting

First Stage- Drying, Removing Chemically Bound Water, Hydrothermal Reactions, Crystalline Inversions and Solid State Reactions

Second Stage- Vigorous Reactions, Presence of Molten Salts, Melt Develops, Formation of Intermediate Compounds

Redox/Gas Generating Reactions

Third Stage- Dissolution of Solid Residues, Bubble Removal

Differences in nuclear waste vitrification and conventional glass

Raw Materials and their Introduction to the Melter
Conv.- raw material choice, carbonate batches, refining agents matched; powder/pellet
NW- batch contains nitrates and multivalent oxides, redox control via additives; slurry

Frit-
Conv.- cullet and batch are nearly identical in composition
NW- vitrification chemicals are premelted into frit

Previous Work

Ch. Krause and B. Luckscheiter, **6**, 2535, J. Mater Res (1991)
Noble metal effects on microstructure evolution

T.V. Palmiter, et al **212**, 153, Mat. Res. Soc. Proc. (1991)
Heat treatment effects on WV glass

L.D. Anderson et al 39, 213, Ceramic Trans. (1993)
Waste glass melting stages

JD Vienna et al **45**, Ceramic Trans. (1994)
Frit effects in nuclear waste vitrification

Laboratory Investigations of Foaming

reboil pressure
indirect observation of melt ring height
direct observation of foaming

Pacific Northwest Laboratory

Cold Cap Process

Cold cap- region of unreacted feed floating on the melt in a continuous melter
Melting reactions have largest effect in this region

<u>4 zones of gas</u>

unrestrained-gas escape	**feed expansion**
bubbly layer	**glass melt**

Crucible experiments show max T of decomposition gas free escape

Gas retention affects heat transfer
Feed expansion zone and bubbly layer have low k

Batches prone to expansion- correlated w/ low melting rate?

Summary

For samples (except sugar) prepared under inert atmosphere, the iron redox was not a function of the batch chemistry.

As expected, temperature strongly affected iron redox.

Differences in volume expansion were attributed to reaction paths which resulted from the batch chemistry.

The use of a reductant for foam mitigation may be unneccessary.

Table 5.8. Volume Expansion Summary

Sample	Expansion Temperatures (°C)					Detected Gases[a]		
	Range[b]	Begin Shrinkage	Maximum Shrinkage	Return to Original Volume	Maximum Expansion	Species	Amount (mmol)	Temperature Range (°C)
Formated #1	700-853	NA	NA	NA	816	O_2	0.215	448-708
Formated #2	710-873	710	735	750	783		0.048	718-838
						CO_2	0.176	691-1200
							0.009	700-873
						N_2	0.252	228-778
							0.012	700-778
						NO	1.9	488-708
							0.361	718-878
							0.399	700-873
Nitric #1	740-890	740	785	820	865	O_2	0.150	605-805
Nitric #2	720-885	720	755	802	845		0.002	720-805
Nitric #3	720-858	720	755	805	858	CO_2	4.34	559-819
							0.695	720-819
						NO	0.980	625-765
							0.085	720-765
Unformated #1	720-852	720	737	757	830	O_2	0.314	538-808
Unformated #2	730-865	730	740	745	854		0.011	818-908
							0.069	720-865
						CO_2	5.93	461-761
							0.016	720-761
						NO	0.922	598-888
							0.523	720-865
Nitric acid 4X weight	160-763	NA	NA	NA	280	O_2	0.34	446-746
							0.023	700-746
(2 ranges)	763-852	NA	NA	NA	850	CO_2	18.5	449-719
							0.080	700-719
						NO	2.67	576-776
							0.066	700-776
Oxide/Carbonate	743-894	NA	NA	NA	893	CO_2	0.004	743-785

(a) Only one measurement of the gas products was obtained.
(b) Expansion temperature range corresponds to recorded deviation of normalized volume from 1 cm^3.

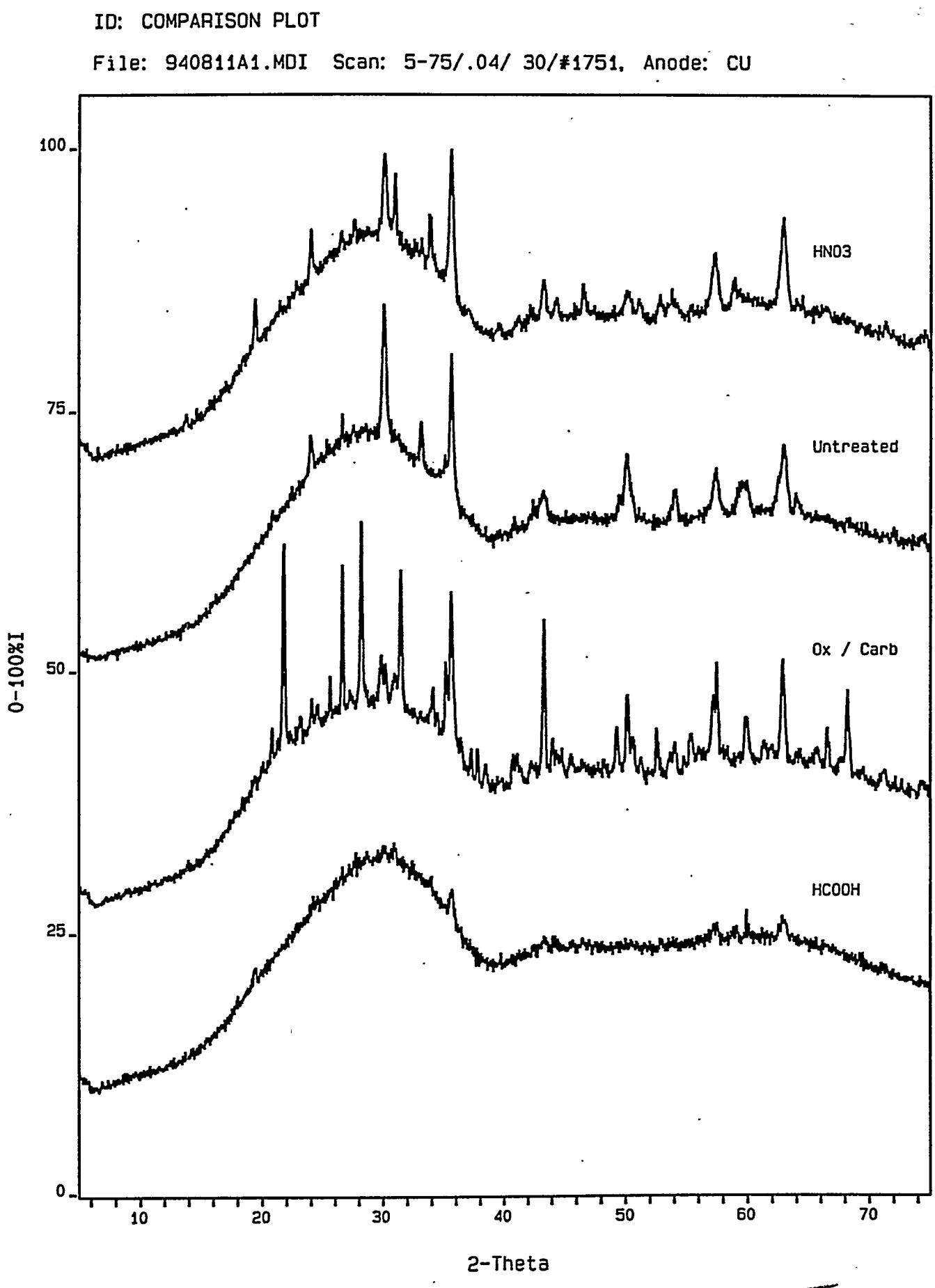
ID: COMPARISON PLOT
File: 940811A1.MDI Scan: 5-75/.04/ 30/#1751, Anode: CU
100
75
50
25
0
0-100%I
HNO3
Untreated
Ox / Carb
HCOOH
10
20
30
40
50
60
70
2-Theta

Figure 11

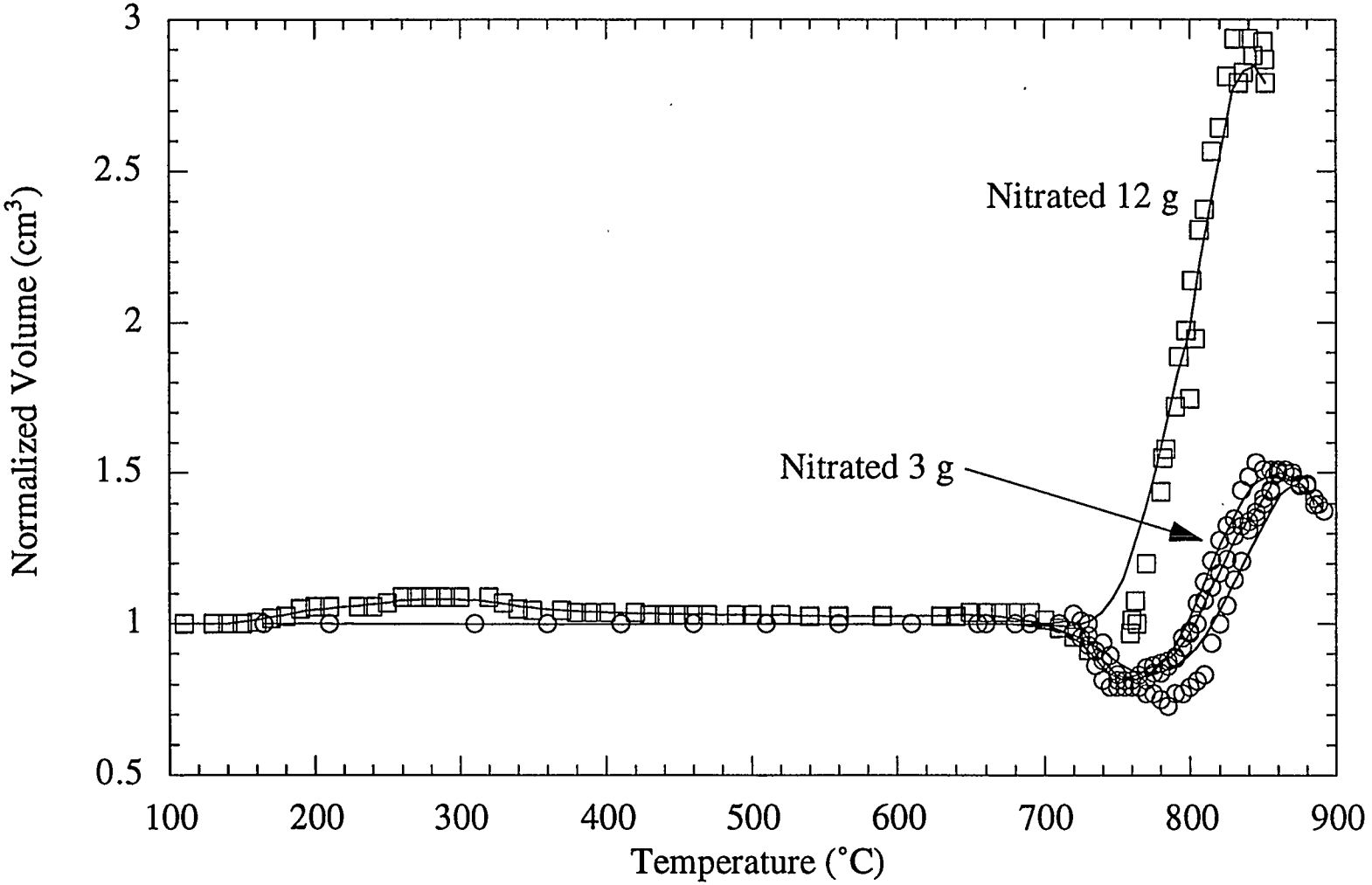
Normalized Volume (cm3)
3
2.5
2
1.5
1
0.5
100
200
300
400
500
600
700
800
900
Temperature (°C)
Nitrated 12 g
Nitrated 3 g

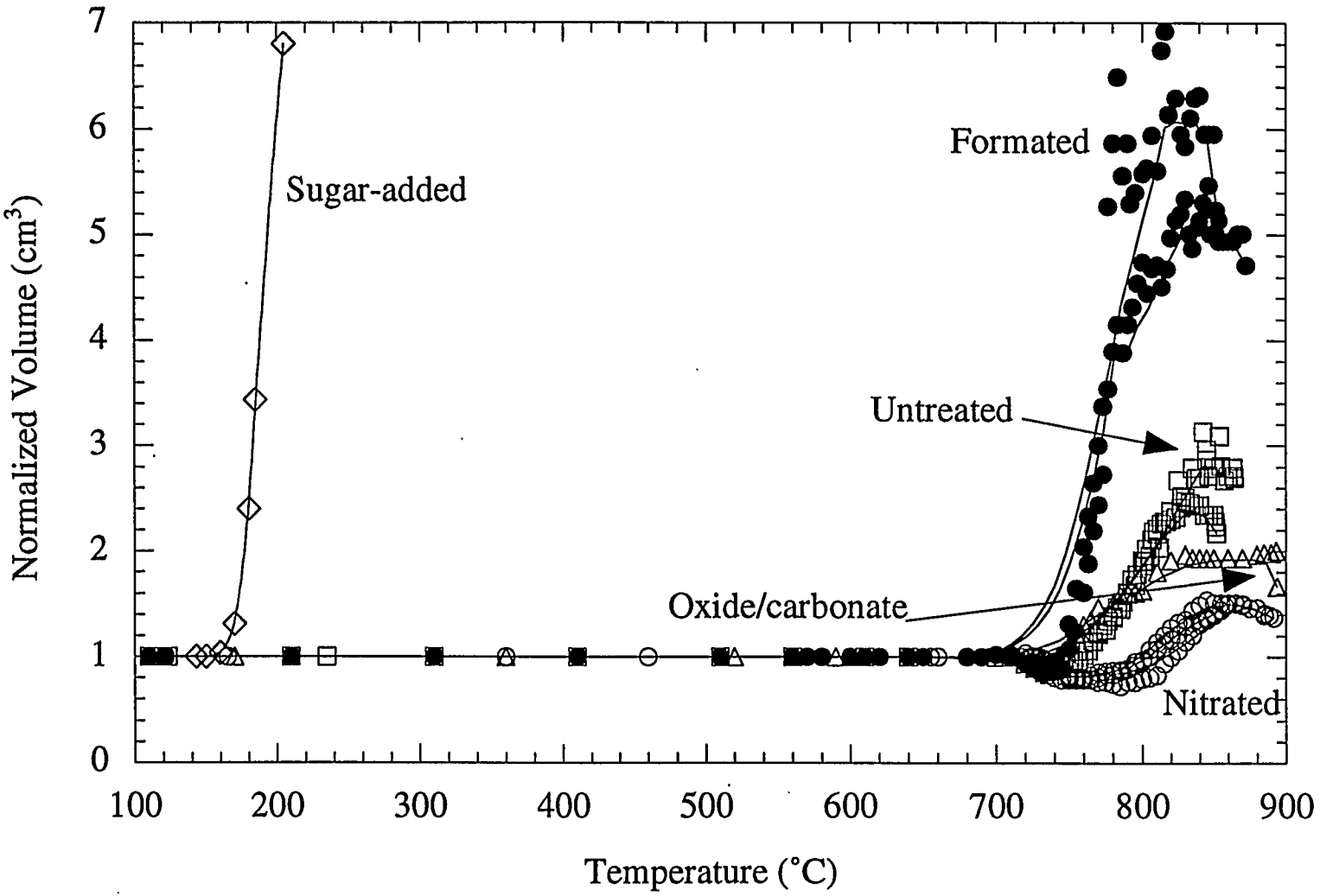
Normalized Volume (cm3)
Temperature (°C)
Sugar-added
Formated
Untreated
Oxide/carbonate
Nitrated
0
1
2
3
4
5
6
7
100
200
300
400
500
600
700
800
900

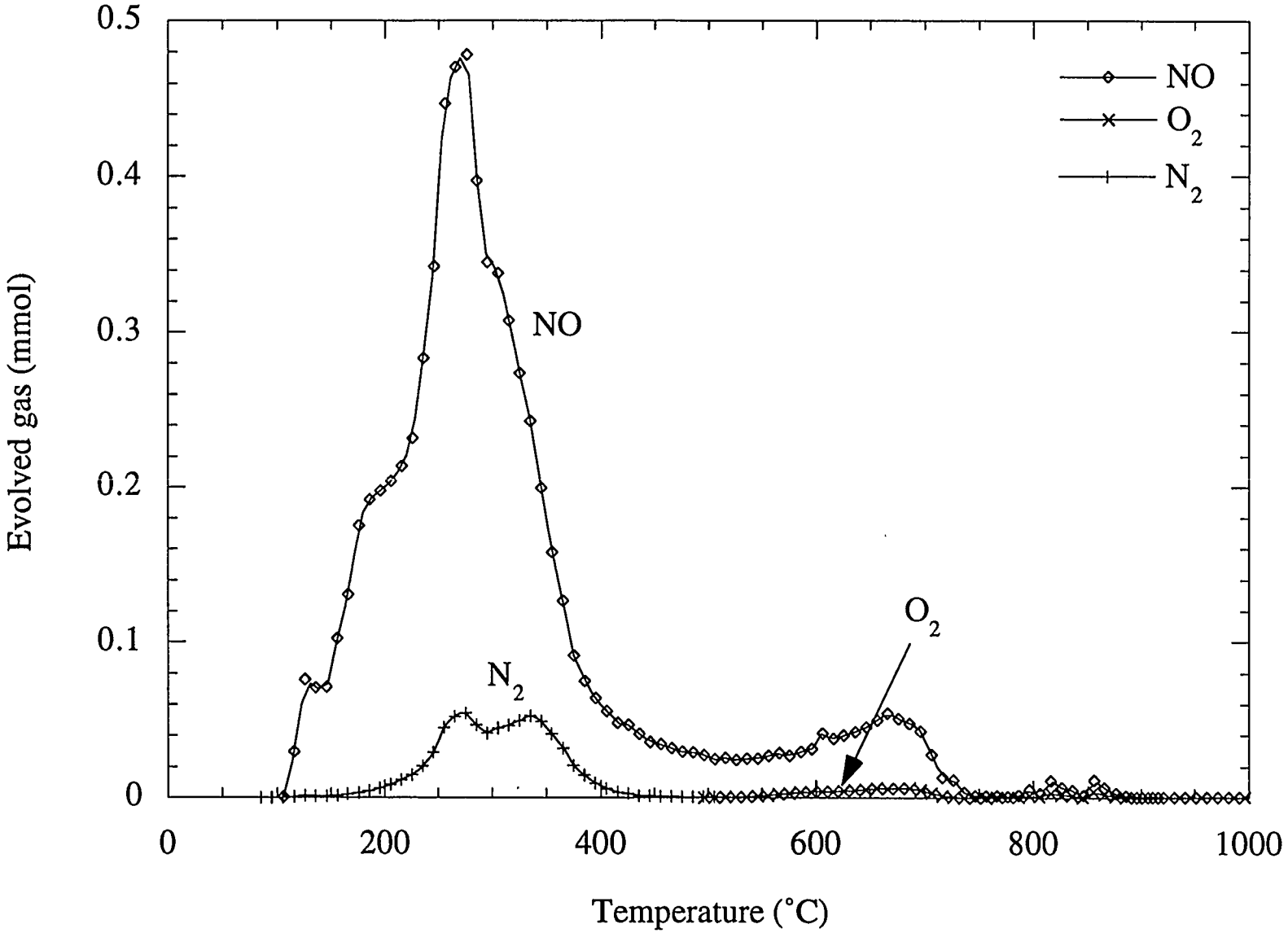
0.5
0.4
0.3
0.2
0.1
0
Evolved gas (mmol)
0
200
400
600
800
1000
Temperature (°C)
NO
O2
N2
NO
N2
O2

LLW thermal analysis observations

158-292 C

Na_4EDTA melts

$Na_4EDTA + NaNOx$ (s) ⟶

292-363 C

$NaNO_2$, $NaNO_3$ melt ⟶

$Na_4EDTA + NaNOx$ (l) ⟶

NOx

CH_4

H_2

CO_2

327-567 EDTA decomposes CO_2

514-804 $NaNOx(l) + SiO_2$ NOx, O_2 CH_4

Pacific Northwest Laboratory

Sodium Nitrite/Nitrate Decomposition

$$NaNO_3 \rightarrow NaNO_2 + (1/2)O_2$$

$$2NaNO_2 \rightarrow Na_2O + 2NO + (1/2)O_2$$

$$2NaNO_2 \rightarrow Na_2O + N_2 + (3/2)O_2$$

Abe et al (1983) reacted sodium nitrite with silica
T < 500C, NO observed
T > 600C, NO and O_2 observed

Pacific Northwest Laboratory

Experimental

Samples- Untreated, Formated, Nitrated, Sugar-Added, Oxide/Carbonate

Heat treatments- 3 g of melter feed; heated 10C/min

Temperatures- 1000, 1044, 1200C; immediate quench

Iron redox measured by colorimetric titration

Offgas measured by GC-MS

Volume expansion measured by recorded images using a video camera

Analysis of quenched foam- Microscopy, XRD, bubble composition

Pacific Northwest Laboratory

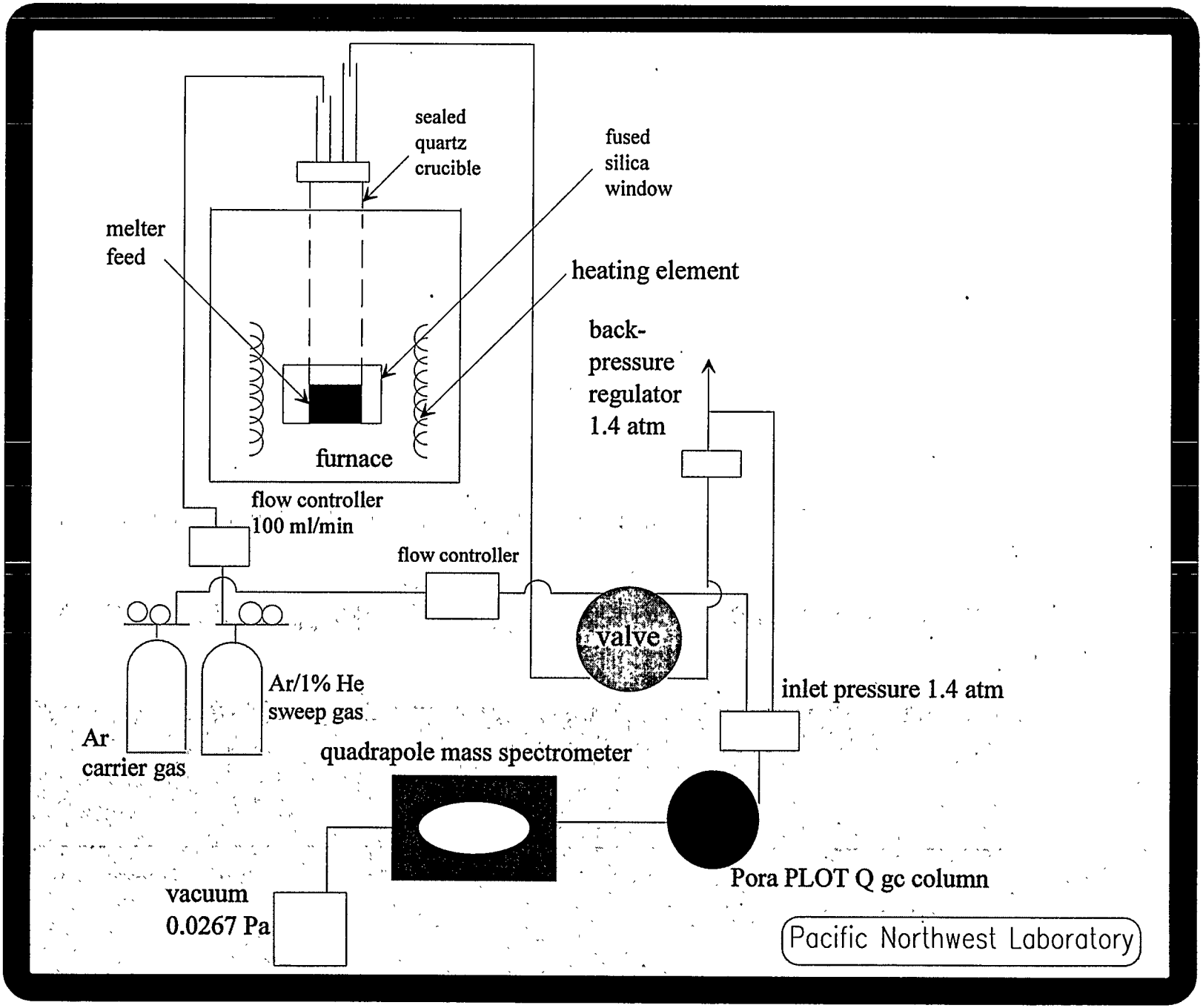
sealed
quartz
crucible
fused
silica
window
melter
feed
heating element
back-
pressure
regulator
1.4 atm
furnace
flow controller
100 ml/min
flow controller
valve
Ar/1% He
sweep gas
Ar
carrier gas
inlet pressure 1.4 atm
quadrapole mass spectrometer
Pora PLOT Q gc column
vacuum
0.0267 Pa
Pacific Northwest Laboratory

Compositional Analysis of Bubbles (wt% of each component)

Sample	N_2	O_2	Ar	CO_2	NO
Formated	17.6	66.0	1.8	1.7	12.9
Untreated	6.1	74.3	1.5	14.6	3.5
Ox/Carbon	25.5	6.9	2.1	65.5	NA
Nitrated	21.2	62.0	2.8	12.7	1.4

Pacific Northwest Laboratory

Previous Work

Ch. Krause and B. Luckscheiter, **6**, 2535, J. Mater Res (1991)
Noble metal effects on microstructure evolution

T.V. Palmiter, et al **212**, 153, Mat. Res. Soc. Proc. (1991)
Heat treatment effects on WV glass

L.D. Anderson et al 39, 213, Ceramic Trans. (1993)
Waste glass melting stages

JD Vienna et al **45**, Ceramic Trans. (1994)
Frit effects in nuclear waste vitrification

Motivations for Studying Batch Melting

Slow steady state melting rate- currently

Conventional borosilicate glass production 80-240 kg/h/m2 (Trier 1987)

Best liquid-fed ceramic melter run 56 kg/h/m2 [Compendium of 44 melter runs at PNL, SRL and WV (Elliot et al 1989)]

Avoid oscillatory operation/ batch pile up

LLW thermal analysis observations

158-292 C

Na_4EDTA melts

$Na_4EDTA + NaNOx$ (s) $\longrightarrow$ NOx, CH_4, H_2, CO_2

292-363 C

$NaNO_2$, $NaNO_3$ melt $\longrightarrow$ NOx, CH_4, H_2, CO_2

$Na_4EDTA + NaNOx$ (l) $\longrightarrow$ NOx, CH_4, H_2, CO_2

327-567 EDTA decomposes $\longrightarrow$ CO_2

514-804 $NaNOx(l) + SiO_2$ $\longrightarrow$ NOx, O_2 CH_4

Why study the conversion of nuclear waste to glass?

- Large-scale runs are expensive
- Safety issues can be identified in small scale
- Enhancement of melting rate
- Conventional glass has been experimenting for a long time
- Lack of experience in radioactive vitrification- Only French melters are in operation

The Technetium Problem

Expected in LLW- $HTcO_4$, TcO_4^- , TcO^+ , $TcO(OH)^+$ $TcO(OH)_2^0$

When Tc is oxidized- high vapor pressure, volatile

LLW contains nitrates which oxidize Tc

LLW contains chlorides and fluorides; the stability of Tc halides is uncertain in LLW, However, decomposition of Tc halides produces Tc metal which is non-volatile.

Oxide/Carbonate Batches of LLW >80% Tc volatilization

Nitrate/ EDTA batches- Reduction in Volatilization

Reductant Reactions

Formic acid

$$HCOOH \longrightarrow H_2 + CO$$

$$HCOOH \longrightarrow H_2O + CO_2$$

Sugar

$$C_{12}H_{22}O_{11} + 8NaNO_3 \rightarrow 4\,Na_2O + 4N_2 + 8CO_2 + 4CO + 11\,H_2O$$

$$C_{12}H_{22}O_{11} + 12NaNO_2 \rightarrow 6Na_2O + 6N_2 + 6CO_2 + 6CO + 11H_2O$$

Elemental Carbon

$$3C + 2NaNO_3 \longrightarrow Na_2O + N_2 + 2CO_2 + CO$$

$$2C + 2NaNO_2 \longrightarrow Na_2O + N_2 + CO_2 + CO$$

High Level Waste Redox Issues

Pacific Northwest Laboratory

Reprint request

PROCESSING PROPERTIES OF NUCLEAR WASTE GLASSES

PROPERTY VS. PRIMARY VARIABLES

- glass can be viewed as a mixture of components
- a mixture property (ξ) depends on primary thermodynamic variables ($T, P, \mathbf{g}$):

$$\xi = f(T, P, \mathbf{g})$$

T temperature

P pressure

$\mathbf{g} = (g_1, g_2, \cdots, g_{n-1})$ composition vector

g_i i-th component mass or mole fraction

n number of components

- glass melting operation: $P = const.$

$$\xi = f(T, \mathbf{g})$$

PROPERTIES RELEVANT FOR GLASS MELTING PROCESS:

$$\xi \equiv \eta, \varepsilon, T_g$$

η viscosity

ε electrical conductivity

T_g glass transition temperature

- we need to determine

  $\eta = \hat{\eta}(T, \mathbf{g})$, $\varepsilon = \hat{\varepsilon}(T, \mathbf{g})$, and $T_g = \hat{T}_g(\mathbf{g})$

PROPERTY VS. COMPOSITION FUNCTIONS

<u>experimental design</u>:

- selection of compositions to cover the composition region and property ranges of interest
- manageable data generation: statistical theory of mixtures

<u>data evaluation</u>:

- plausible assumptions regarding the form of the property function

  $\xi = f(T, \mathbf{g})$

EMPIRICAL MODELS

- provide the most accurate practically achievable information regarding the effects of composition on composition-dependent variables

- minimize the amount of laboratory testing by restricting the compositional region

- employ statistical experimental design to optimize the coverage of this region by data points

- assume simple functional forms for the dependence of properties on composition

HANFORD SITE WASTE GLASS COMPOSITION REGION (wt%)

SiO_2	40-60	B_2O_3	≤15
Na_2O	5-25	Li_2O	≤ 7
CaO	≤ 3	MgO	≤ 1
Fe_2O_3	≤15	Al_2O_3	≤17
Zr_2O	≤14	CeO_2	≤ 2
Bi_2O_3	≤ 2	P_2O_5	≤ 3(?)
UO_3	≤17	TiO_2	≤ 9
NiO	≤ 2	Cr_2O_3	≤ 2
MnO	≤ 5		
SO_3	≤ 1	F	≤ 2

- these ranges reflect waste components inventory or solubility limits or both
- these ranges are estimated for statistical test matrices and <u>should not be used as acceptable ranges for engineering calculations</u>

PROPERTY CONSTRAINTS

- the selected composition region is further restricted by imposing property constraints:

$$T_L < T_M - 100°C$$

$$2Pa \cdot s < \eta(T_M) < 10Pa \cdot s$$

T_L liquidus temperature

T_M melting (melter operating) temperature

- low-temperature melter:
  $$T_M = 1050 - 1200°C$$
- high-temperature melter:
  $$T_M = 1200 - 1500°C$$

TEMPERATURE-DEPENDENT PROPERTIES

<u>viscosity</u>

- Vogel-Fulcher-Tammann (VFT) equation is generally used for viscosity as a function of temperature:

$$\eta = \exp[A(\mathbf{g}) + \frac{B(\mathbf{g})}{T - T_0(\mathbf{g})}]$$

- Arrhenius equation (for a narrow temperature interval, i.e., 950-1250°C):

$$\varepsilon = \exp[C(\mathbf{g}) + \frac{D(\mathbf{g})}{T}]$$

A, B, C, D temperature-independent coefficients

<u>electrical conductivity</u>

- both equations (VFT and Arrhenius) can be used

TEMPERATURE INDEPENDENT PROPERTIES VS. COMPOSITION

$$\Phi \equiv (\eta_T, \varepsilon_T, T_g, A, B, T_o)$$

η_T and ε_T viscosity and electrical conductivity at a given (constant) temperature

Scheffé forms:

first-order mixture models:

$$\Phi = \sum_{i=1}^{n} b_i g_i$$

second-order mixture models:

$$\Phi = \sum_{i=1}^{n} b_i g_i + \sum_{i<j} b_{ij} g_i g_j$$

b_i and b_{ij} are first- and second-order coefficients

PHYSICAL MEANING OF FIRST-ORDER COEFFICIENTS

1) replacement of i-th component by a k-th component

$$\partial\Phi / \partial g_i = b_i - b_k$$

2) i-th component addition to the mixture (component effect)

$$\partial\Phi / \partial g_i\big|_{add} = \frac{b_i - \Phi}{1 - g_i}$$

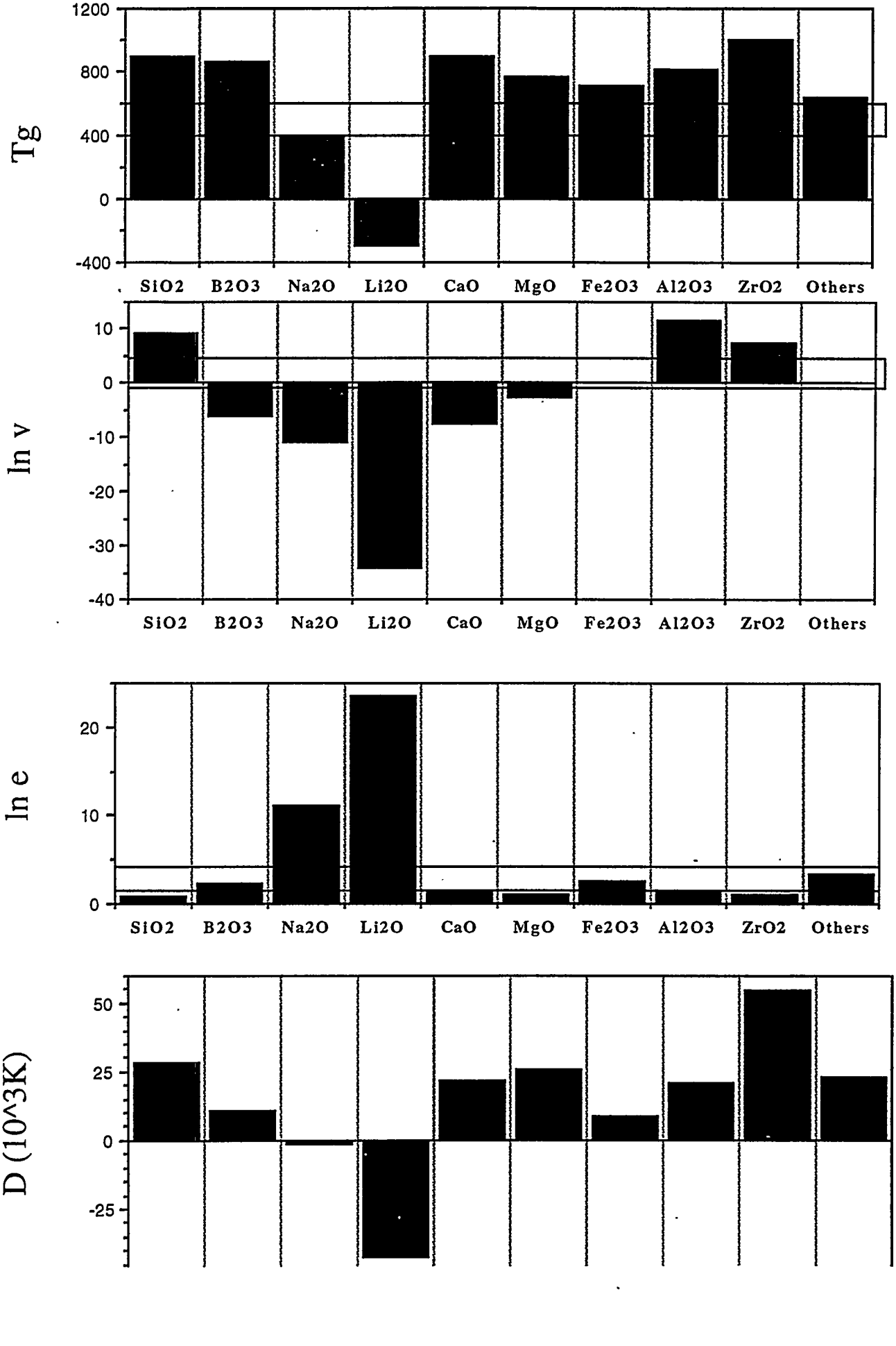
Tg
1200
800
400
0
-400
SiO2
B2O3
Na2O
Li2O
CaO
MgO
Fe2O3
Al2O3
ZrO2
Others
ln v
10
0
-10
-20
-30
-40
SiO2
B2O3
Na2O
Li2O
CaO
MgO
Fe2O3
Al2O3
ZrO2
Others
ln e
20
10
0
SiO2
B2O3
Na2O
Li2O
CaO
MgO
Fe2O3
Al2O3
ZrO2
Others
D (10^3K)
50
25
0
-25

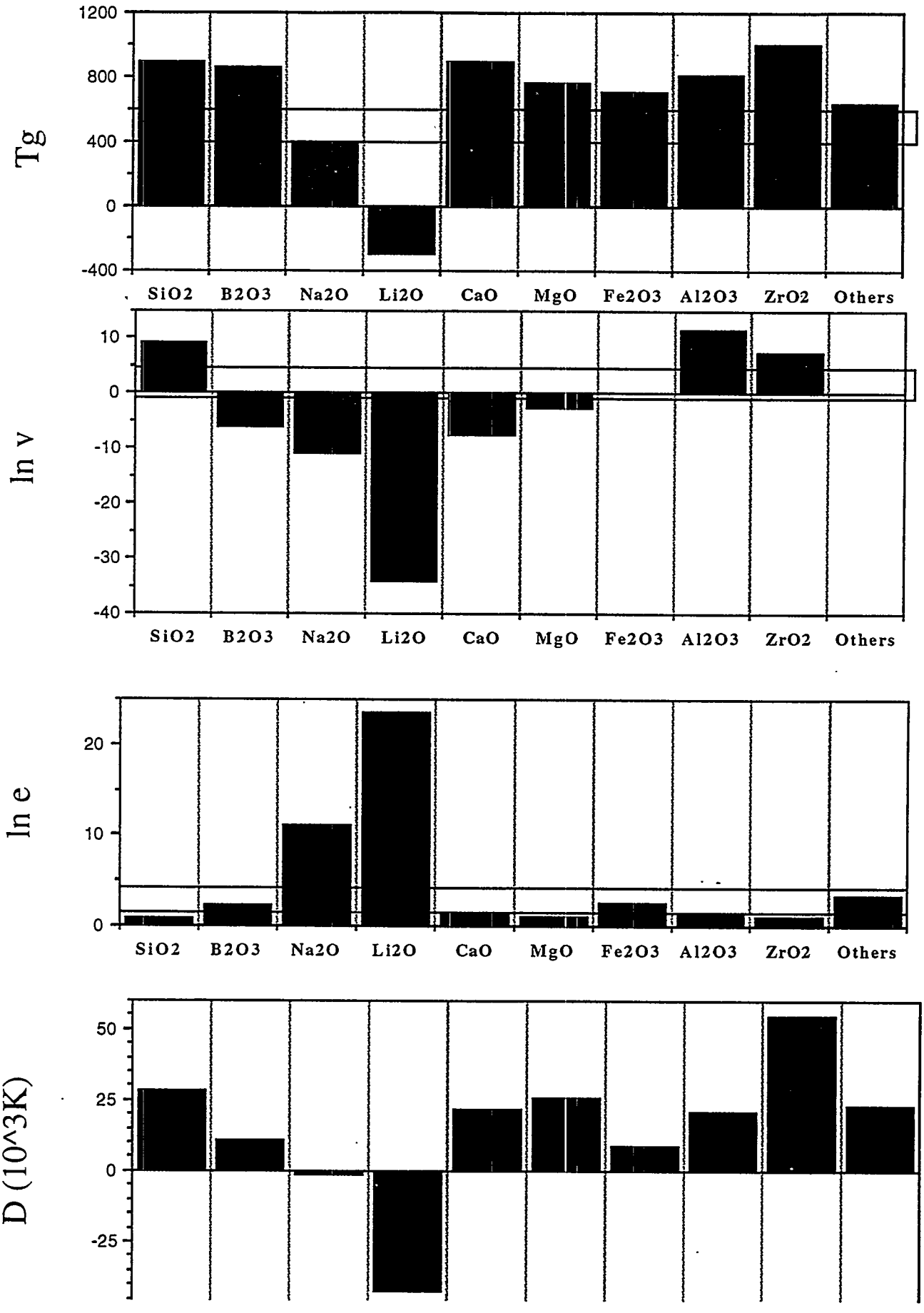
Tg
1200
800
400
0
-400
SiO2
B2O3
Na2O
Li2O
CaO
MgO
Fe2O3
Al2O3
ZrO2
Others
ln v
10
0
-10
-20
-30
-40
SiO2
B2O3
Na2O
Li2O
CaO
MgO
Fe2O3
Al2O3
ZrO2
Others
ln e
20
10
0
SiO2
B2O3
Na2O
Li2O
CaO
MgO
Fe2O3
Al2O3
ZrO2
Others
D (10^3K)
50
25
0
-25

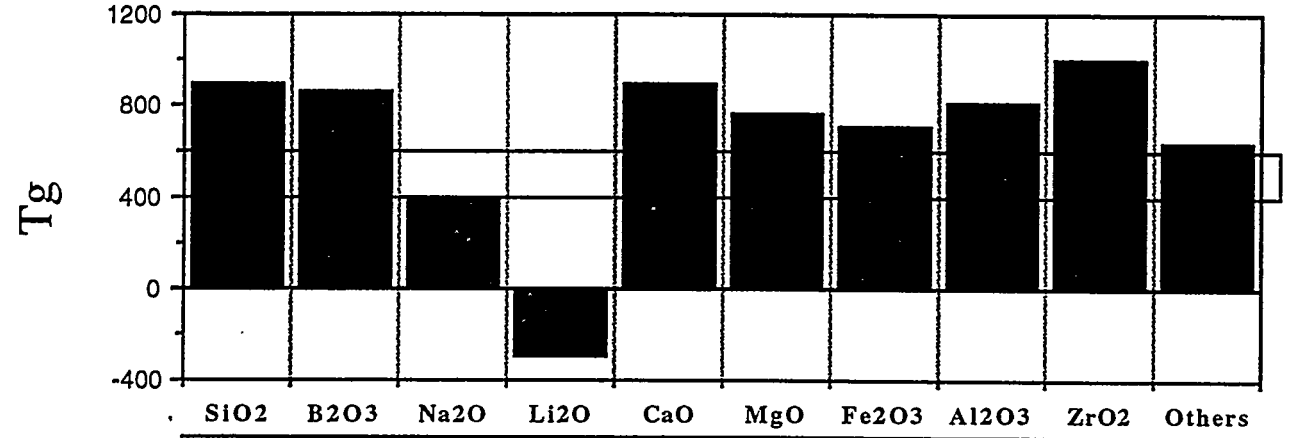
Tg
1200
800
400
0
-400
SiO2
B2O3
Na2O
Li2O
CaO
MgO
Fe2O3
Al2O3
ZrO2
Others

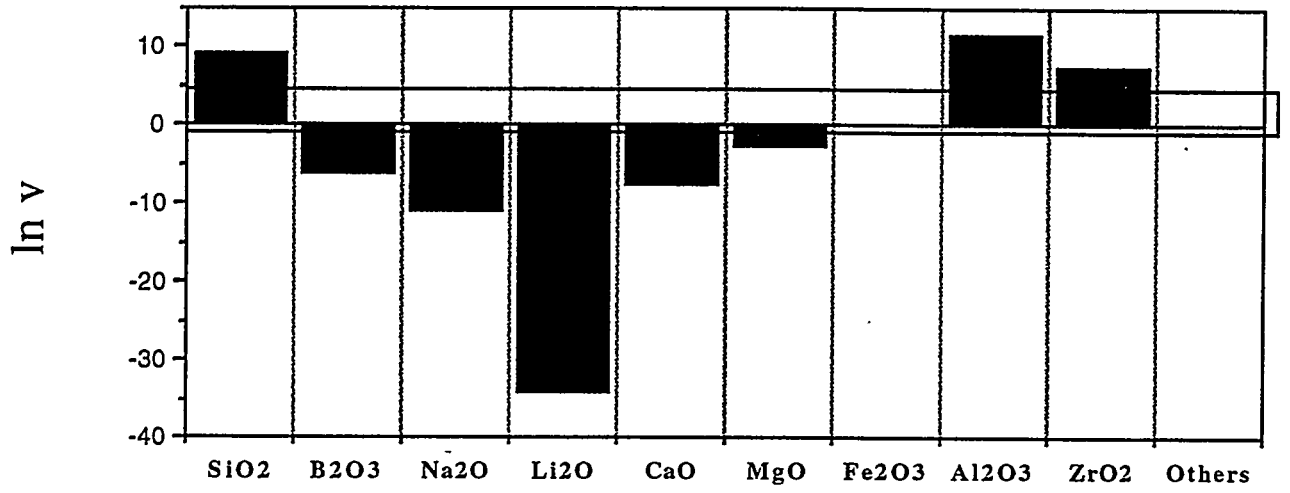
ln v
10
0
-10
-20
-30
-40
SiO2
B2O3
Na2O
Li2O
CaO
MgO
Fe2O3
Al2O3
ZrO2
Others

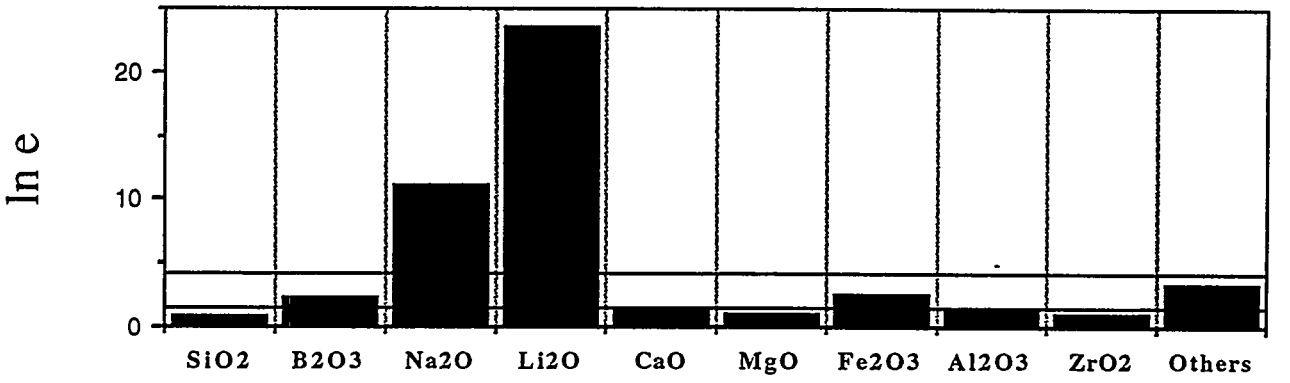
ln e
20
10
0
SiO2
B2O3
Na2O
Li2O
CaO
MgO
Fe2O3
Al2O3
ZrO2
Others


D (10^3K)
50
25
0
-25

GLASS TRANSITION TEMPERATURE (HLW GLASSES FOR LOW-TEMPERATURE MELTER)

T_g first-order coefficients, $T_{gi}(^\circ C)$

comp.	SiO_2	B_2O_3	Na_2O	Li_2O	CaO	MgO	Fe_2O_3	Al_2O_3	ZrO_2	Other	R^2
mass	623	585	129	-571	622	494	427	544	730	364	0.89
mole	615	589	138	-6	606	490	331	579	953	162	0.88

$T_g \uparrow$ if $T_{gi} > 600^\circ C$: $ZrO_2 > SiO_2 > CaO$

$T_g \downarrow$ if $T_{gi} < 400^\circ C$: $Li_2O << Na_2O <$ Others

$T_g \updownarrow$ if $400^\circ C < T_{gi} < 600^\circ C$:

$B_2O_3 \approx Al_2O_3 > MgO > Fe_2O_3$

VISCOSITY AT 1150°C (HLW GLASSES FOR LOW-TEMPERATURE MELTER)

$\eta(1150°C)$ first-order coefficients, $\ln \eta_i (Pa \cdot s)$

comp.	SiO_2	B_2O_3	Na_2O	Li_2O	CaO	MgO	Fe_2O_3	Al_2O_3	ZrO_2	Other	R^2
mass	9.0	-6.2	-11.0	-34.2	-7.5	-2.8	0.0	11.3	7.4	-0.2	0.94
mole	8.5	-6.8	-10.7	-15.0	-6.3	-1.2	-2.5	17.1	12.8	-3.6	0.95

$\eta \uparrow$ if $\ln \eta_i > 4.5$ $\quad Al_2O_3 > ZrO_2 > SiO_2$

$\eta \downarrow$ if $\ln \eta_i < -1$ $\quad Li_2O < Na_2O < CaO \approx B_2O_3 < MgO$

$\eta \updownarrow$ if $-1 < \ln \eta_i < 4.5$ $\quad$ Others $\approx Fe_2O_3$

ELECTRICAL CONDUCTIVITY AT 1150°C (HLW GLASSES FOR LTM)

$\varepsilon(1150°C)$ first-order coefficients, $\ln \varepsilon_i (S/m)$

comp.	SiO_2	B_2O_3	Na_2O	Li_2O	CaO	MgO	Fe_2O_3	Al_2O_3	ZrO_2	Other	R^2
mass	0.9	2.3	11.0	23.5	1.4	1.1	2.6	1.3	1.1	3.5	0.93
mole	1.0	2.2	10.8	12.7	1.6	3.0	1.8	0.2	-0.9	3.9	0.94

$\varepsilon \uparrow$ if $\ln \varepsilon_i > 4.6$ $\quad Li_2O > Na_2O$

$\varepsilon \downarrow$ if $\ln \varepsilon_i < 1.8$ all non-alkali components except B_2O_3, Fe_2O_3, and Others

- electricity in molten glass is conducted by alkali ions
- relation $\eta\varepsilon = const.$ is not valid as glass composition varies

GLASS "LENGTH"

- glass length measures the change of η in response to a change in temperature
- first-order Arrhenius activation energy (D) can be used to measure glass length $\left(\eta = \exp[C(\mathbf{g}) + \frac{D(\mathbf{g})}{T}]\right)$
- component coefficients $D_i \times 10^{-3}(K)$ for the temperature interval 950-1250°C

comp.	SiO_2	B_2O_3	Na_2O	Li_2O	CaO	MgO	Fe_2O_3	Al_2O_3	ZrO_2	Other
mass	28.5	10.9	-1.2	-42.3	21.5	25.8	8.8	21.2	54.6	23.0
mole	28.8	9.1	-2.0	-12.6	20.3	23.3	-5.3	25.1	90.4	29.7

longer glass ($D\downarrow$) $\quad Li_2O << Na_2O < B_2O_3 \approx Fe_2O_3$

shorter glass ($D\uparrow$) $\quad ZrO_2 > SiO_2 > MgO > CaO \approx Al_2O_3$

Effects of Experimental Parameters on Glass Durability

Xiangdong Feng

June 28, 1995

Glass Science and Engineering Tutorial
Westinghouse Hanford Company
Richland, Washington

Topics in Experimental Parameters

- Test methods
  - PCT (Product Consistency Test)
  - Single-Pass Flow-Through Test (SPFT)
  - Vapor Hydration Test (VHT)
- S/V (ratio of glass surface area to solution volume)
- Leachant composition
  - Ionic strength
  - Inorganic/organic
  - Individual cations
  - pH
  - Presence of metals
- Simulated glasses/fully radioactive glasses

Chemical Description of Glass Reaction

- Water diffusion
- Ion exchange
- Hydrolysis
- Secondary phase formation

Ion Exchange

$$\equiv SiO\text{-}M + H_2O \longleftrightarrow \equiv SiO\text{-}H + M^+ + OH^-$$

$$K_M = \frac{[\equiv SiO\text{-}H]\,[M^+]\,[OH^-]}{[\equiv SiO\text{-}H]\,[H_2O]}$$

$$\frac{d}{dt}\,[M^+] = \frac{SA}{V}\,k_M\,[H_2O]\,\left(1 - \frac{[M^+]\,[OH^-]}{K_M}\right)$$

Hydrolysis

$$\equiv Si\text{-}O\text{-}Si(OH)_3 + OH^- \longleftrightarrow \equiv SiO^- + HO^-Si(OH)_3$$

$$K_{Si} = \frac{[\equiv Si\text{-}O^-]\ [H_4SiO_4]}{[\equiv SiO\text{-}Si(OH)_3]\ [OH^-]}$$

$$\frac{d}{dt}[H_4SiO_4] = \frac{SA}{V} k_{Si} [OH^-]\ \left(1 - \frac{[H_4SiO_4]}{K_{Si}}\right)$$

- Description of glass reaction must account for influence of all processes

- Test conditions may be used to promote or quench specific processes of water diffusion, ion exchange, hydrolysis, or secondary phase formation

S/V Effects on Glass Corrosion

- S/V has been used as a reaction acceleration parameter to speed up glass reaction progress, i.e., equal leachate concentration can be obtained as long as:

$$\left(\frac{S}{V}\right)_1 \cdot t_1 = \left(\frac{S}{V}\right)_2 \cdot t_2$$

- Waste glasses may experience different S/V conditions under disposal conditions due to:
  - Glass cracking
  - Change in groundwater flow through the disposal site

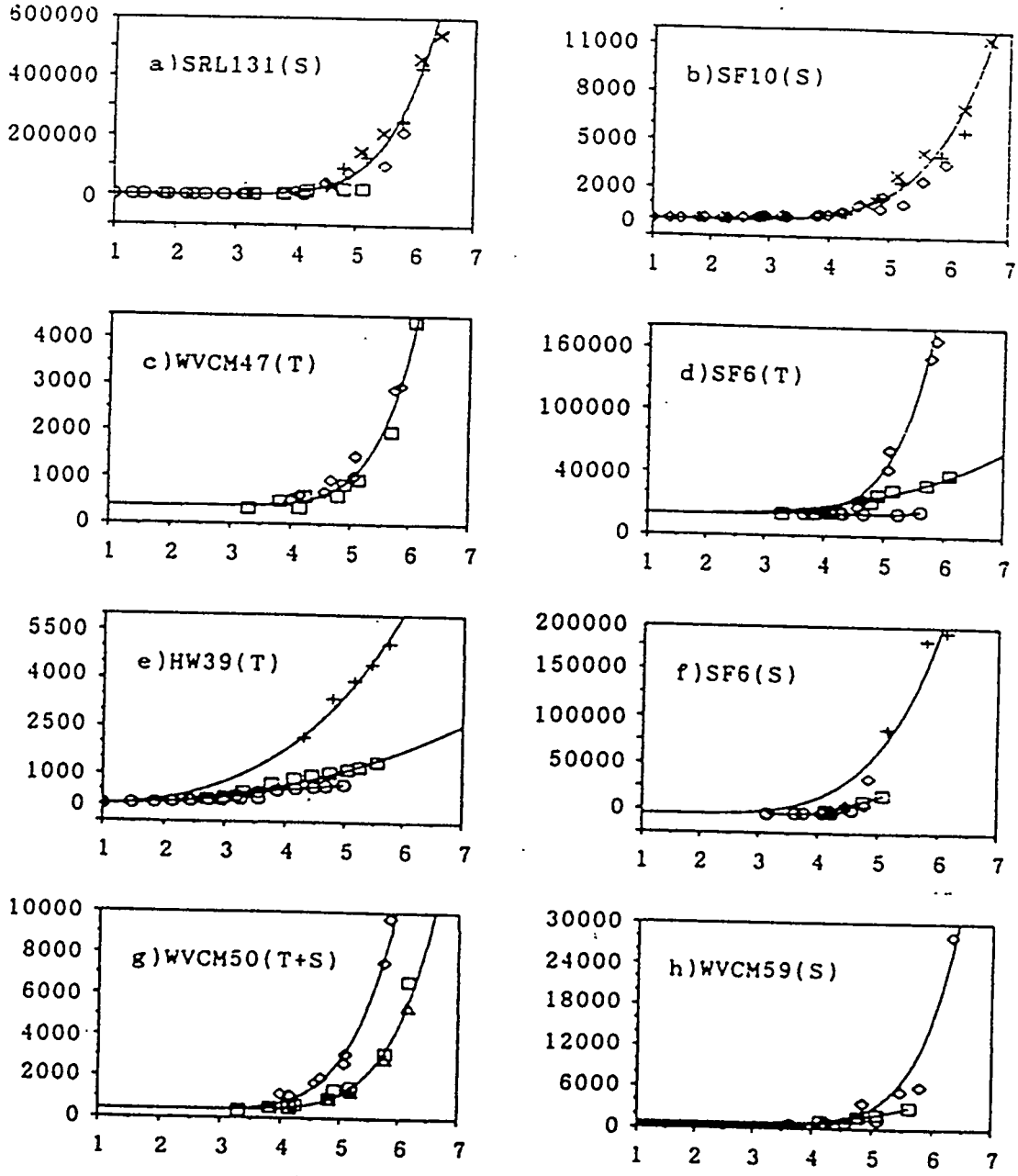

Normalized Boron Concentration (PPM)
vs log[(S/V)·t] (day·m^{-1})

○ S/V ≤ 600 M^{-1} □ S/V = 2000 M^{-1} (T) △ S/V = 2000 M^{-1} (S)

◇ S/V = 10000 M^{-1} ▽ S/V = 14000 M^{-1} + S/V = 20000 M^{-1}

× S/V = 40000 M^{-1}

Feng et al., MRS Proc. (1990)

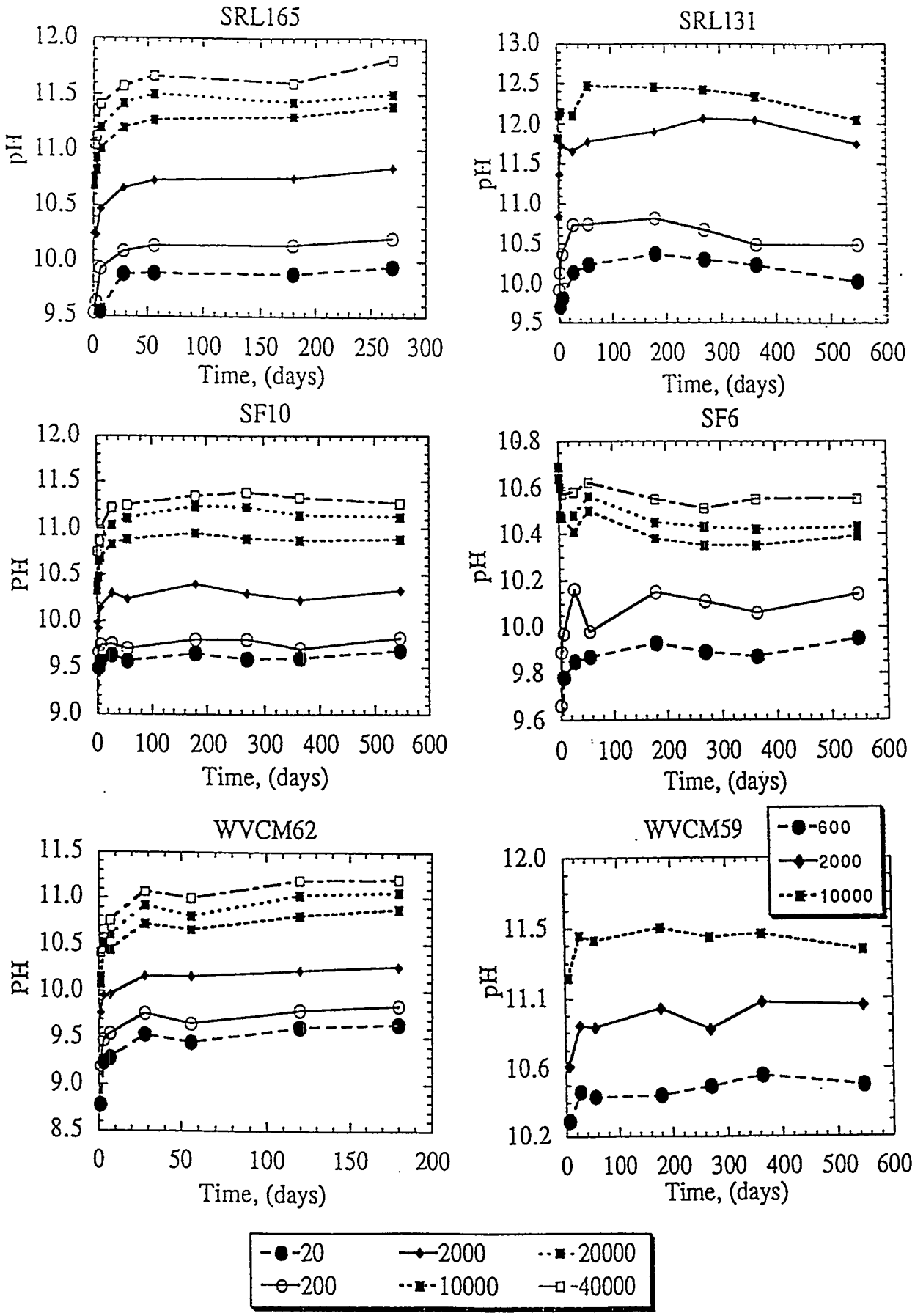

Feng et al. J. Non-Cryst. Solids, (1994)

Ion Exchange

$$\equiv SiO\text{-}M + H_2O \longleftrightarrow \equiv SiO\text{-}H + M^+ + OH^-$$

$$K_M = \frac{[\equiv SiO\text{-}H]\,[M^+]\,[OH^-]}{[\equiv SiO\text{-}H]\,[H_2O]}$$

$$\frac{d}{dt}\,[OH^-] = \frac{SA}{V}\,k_M\,[H_2O]\,\left(1 - \frac{[M^+]\,[OH^-]}{K_M}\right)$$

Isotope Effects Summary (H_2O/D_2O)

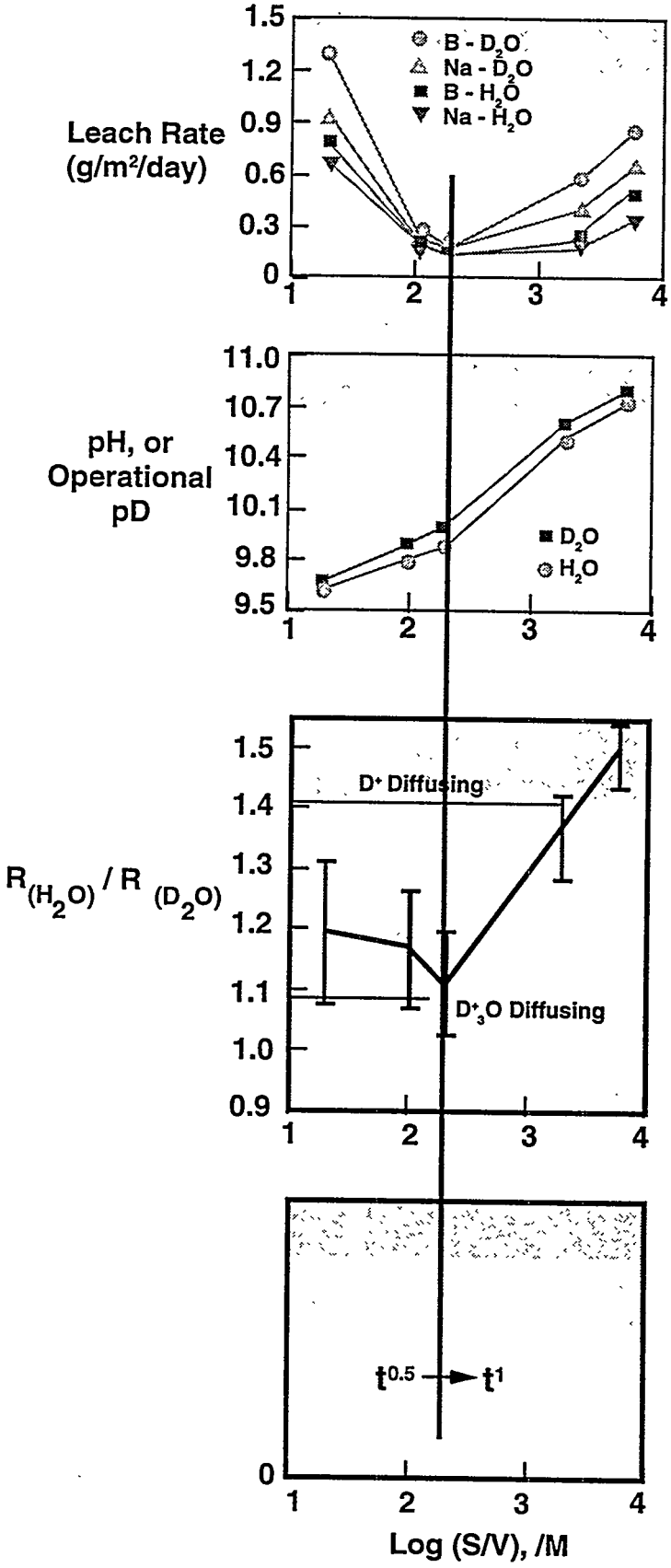

When SA/V Changes:

Rate Changes

pH Changes

Isotope Effect Changes

Solution Kinetics Changes

Mechanism Transition: $t^{0.5} \rightarrow t^{1}$

Feng et al., MRS Proc. 1991

Mechanistic Investigation pH Effects on Mechanisms

- In pH = 8.5 buffers
  - Solution kinetics
    S/V = 200/m → $t^{0.5}$
    S/V = 2000/m → $t^{0.5}$
  - Isotope effects, support diffusion
    S/V = 200/m → 1.1*
    S/V = 2000/m → 1.1*

- In pH = 10.0 buffers
  - Solution kinetics
    S/V = 200/m → t^{1}
    S/V = 2000/m → t^{1}
  - Isotope effects, matrix dissolution
    S/V = 200/m > > 1.1*
    S/V = 2000/m > > 1.1*

Feng et al., Nucl. Waste Mgmt. (1991)

Isotope Effects Summary (H_2O/D_2O)

When SA/V Changes:

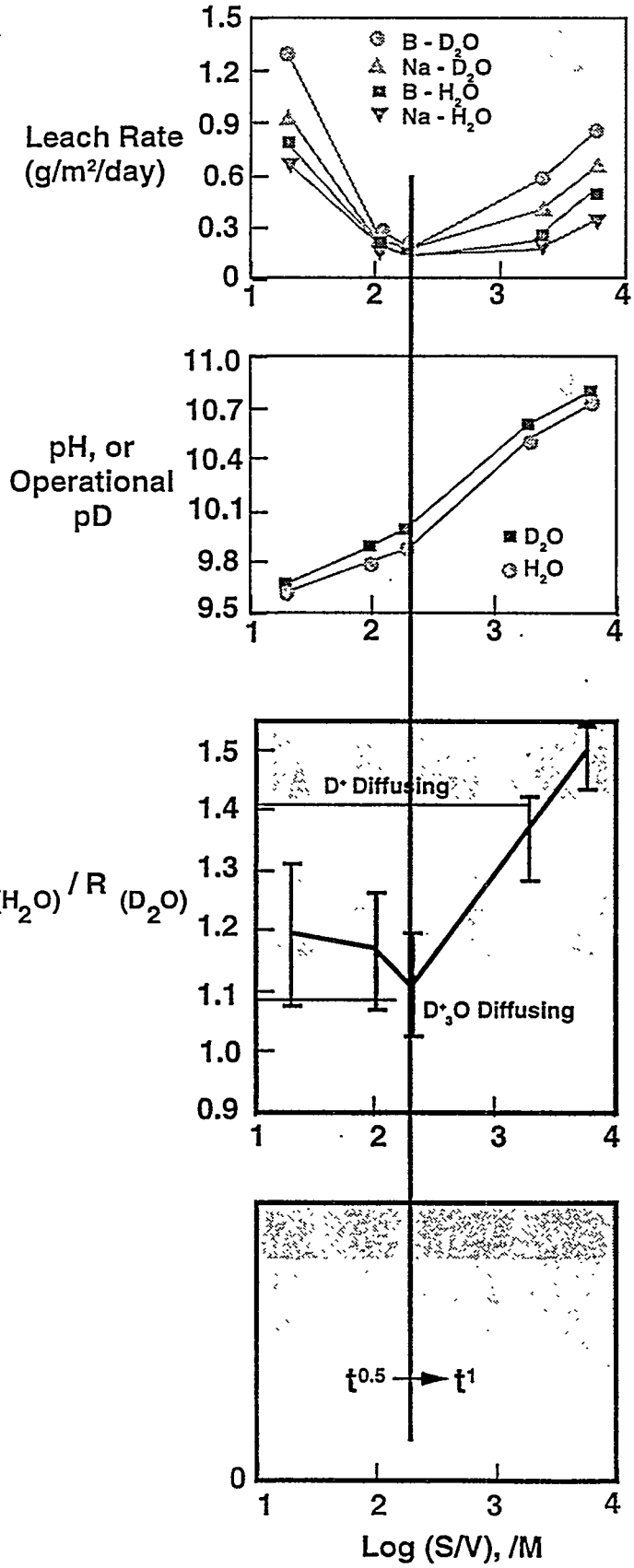

Rate Changes

pH Changes

Isotope Effect Changes

Solution Kinetics Changes

Mechanism Transition: $t^{0.5} \rightarrow t^{1}$

Feng et al., MRS Proc. 1991

R9506086.32 C

The Nature of S/V Effect

- It is the combination of pH and concentration effect
- pH
  - Determines controlling glass RXN mechanism
  - Dominates glass RXN rates
  - Influences identities of alteration phases
  - Dominates thickness of alteration layers
- Concentration
  - Contributes to glass RXN rates
  - Determines when secondary phases form (if nucleation is not hindered)
  - Controls amount of secondary phases formed
  - Affects thickness of alteration layer
- pH is a more dominant factor in glass RXN

Feng et al. Acers Meeting (1992)

Summary of S/V Effects

- S/V is a very important parameter in glass reaction
- Understanding S/V effect is the key to proper modeling
- The S/V induces pH change and mechanism change need to be incorporated into the existing modeling effects

Feng et al. Acers Meeting (1992)

Leachant Composition Effects on Glass Durability

- **Ionic strength**
  - *Feng et al., Phys. Chem. Glasses, (1994)*
- **Inorganic/organic**
  - *Feng et al., MRS Proc. (1986)*
- **Individual cations**
  - *Feng et al., Proc. Intern. SEE (1992)*
  - *Feng, UMI (1988)*
- **pH**
  - *Feng et al., Nucl. Waste Mgmt. (1991)*
- **Presence of metals**
  - *Feng, Waste Mgmt. (1994)*

Concentration vs. Time

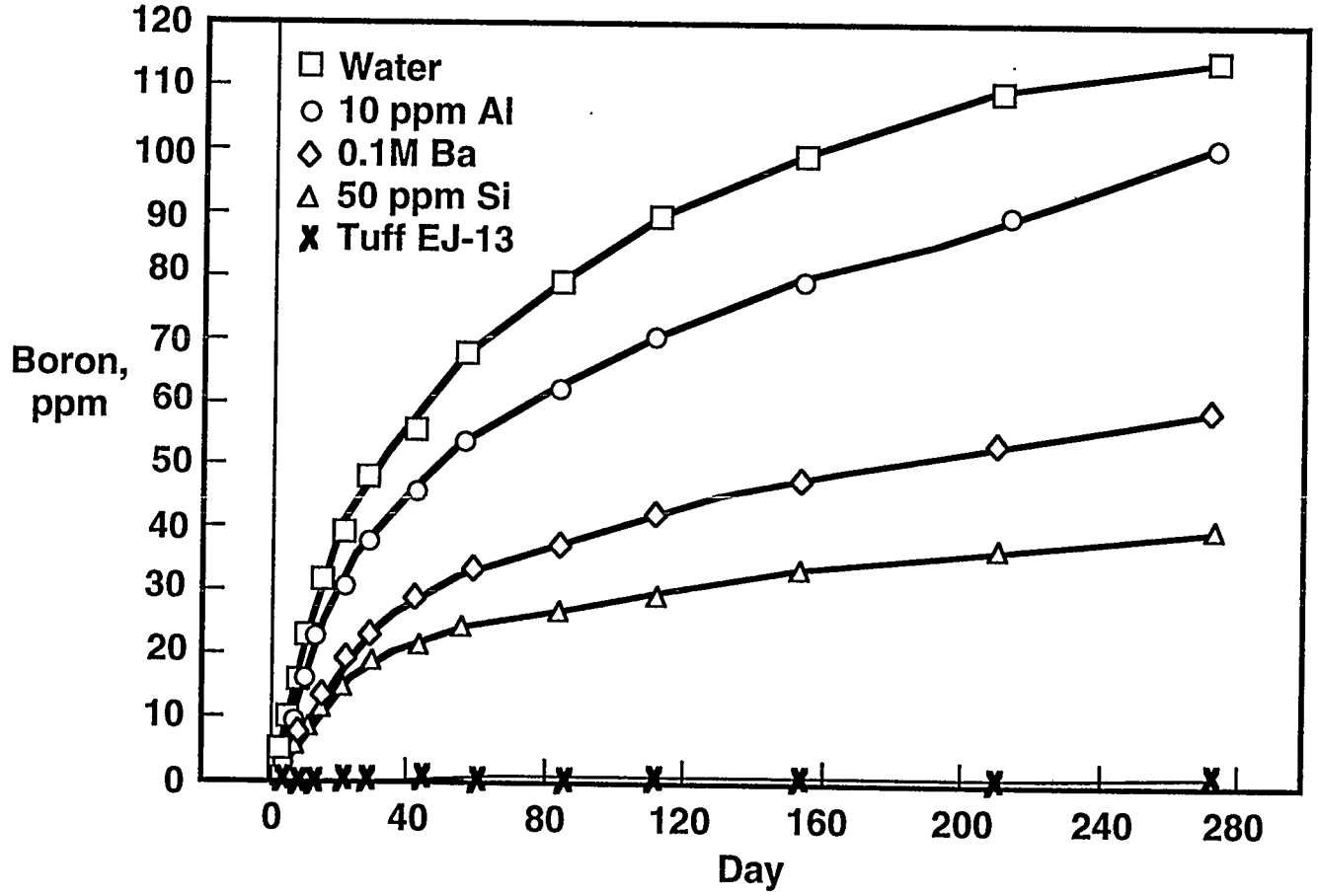

Ion Exchange

(A) Destructive exchange:

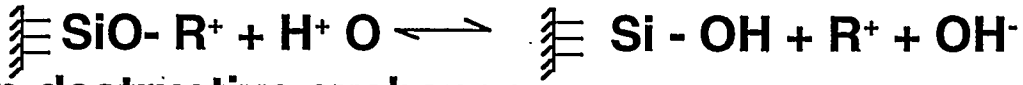

(B) Non-destructive exchange:

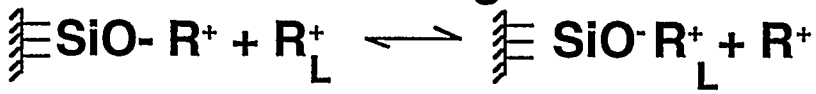

- Salt suppresses Case A
  - Facilitates competing reaction in Case B
  - ⟶ Reduces glass leaching
  - Lower pH
- Expect:
  - Small effect for non-exchangeable R^+_L
  - Dependence on mobility of R^+_L

Cation Effects

Relative Mobility of Cations

	Li	Na	K	Cs
Crystal Radii (Å)	0.86	1.12	1.44	1.84
Hydrated Radii (Å)	3.40	2.76	2.32	2.28
Relative Mobility in Water	33.5	43.5	64.6	68.0

Summary of Solution Composition Effects

- **Ionic strength (salt effects)**
  - **Salt reduces corrosion rate**
    - **Due to kinetic ion exchange**
    - **Not thermodynamic ionic strength effects**

  Feng et al., Phys. Chem. Glasses (1994)

- **Inorganic/organic buffers at the same pH**
  - **L.R. in inorganic > that in organic due to hydrophobic coating on and complexing with glass surfaces**

  Feng et al., MRS Proc. 1986

Summary of Solution Composition Effects (cont.)

- **Individual cations**
  - **Corrosiveness of solutions:**
  - **$Li^+ > Na^+ > K^+ > Cs^+$**
  - **Due to differences in mobility and size, which affect ion exchange reactions**

    Feng et al., Proc. Intern. SEE 1992

- **Silicate or aluminate water**
  - **Reduce corrosion by reducing reaction affinity**

    Feng Waste Mgmt. 1994

- **pH**
  - **Affect corrosion mechanism and secondary phase formation**

    Feng et al., Nucl. Waste Mgmt. 1991

Summary of Solution Composition Effects (cont.)

- **EJ-13 groundwater**
  - **Lowest leach rate under dynamic test condition**
  - **Due to compounding effects of salt, alumina and silica, and buffering capability**

    Feng et al., MRS Proc. 1986

- **Presence of metals**
  - **Fe enhances corrosion**
  - **Due to formation of Fe(II)-silicates in solution, that affects reaction affinity**

    Feng, UMI 1988
    Feng, Waste Mgmt. 1994

Comparison of Durability Between Simulated and Fully Radioactive Glasses

- Most waste glass durability data are generated from simulated glasses
- Needs to investigate and understand the different corrosion behavior between them in order to make use of the data simulated glass for performance assessment of radioactive glasses

SRL 165/42 glasses were tested at 2000 m^{-1}. R- and S-glasses show similar corrosion behavior

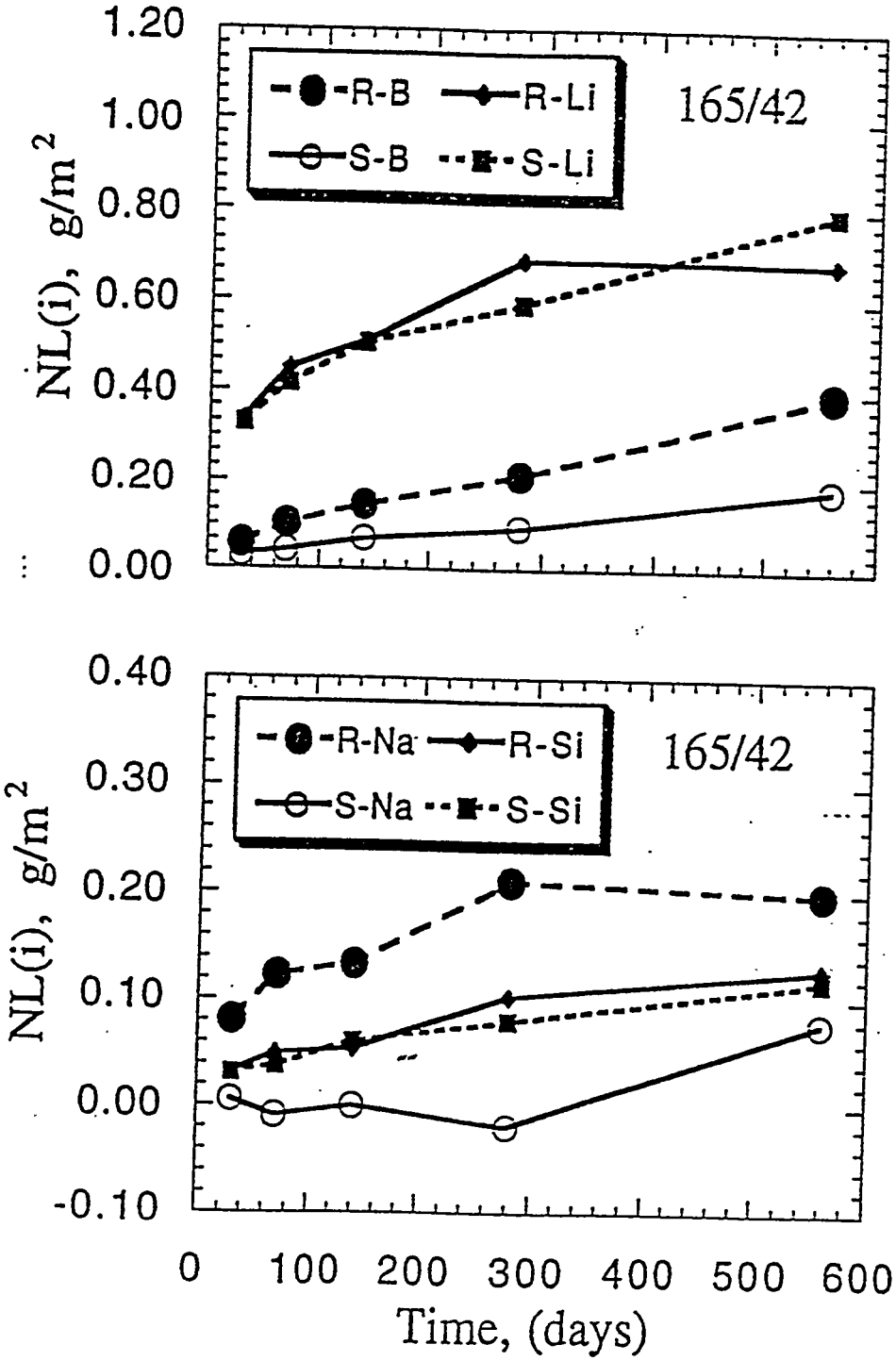

SRL 200 glasses were tested at 2000 m^{-1} and similar corrosion behavior was observed

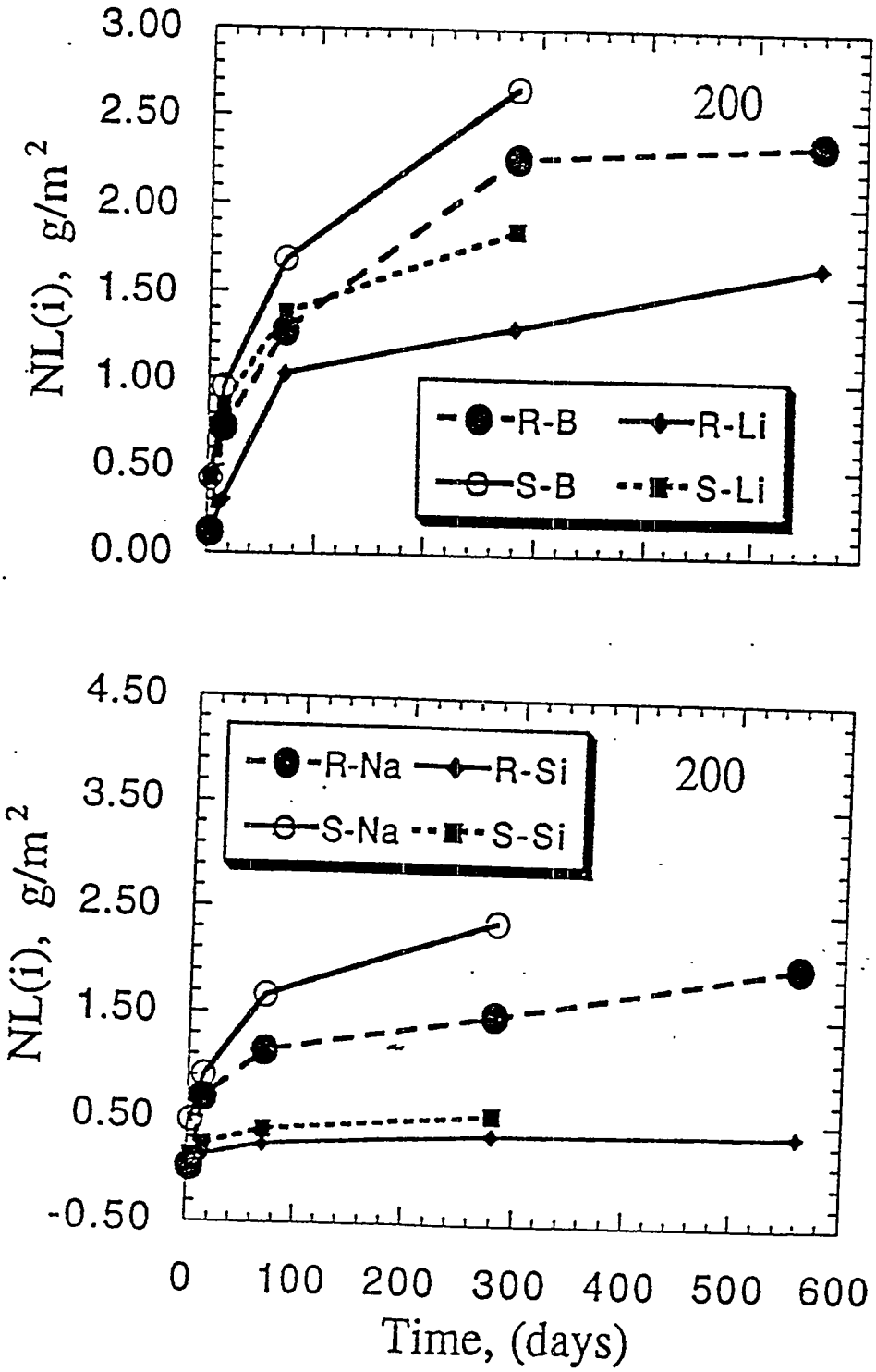

A large difference in corrosion behavior was observed for SRL 200R and SRL 200S glasses when these glasses were tested at 20,000 m^{-1} for one year or longer

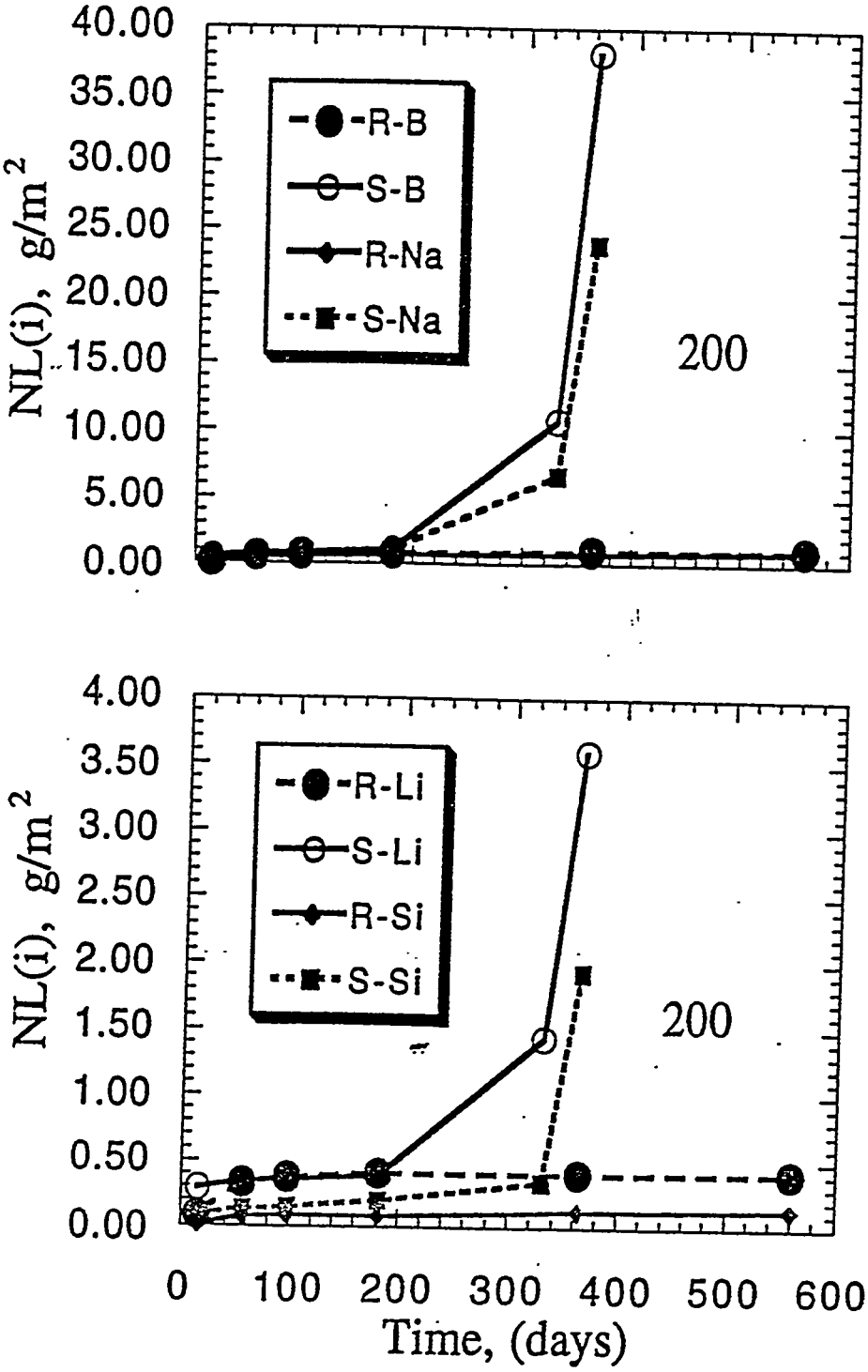

200 at 20,000 m-1

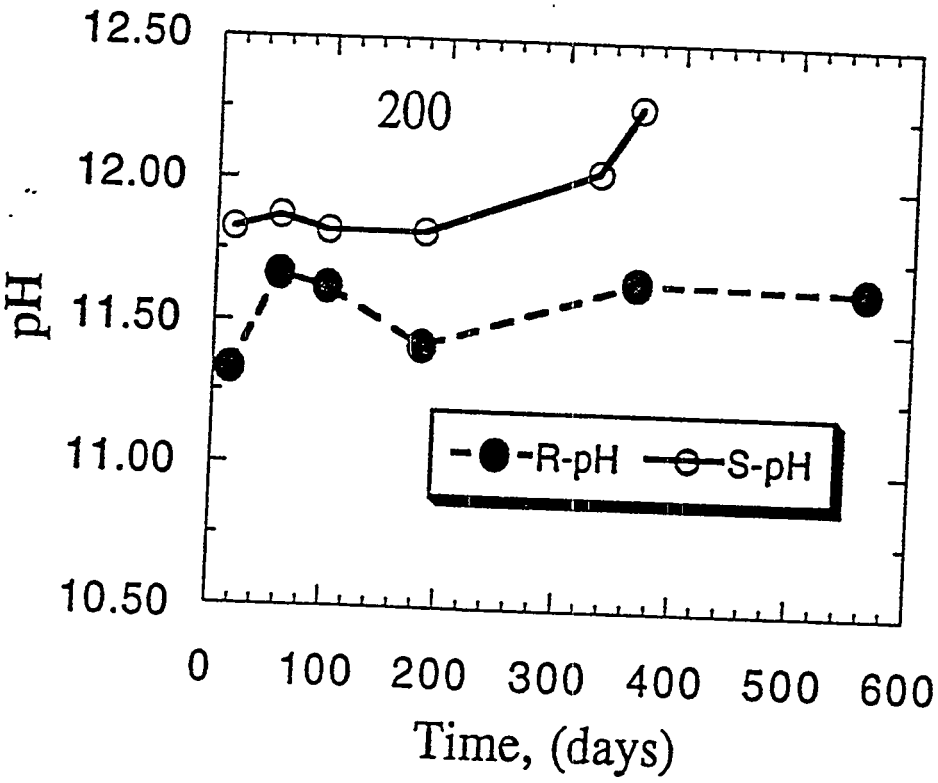

SURFACE LAYER THICKNESS
(200S at 20,000 m^{-1})

98 day

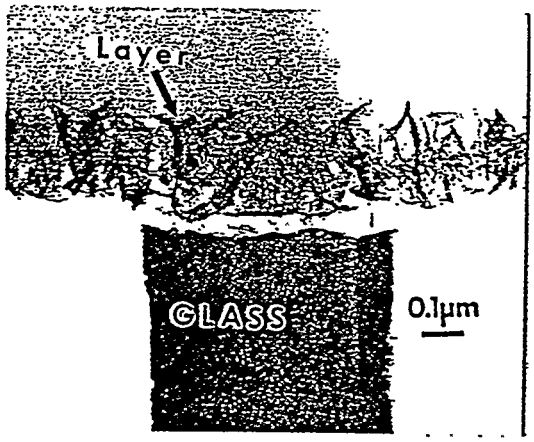

182 day

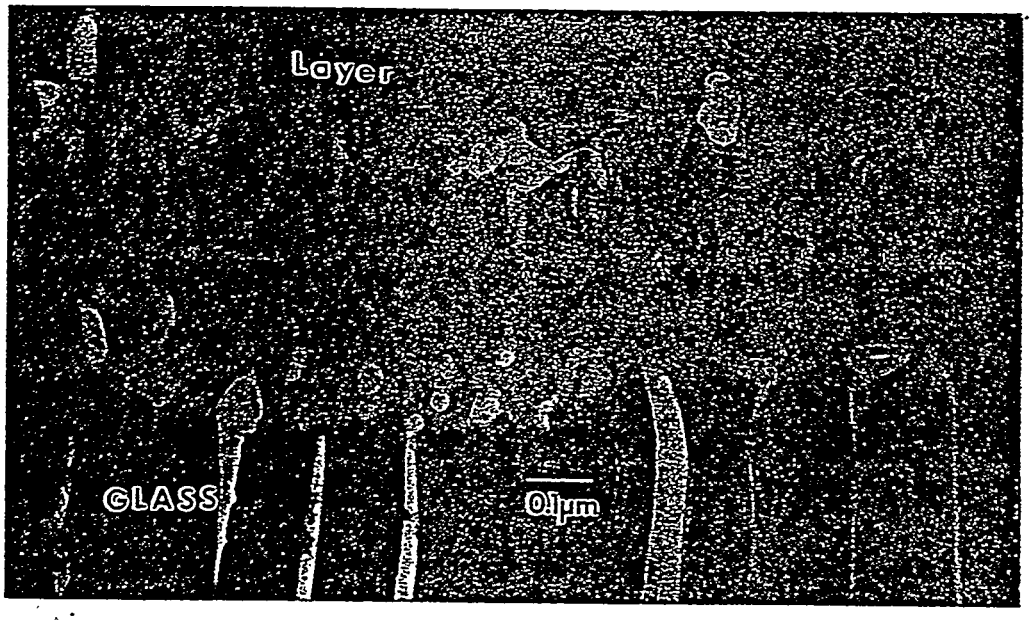

SURFACE LAYER THICKNESS
(200S at 20,000 m-1)

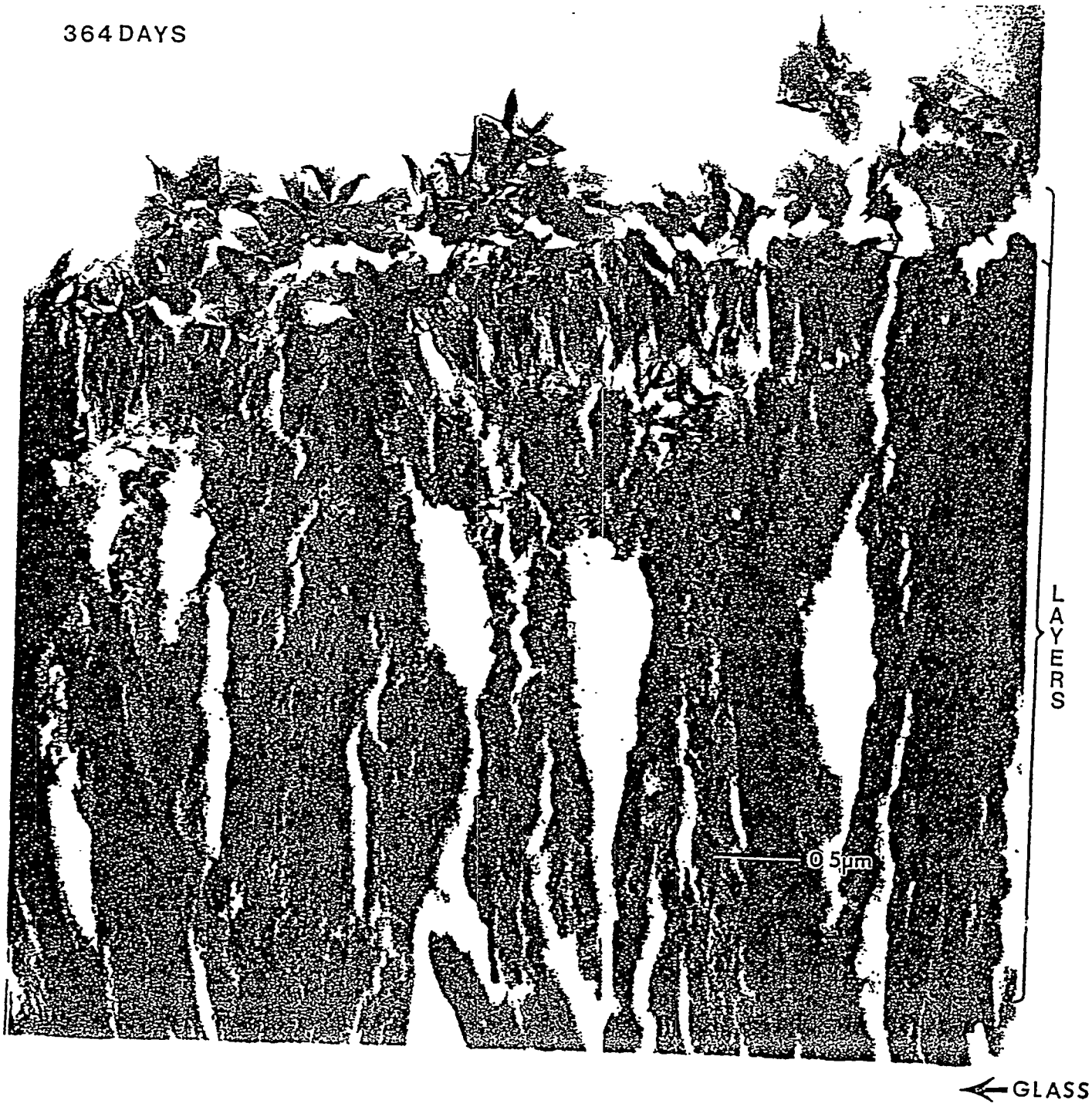

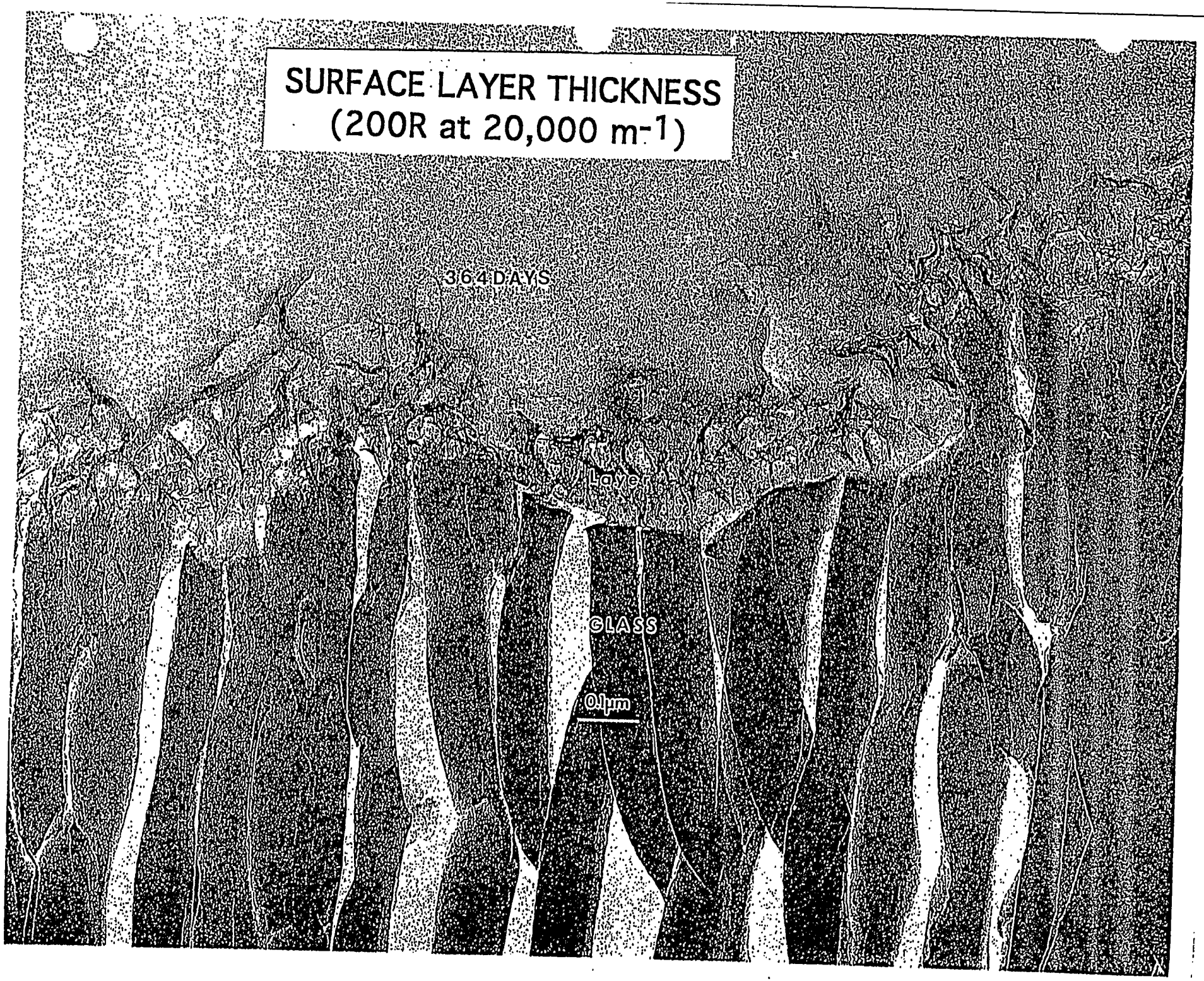
SURFACE LAYER THICKNESS
(200R at 20,000 m-1)
364 DAYS
Layer
GLASS
0.1μm

SECONDARY PHASE FORMATION
(200S at 20,000 m^{-1})

98 day

182 day

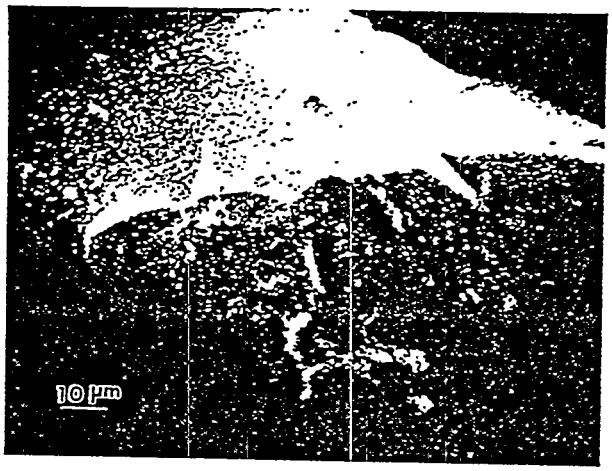

364 day

The possible secondary phases identified in the surface layers of SRL 200S reacted for 364 days at 20,000 m^{-1}:

- Clinoptilolite
- Si-Ca phase
- Fe-rich clay phase
- Amorphous silica phases

Possible Explanations

- Radiation-induced lowering of pH of R-glass leachate prevents accelerated glass reaction in R-glass
- Extensive secondary phase formation in tests with S-glass increased the reaction affinity and resulted in increased glass reaction rate

Implications

- Utilization of S-glass corrosion data for modeling fully radioactive waste glasses requires caution
- Radiation effects (such as the effects on leachate pH) have to be incorporated in the long-term modeling
- A meaningful comparison study between R- and S-glasses should include tests at both high- and low-SA/V's and for long-term
- Long-term testing of fully radioactive glasses is a MUST for performance assessment of nuclear waste glasses

Test Methods for Evaluation of Glass Durability

- Different tests subject glass to different corrosion conditions, which selectively promote or reduce certain glass reaction processes
- Generate different extent of glass reaction during similar test duration
- Provide information of different stages of glass reaction

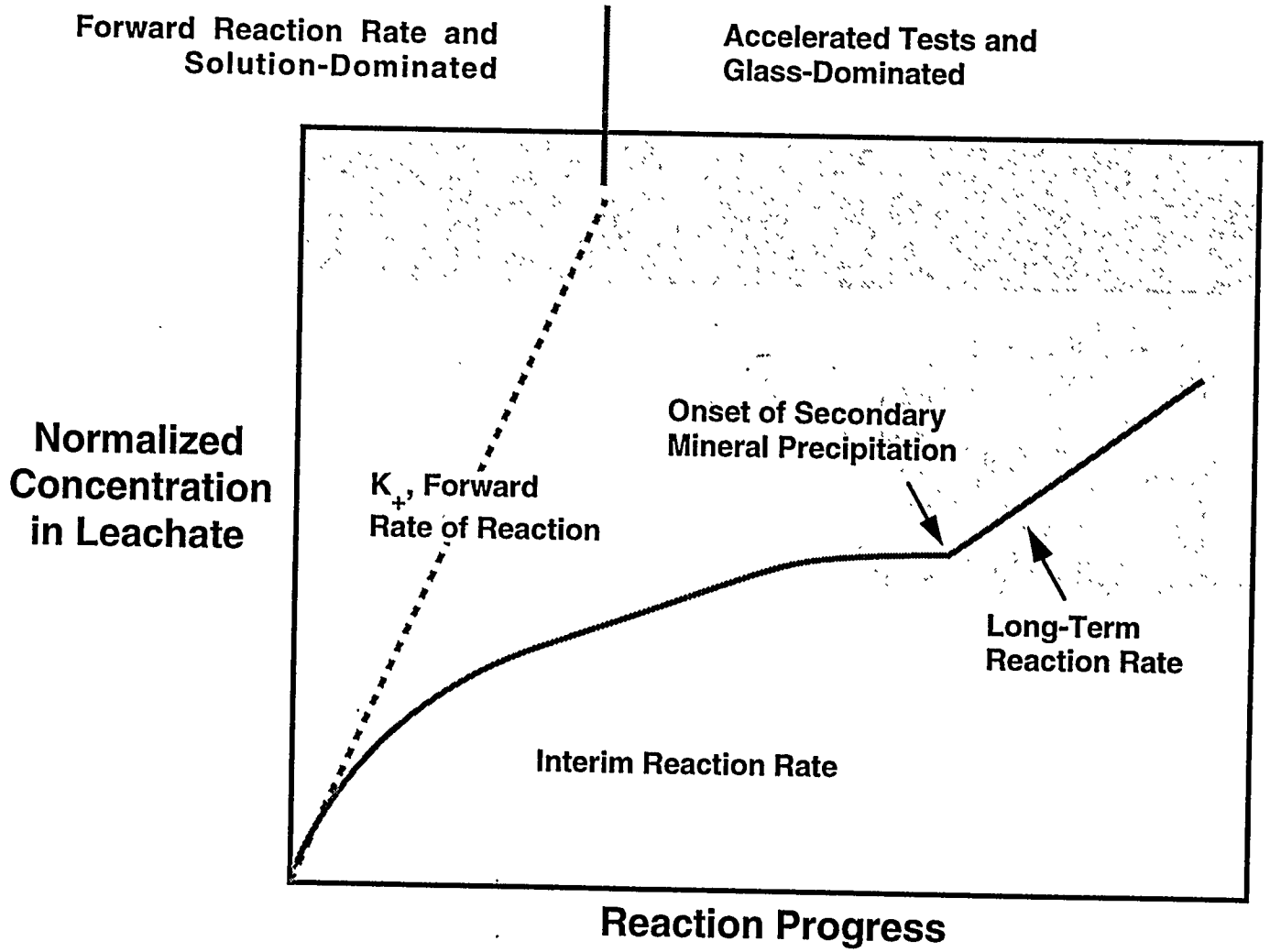
Forward Reaction Rate and
Solution-Dominated
Accelerated Tests and
Glass-Dominated
Normalized
Concentration
in Leachate
K_+, Forward
Rate of Reaction
Onset of Secondary
Mineral Precipitation
Long-Term
Reaction Rate
Interim Reaction Rate
Reaction Progress

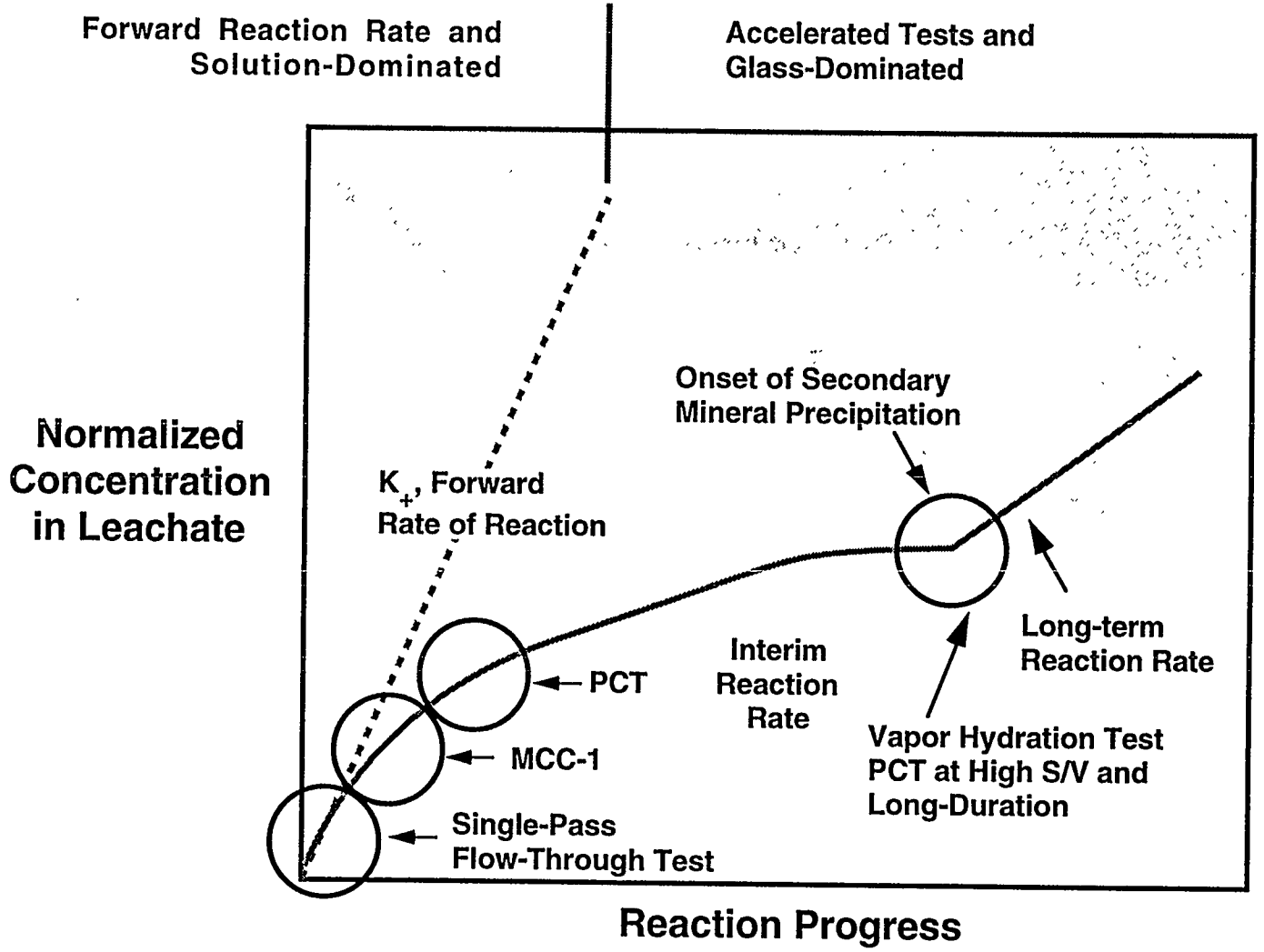
Forward Reaction Rate and
Solution-Dominated
Accelerated Tests and
Glass-Dominated
Normalized
Concentration
in Leachate
Onset of Secondary
Mineral Precipitation
K+, Forward
Rate of Reaction
PCT
MCC-1
Single-Pass
Flow-Through Test
Interim
Reaction
Rate
Long-term
Reaction Rate
Vapor Hydration Test
PCT at High S/V and
Long-Duration
Reaction Progress

Single-Pass Flow-Through Test (SPFT)
Product Consistency Test (PCT)
Vapor Hydration Test (VHT)

Temp. °C	Leachant	S/V	Glass Samples	Flow Rate	pH
SPFT 20-90°C	variable	variable	monolith or powders	variable	constant
PCT 20-200	deionized water	variable	powders	static	changing
VHT up to 300	adsorbed water vapor	much higher than 2000/m	monolith usually	static	changing

Cpmparison of Durability Using PCT (90C) VS. Single-Pass Flow Through Test (SPFT) (at 90C and pH=12.0)

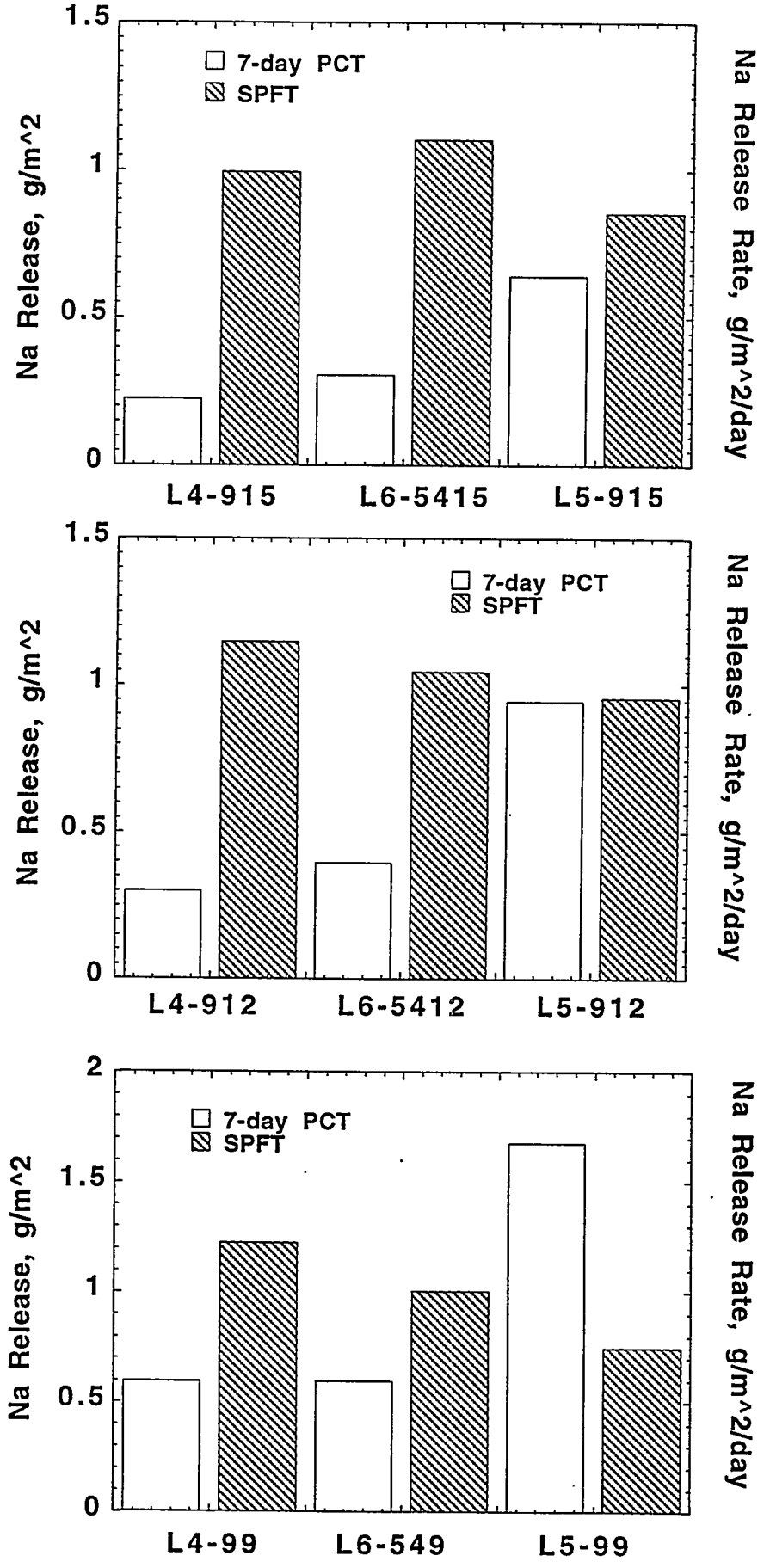

Cpmparison of Durability Using PCT (90C) VS. Single-Pass Flow Through Test (SPFT) (at 90C and pH=12.0)

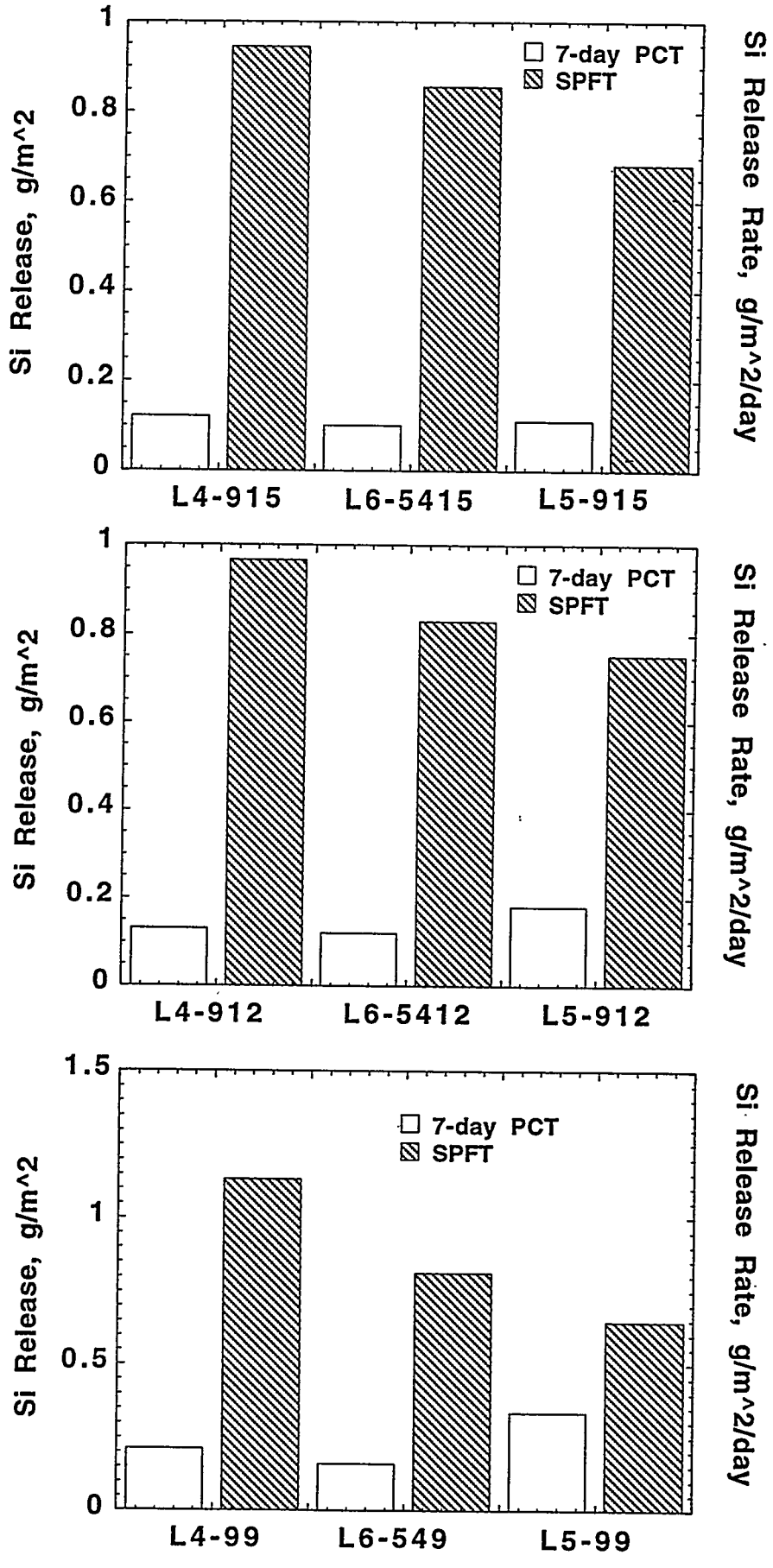

Durability Order Measured with PCT and SPFT:

- On Glass Systems
  - L4 - Boron only glasses
  - L5 - Calcium only glasses
  - L6 - Mixture of boron and calcium

- In PCT (90°C)
  - L4 > L6 > L5

- In SPFT (90°C, pH = 12)
  - L5 > L6 > L4

PCT Durability Order:
B-Glass > (B + Ca) - Glass > Ca-Glass

- Understandable based on glass structure
  - B_2O_3 replaces NBO bonds with BO
  - CaO replaces NBO with hybrid of BO + NBO
  - More durability improvement is expected for B_2O_3 than for CaO
- Boron containing glasses releases boron that buffers leachate pH in static test. Lower pH results in lower glass corrosion rate.
- Observation: Boron-only glasses have pH's lower by 1-2 pH units than the corresponding Ca-only glasses.

SPFT (at pH12) Durability Order:
Ca-Glass > (B + Ca)-Glass > Ca-Glass

- Difficult to understand based on glass structure
- Understandable based on solution chemistry:
  - Ca-compound, such as $Ca(OH)_2$ have low solubilities at pH 12 while boron compound are easily dissolved at pH12
  - Observation: (1) Ca release is very low compared with any other glass components. (2) Possible Ca phases on glass surfaces.
- The boron buffering effects can not be realized in a buffered and flow-through test system

Vapor Hydration Results

Durability is measured by the thickness of the alteration layers formed on corroded glasses

	Alteration Layer Thickness (μm)			Glass Composition (wt%)		
Glass	7 day	14 day	28 day	B_2O_3	CaO	Al_2O_3
L4-96	0	300	0	9	0	6
L4-99	0	0	0	9	0	9
L4-612	0	0	300	6	0	12
L4-912	0	0	0	9	0	12
L4-1212	0	0	0	12	0	12
L5-96	30	100	300	0	9	6
L5-912	40	50	>	0	9	12
L6-546	50	>	>	5	4	6
L6-549	300	>	>	5	4	9
L6-5412	0	400	>	5	4	12
L6-5412	0	200	>	5	4	12

> Completely altered

Durability order: L4 > L5 ≈ L6 i.e., Boron Only > Ca-only ≈ (Ca + B)

This order is similar to PCT results and can be understood based on glass structure and pH effect of boron.

Summary of Effects of Test Methods

- PCT and VHT results are easy to understand based on glass structure
- SPFT (at pH 12) results are understandable based on solution chemistry
- PCT results are similar to VHT results, which is relevant to long-term glass corrosions AND PCT results are more relevant to glass composition effects. THEREFORE, PCT may be a viable test for the glass optimization program that requires testing on every glass within short time and optimizes glass to have good long-term durability

Conclusions

- Testing parameters affect glass corrosion process
- These effects can be understood in terms of solution chemistry
- Description of glass reaction must account for influence on all processes
- A good understanding of experimental parameter effects can help the proper selection of a combination of tests to achieve glass optimization and to develop test methods that are more relevant to long-term glass durability

List of References in X. Feng's Talk on June 28, 1995

1. X. Feng and A. Barkatt, "Effects of Aqueous Phase Composition on the Leach Behavior of Nuclear Waste Glasses," Scientific Basis for Nuclear Waste Management X, Eds., J. K. Bates and W. B. Seefeldt, Vol.8 4, 519-531 (1987).

2. X. Feng, "Composition Effects on Chemical Durability and Viscosity of Nuclear Waste Glasses - Systematic Studies and Structural Thermodynamic Models," Ph.D. Thesis, The Catholic University of America (1988), published by UMI (1988), 300 N. Zeeb Rd., Ann Arbor, Michigan 48106, U.S.A., Order No. 8820009.

3. X. Feng, I. L. Pegg, Aa. Barkatt, and P. B. Macedo, "Effects of Surface-Area-To-Solution Volume on the Chemical Durability of Nuclear Waste Glasses," Scientific Basis for Nuclear Waste Management XIII, Eds., V. M. Oversby and P. W. Brown, Vol. 176, 383-402 (1990).

4. X. Feng, L. Fu; T. K. Choudhury, I. L. Pegg, and P. B. Macedo, "Mechanistic Effects of Deuteration on the Aqueous Corrosion of Nuclear Waste Glasses," Scientific Basis for Nuclear Waste Management XIV, Eds., T. A. Abrajano, Jr. and L. H. Johnson, Vol. 212, 49-56 (1991).

5. X. Feng, I. L. Pegg, Q. Yan, X. Mao, and P. B. Macedo, "Effect of pH on the Leaching Mechanism of Nuclear Waste Glasses," Nuclear Waste Management IV, Ceramic Transactions, Vol. 23, Eds., G. G. Wicks, D. F. Bickford, and L. R. Bunnell, 95-104 (1991).

6. X. Feng and J. K. Bates, "Initial Comparison of Leach Behavior Between Fully Radioactive and Simulated Nuclear Waste Glasses through Long-term Testing. Part 1. Solution Analysis," Proceeding of 1992 international High-Level Radioactive Waste Management Conference, Las Vegas, Nevada, April 12-16, 1992, 925-933.

7. X. Feng and I. L. Pegg, "Kinetic Ion Exchange Salt Effects on Waste Glass Leaching," Proceedings of International Symposium on Energy, Environment, and Information Management, Chicago, Illinois, September 15-18, 1992, 7.9-7.16 (1992).

8. X. Feng, J. K. Bates, C. R. Bradley, and E. C. Buck, "Does Fully Radioactive Glass Behave Differently Than Simulated Waste Glass?" Scientific Basis for Nuclear Waste Management XVI, Eds., C. G. Interrante and R. T. Pabalan, Vol. 294, 207-214 (1993).

9. J. C. Cunnane, J. K. Bates, W. L. Ebert, X. Feng, J. J. Mazer, D. J. Wronkiewicz, J. Sproull, W. L. Bourcier, and P. McGrail, "High-Level Nuclear Waste Borosilicate Glass: A Compendium of Characteristics," Scientific Basis for Nuclear Waste Management XVI, Eds., C. G. Interrante and R. T. Pabalan, Vol. 294, 577-582 (1993).

10. W. L. Bourcier, W. L. Ebert, and X. Feng, "Modeling Surface Area to Volume Effects on Borosilicate Glass Dissolution," Scientific Basis for Nuclear Waste Management

XVI, Eds., C. G. Interrante and R. T. Pabalan, Vol. 294, 225-232 (1993).

11. X. Feng and J. K. Bates, "Factors Influencing Chemical Durability of Nuclear Waste Glasses," Proceedings of the Ninth International Conference on Advanced Science and Technology, March 27, 1993, Schaumburg, Illinois, 128-135 (1993).

12. X. Feng, J. K. Bates, E. C. Buck, C. R. Bradley, and M. Gong, "Long-Term Comparison of Dissolution Behavior Between Fully Radioactive and Simulated Nuclear Waste Glasses," Nuclear Technology 104, 193-206 (1993).

13. X. Feng and I. L. Pegg, "Kinetic Ion Exchange Salt Effects on Glass/Water Reactions," Phys. Chem. Glasses, 35(2), 98-103 (1994).

14. X. Feng and I. L. Pegg, "A Glass Dissolution Model for the Effects of S/V on Leachate pH," Journal of Non-Crystalline Solids, 175, 281-293 (1994).

15. X. Feng, J. K. Bates, E. C. Buck, C. Mertz, J. C. Cunnane, and D. J. Chaiko, "Characteristics of the Colloids Generated from Interaction of Nuclear Waste Glasses with Groundwater," Roadiochimica Acta 66/67, 197-205 (1994).

16. X. Feng, "Surface Layer Effects on Glass Corrosion," Mat. Res. Soc. Symp. Proc., 333, 55-68 (1994).

PREDICTION OF NUCLEAR WASTE GLASS DISSOLUTION AS A FUNCTION OF COMPOSITION

GLASS DURABILITY

- glass durability = the resistance of glass against environmental corrosive effects
- dissolution of glass is a complex process of interaction between glass and water (or a humid environment)
- it involves
  - glass matrix hydration
  - formation of gel layer on the glass surface
  - nucleation and growth of secondary phases
- glass durability has not yet been fully resolved into well-defined easy-to-measure thermo-chemical properties, for which component and temperature coefficients could be determined

GLASS DURABILITY MEASUREMENT TECHNIQUES

- various techniques have been used by commercial and waste glass industries to measure the extent of glass dissolution under a constant temperature and fixed hydrodynamic conditions:
  - static tests
  - flow-through tests
- component and temperature coefficients can be determined from the test results
- these coefficients do not represent thermo-chemical properties of the glass-water system
- they can be used, with caution, for glass formulation and prediction of glass dissolution as a function of composition.

STATIC TESTS FOR WASTE GLASS DURABILITY

- Product Consistency Test (PCT)
- Materials Characterization Center MCC-1 test

<u>test conditions</u>

- deionized water
- 90°C
- glass surface area to solution volume ratio
  - PCT 2000 m^{-1}
  - MCC-1 10 m^{-1}
- standard duration
  - PCT 7 days
  - MCC-1 28 days

<u>test data</u>

- concentrations of elements in the solution (determined by ICP and AA)

α-TH ELEMENT NORMALIZED RELEASE

$$R_\alpha = c_\alpha / (\sigma g_\alpha)$$

c_α α-th element concentration in the solution
σ glass surface area to solution volume ratio
g_α α-th element mass fraction in the glass

<u>congruent dissolution assumption</u>

- normalized B release = glass loss per unit glass surface area

- normalized releases of other elements indicate secondary effects associated with glass dissolution

FIRST- AND SECOND-ORDER MIXTURE MODELS

$$L_\alpha = \sum_{i=1}^{n} b_{\alpha i} g_i$$

$$L_\alpha = \sum_{i=1}^{n} b_{\alpha i} g_i + \sum_{i \le j} b_{\alpha ij} g_i g_j$$

$L_\alpha = \ln R_\alpha$

$b_{\alpha i}$ i-th component first-order coefficient for α-th element

$b_{\alpha ij}$ i-th and j-th components second-order coefficient for α-th element

FIRST-ORDER MODELS

- first-order coefficients provide information about the effect of individual components on glass dissolution

- effect of replacing an k-th component by an equivalent of an i-th component while keeping the fractions of all other components constant:

$$\partial L_\alpha / \partial g_i = b_{\alpha i} - b_{\alpha k}$$

- effect of adding i-th component to the mixture (component effect)

$$\partial L_\alpha(\mathbf{g}) / \partial g_i\big|_{add} = \frac{b_{\alpha i} - L_\alpha(\mathbf{g})}{1 - g_i}$$

TYPICAL VALUES AND DATA RANGES

- 7-day PCT normalized B release
  $R_B = 0.3 g/m^2$ (0.1 to $30 g/m^2$)
  $L_B \approx -1$ (-3 to 4)

- 28-day MCC-1 normalized B release
  $R_B = 15 g/m^2$ (3 to $100 g/m^2$)
  $L_B \approx 2.5$ (1 to 5)

- there is no direct or simple correlation between the results of the MCC-1 tests and the PCT
- in other words, the component coefficients for these two tests (their vectors in the composition space) are not collinear

RELEASES OF OTHER ELEMENTS

<u>alkalis</u>

- initial ion exchange
- participation in secondary phases
- normalized releases of Na, Li, and B have similar values

<u>silica</u>

- solubility of silica in water is limited:

$$R_{Si} / R_B \leq 1$$

- there is no direct or simple correlation between the releases of different elements from a glass treated in a given test if these elements participate in gel layer formation and secondary reactions

PCT NORMALIZED B RELEASE (HLW GLASSES FOR LOW-TEMPERATURE MELTER)

first-order coefficients (based on mass fractions)

comp.	SiO_2	B_2O_3	Na_2O	Li_2O	CaO	MgO	Fe_2O_3	Al_2O_3	ZrO_2	Other	R^2
PCT	-4.3	12.0	17.6	22.6	-8.7	10.9	-3.2	-25.4	-10.6	0.2	0.81

$R_B \uparrow$ if $L_{Bi} > 4$: $Li_2O > Na_2O > B_2O_3 > MgO$

$R_B \downarrow$ if $L_{Bi} < -3$: $Al_2O_3 < ZrO_2 < CaO < SiO_2 < Fe_2O_3$

$R_B \updownarrow$ if $-3 < L_{Bi} < 4$: Others

<u>MgO</u> enhances dissolution

- by precipitation of magnesium silicate secondary phases
- not recommended for frits

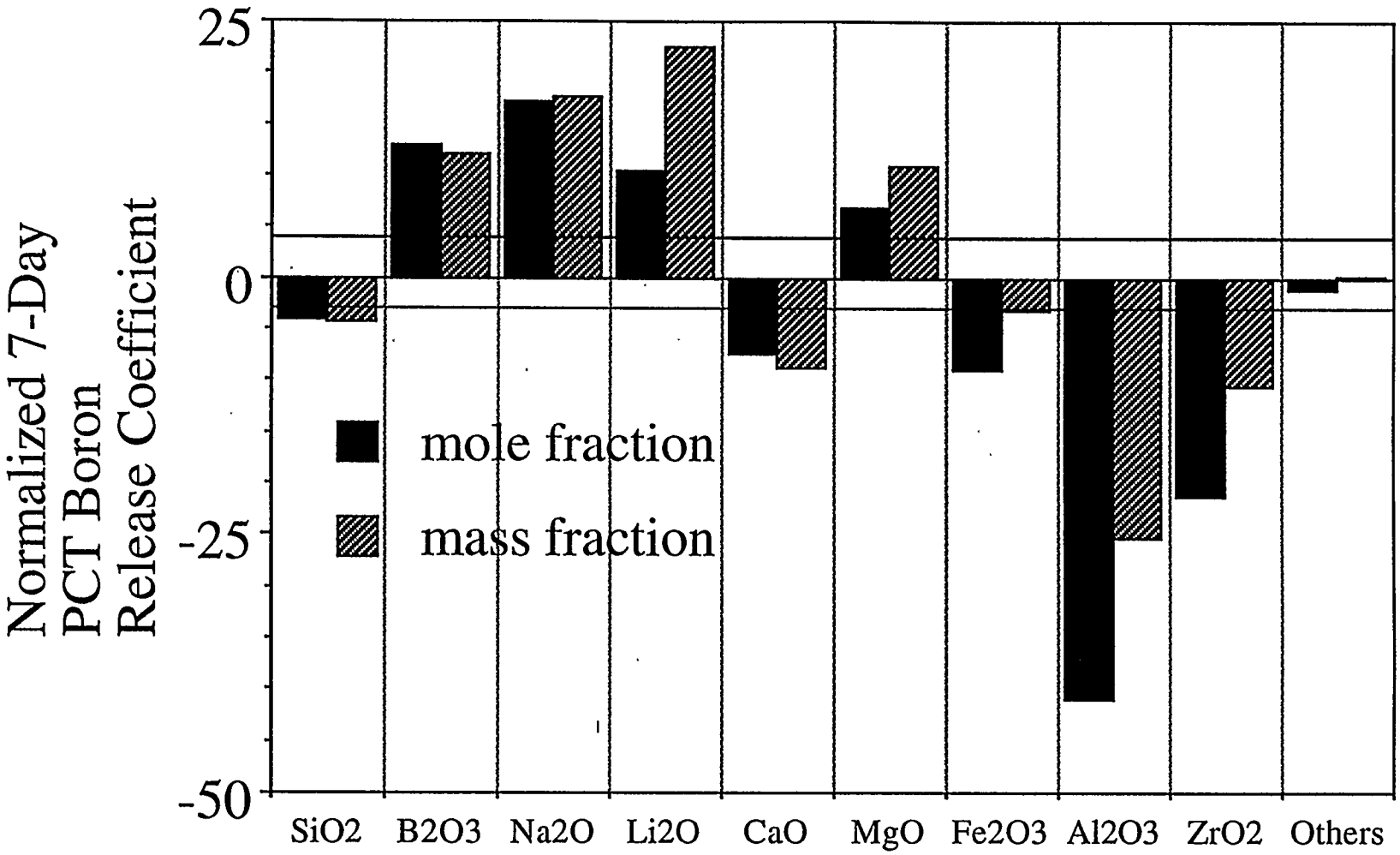
Normalized 7-Day
PCT Boron
Release Coefficient
25
0
-25
-50
mole fraction
mass fraction
SiO2
B2O3
Na2O
Li2O
CaO
MgO
Fe2O3
Al2O3
ZrO2
Others

MCC-1 NORMALIZED B RELEASE (HLW GLASSES FOR LOW-TEMPERATURE MELTER)

first-order coefficients (based on mass fractions)

comp.	SiO_2	B_2O_3	Na_2O	Li_2O	CaO	MgO	Fe_2O_3	Al_2O_3	ZrO_2	Other	R^2
MCC-1	-0.1	9.7	9.6	11.8	3.8	5.1	5.7	-6.3	-0.6	3.7	0.65

$R_B \uparrow$ if $L_{Bi} > 5$: $Li_2O > B_2O_3 > Na_2O > Fe_2O_3 > MgO$

$R_B \downarrow$ if $L_{Bi} < 1$: $Al_2O_3 < ZrO_2 < SiO_2$

$R_B \updownarrow$ if $1 < L_{Bi} < 5$: Others > CaO

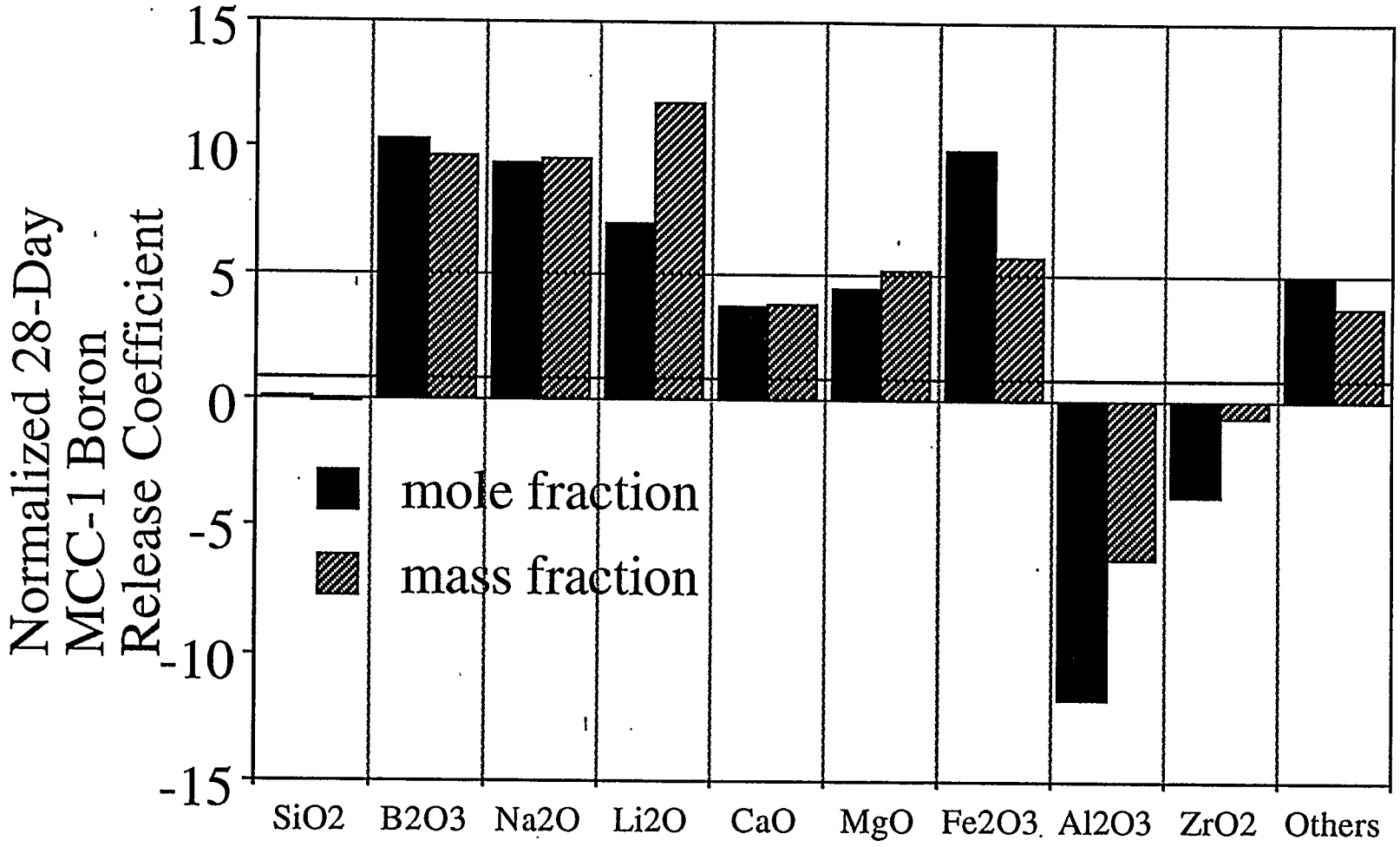
Normalized 28-Day
MCC-1 Boron
Release Coefficient
15
10
5
0
-5
-10
-15
mole fraction
mass fraction
SiO2
B2O3
Na2O
Li2O
CaO
MgO
Fe2O3
Al2O3
ZrO2
Others

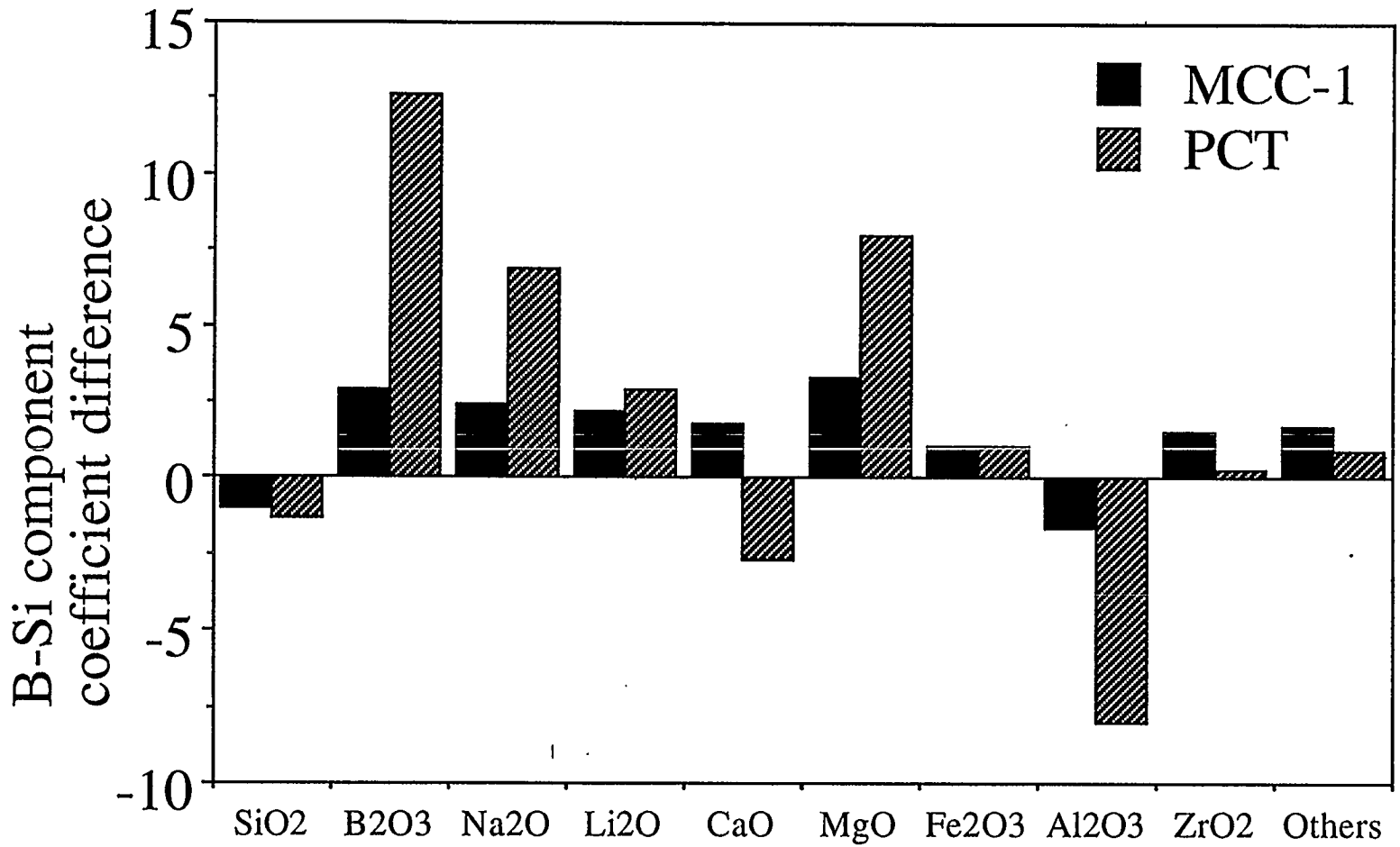
B-Si component
coefficient difference
15
10
5
0
-5
-10
MCC-1
PCT
SiO2
B2O3
Na2O
Li2O
CaO
MgO
Fe2O3
Al2O3
ZrO2
Others

pH VALUES (HLW GLASSES FOR LOW-TEMPERATURE MELTER)

comp.	SiO_2	B_2O_3	Na_2O	Li_2O	CaO	MgO	Fe_2O_3	Al_2O_3	ZrO_2	Other	R^2
PCT	8.19	3.33	23.60	31.20	17.20	15.30	8.59	5.36	7.61	9.27	0.91
MCC-1	7.34	9.12	17.80	24.50	13.30	13.20	10.18	4.05	7.59	8.68	0.75

pH ↓:

PCT $B_2O_3 < Al_2O_3 < ZrO_2 < SiO_2$

MCC-1 $Al_2O_3 < SiO_2 \approx ZrO_2$

pH ↑:

PCT $Li_2O > Na_2O > CaO > MgO$

MCC-1 $Li_2O > Na_2O > CaO \approx MgO$

SECOND-ORDER TERMS (HLW GLASSES FOR LOW-TEMPERATURE MELTER)

PCT

$Al_2O_3 \times Al_2O_3, B_2O_3 \times B_2O_3, SiO_2 \times MgO,$
$Na_2O \times CaO, B_2O_3 \times CaO, MgO \times ZrO_2$ $R^2 = 0.90$

MCC-1

$Al_2O_3 \times Al_2O_3, Al_2O_3 \times B_2O_3, CaO \times SiO_2$ $R^2 = 0.88$

expected terms:

squared terms: Al_2O_3, B_2O_3

crossproduct terms:

- $Al_2O_3 \times Na_2O$ (electric charge balance)
- $Na_2O \times Li_2O$ (mixed alkali effect)
- $SiO_2 \times MgO$ (reaction in the solution)

HYDRATION ENERGY APPROACH

- estimates the hydration energy of glass as a weighted sum of hydration energies of silicates and oxides
- linearly correlates these estimates with logarithmic normalized elemental releases obtained by the MCC-1 test or the PCT
- is identical in form with the first-order model except that the component coefficients are not derived from data
- works whenever a binary variation dominates and the R_α versus ΔG plot is close to linear
- R_α versus ΔG correlation is poor for glasses tested in this work

Effect of Al_2O_3

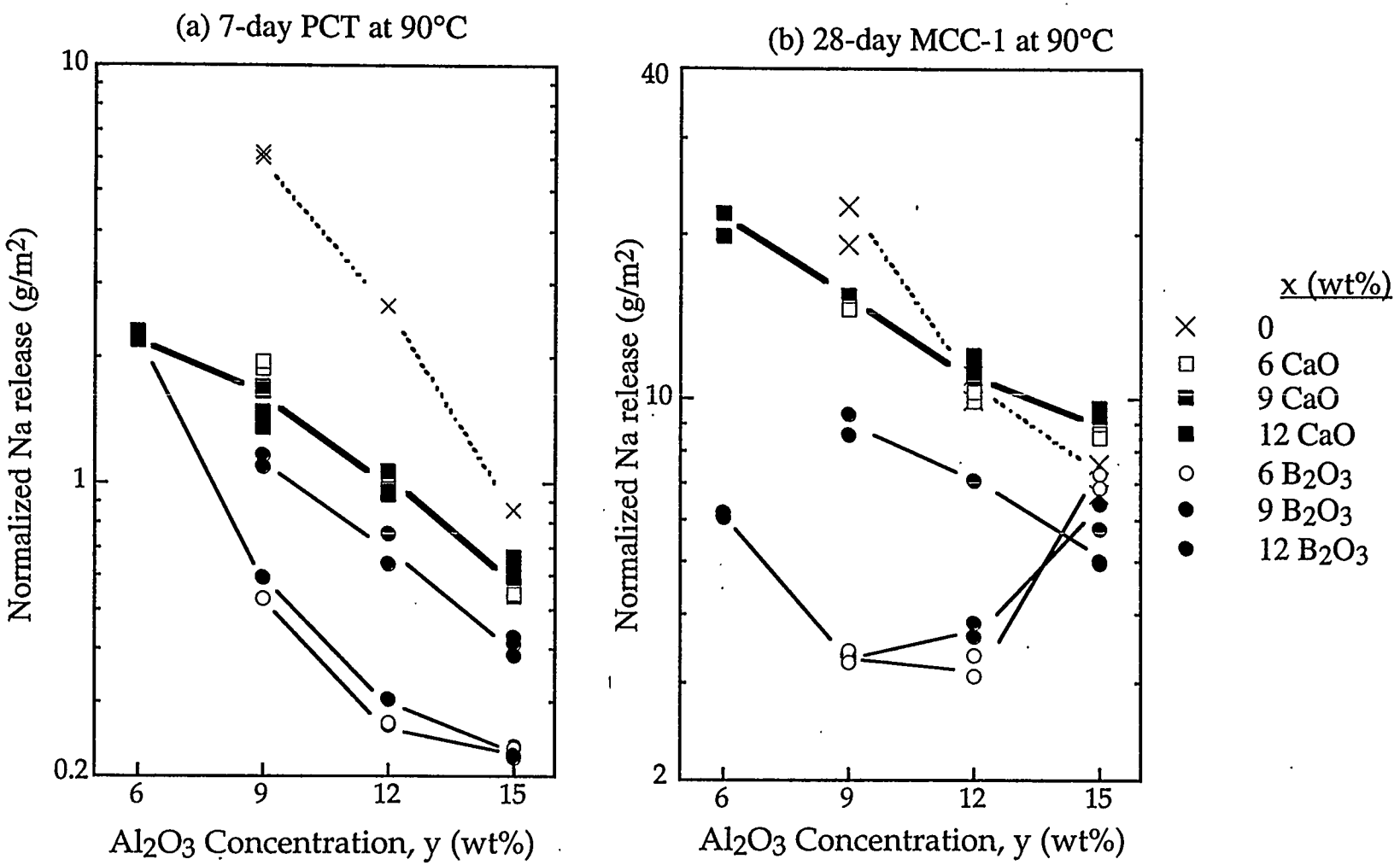

7-day PCT at 90°C, Effect of B_2O_3

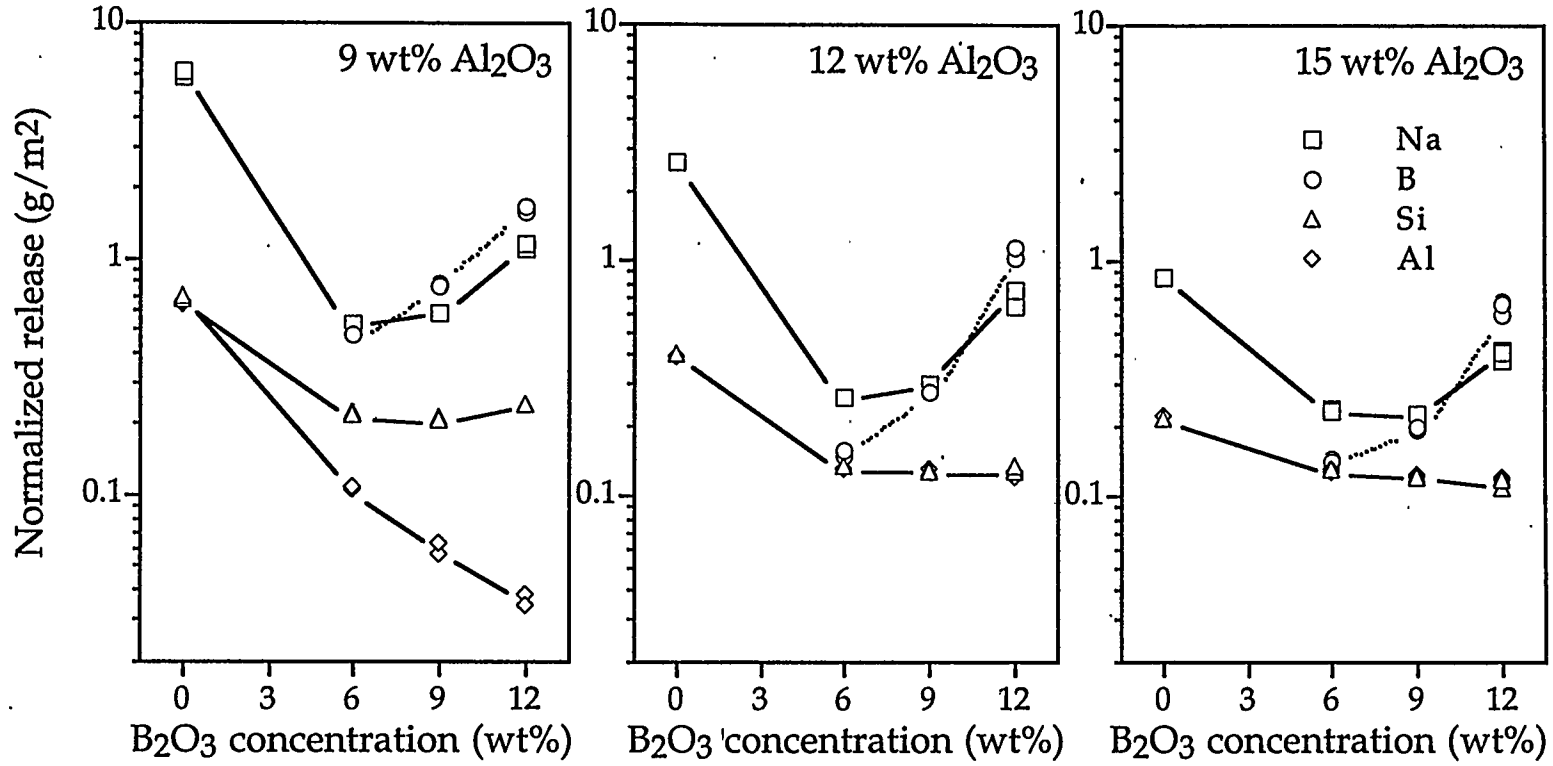

7-day PCT at 90°C, Effect of CaO

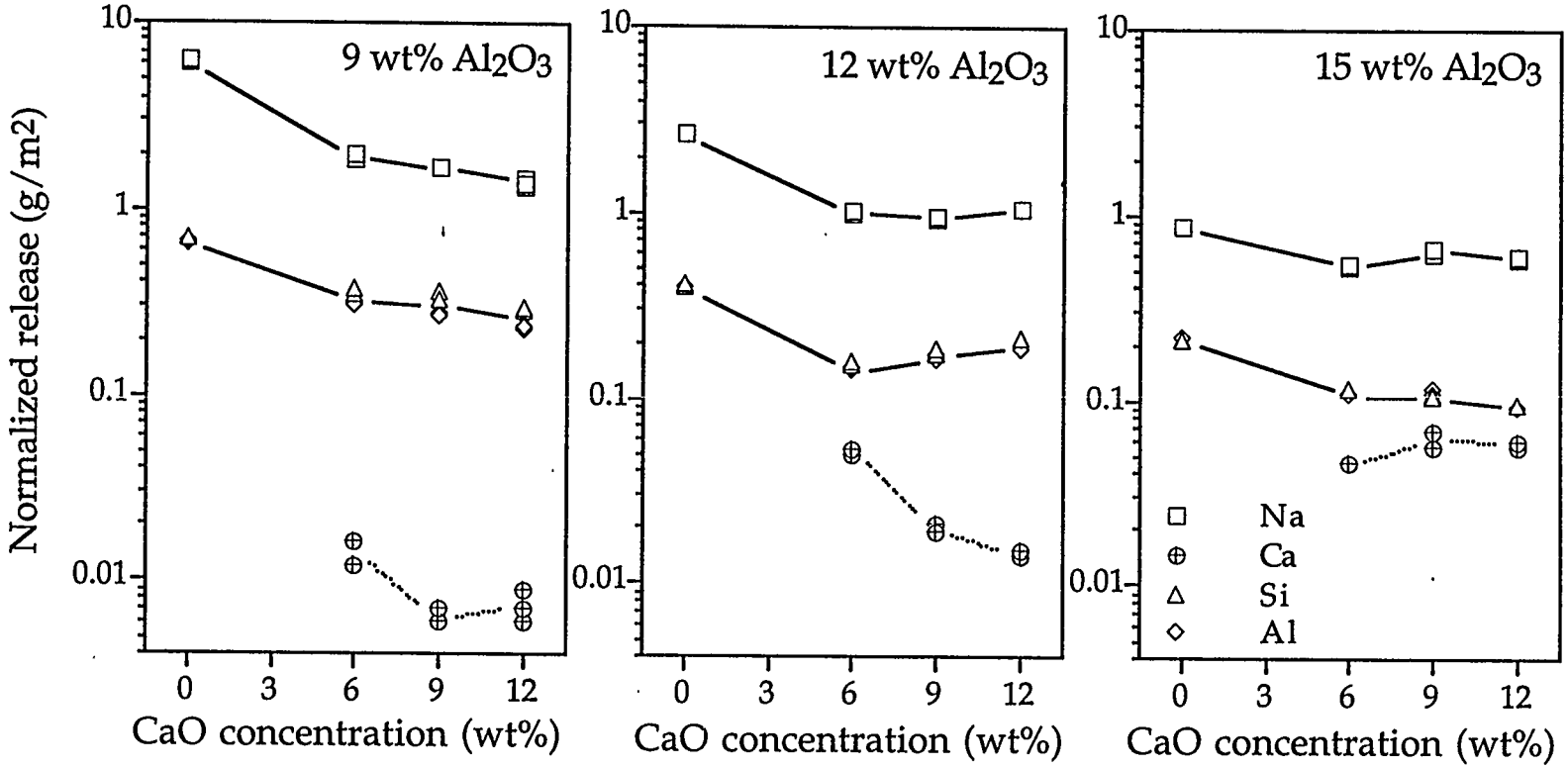

28-day MCC-1 at 90°C, Effect of B_2O_3

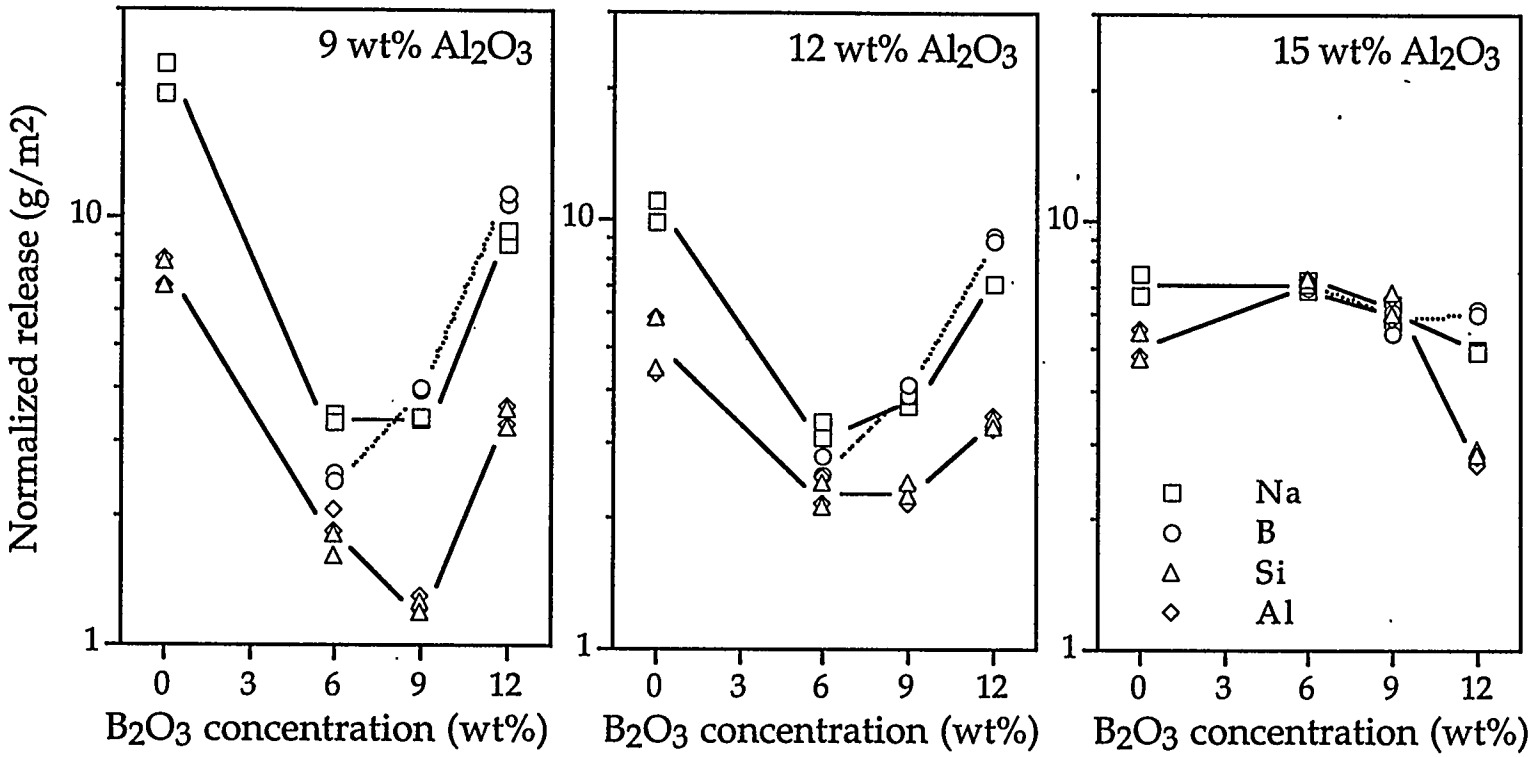

28-day MCC-1 at 90°C, Effect of CaO

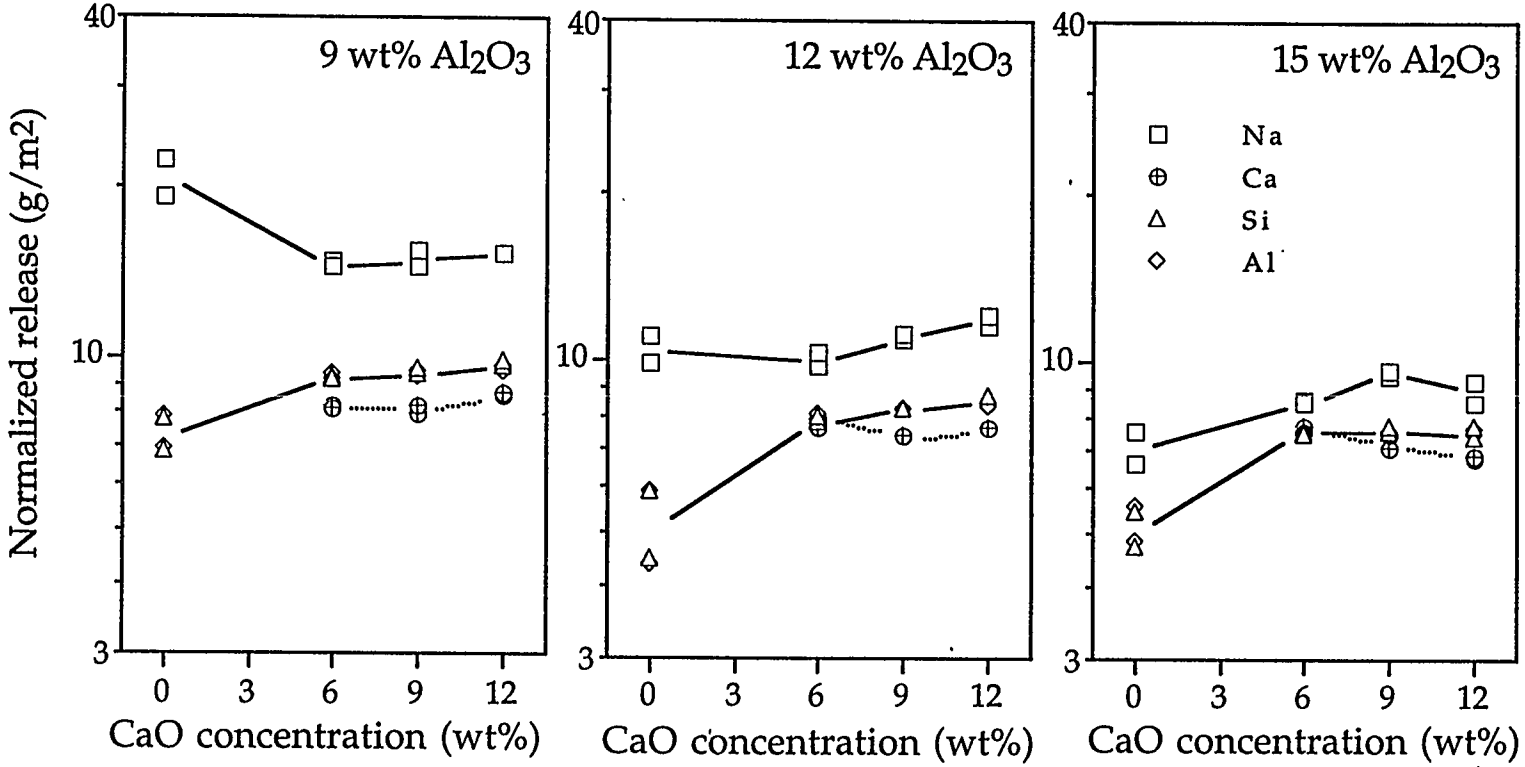

Effect of Crystallization on the Chemical Durability of Simulated Nuclear Waste Glasses

Chemical Durability

- Chemical durability is a key property in meeting radioactive waste glass acceptability
- Extent of reaction in an aqueous medium is used as a relative measure of durability
- Aqueous dissolution depends on factors both internal and external to the glass

External Factors

- Nature of aqueous medium
- Static versus dynamic dissolution conditions
- Surface area to volume ratio
- Repository conditions
  - Radiation environment
  - Soil chemistry
  - Ambient soil temperature
  - Pressure

Internal Glass Factors

- Primary internal factors
  - Composition
  - Thermal history
- Microstructural characteristics
  - Crystallization
  - Amorphous phase separation
  - Structural integrity

Thermal History

- Influences the kinetics of crystallization
- Rapid cooling (quenching) kinetically limits crystallization
- Slower cooling favors crystallization, if thermodynamically favorable
- HLW glasses will have a complex thermal history - canistered
- Quenched vs canistered centerline cooled (CCC)
- CCC represents the slowest cooling rate of canistered glass
- Highest potential for crystallization

Crystallization

- Effect on durability depends on:
  - Type of crystallization
  - Extent (or fraction) of crystallization
- Durability can increase or decrease
- Associated effects:
  - Change of residual glass composition
  - Internal stresses or microcracking formed by thermal expansion and density mismatches
  - Preferential attack at the glass-crystal interface
- Dependent upon the glass composition and thermal history

Objective

- **Determine the effect of crystallization on the chemical durability of simulated HLW nuclear waste glasses**
  - **Identify the type and extent of crystallization for 121 CVS (Compositional Variation Study) glasses**
  - **Bound "extreme" thermal history profiles (quenched versus CCC)**
  - **Correlate predicted durability (PCT B release) with calculated residual phase composition**

Experimental

- 121 CVS simulated HLW glasses
- Thermal history
  - Quenched or as-melted
  - CCC simulated time-temperature schedule
- SEM/EDS, XRD, optical microscopy
  - Semi-quantitative volume fractions of various phases
  - Qualitative identification of crystalline phases
- Chemical durability
  - 7-day PCT (90°C)
  - Both quenched and CCC glasses
  - Normalized boron release

Composition Region of CVS Glasses

Oxide	Range (wt%)
SiO_2	42 - 57
B_2O_3	5 - 20
Na_2O	5 - 20
Li_2O	1 - 7
CaO	0 - 10
MgO	0 - 8
Fe_2O_3	0.5 - 15
Al_2O_3	0 - 17
ZrO_2	0 - 13
"Others"	1 - 10

- "Others" component was composed of BaO, CdO, CeO_2, Cr_2O_3, Cs_2O, CuO, F, La_2O_3, MnO_2, MoO_3, Nd_2O_3, NiO, P_2O_5, PdO, Pr_6O_{11}, Rb_2O, Rh_2O_3, RuO_2, SO_3, Sm_2O_3, SrO, and Y_2O_3.

Crystallization of Quenched Glasses

- Quenched or as-melted glasses virtually crystal-free
- 31 of the 121 CVS glasses checked by SEM/EDS and optical microscopy
- <1 vol% undissolved ZrO_2 in two glasses
- Al-containing crystals in one glass
- CCC treatment of these three glasses produced ≥14 vol% crystallization

Effect of CCC on Normalized Boron Release

- No or negligible effect
- Moderate increase
- Strong increase
- Moderate decrease

Crystallinity of CCC Glasses: Classifications

- Glasses with no crystallization
- Glasses with <7 volume %
- Glasses with ≥7 volume %

**Volume % based on XRD data of primary crystalline phase*

Results

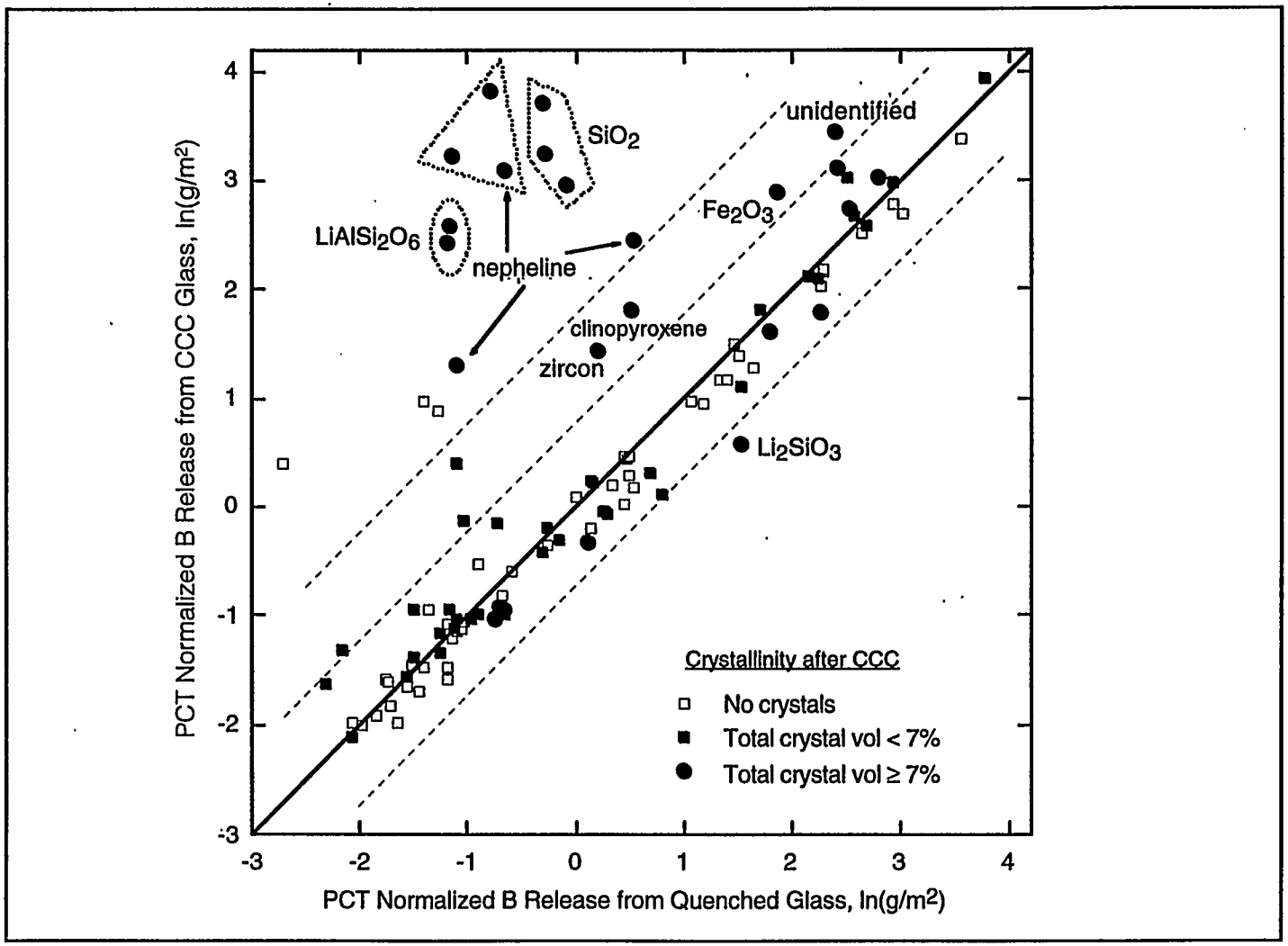
PCT Normalized B Release from CCC Glass, ln(g/m²)
PCT Normalized B Release from Quenched Glass, ln(g/m²)
4
3
2
1
0
-1
-2
-3
-3
-2
-1
0
1
2
3
4
SiO2
unidentified
Fe2O3
LiAlSi2O6
nepheline
clinopyroxene
zircon
Li2SiO3
Crystallinity after CCC
No crystals
Total crystal vol < 7%
Total crystal vol ≥ 7%

Normalized Boron Release Versus Crystallinity on CCC Glasses

	No Crystals	Low Crystal (<7 vol%)	High Crystal (≥7 vol%)	Total
No Change	49	31	9	89
Moderate Increase	0	3	4	7
Strong Increase	3	0	10	13
Moderate Decrease	0	0	1	1
Total	52	34	24	110*

**11 replicates*

CCC Glasses with No Crystallinity

- **Effect on Normalized Boron Release**

No Change	49
Moderate Increase	0
Strong Increase	3
Moderate Decrease	0
Total	*52*

- **Majority show no change in durability upon CCC**
- **Three glasses have a "strong increase" in B release after CCC (decrease in durability)**
- **Not an effect of crystallization**
- **Amorphous phase separation**
  - **Compositionally not prone**
  - **SEM/TEM failed to detect**

CCC Glasses with Low Crystallization (<7 vol%)

- Effect on Normalized Boron Release

No Change	31
Moderate Increase	3
Strong Increase	0
Moderate Decrease	0
Total	*34*

- Majority show no change in durability
- Three glasses show a moderate increase in boron release (decrease in durability)
  - Spinel or nepheline ($NaAlSiO_4$)
  - Although classified as "moderate increase", both quenched and CCC well below the EA glass limit (r_B = 8.35 g/m^2/7-day)

CCC Glasses with High Crystallinity (≥7 vol %)

- **Effect on Normalized Boron Release**

No Change	9
Moderate Increase	4
Strong Increase	10
Moderate Decrease	1
Total	*24*

- **10 glasses show a "strong increase" in boron release (decrease durability)**
  - **Nepheline ($NaAlSiO_4$), $LiAlSi_2O_6$, or crystalline SiO_2 as primary phase**
  - **Effects of residual glass composition**

CCC Glasses with High Crystallinity (≥7 vol %) (cont.)

- Nine glasses show no change in durability after CCC
  - Nepheline ($NaAlSiO_4$), $LiAlSi_2O_6$, crystalline SiO_2 not present as primary phase
- Four glasses show a "moderate increase" in boron release after CCC
  - Zircon, hematite, clinopyroxene as primary phase
  - Does not effect durability as dramatically as other phases in composition region studied
- One glass shows a "moderate decrease" in boron release (increase durability) after CCC
  - High content of Li_2SiO_3 (10 vol %) and clinopyroxene (8 vol %)
  - Removal of Li from the glass matrix has a more dominant effect on increasing durability than the effect of Si removal decreasing durability

Residual Glass Composition

- Crystalline phase formation extracts specific elements from the glass matrix
- Chemical durability of the residual glass may be affected
- Component mass balance equation for crystallization:

$$g_i = \sum_{j=1}^{n} c_{ij} f_j + r_i \left(1 - \sum_{j=1}^{n} f_j\right)$$

g_i : mass fraction of the i-th component in glass before crystallization

r_i : mass fraction of the i-th component after crystallization

c_{ij} : mass fraction of the i-th component in the j-th crystal

f_j : mass fraction of the j-th crystal in the partially crystallized glass

n : number of different crystal types

Component Mass Balance Equation

- Assume only one type of crystal forms (n=1)

$$g_i = c_i f + r_i (1-f)$$

- Rearranging, we obtain the residual glass composition as a function of crystal mass fraction (f)

$$r_i = \frac{g_i - c_i f}{1 - f}$$

- i-th component concentration in the residual glass (after crystallization) increases if its fraction in the crystalline phase is smaller than in the original glass ($g_i > c_i$)

Composition of CVS1-1 Glass

Oxide	(wt%)
SiO_2	48.0
B_2O_3	11.4
Na_2O	10.0
Li_2O	3.8
CaO	2.8
MgO	3.6
Fe_2O_3	5.7
Al_2O_3	6.4
ZrO_2	4.3
"Others"	4.1

- "Others" component was composed of BaO, CdO, CeO_2, Cr_2O_3, Cs_2O, CuO, F, La_2O_3, MnO_2, MoO_3, Nd_2O_3, NiO, P_2O_5, PdO, Pr_6O_{11}, Rb_2O, Rh_2O_3, RuO_2, SO_3, Sm_2O_3, SrO, and Y_2O_3.

Predicted Normalized Boron Release from CVS1-1 Glass as a Function of Primary Crystalline Phases

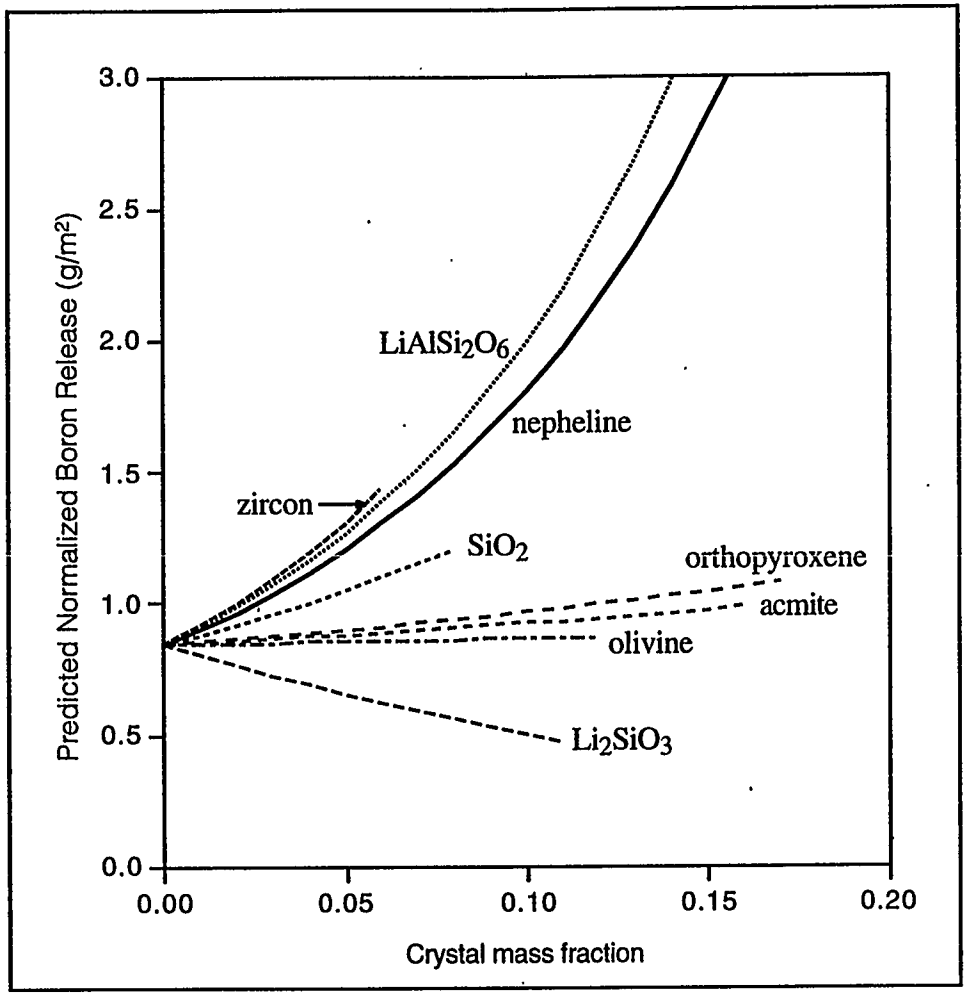

Predicted normalized release calculated using the CVS first-order model

Predicted Effects of Residual Glass Composition

- No or negligible effect with crystallization of orthopyroxene, acmite, or olivine
- Formation of Li_2SiO_3 causes a decrease in predicted boron release
  - Agrees with experimental observations
  - Effect not observed in a glass with higher crystallization of Li_2SiO_3 and Li_2MgSiO_4
- Crystallization of nepheline ($NaAlSiO_4$), $LiAlSi_2O_6$, crystalline SiO_2 and/or zircon as primary phase has a pronounced negative effect on the predicted durability
  - Nepheline ($NaAlSiO_4$), $LiAlSi_2O_6$, crystalline SiO_2 experimentally agrees
  - The predicted strong effect of zircon was not observed experimentally

Results

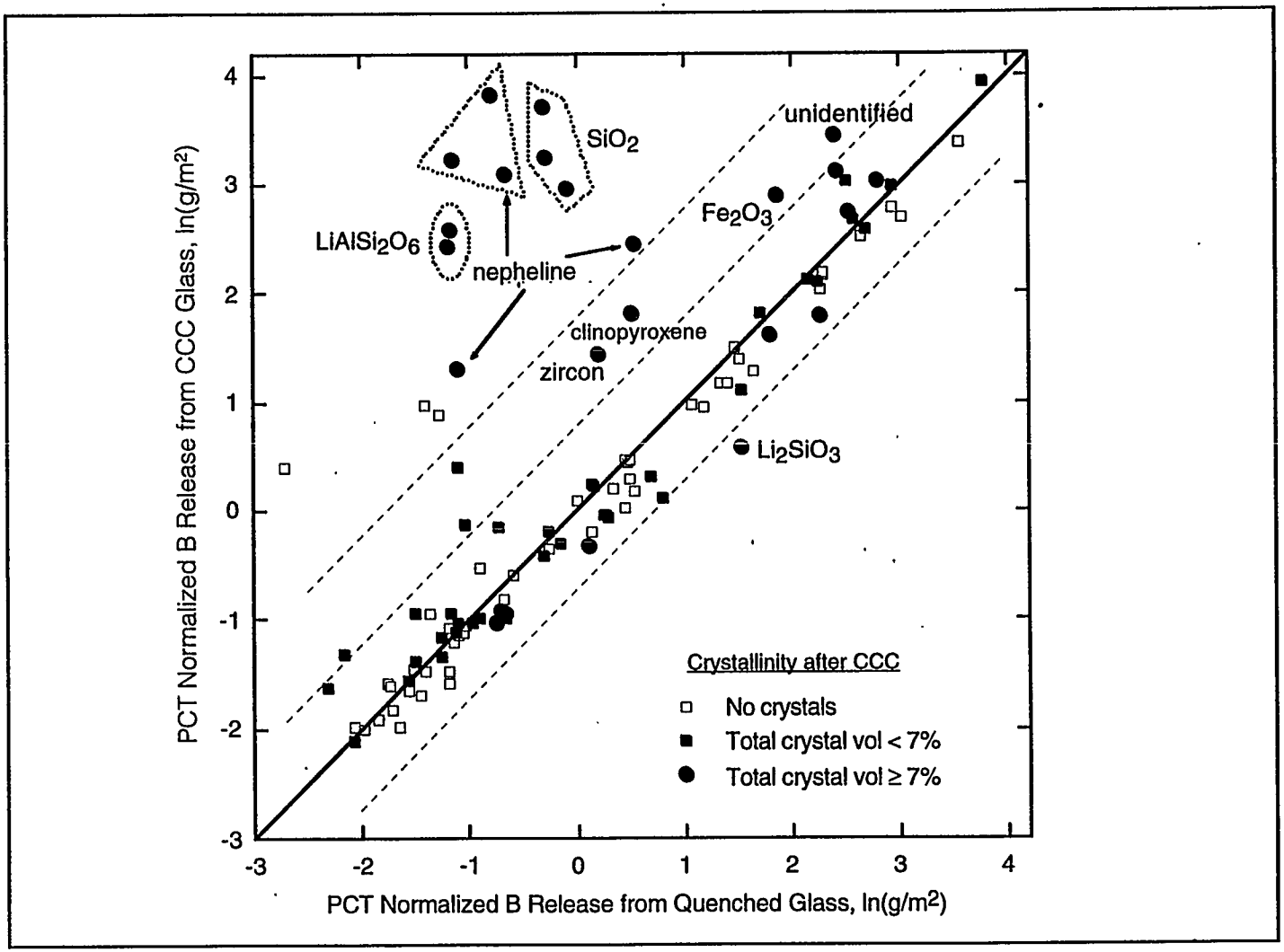
PCT Normalized B Release from CCC Glass, ln(g/m²)
PCT Normalized B Release from Quenched Glass, ln(g/m²)
4
3
2
1
0
-1
-2
-3
-3
-2
-1
0
1
2
3
4
SiO2
unidentified
Fe2O3
LiAlSi2O6
nepheline
clinopyroxene
zircon
Li2SiO3
Crystallinity after CCC
No crystals
Total crystal vol < 7%
Total crystal vol ≥ 7%

Summary

- Kinetics of crystallization highly dependent upon thermal history
- Quenched glasses virtually crystal-free, CCC treatment had a higher probability of crystallization
- Effect on durability depends upon the type and extent of crystallization
- Glasses containing Al-bearing crystals ($NaAlSiO_4$ and $LiAlSi_2O_6$) and crystalline SiO_2 generally produce a high increase in boron release (negative effect on durability)
- Predicted crystallization effects on durability based on residual glass composition calculations generally agree with experimental observations
- Discrepancies between observed and predicted effects suggest that factors other than the change in residual glass composition play a role in defining the overall durability

Amorphous Phase Separation: Theory, Prediction, and Application

Inhomogeneous Microstructure Development:

- Crystallization or devitrification
  - crystalline phases nucleate and grow

- Amorphous phase separation
  - the separation of a homogeneous melt into two or more liquid phases

Free Energy of Mixing

$$\Delta G_M = \Delta H_M - T\Delta S_M$$

where:
ΔG_M = free energy of mixing
ΔH_M = enthalpy of mixing (heat or bond energy)
ΔS_M = entropy of mixing (degree of randomness)

- System can reduce its free energy by separating into two or more phases
- For overall system to reduce free energy ΔG_M:

  1. ΔS_M must increase, or
  2. ΔH_M must decrease.

Entropy of Mixing (ΔS_M) in a Two Component (A and B) System:

- Defined as the entropy of mixing (or degree of randomness)

$$\Delta S_M = -R[(1-c)\ln(1-c) + c\ln c]$$

where:

R = gas constant
c = mole fraction of component A

- Since $c < 1$, the expression $[(1-c)\ln(1-c) + c\ln c]$ is always a negative number

- The entropy of the system will increase upon mixing

Enthalpy of Mixing (ΔH_M):

Ideal solutions:

- $\Delta H_M = 0$
- $\Delta G_M = \Delta H_M - T\Delta S_M = -T\Delta S_M$
- ΔS_M increases upon mixing ($c < 1$)
- ΔG_M is negative at all temperatures and the resulting material will be a mixed solution

Enthalpy of Mixing (ΔH_M): (continued)

Regular solutions:

- $\Delta S_M = -R[(1-c)\ln(1-c) + c \ln c]$
- $\Delta H_M \neq 0$, and is given by:

$$\Delta H_M = \alpha c(1-c)$$

α is defined as the excess interaction energy

$$= NZ[E_{AB} - (E_{AA} - E_{BB})/2]$$

where: N is Avogadro's number
Z is the coordination number
E's are the energies of the various bonds between atoms (A and B)

Negative ΔH_M (α is negative):

- The system gives off heat upon mixing (exothermic)
- $\Delta G_M = \Delta H_M - T\Delta S_M$ is negative at all temperatures
- Mixing of the system is "encouraged" - (single-phase) thermodynamically favorable

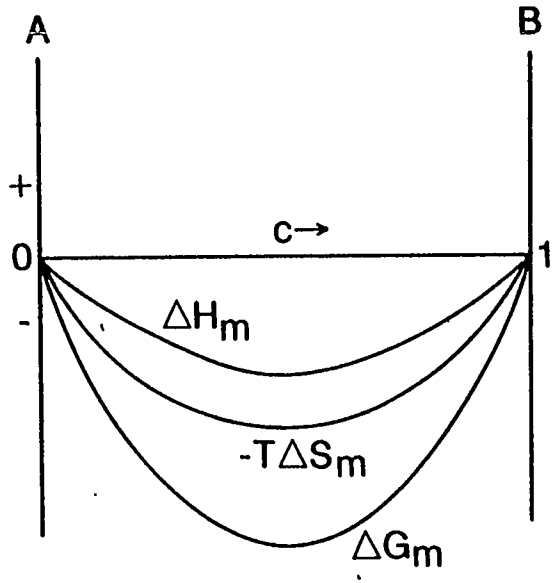

Positive ΔH_M (α is positive):

- The system takes in heat upon mixing (endothermic)

- $\Delta G_M = \Delta H_M - T\Delta S_M$:

  - the shape of the ΔG_M variation with composition (c) depends upon the magnitude of the ΔH_M term compared to the $T\Delta S_M$ term

  - highly dependent upon the temperature

Positive ΔH_M (α is positive): (continued)

- At high temperatures, the term $-T\Delta S_M$ is greater than the ΔH_M term so ΔG_M is negative everywhere
  - the system is single-phased at sufficiently high temperatures

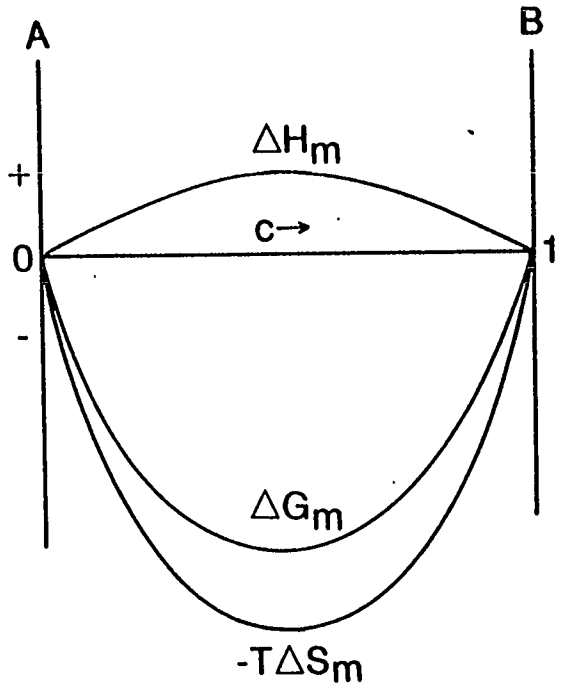

Positive ΔH_M (α is positive): (continued)

- As the temperature decreases ($T < T_c$), the ΔG_M curve begins to flatten out - "saddle" develops
- $-T\Delta S$ term becomes less dominant

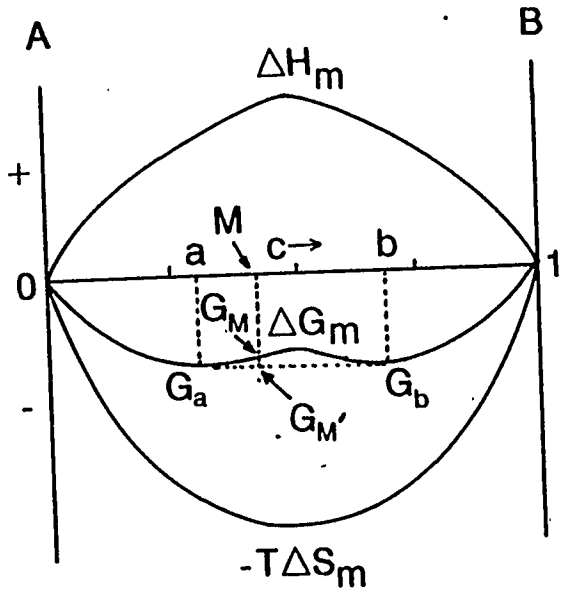

- Although the mixed system has a lower ΔG_M than the unmixed end components (A and B), between points "a" and "b", ΔG_M of the fully mixed system is higher that those of "a" and "b"

- The free energy G_M of composition M (lying between "a" and "b) can be lowered to G_M by separating into compositions a and b.

- Separation into two phases will occur when the total enthalpy increase ($+\Delta H_M$) is greater that the increase in free energy (ΔG_M) due to the entropy (ΔS_M) consideration
  - highly dependent upon temperature

FREE ENERGY VERSUS COMPOSITION

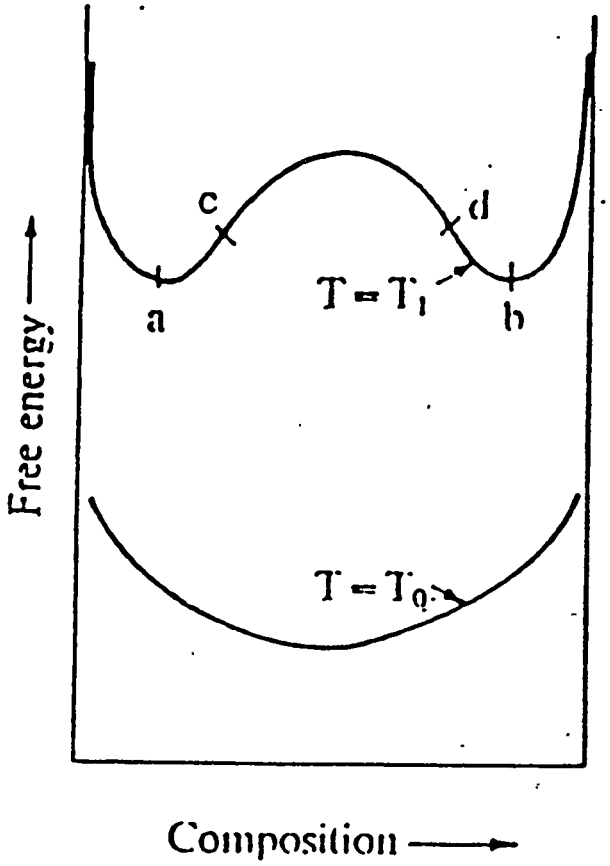

- Above Tc, single phase
  - ΔG_M has a positive curvature
- As temperature decreases, "saddle" develops between "a" and "b"
- Define position at which $\delta G/\delta c = 0$, T = T1
- Immiscibility dome or phase boundary

PHASE DIAGRAM

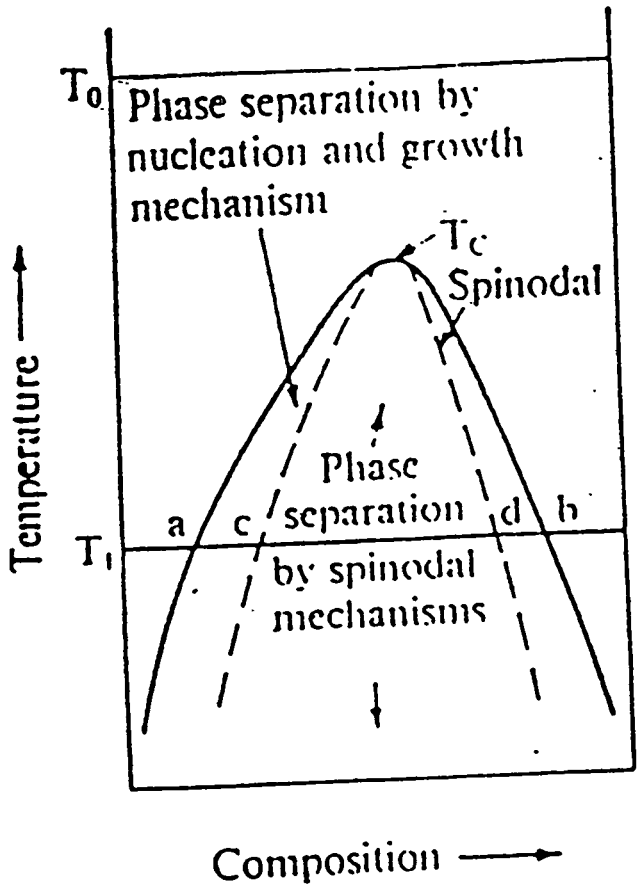

- $\delta^2G/\delta c^2 = 0$, $T = T_1$ defines points "c" and "d" - inflection points
- Inflection points define composition field within the immiscibility dome in which the mechanism of separation differs - morphology changes due to mechanism change
- Nucleation growth versus spinodal decomposition

THEORY SUMMARY:

- Relative magnitudes of the $T\Delta S_M$ and ΔH_M terms determine shape of the ΔG_M curve

- Highly dependent upon temperature
  - high temperature $-T\Delta S_M$ dominants - (single-phase)
  - lower temperature ΔH_M plays "major role"

- Phase separation can occur if thermodynamically favorable
  - composition dependent

- No assumptions regarding the kinetics of the separation process or the mechanisms have been made

Nucleation/Growth Mechanism

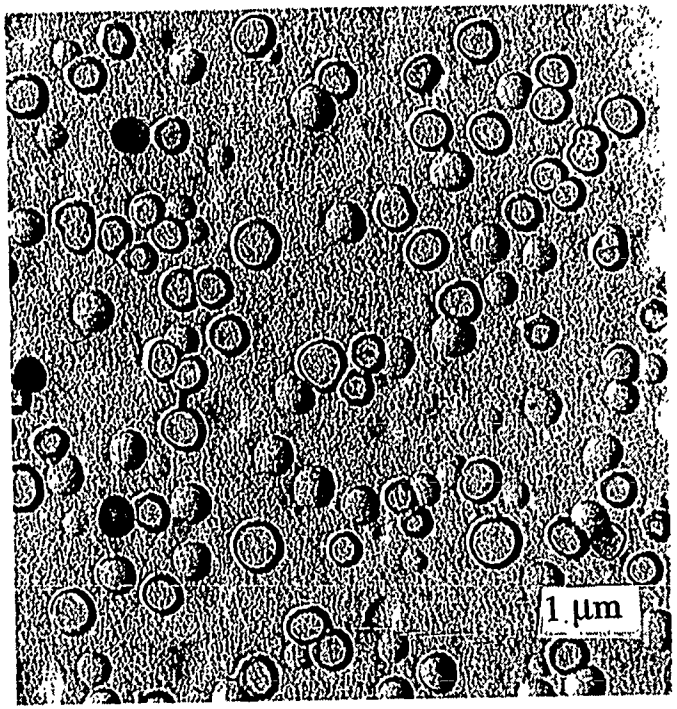

(a)

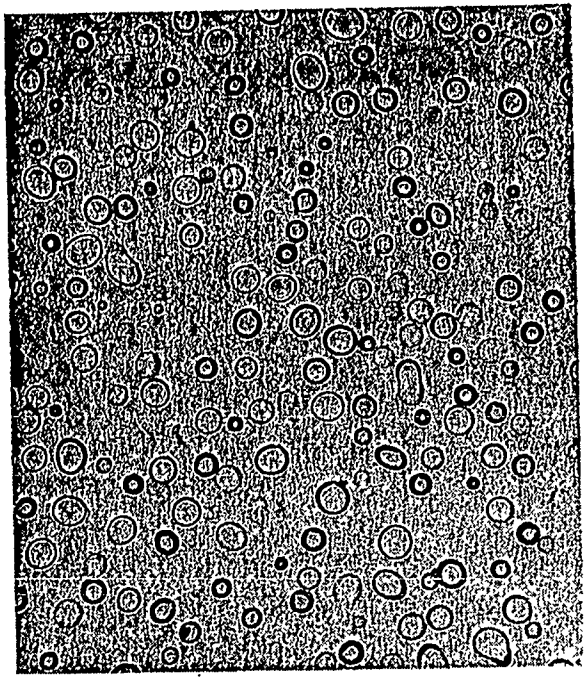

(b)

- Dispersed phase is isolated in continuous matrix

(a) W. Vogel, Chemistry of Glass, Figure 7.21, p. 11, American Ceramic Society, Columbus, Ohio,1985.

(b) H. Rawson, Properties and Applications of Glass, Figure 10, Elsevier Science Publishers, Amsterdam, Netherlands, 1980.

Spinodal Decomposition Mechanism:

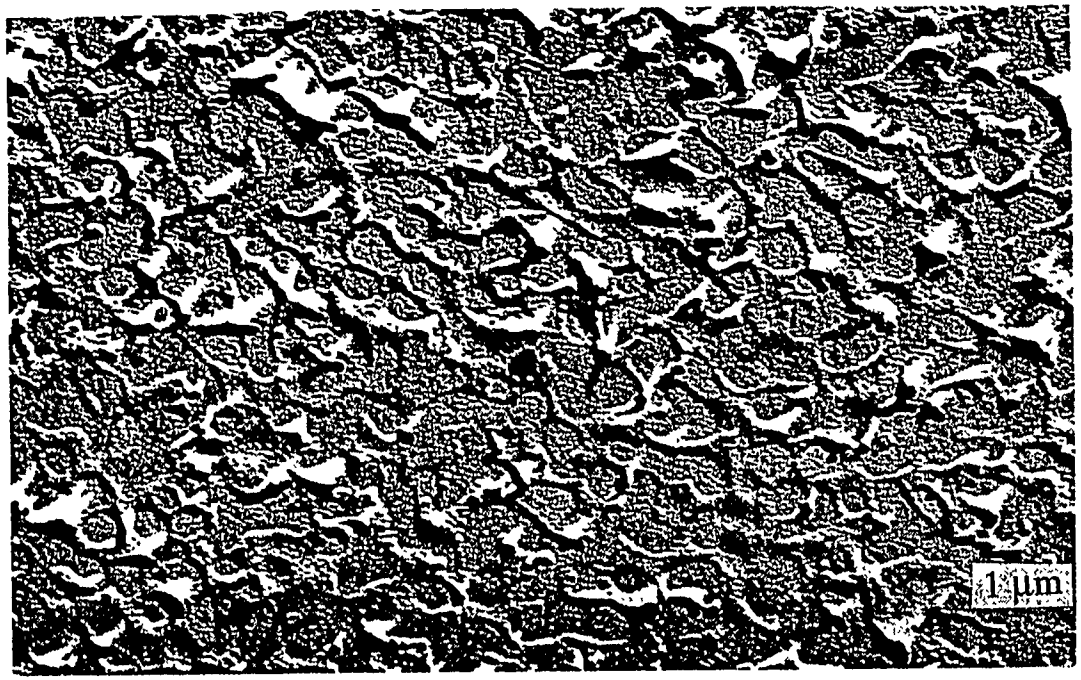

(a)

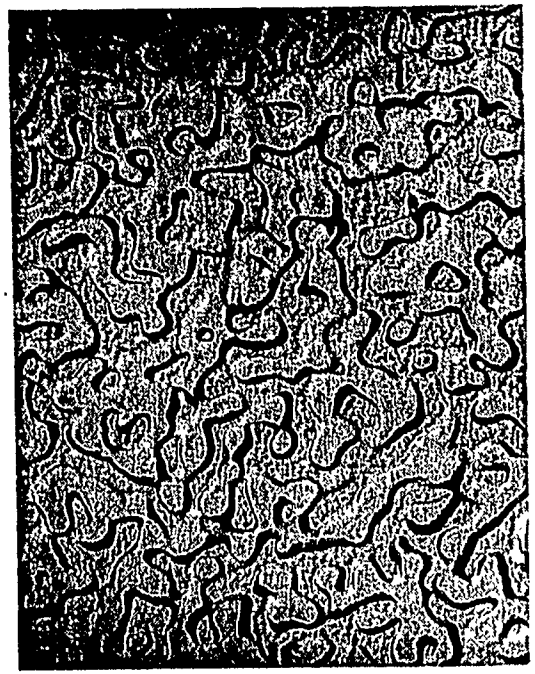

(b)

- Both phases highly continuous

(a) W. Vogel, Chemistry of Glass, Figure 7.21, p. 11, American Ceramic Society, Columbus, Ohio,1985.

(b) H. Rawson, Properties and Applications of Glass, Figure 10, Elsevier Science Publishers, Amsterdam, Netherlands, 1980.

Distinction Between Phase Separation Mechanisms

Nucleation/Growth

Interface between phases is always same degree of sharpness during growth

Tendency for random distributions of particle sizes and positions in matrix

Tendency for separation of second-phase spherical particles with low connectivity

Spinodal Decomposition

Interface between phases initially is very diffuse, eventually sharpens

Regularity of second-phase distribution in size and positions characterized by a geometrical spacing

Tendency for separation of second-phase, non-spherical particles with high connectivity

* J.W. Cahn and R.J. Charles, *Phys. Chem. Glasses*, 6 (5), 181-191, (1965)

* Fundamental of Inorganic Chemistry, A.K. Varshneya, Academic Press, Inc., 1994

Microstructural Types for Borosilicate Systems:

Type A: both phase highly interconnected (spinodal decomposition)

Type B: Si-rich dispersed phase, B-rich continuous matrix (nucleation/growth)

Type C: B-rich dispersed phase, Si-rich continuous matrix (nucleation/growth)

* Tomozawa, M., "Phase Separation in Glass," In Treatise on Materials Science and Technology, Vol. 17, Edited by M. Tomozawa and R.H. Doremus, Academic Press, New York, pp. 71-113, (1972).

Predicting Liquid Immiscibility in Multicomponent Nuclear Waste Glasses

Predicting Amorphous Phase Separation

- Commonly used experimental techniques to define immiscibility domes of simple binary and some ternary systems include:

  - opalescence method
  - SEM/TEM techniques
  - Small Angle X-ray Scattering (SAXS)

- As the systems progress from binary through ternary to multicomponent systems, detailed mapping of the immiscibility dome requires the preparation and characterization of a rapidly increasing number of glasses (extremely complex and time consuming)

- Advantageous to predict/model immiscibility in multicomponent systems based on knowledge of the more simple systems

IMMISCIBILITY IN BINARY SILICATE SYSTEMS

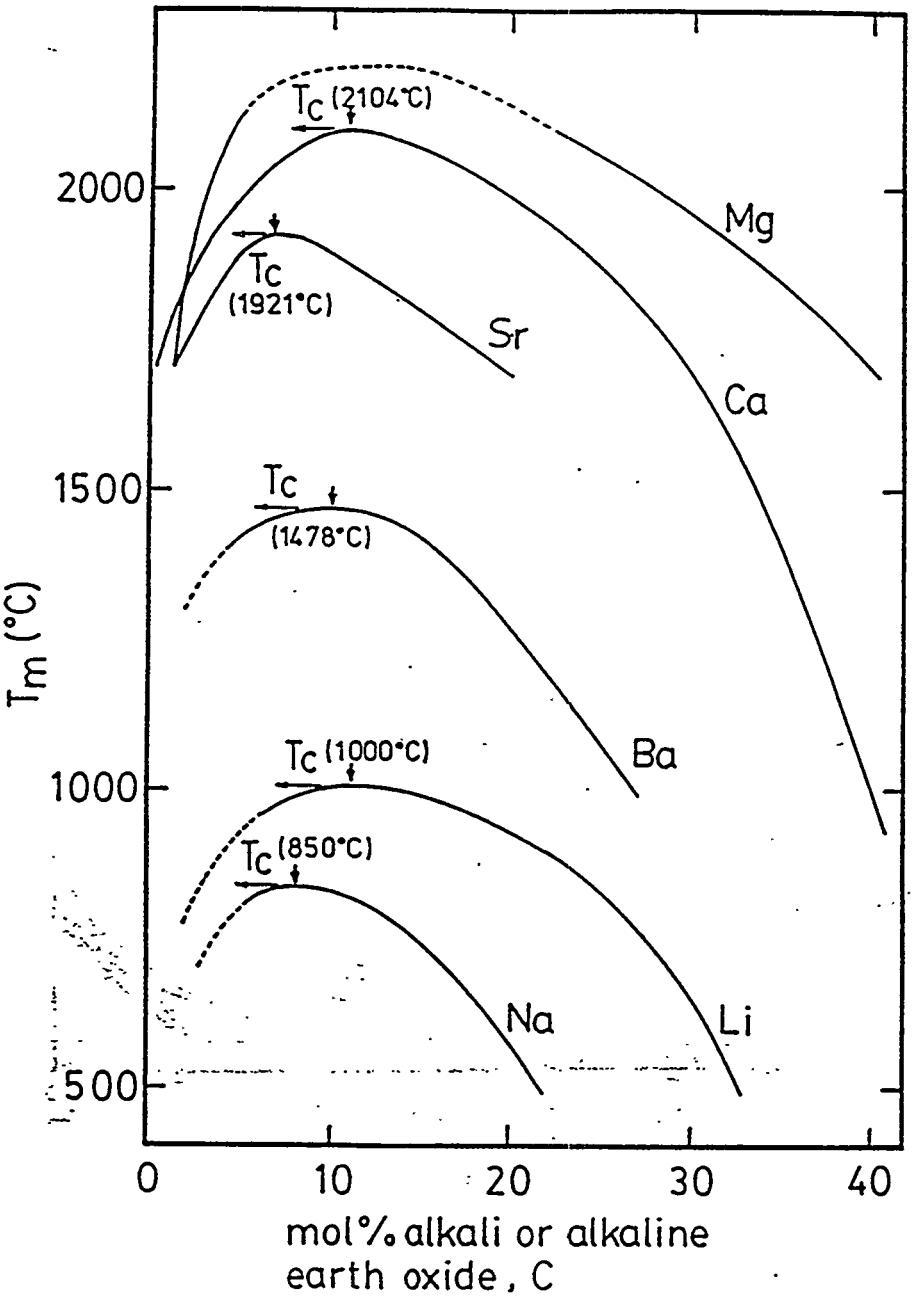

- In general, the greater the polarization power of the cation (Z/r^2), the more extensive is the immiscibility gap in terms of both temperature and composition
- MO-SiO_2 systems generally have more extensive immiscibility gaps than the X_2O-SiO_2 systems

Immiscibility in the Na_2O-B_2O_3-SiO_2 System

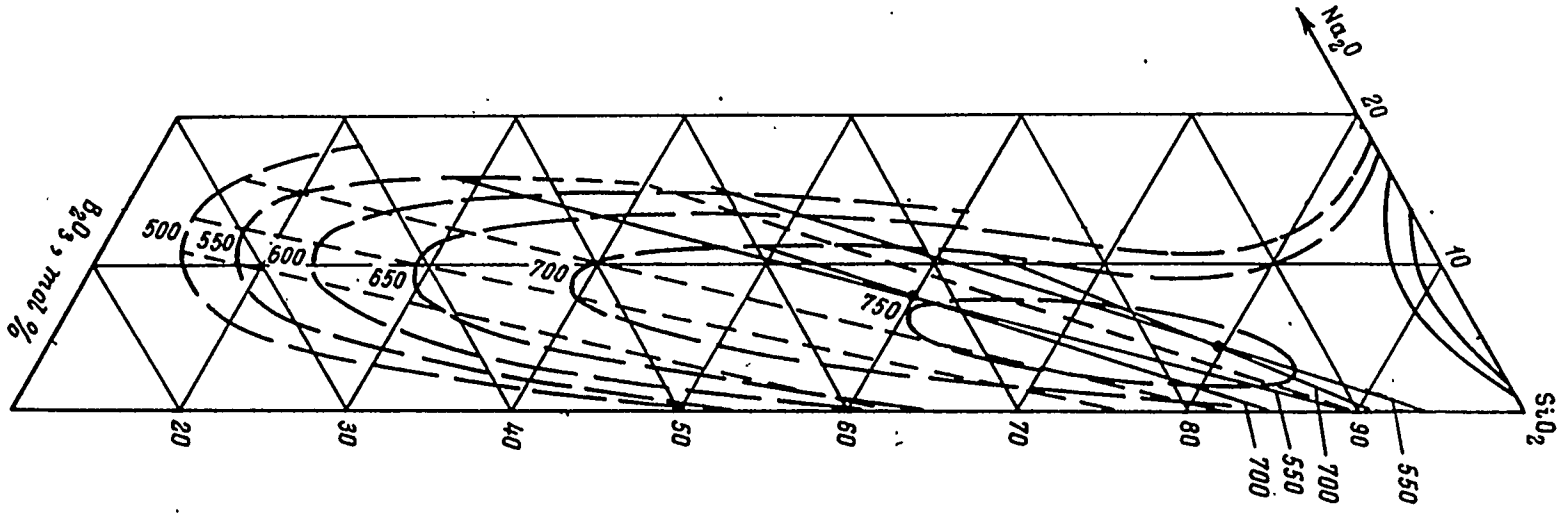

* Fundamental of Inorganic Chemistry, A.K. Varshneya, Academic Press, Inc., 1994

- Vycor® process (Corning Glass Works) to produce a 96% silica glass
- Not applied to multicomponent borosilicate systems typical of nuclear waste vitrification

Composition Region of CVS Glasses

Oxide	Range (wt%)
SiO_2	42 - 57
B_2O_3	5 - 20
Na_2O	5 - 20
Li_2O	1 - 7
CaO	0 - 10
MgO	0 - 8
Fe_2O_3	0.5 - 15
Al_2O_3	0 - 17
ZrO_2	0 - 13
"Others"	1 - 10

- "Others" component was composed of BaO, CdO, CeO_2, Cr_2O_3, Cs_2O, CuO, F, La_2O_3, MnO_2, MoO_3, Nd_2O_3, NiO, P_2O_5, PdO, Pr_6O_{11}, Rb_2O, Rh_2O_3, RuO_2, SO_3, Sm_2O_3, SrO, and Y_2O_3.

Experimental Basis

- Compositional submixture (Na_2O-Li_2O-B_2O_3-SiO_2)
  - Compositional subspace embedded in an overall space defining the multicomponent glass composition
  - 1 to 1 correspondence between submixture and the multicomponent glass
  - NLBS submixture effective in predicting the development of phase separation in multicomponent, canistered glasses and also provides a basis for the composition/durability relationship
- MCC-1 durability data of all quenched and select CCC glasses was used to obtain insight into the relation between composition and durability as a function of thermal history

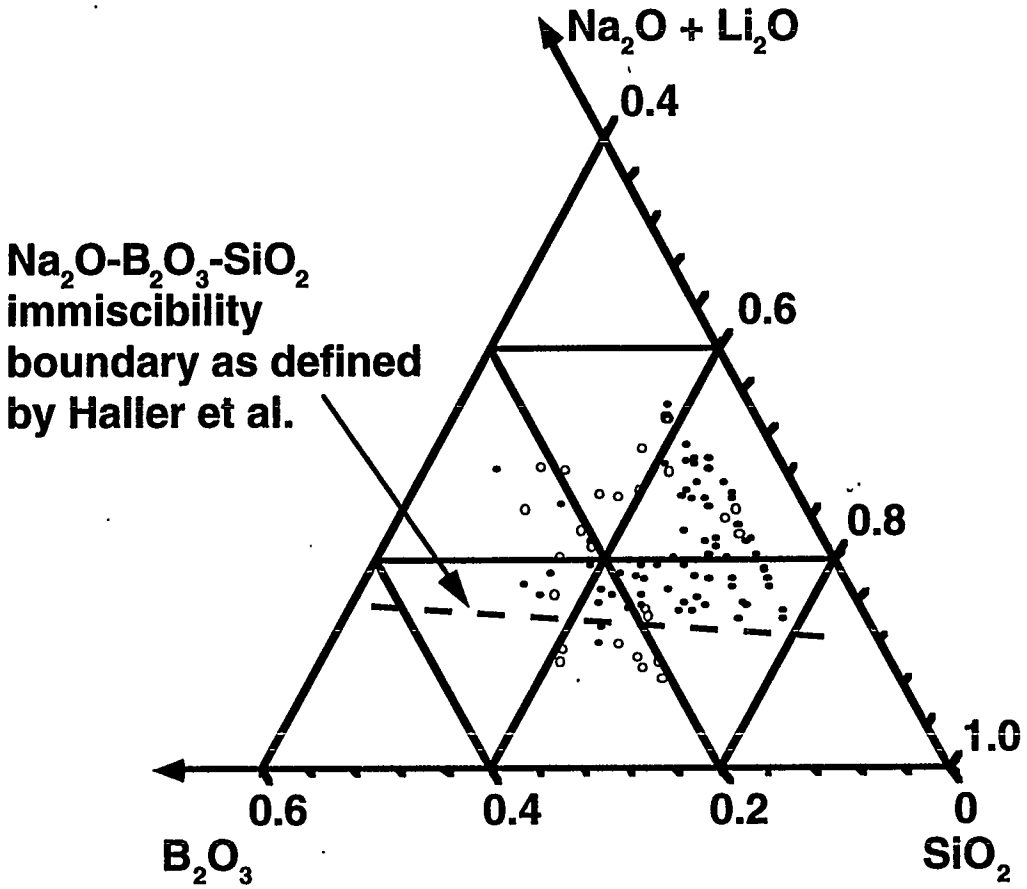

- Distribution of 123 CVS glasses within the normalized NLBS submixture
- Solid (•) and open (o) points represent high- and low-durability glasses, respectively
- Durability based on 28-day MCC-1 normalized boron (B) release values
- Three defined regions of durability
- Glasses deviating from this relation within each region

NBS and NLBS Submixtures

High Durability

CVS Glass	Microstructure	NBS	NLBS
CVS2-30	–	Y	Y
CVS1-11	–	Y	Y
CVS2-52	–	Y	–
CVS2-6	–	Y	–
CVS2-43	–	Y	–
CVS2-74	–	Y	–
CVS2-24	–	Y	–
CVS1-10	–	Y	–
CVS2-12	–	Y	–
CVS2-73	–	Y	–
CVS1-7	–	–	–
CVS2-47	–	–	–
CVS2-38	–	–	–

Low Durability

CVS Glass	Microstructure	NBS	NLBS
CVS1-4	Y	Y	Y
CVS2-29	Y	Y	Y
CVS2-31	Y	Y	Y
CVS1-9	C	Y	Y
CVS2-80	C	Y	Y
CVS2-78	C	Y	Y
CVS2-90	–	Y	–
CVS2-26	–	Y	–
CVS1-14	–	–	–
CVS2-25	–	–	–
CVS2-81	–	–	–

- Majority of the high durability, non-phase separated glasses move outside the dome
- Low durability glasses relatively stable (phase separated and extensive crystallization)
- Only two glasses can not be accounted for by the modified submixture (CVS1-11 and CVS2-30); borderline glasses

R9404074 1 0

Amorphous Phase Separation

- Some borosilicate glasses are prone to phase separation
- Two domains develop when an alkali-borosilicate glass undergoes phase separation
    1. Si-rich phase
    2. B-rich phase
- Three microstructural types defined by Tomozawa
    - Type A: both phases highly interconnected (spinodal decomposition)
    - Type B: Si-rich dispersed phase, B-rich continuous matrix (nucleation/growth)
    - Type C: B-rich dispersed phase, Si-rich continuous matrix (nucleation/growth)

Amorphous Phase Separation (cont.)

- Type A or Type B: Durability deteriorates since "low-durability" B-rich phase is continuous
- Type C: Little effect on durability, and in some cases, has been shown to improve durability (Si-rich phase is continuous)
- Formation of amorphous phase separation will depend on:
    1. Composition, position with respect to immiscibility dome, and
    2. Thermal history that will govern kinetics

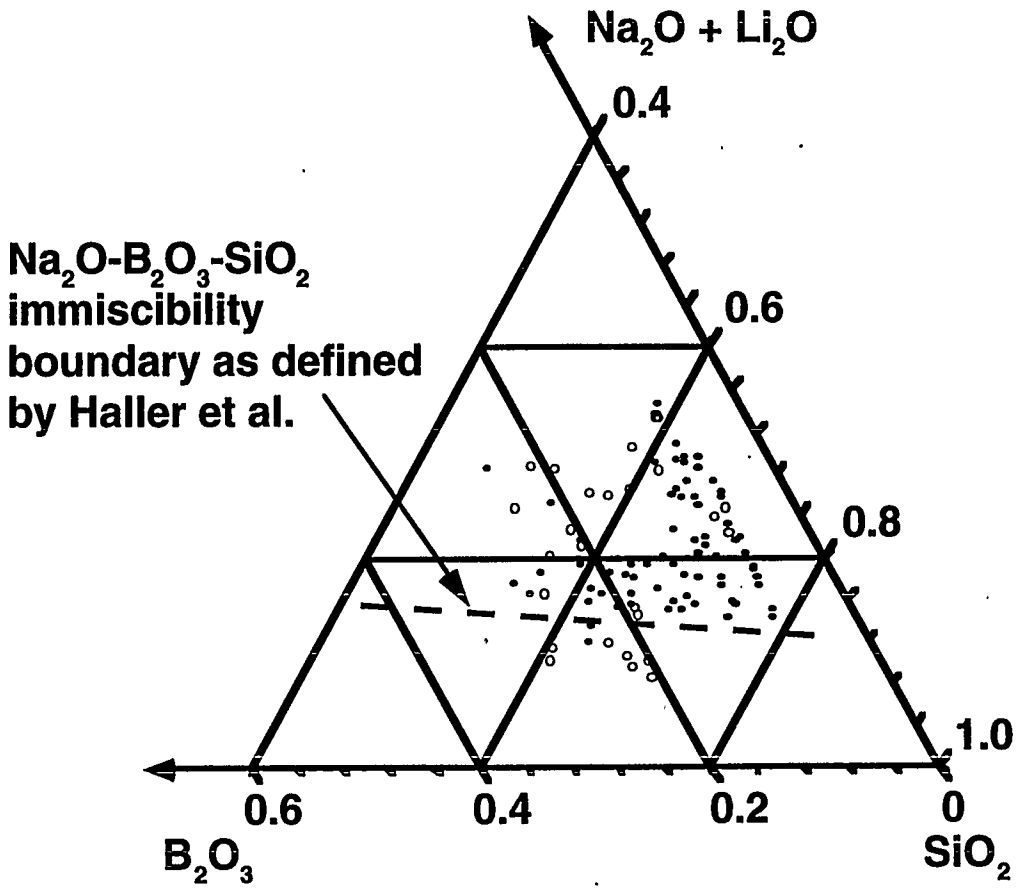

- Nine glasses lying within the immiscibility dome are compositionally prone to amorphous phase separation
- Majority of glasses within immiscibility dome are low-durability systems
- SEM confirmed development of phase separation in three CCC glasses (CVS1-9, CVS2-29, and CVS2-31)
- Of the remaining six, four were characterized by a high degree of crystallization and two were homogeneous with respect to amorphous phase separation

SEM/TEM Micrographs of CVS2-29 (CCC)

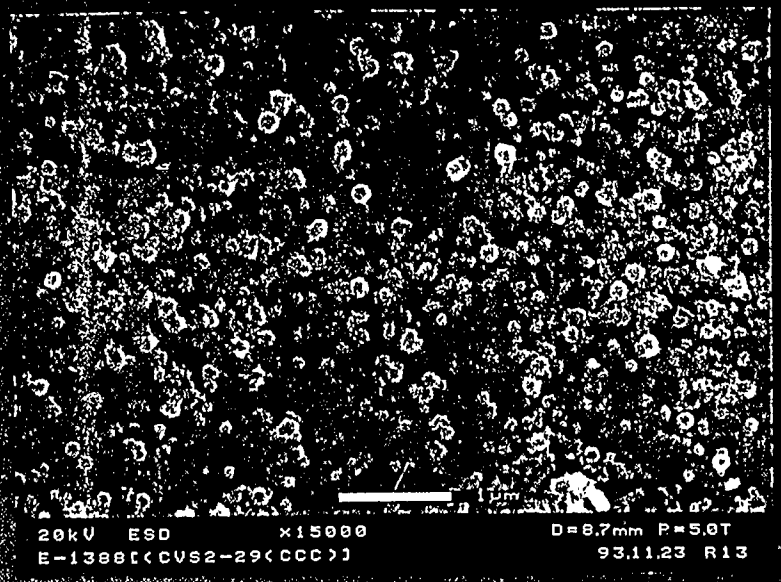

(a) SEM Micrograph (x 15,000)

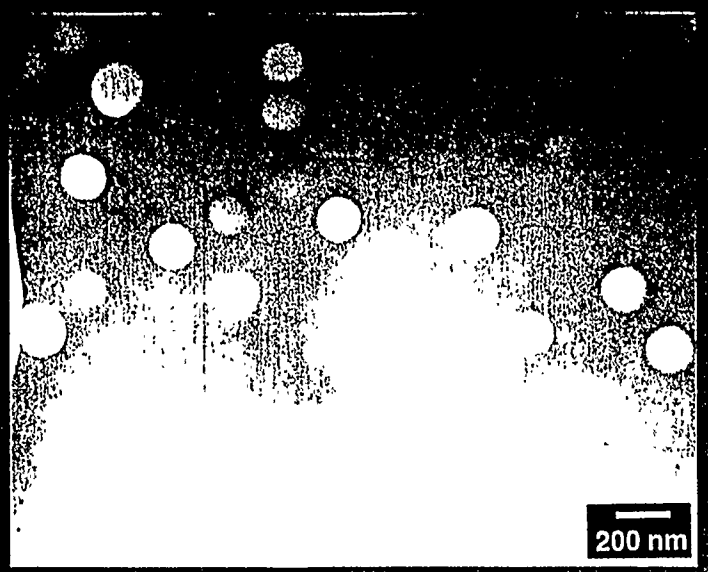

(b) TEM Micrograph (x 40,000)

- Microstructure typical of nucleation/growth

Average TEM EDS Compositional Analysis of CVS2-29

Element	Dispersed Phase (Wt%)	Matrix Phase (Wt%)
Na-K	2.54	6.64
Si-K	91.72	51.97
Ca-K	1.04	12.41
Fe-K	1.27	3.54
Ni-K	0.02	1.94
Zr-L	2.85	17.08
Nd-L	0.03	4.55
Cd-L	0.11	1.88

B not detected in TEM EDS system; EELS performed

EELS Spectra for CVS2-29 (CCC)

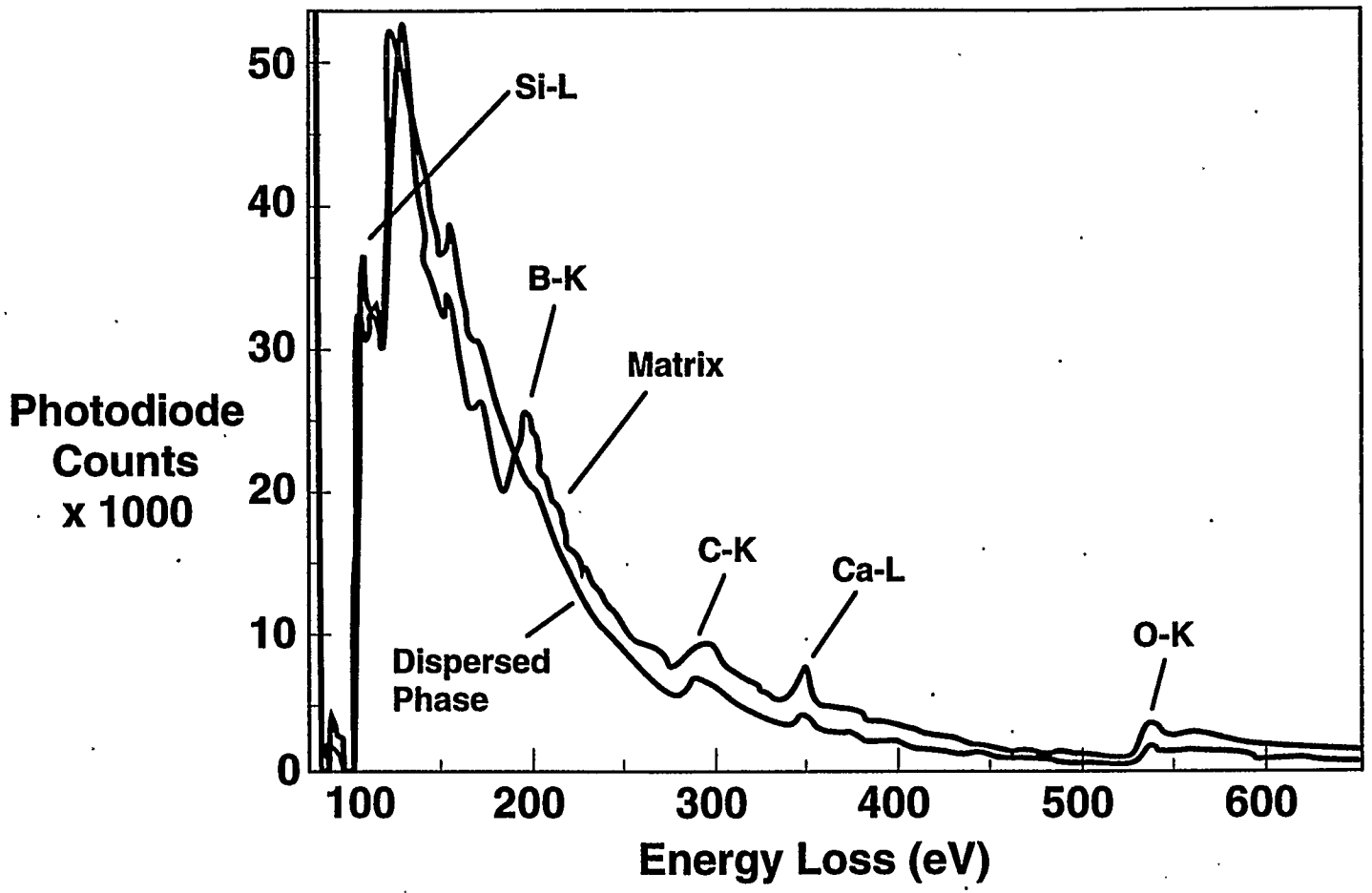

- Confirmation of Type B microstructure: Si-rich dispersed phase and B-rich matrix phase
- Microstructure detrimental to system durability

SEM/TEM Micrographs of CVS2-31 (CCC)

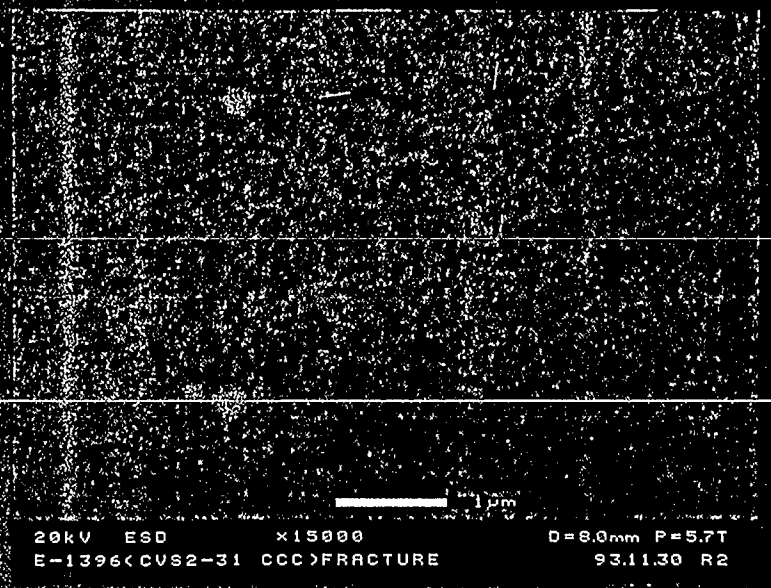

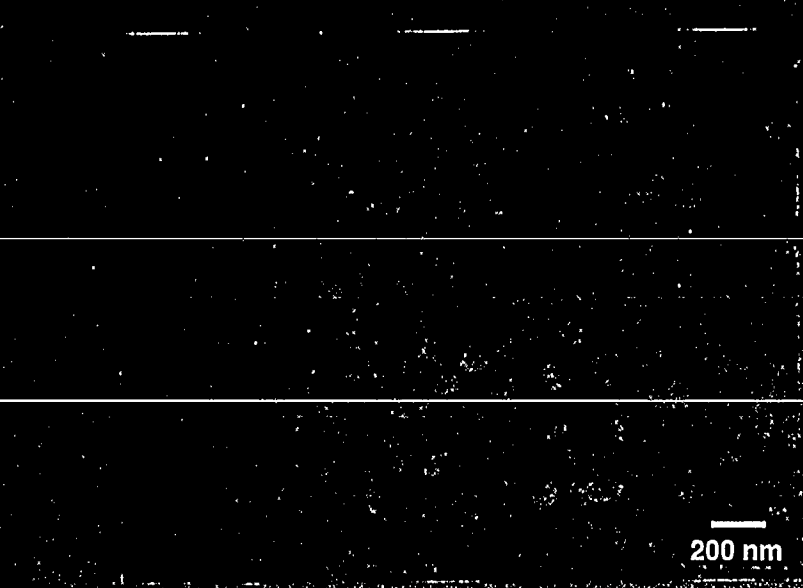

(a) SEM Micrograph (x 15,000) (b) TEM Micrograph (x 40,000)

- Microstructure typical of spinodal decomposition
- Both phases appear to be interconnected and continuous
- TEM EDS unable to differentiate Si content between two phases

EELS Spectra for CVS2-31 (CCC)

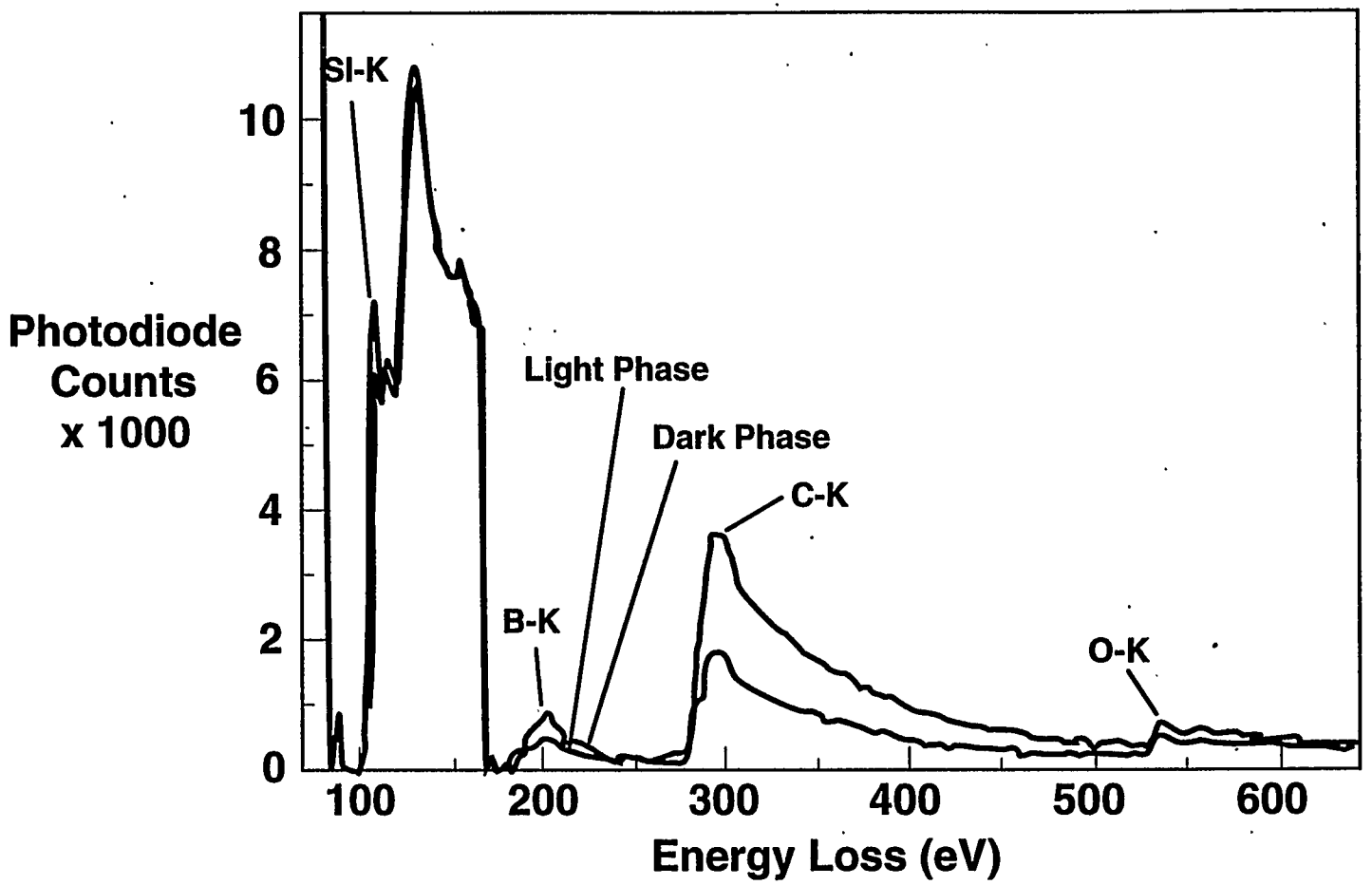

- EELS indicates a boron-rich phase
- Type A microstructure (spinodal decomposition)
- Detrimental to system's durability

Amorphous Phase Separation

Durability Data for Two Phase Separated Glasses

- MCC-1 normalized boron released values for CVS2-29 and CVS2-31

Glass	Quenched*	CCC
CVS2-29	42.29	45.10
CVS2-31	47.02	44.49

*Quenched samples showed no indication of phase separation by SEM

- CCC CVS2-29 (Type B microstructure) shows a slightly higher B release than its counterpart non-phase separated quenched glass
- Indicates that the development of amorphous phase separation may slightly reduce the systems durability
- CCC CVS2-31 (Type C microstructure) unexpectedly shows a slight increase in durability from its counterpart non-phase separated sample
- However, both cooling schedules produce unacceptable glasses in terms of boron release values (>28 g/m^2)

Amorphous Phase Separation (cont.)

- Due to only slight differences in release values between quenched (non-phase separated) and CCC (phase separated) samples, there seems to be very little effect of the development of phase separation on the overall durability
- Composition is inherently low in Al_2O_3 and /or ZrO_2:

Glass	Al_2O_3 (wt%)	ZrO_2 (wt%)
CVS2-29	0.0	8.3
CVS2-31	5.3	0.0

- Composition lacks sufficient network forming oxides to provide the required 3-D network
- The effect of structural integrity (or lack thereof) dominates these two glasses not the development of amorphous phase separation
- No crystallization effects

"Highly" Crystalline Samples

- Four glasses prone to amorphous phase separation were characterized by a high degree of crystallization (CCC samples)

Primary Phase for "Highly" Crystalline Glasses Prone to Amorphous Phase Separation

Glass	Primary Crystalline Phase	Estimated Volume %
CVS2-78	SiO_2, cristobalite	22
CVS2-79	SiO_2, cristobalite	20
CVS2-80	SiO_2, cristobalite	15
CVS1-9	Unidentified	5 - 7

- Early development of a Type B microstructure (Si-rich dispersed phase) may act as a precursor to SiO_2 crystallization upon further cooling
- Development of amorphous phase separation may lower the kinetic and thermodynamic barriers to crystallization
- However, internal crystallization can occur without prior phase separation

REFERENCES

1. Tomozawa, M., "Phase Separation in Glass," In Treatise on Materials Science and Technology, Vol. 17, Edited by M. Tomozawa and R.H. Doremus, Academic Press, New York, pp. 71-113, (1972).

2. Tomozawa, M., G.M. Singer, Y. Oka, and J.T. Warden, "Phase Separation in Nuclear Waste Glasses," In Ceramics in Nuclear Waste Management, Proceedings of Symposium in Cincinnati, OH, April/May 1979. Edited by T.D. Chikalla and J.E. Mendel, U.S. Dept. of Energy, Tech. Info. Center, pp. 193-197.

3. Peeler, D.K. and P.R. Hrma, "Predicting Liquid Immiscibility in Multicomponent Nuclear Waste Glasses," Ceramic Transaction Series, Environmental and Waste Management in the Ceramic Industry II, Volume 45, pp. 219 - 229 (1994).

4. Piepel, G.F., P.R. Hrma, S.O. Bates, M.J. Schweiger, and D.E. Smith, First-Order Study of Property/Composition Relationships for Hanford Waste Vitrification Plant Glasses, PNL-8502, Chapter 12, Section 11.4, Pacific Northwest Laboratory, Richland, Washington, (1993).

5. Ehrt, D., H. Reiss, and W. Vogel, "Microstructural Study of CoO-containing Na_2O-B_2O_3-SiO_2 Glasses, *Silikattechnik*, Vol. 28, pp. 359-364, 1977.

6. Taylor, P., "A Review of Phase Separation in Borosilicate Glasses, with Reference to Nuclear Fuel Waste Immobilization," Whiteshell Nuclear Research Establishment, AECL-10173 (1990).

7. Danilova, N.P., O.V. Mazurin, and T.S. Tschomskaya, "The Influence of the Structure of Phase Separated Glasses on Their Chemical Durability," Proc. Int. Cong. Glass (9^{th}), Versailles, pp. 825-841 (1971).

8. Taylor, P., S.D. Ashmore, and D.G. Owen, "Chemical Durability of Some Sodium Borosilicate Glasses Improved by Phase Separation," *J. Amer. Ceram. Soc.*, 70 [5] 333-338 (1987).

9. Dietzel, A., "The Cation Field Strength and the Relation to Devitrifying Processes, to Compound Formation, and to the Melting Points of Silicates," *Z. Electrochem.*, 48 [1] 9 - 23 (1942).

10. Warren, B.E. and A.G Pincus, "Atomic Considerations of Immiscibility in Glass Systems," *J. Amer. Ceram. Soc.*, 23 [10] 301 - 304 (1940).

11. Haller, W., D.H. Blackburn, F.E. Wagstaff, and R.J. Charles, "Metastable Immiscibility Surface in the System Na_2O-B_2O_3-SiO_2," *J. Amer. Ceram. Soc.*, 53 [1] 34 - 39 (1970).

12. Kawamoto, Y. and M. Tomozawa, "Prediction of Immiscibility Boundaries of Ternary Silicate Glasses," *Phys. Chem. Glasses*, 22 [1] 11 - 16 (1987).

13. Charles, R.J., "Metastable Immiscibility in the BaO-Li_2O-SiO_2 System," *Phys. Chem. Glasses*, 8 [5] 185 - 189 (1967).

14. Levin, E.M. and S. Block, "Structural Interpretation of Immiscibility in Oxide Systems: I, Analysis and Calculation of Immiscibility," *J. Amer. Ceram. Soc.*, 40 [3] 95 - 106 (1957).

15. Strand, Z. and P. Strand, "Calculation of Metastable Two-Liquid Tie Lines in Ternary Glass-Forming Systems," *J. Amer. Ceram. Soc.*, 61 [7/8] 283 - 286 (1978).

16. Burnett, D.G. and R.W. Douglas, "Liquid-Liquid Phase Separation in the Soda-Lime-Silica System," *Phys. Chem. Glasses*, 11 [5] 125 - 135 (1970).

17. Taylor, P. and D.G. Owen, "Liquid Immiscibility in the System Na_2O-ZnO-B_2O_3-SiO_2," *J. Amer. Ceram. Soc.*, 64 [6] 360-367 (1981).

18. Taylor, P., A.B. Campbell, and D.G. Owen, "Liquid Immiscibility in the Systems X_2O-MO-B_2O_3-SiO_2 (X=Na,K; M=Mg, Ca,Ba) and Na_2O-MgO-BaO-B_2O_3-SiO_2," *J. Amer. Ceram. Soc.*, 66 [5] 347-351 (1983).

19. Taylor, P., S.D. Ashmore, and A.B. Campbell, "Liquid Immiscibility in the Systems Na_2O-Yb_2O_3-B_2O_3-SiO_2 and K_2O-Yb_2O_3-B_2O_3-SiO_2," *J. Amer. Ceram. Soc.*, C-186 (1984).

20. Tomozawa, M., "Liquid Phase Separation and Crystal Nucleation in Li_2O-SiO_2 Glasses," *Phys. Chem. Glasses*, 13, 161 - 166 (1972).

21. Matusita, K., J. Maki, and M. Tashiro, "Effect of Added Oxides on the Crystallization and Phase Separation of Li_2O-$3SiO_2$ Glasses," *Phys. Chem. Glasses*, 15, 106 - 108 (1974).

22. Zanotto, E.D., "The Effect of Amorphous Phase Separation on Crystal Nucleation in Baria-Silica and Lithia-Silica Glasses," Ph.D. Thesis, Sheffield University (1981).

Minor Components in Nuclear Waste Glasses

Hong Li

June, 1995

Materials Applications Section
Pacific Northwest Laboratory
Richland, Washington 99352

Collaborators:

S. Crichton
J. Coleman
J.G. Darab
X. Feng
M. Gong
P.R. Hrma
D.S. Kim
M.H. Langowski
D. MaCready
S. Palmer
D.K. Peeler
K. Pool
R. Sanders
M.J. Schweiger
D.E. Smith
P.A. Smith
M. Tomozawa
J.D. Vienna
J.H. Westsik, Jr.

BACKGROUND

WHAT DO WE KNOW ABOUT MINOR COMPONENTS ?

Cl, F, and SO_3 : Volatility

All components : Phase Seg./Sep.

Cr_2O_3 : Crystallization

WHAT DO WE NEED TO KNOW ?

Minor component solubility limits as a function of waste glass compositions

Effects on batch melting process

Effects on glass durability


Minor Component
Study of LLW Glasses

WORKING SCOPE

- Solubility Limits of Minor Components

- Glass Melting Process

  Phase Segregation
  Crystallization
  Volatility
  Viscosity

- Glass Durability

  7-Day Product Consistency Test
  Flow-Through Test

LLW Glass Compositions (wt%)

Oxide	L6-5412	L4-9012	(L4-909)	(L5-0912)
SiO_2	56.78	56.78	59.78	56.78
B_2O_3	5.00	9.00	9.00	0.00
Na_2O	20.00	20.00	20.00	20.00
CaO	4.00	0.00	0.00	9.00
Al_2O_3	12.00	12.00	9.00	12.00
Others Bi_2O_3, Cl, F, Fe_2O_3, K_2O, MnO, Nd_2O_3, P_2O_5 SO_3, Cr_2O_3, ZrO_2	2.20 Spiked with Cl, F, P_2O_5, SO_3, Cr_2O_3	2.20 Spiked with Cl, F, P_2O_5, SO_3, Cr_2O_3	2.22 Spiked with Cl, F, P_2O_5, SO_3, Cr_2O_3	2.22 Spiked with Cl, F, P_2O_5, SO_3, Cr_2O_3

(Batch: Oxides, Boric Acid and Sodium-Containing Salts)

• Minor Component Solubility

Maximum concentration in the glass (quenched and annealed samples) :

☞ free from crystals under an optical microscope

☞ amorphous to x-ray

☞ melted in ambient air

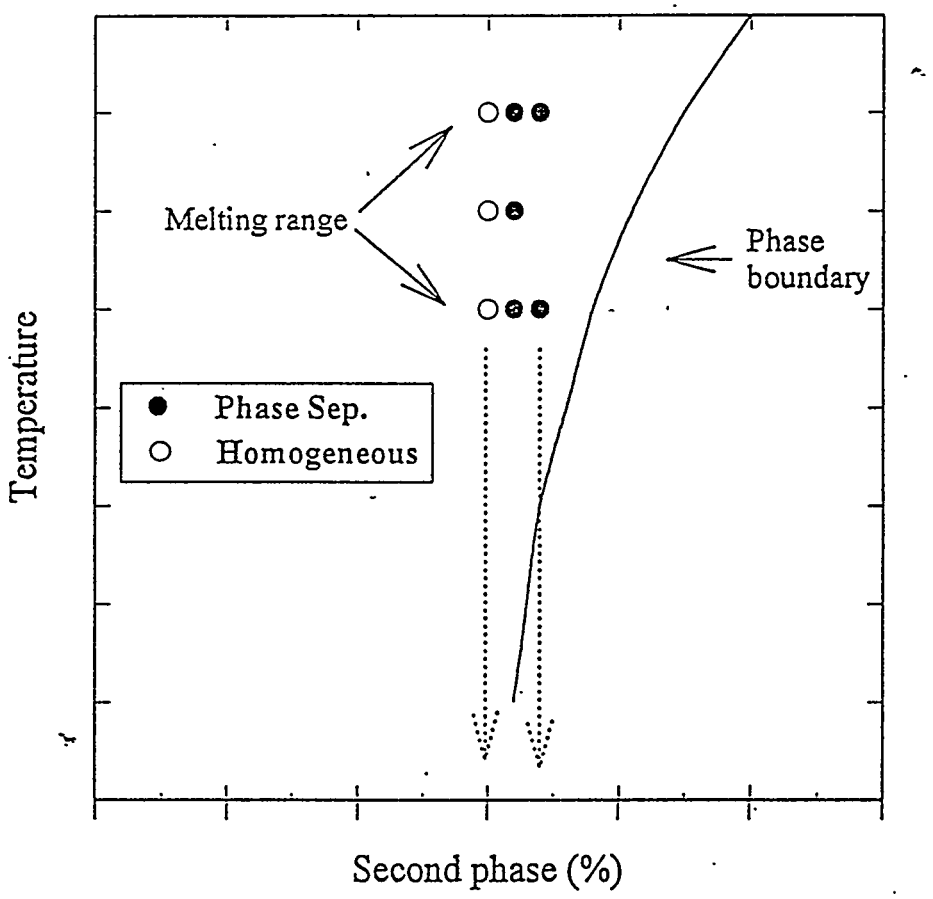

Figure 1. Schematic diagram of a system that is homogeneous in the melting range but becomes phase separated during cooling. The observed solubility is independent of temperature.

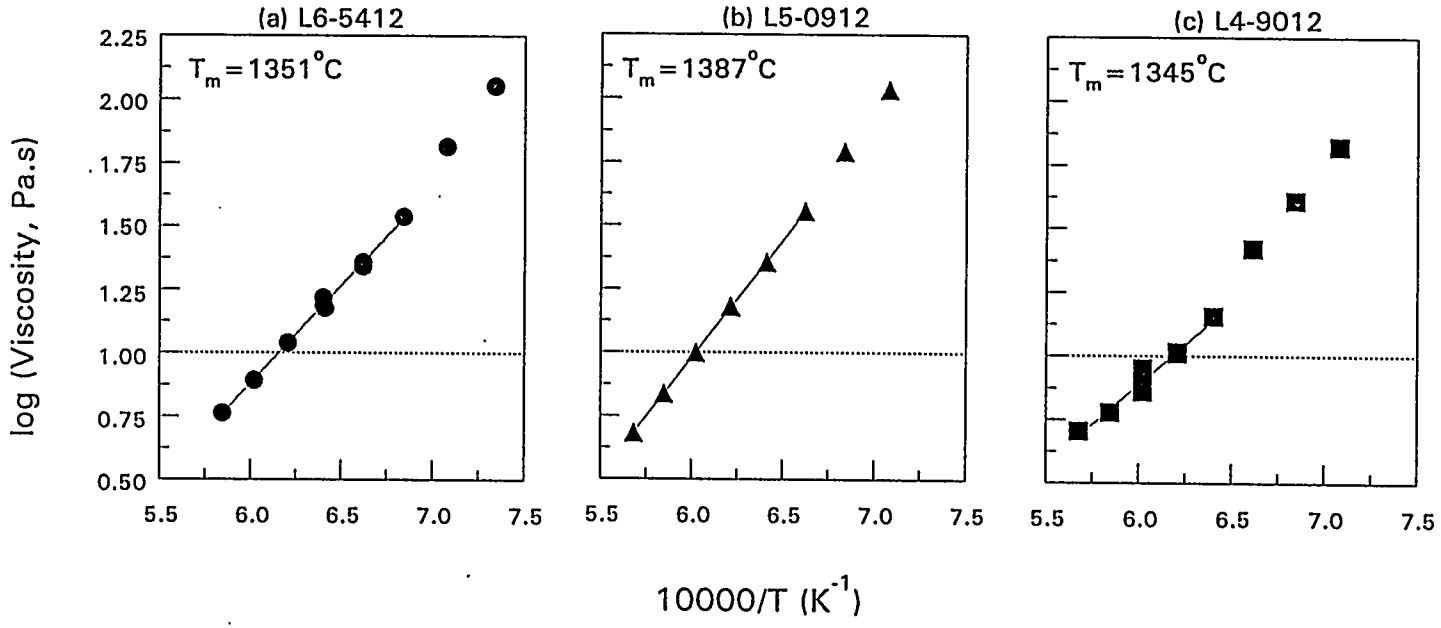

Figure Melt viscosity as a function of temperature for L6-5412 L5-0912 and L4-9012 glasses.

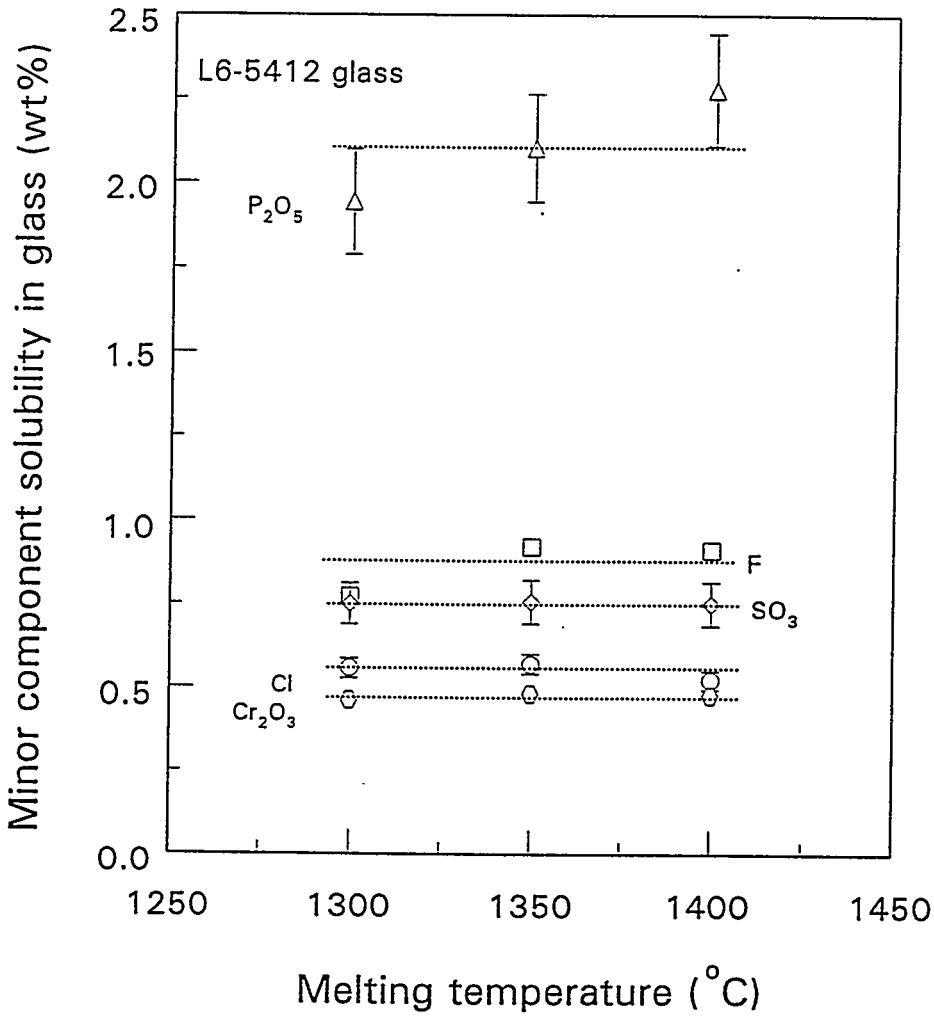
L6-5412 glass
P_2O_5
F
SO_3
Cl
Cr_2O_3
Minor component solubility in glass (wt%)
Melting temperature (°C)
2.5
2.0
1.5
1.0
0.5
0.0
1250
1300
1350
1400
1450

Solubility of Minor Components in LLW Glasses (wt%)

Tm = 1350 C / Time = 2 h (ambient air)

Glass	L6-5412	L4-9012
	B2O3 : 5 wt% CaO : 4 wt%	B2O3 : 9 wt% CaO : 0 wt%
Chlorine, Cl	0.57	0.49
Fluorine, F	0.92	1.18 < X < 1.45
Phosphate, P2O5	2.10	4.72 < X < 5.72
Sulfate, SO3	0.75	0.47
Chromium Oxide, Cr2O3	0.48	1.04

Sulfate Solubility in Silicate Glass

$$\equiv Si\text{-}O\text{-}Si\equiv + 2Na^{+} : O^{2-}\ (glass) \Longleftrightarrow 2(\equiv Si\text{-}O^{-} : Na^{+})\ (glass)$$

$$SO_3\ (gas) + 2Na^{+} : O^{2-}\ (molten\ salt) \Longleftrightarrow 2Na^{+} : SO_4^{2-}\ (molten\ salt)$$

$$[SO_4^{2-}] \propto P(SO_3) * [Na^{+}]^2[\equiv S\text{-}O^{-}]^2 / [\equiv Si\text{-}O\text{-}Si\equiv]$$

(Ref: K. Papadopoulos, Phys. Chem. Glasses, 14 (1973) 60-65)

- Volatilization

Minor Component - Cl, F, and SO_3

High B_2O_3 Enhances Volatility of Cl, F, and SO_3

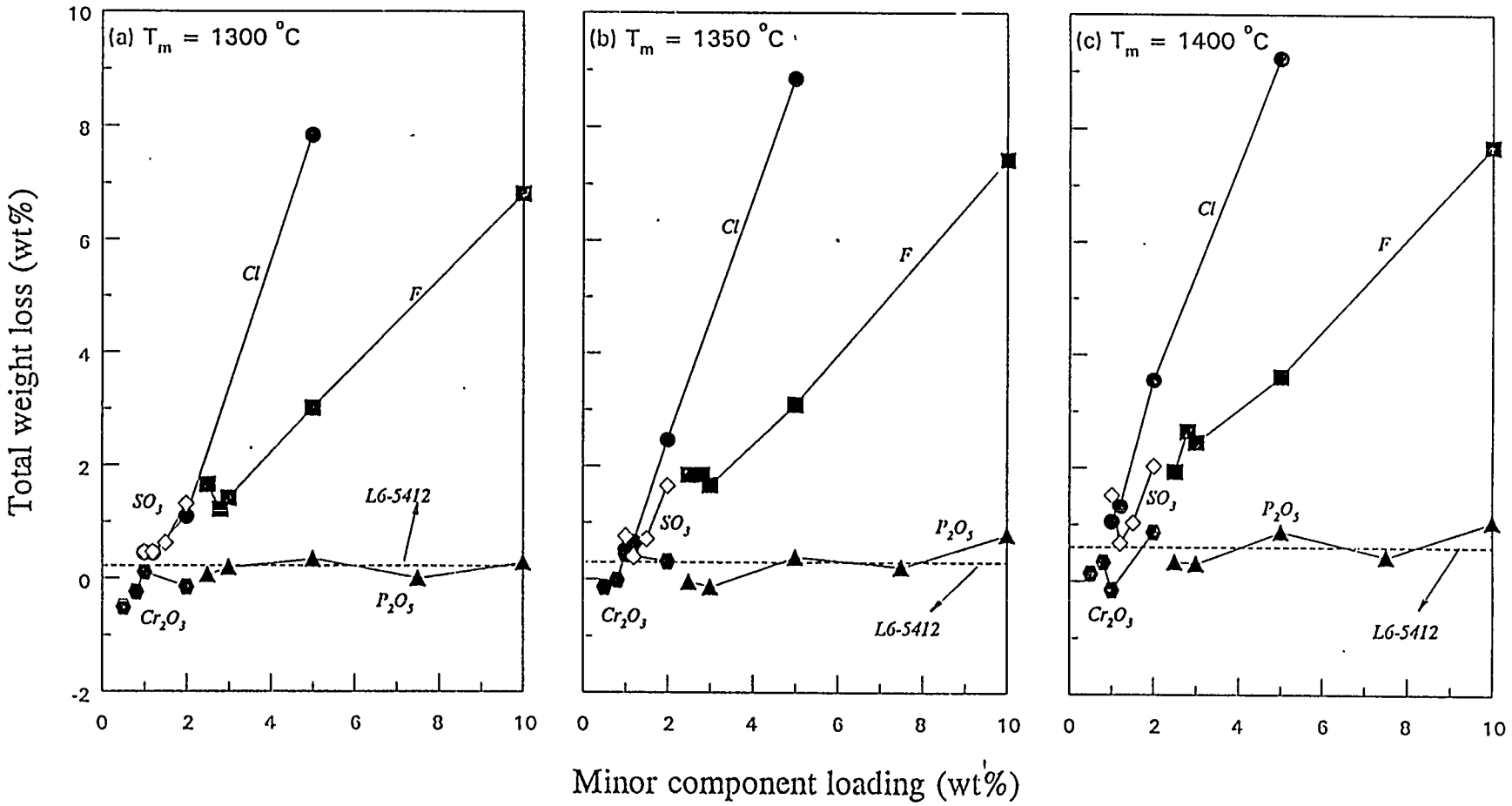

Figure 1. Total weight loss of L6-5412 based glasses spiked with minor components and melted at (a) 1300 °C, (b) 1350 °C and (c) 1400 °C.

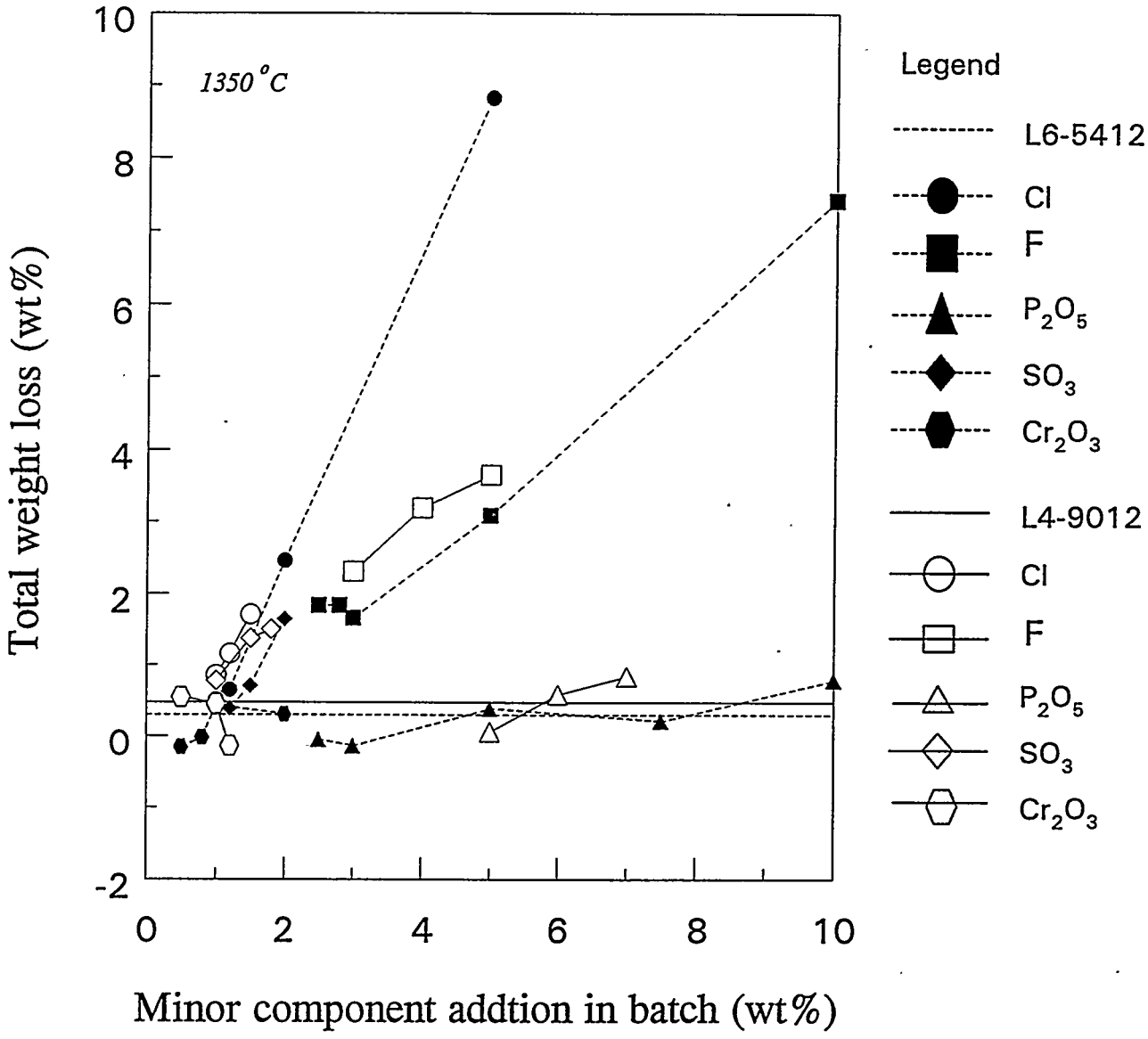
1350 °C
Total weight loss (wt%)
Minor component addtion in batch (wt%)
10
8
6
4
2
0
-2
0
2
4
6
8
10
Legend
L6-5412
Cl
F
P2O5
SO3
Cr2O3
L4-9012
Cl
F
P2O5
SO3
Cr2O3

• Crystallization

Crystalline Phases in Na-Ca-Al-B-Si Glass Over-saturated with Minor Components

Minor Component	Crystalline Phases
Chlorine	NaCl
Fluorine	NaF CaF_2
Phosphate	Na_3PO_4 $Na_2Ca_4(PO_4)_2SiO_4$
Sulfate	Na_2SO_4
Chromium Oxide	Cr_2O_3

(glass : L6-5412)

• Phase Segregation

Cl and SO_3 :

Precipitation from the melt
Accumulation on the melt surface
Occurred at glass processing temperature

F and P_2O_5 :

Precipitation from the melt
Occurred during the melt cooling

Cr_2O_3 :

Precipitation from the melt
Occurred probably during the melt cooling

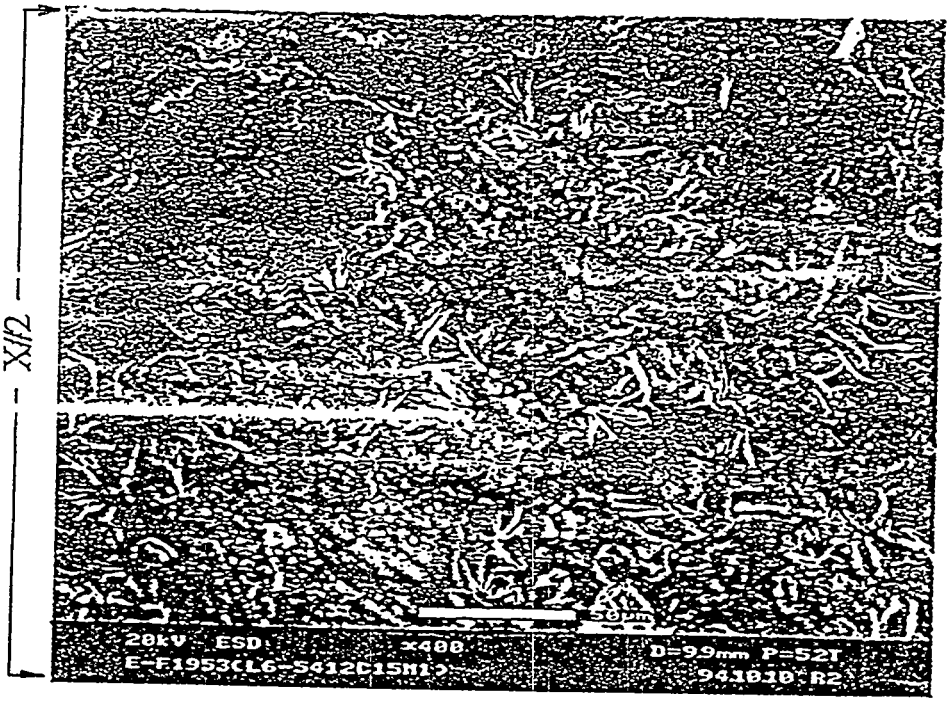

(a)

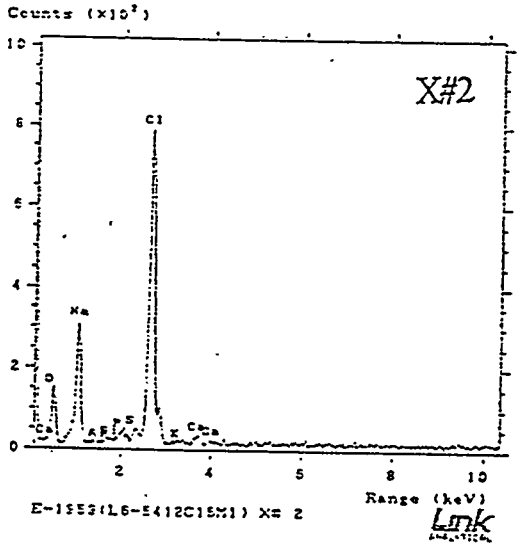

(b)

Figure 3. (a) SEM micrograph of a molten salt layer and (b) its corresponding EDS pattern for glass spiked with 5.0 wt%Cl and melted at 1300 °C.

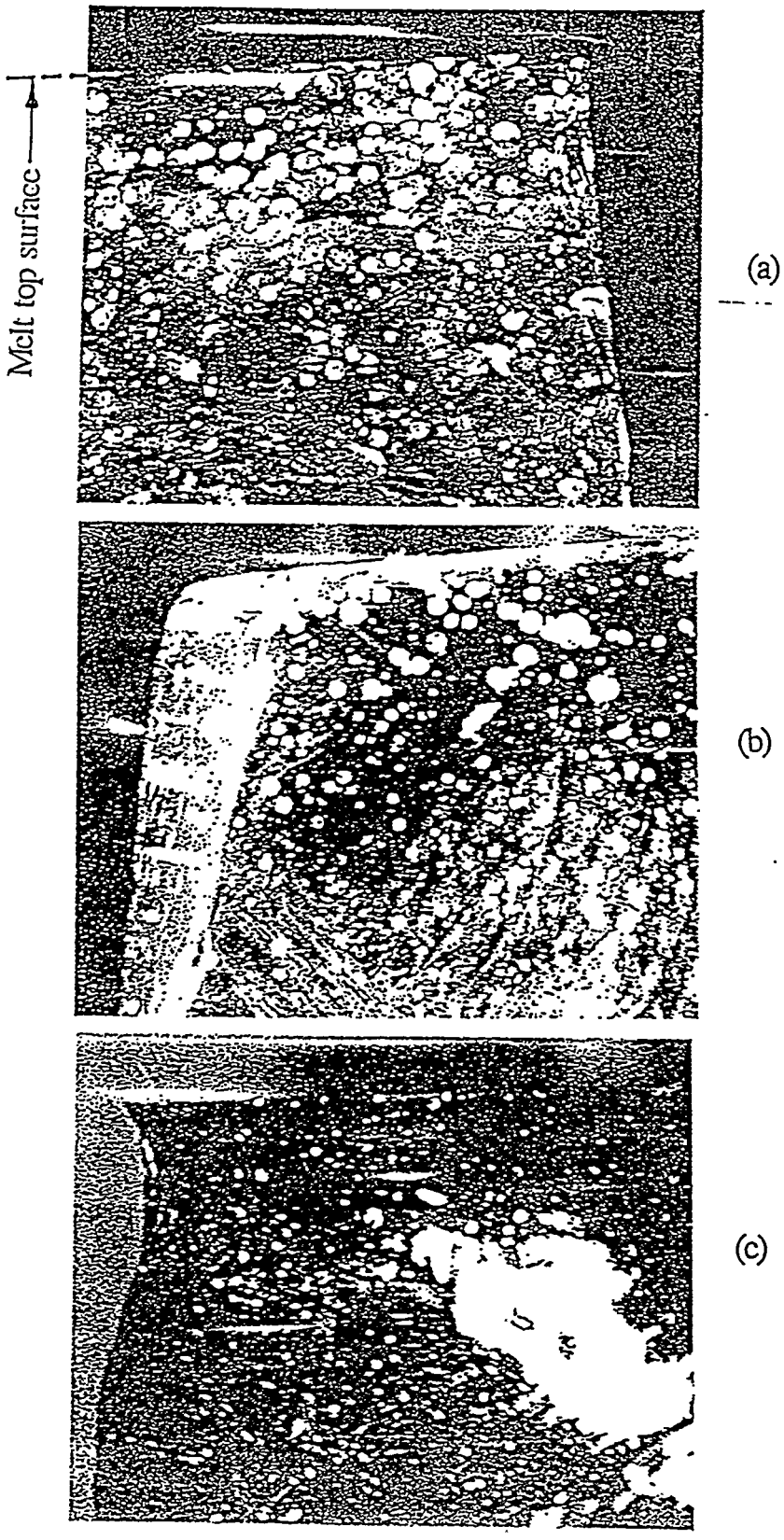

Figure 2. Optical micrographs of cross sections of quenched glasses melted at (a) 1300 °C, (b) 1350 °C and (c) 1400 °C for L6-5412 glass spiked with 5.0 wt%Cl (mag. 8X).

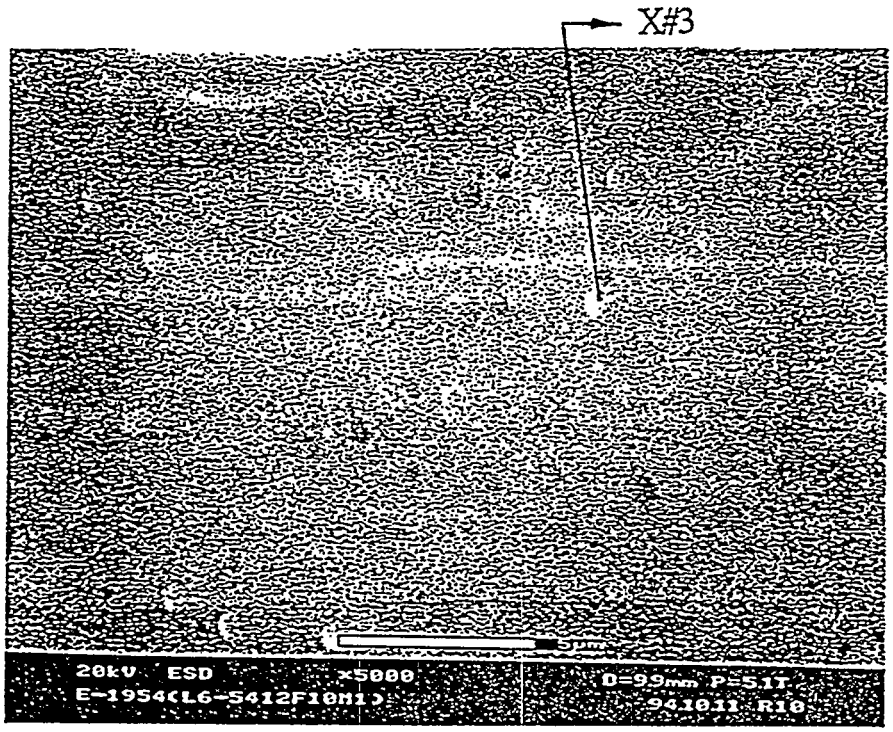

(a)

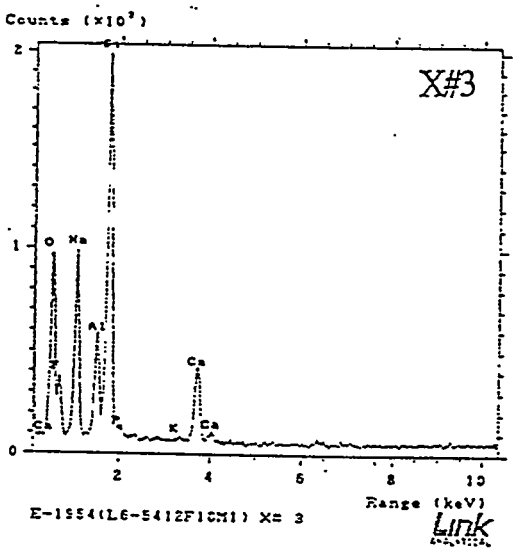

(b)

Figure 7. (a) SEM micrograph of L6-5412 glass spiked with 10.0 wt%F and melted at 1300 °C and (b) its corresponding EDS pattern, X#3.

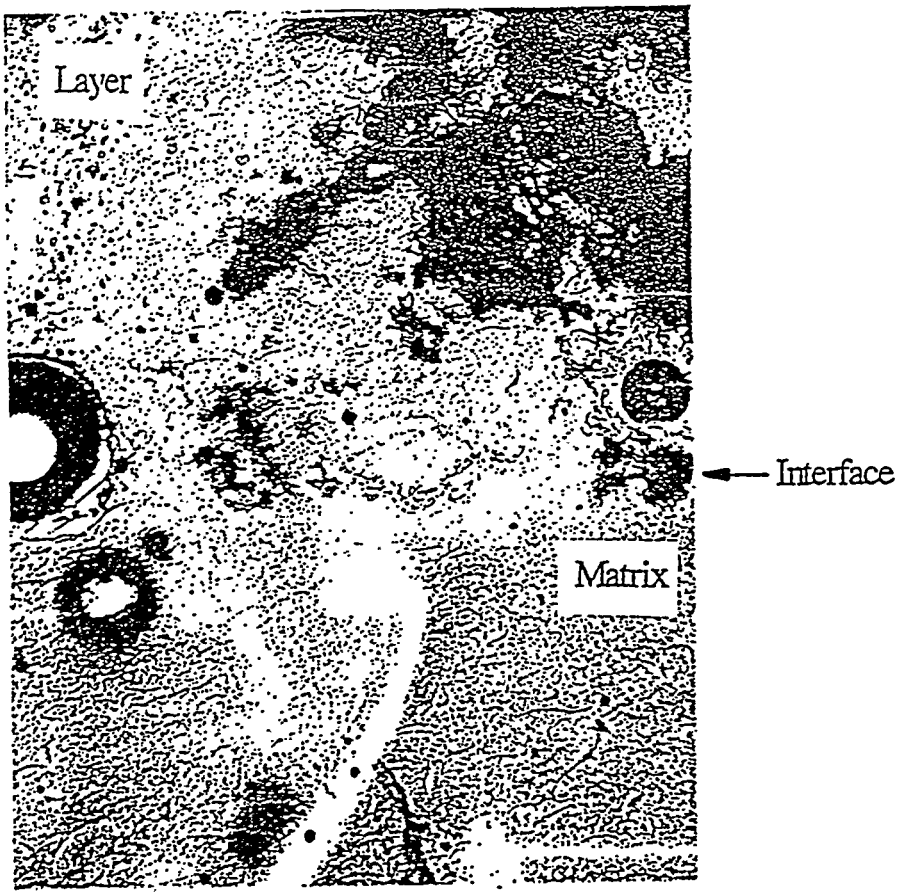

Figure 11. Optical micrograph of L6-5412 glass spiked with 10.0 wt%P_2O_5 and and melted at 1300 °C, showing a phase segregated layer at the top of the melt (mag. 200X).

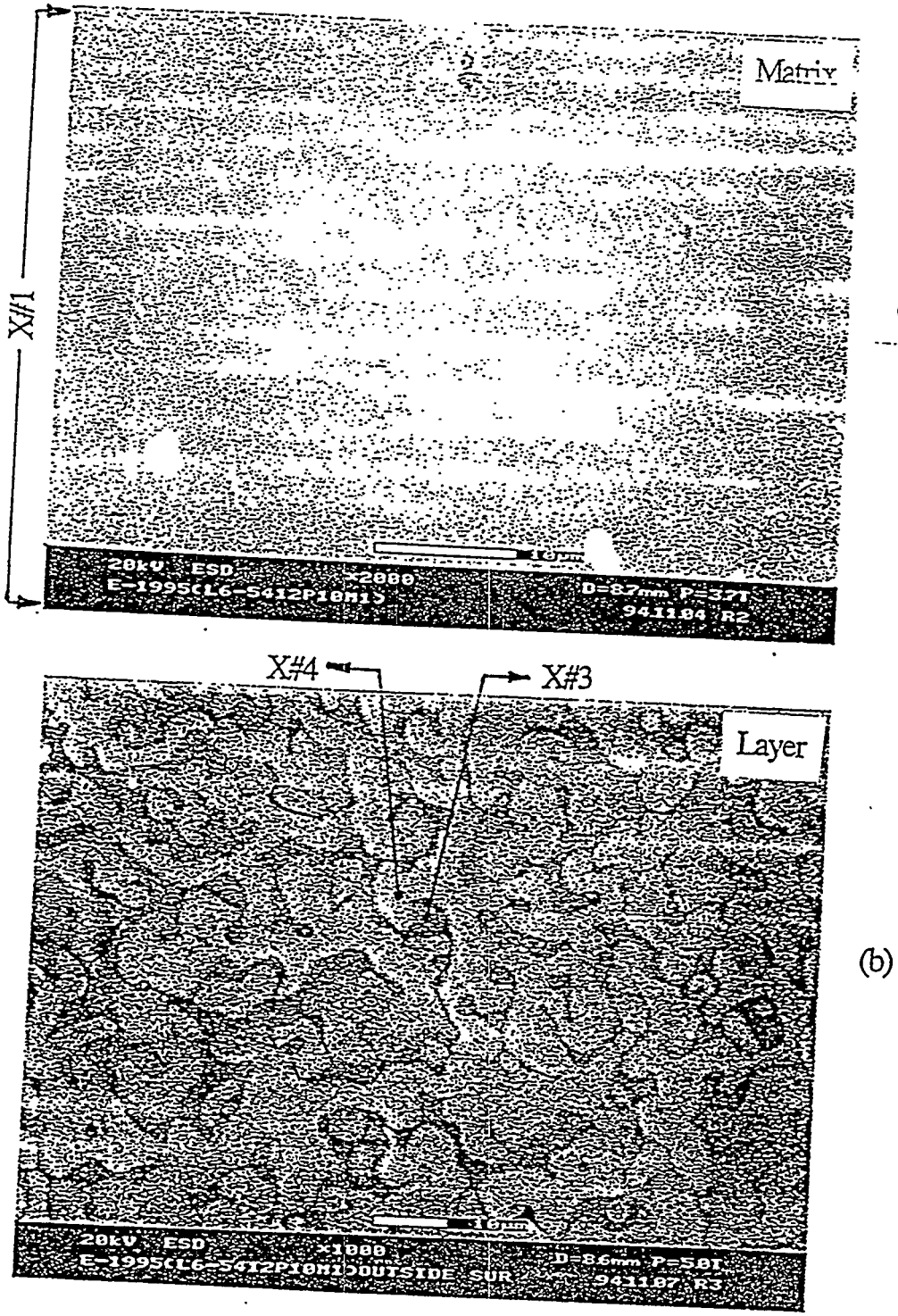

Figure 12. SEM micrographs of for L6-5412 glass spiked with 10.0 wt%P_2O_5 and melted at 1300 °C, showing (a) homogeneous matrix, X#1, and (b) phase separation at the top of the melt, X#3 and X#4.

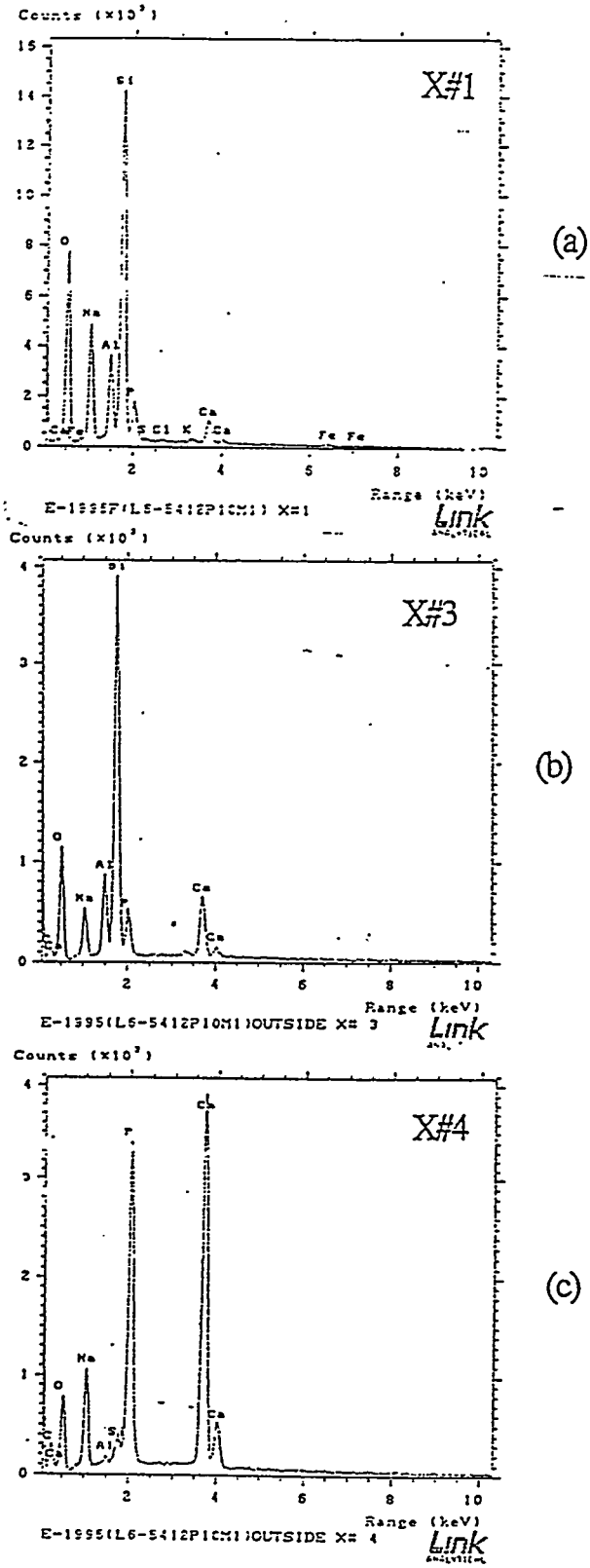

Figure 13. EDS patterns corresponding to the areas, X#1, 2, and 3 shown in Figure 12.

L4-9012S1 (1 wt% SO_3, 1350 °C)

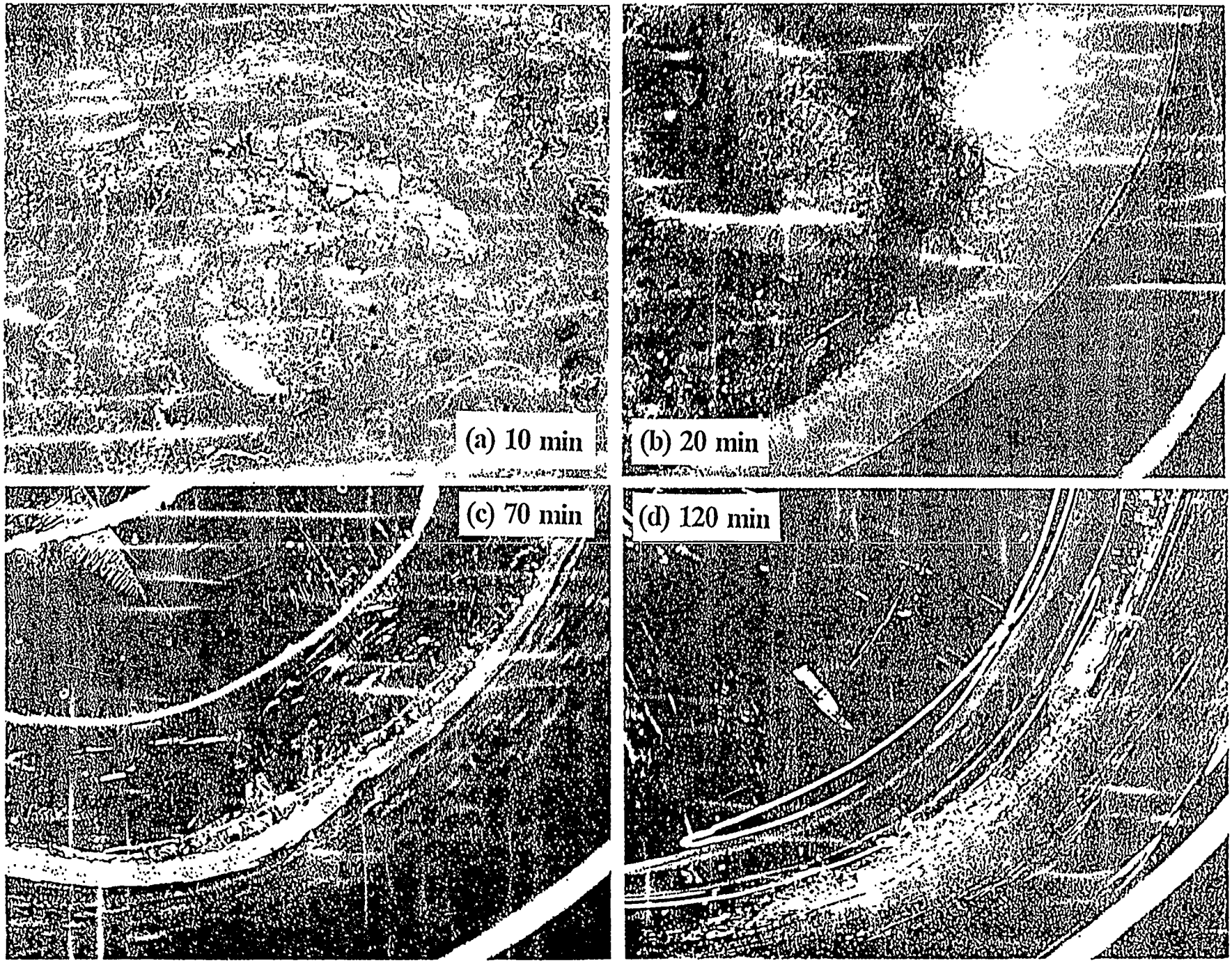

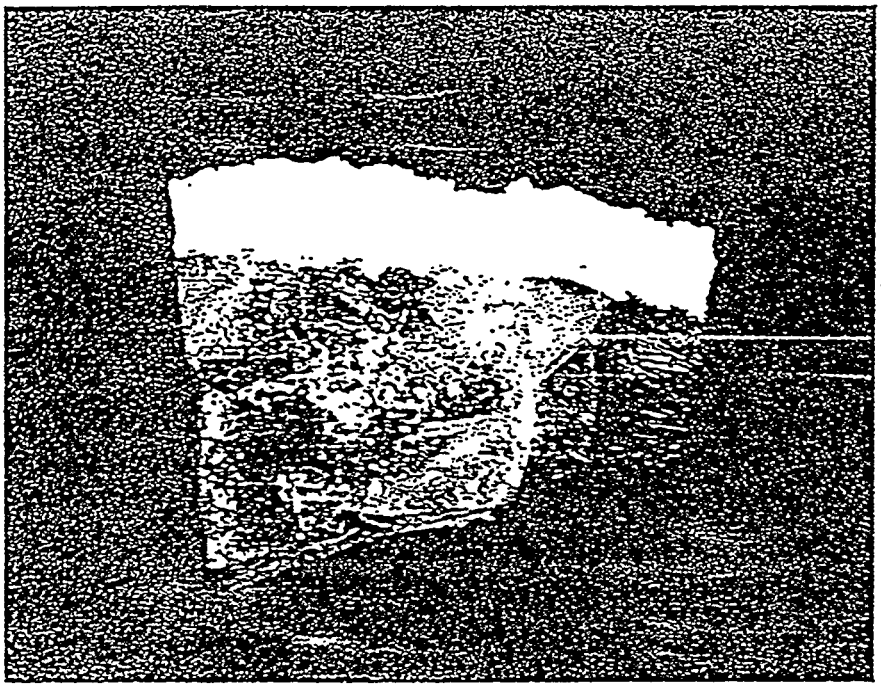

Figure 14. Optical micrograph of L6-5412 glass spiked with 2.0 wt%SO_3 and melted at 1300 °C, showing phase segregation in a meniscus area (mag. 8X).

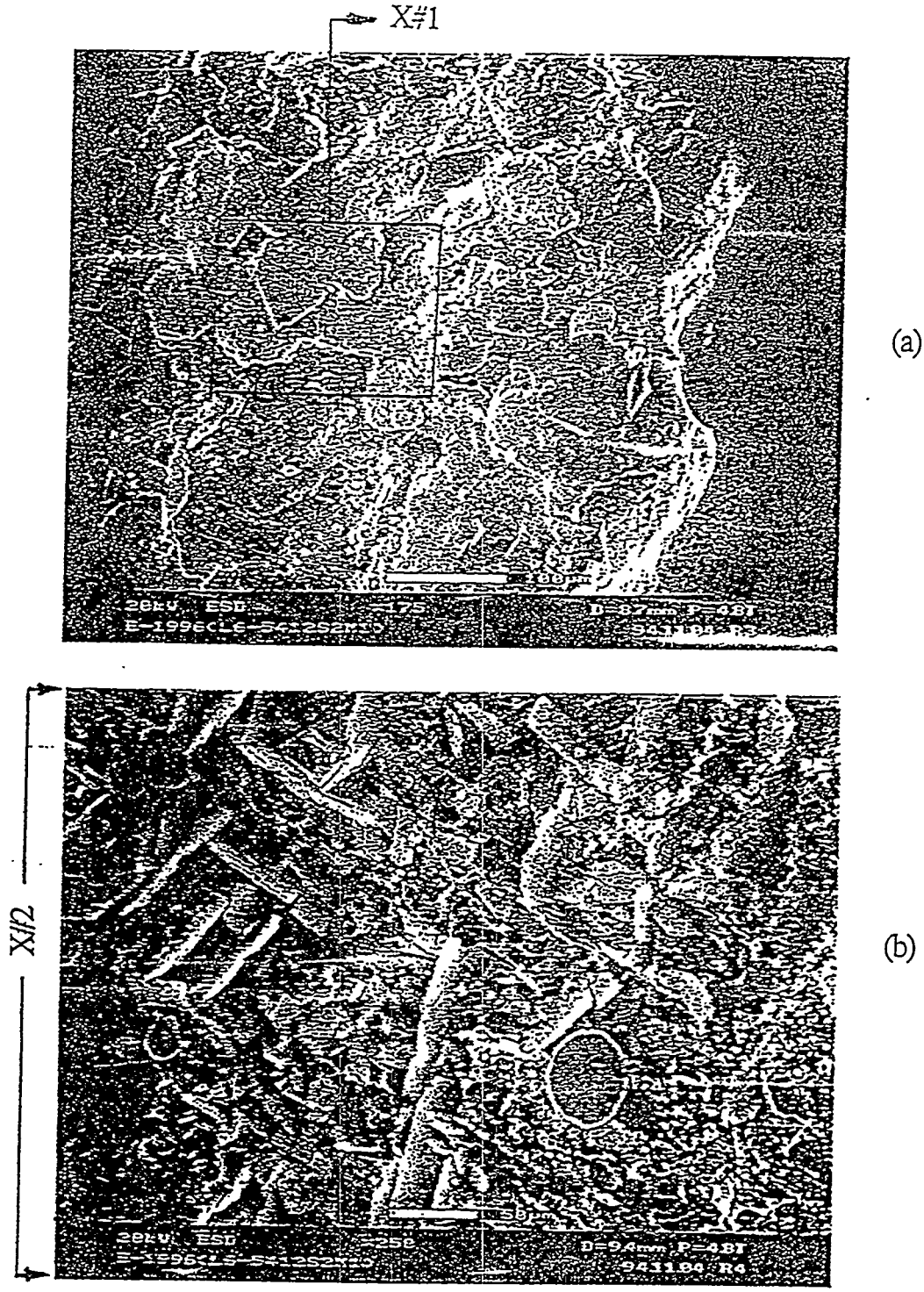

Figure 16. SEM micrographs of L6-5412 glass spiked with 2.0 wt%SO_3 and melted at 1300°C, showing (a) plate-like, X#1, and (b) rod-like crystalline phases, X#2.

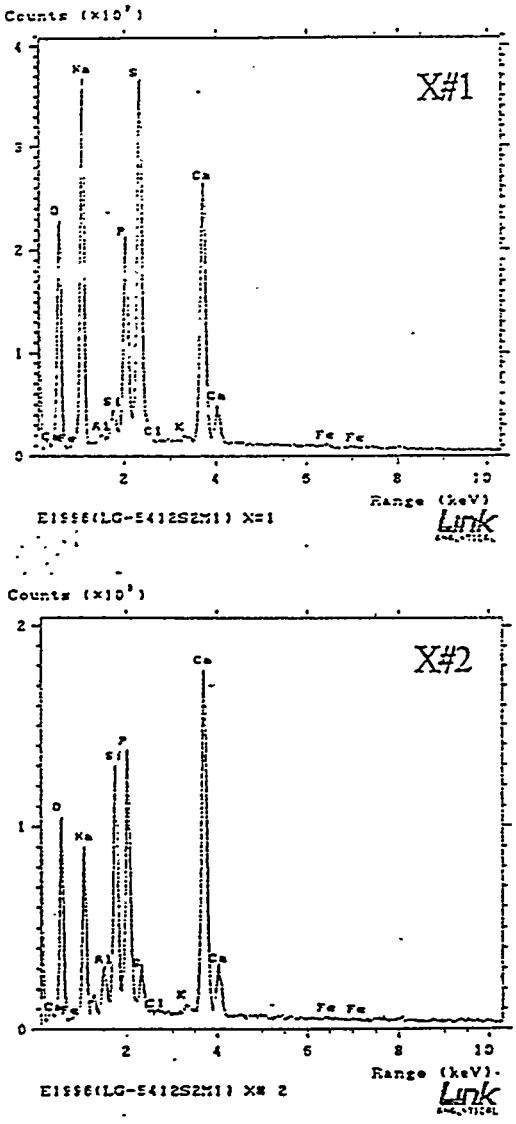

Figure 17. EDS patterns of (a) plate-like and (b) rod-like crystalline phases shown in Figure 16.

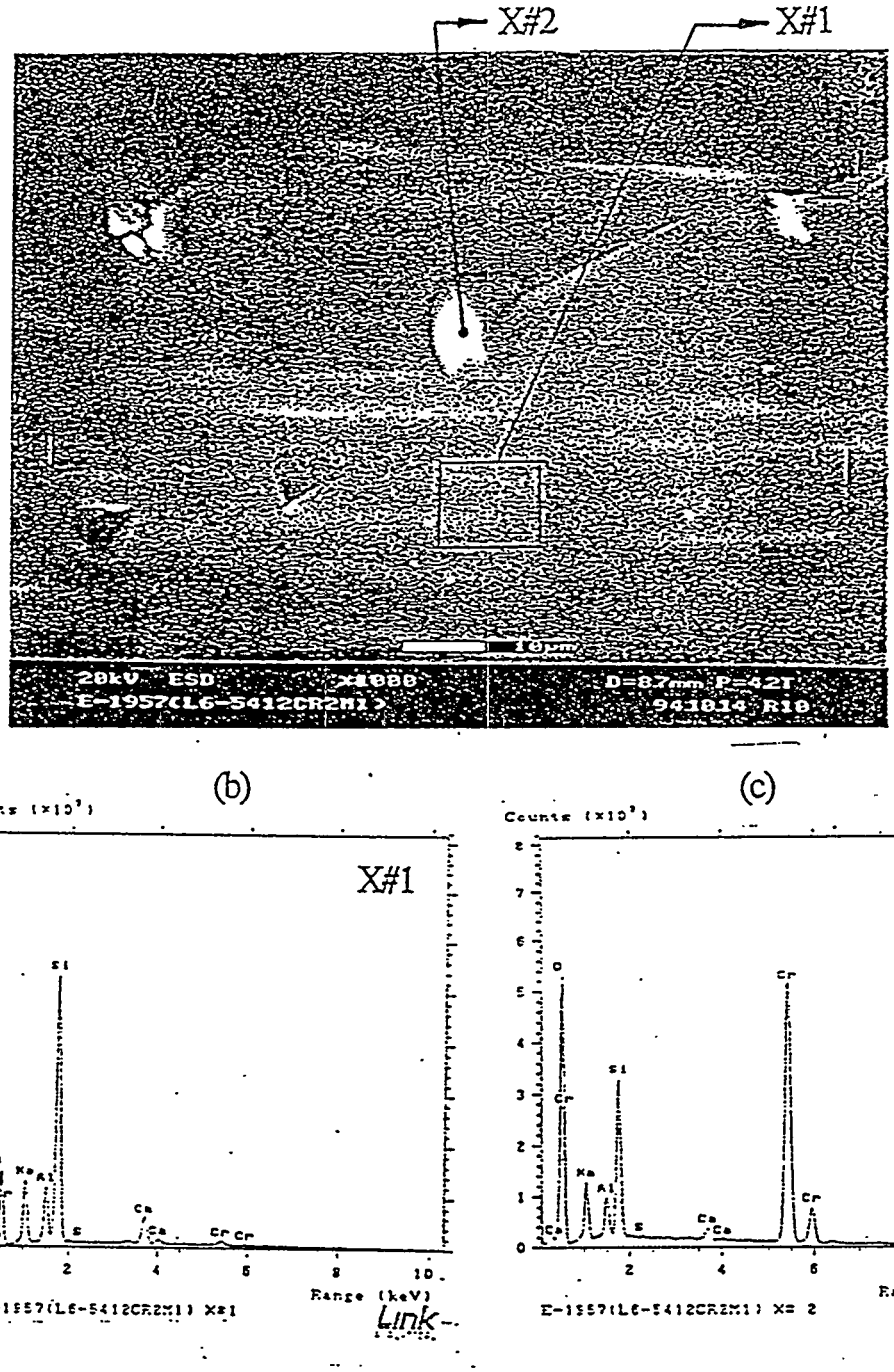

Figure 18. (a) SEM micrograph and (b-c) its corresponding EDS patterns, X#1 and X#2, for L6-5412 glass spiked with 2.0 wt%Cr_2O_3 and melted at 1300°C.

Effect of S-P Mutual Reaction on Melt Phase Segregation and Glass Phase Separation

Glass	L4-9012		L4-909		L6-5412		L5-0912	
	Conc.	Solubility	Conc.	Solubility	Conc.	Solubility	Conc.	Solubility
P2O5	2.20	4.97	2.05	(< 4.97)	2.24	2.50	2.29	(< 2.50)
SO3	0.57	0.47	0.68	(> 0.47)	0.88	0.75	1.00	(> 1.00)
Segregation	+++		+++		++		-	
Separation	+++		++		+		-	

Segregation : Accumulation of Molten Salts on the Melt Surafce (crystalline phase).

Separation : Two amorphous phases coexist in the bulk of glass, which have different compositions.

L6-5412 GLASS 1350°C

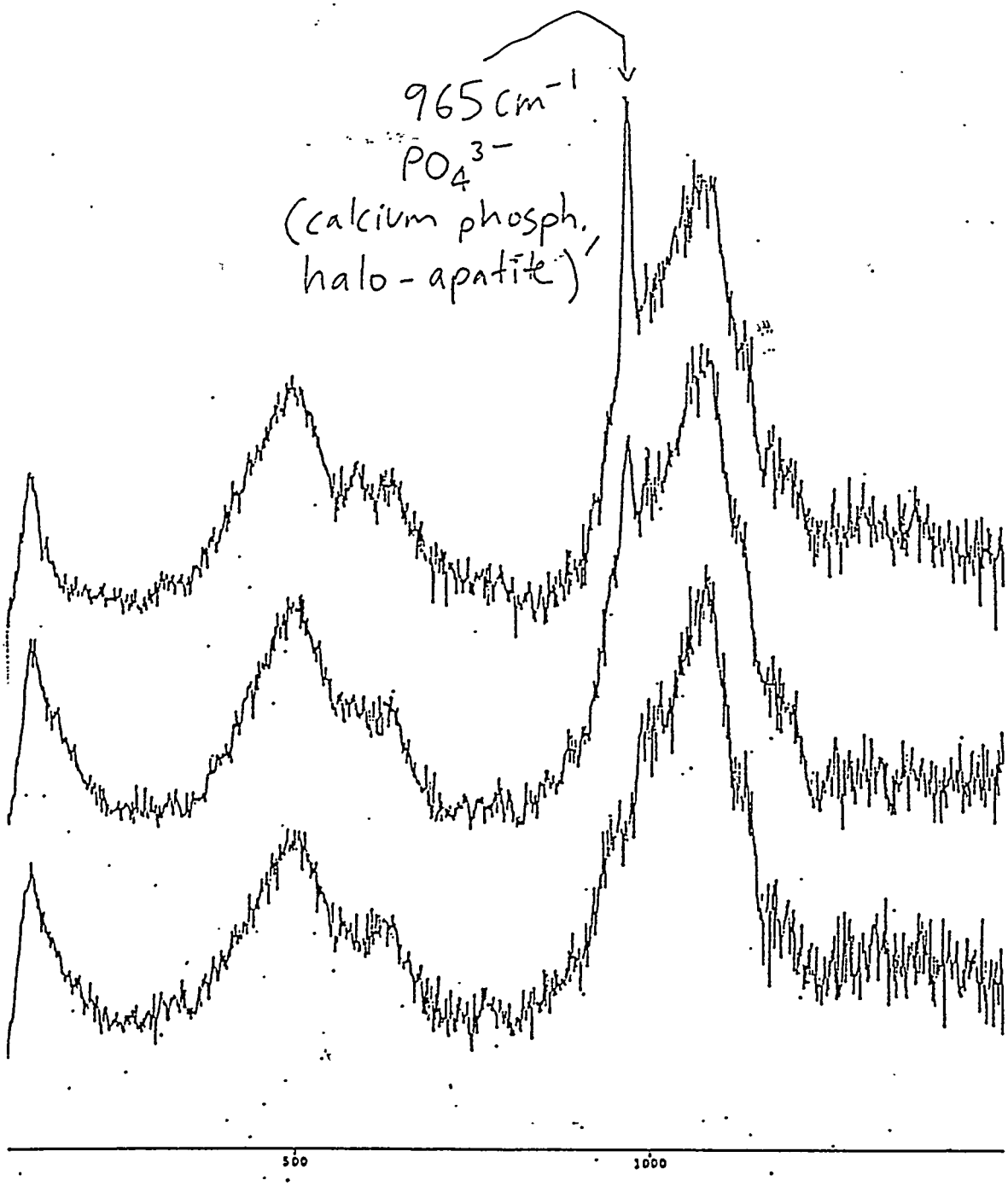

L4-9012 GLASS 1350°C

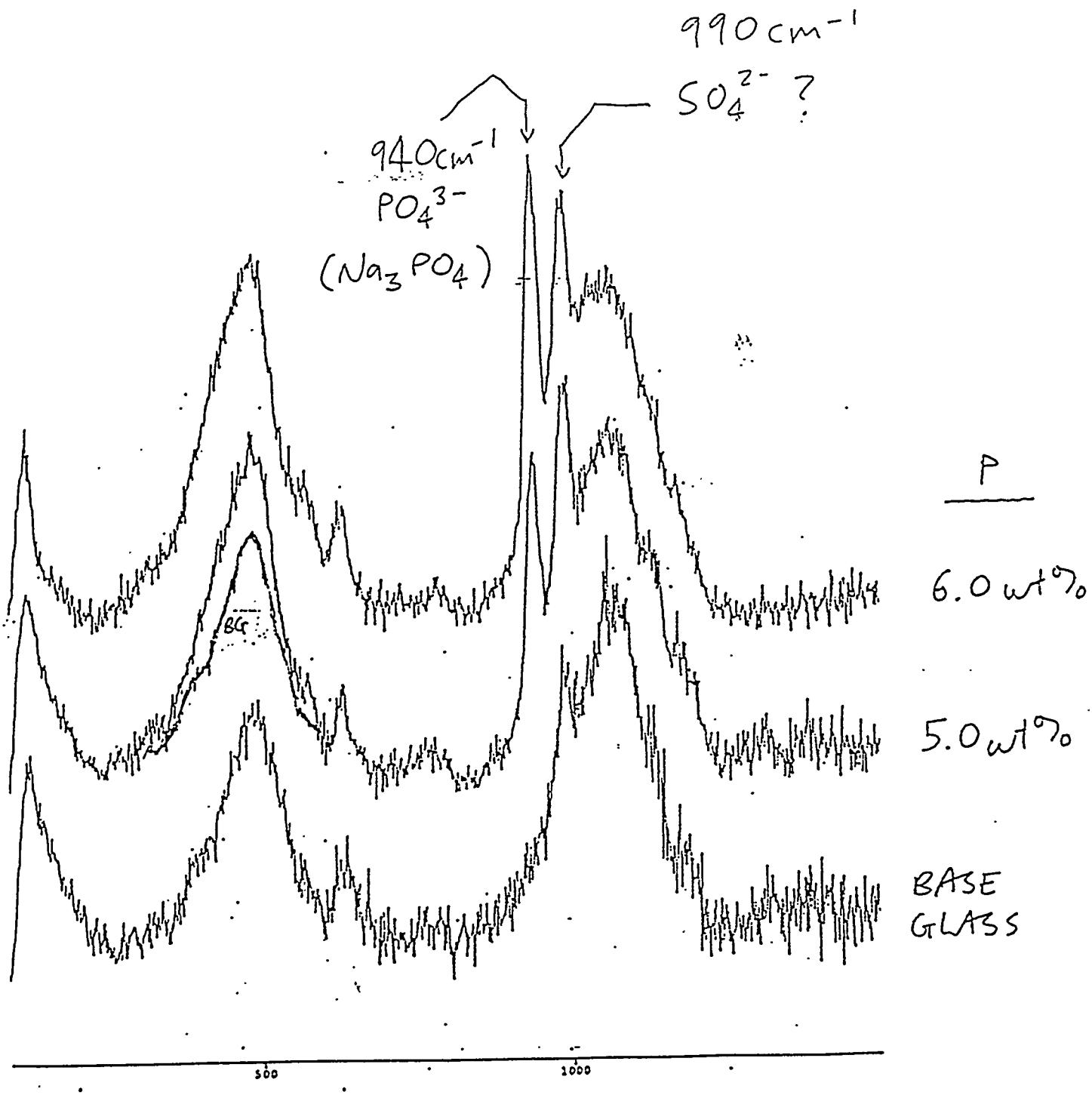

Effect of Minor Components on Glass Melting Temperature

Minor Component	L6-5412		L4-9012	
	ΔT_m (K)	$\Delta T_m/\Delta C_{MC}$ (K/wt%)	ΔT_m (K)	$\Delta T_m/\Delta C_{MC}$ (K/wt%)
Cl	23.0	48.0	7.0	18.0
F	-67.0	-94.0	-129.0	-117.0
P_2O_5	10.0	11.0	21.0	5.0
SO_3	10.0	23.0	-3.0	-23.0
Cr_2O_3	3.0	7.0	-25.0	-25.0

Effect of Minor Components on Glass Durability

Minor Component	PCT		FTT	
	ΔNL_{Na} (%)	$\Delta NL_{Na}/\Delta C_{MC}$ (%/wt%)	ΔNR_{Na} (%)	$\Delta NR_{Na}/\Delta C_{MC}$ (%/wt%)
Cl	12.0	25.0	-17.0	-36.0
F	-9.0	-13.0	110.0	155.0
P_2O_5	20.0	21.0	6.0	7.0
SO_3	8.0	18.0	5.0	14.0
Cr_2O_3	25.0	57.0	13.0	30.0

• Glass Melt Viscosity

Cl and P_2O_5 : Increasing

F : Decreasing

SO_3 and Cr_2O_3 :

Increasing (low B_2O_3 glass)
Decreasing (high B_2O_3 glass)

Effects of Minor Components on Melt Viscosity of L6-5412 Glass

Temperature range : 1200 - 1450 °C

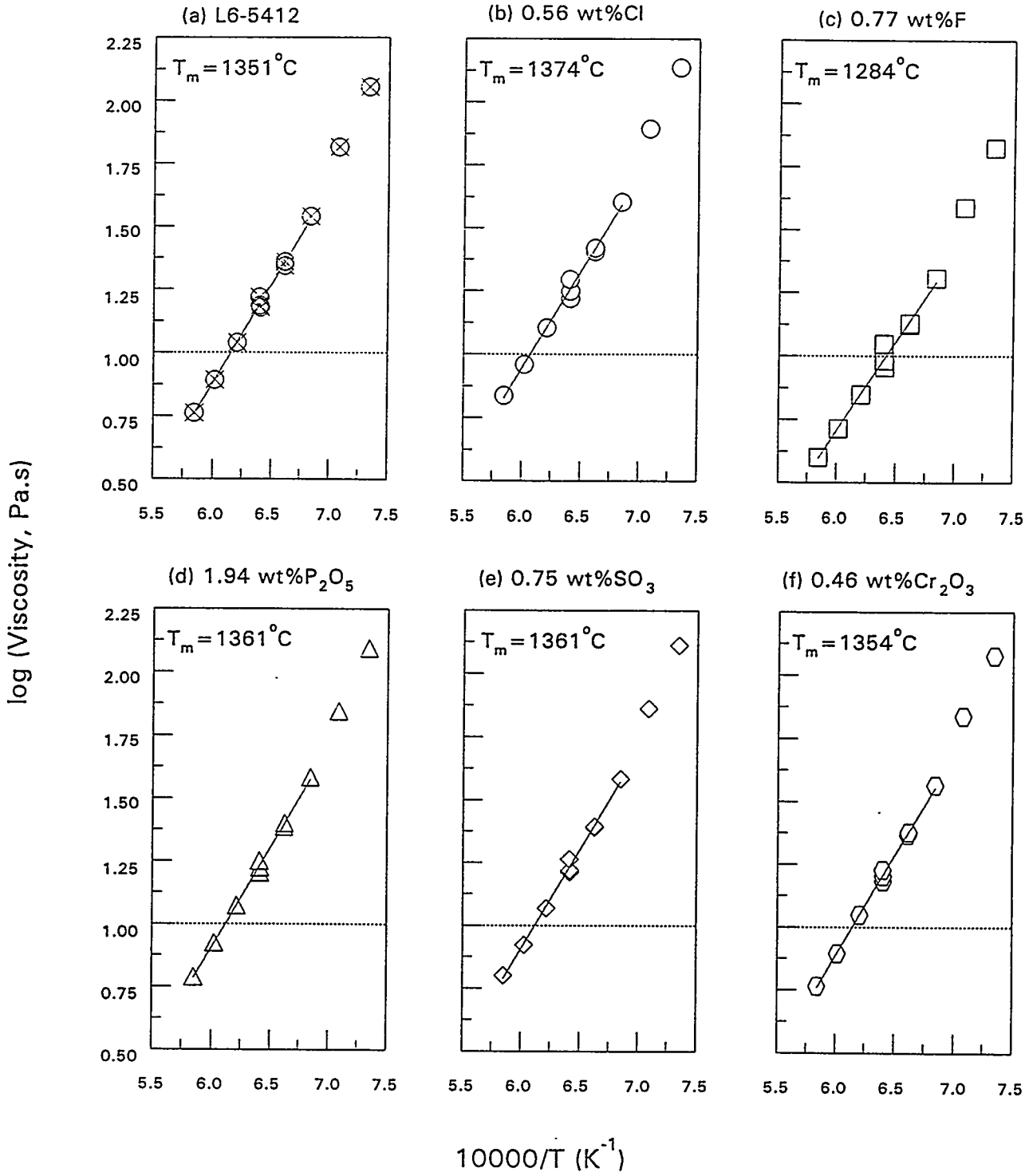

Effects of Minor Components on Melt Viscosity of L4-9012 Glass

Temperature range : 1150 - 1450 °C

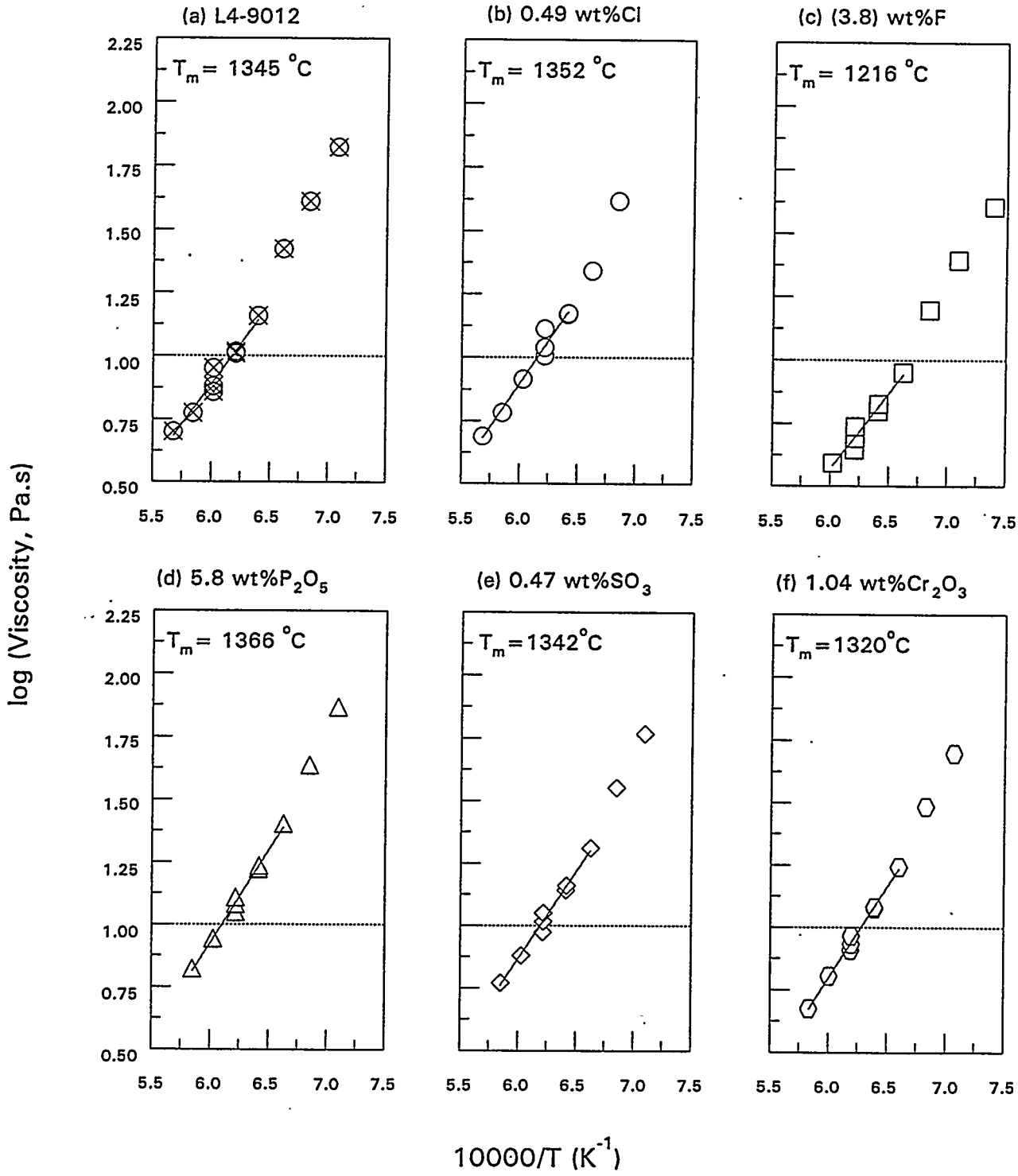

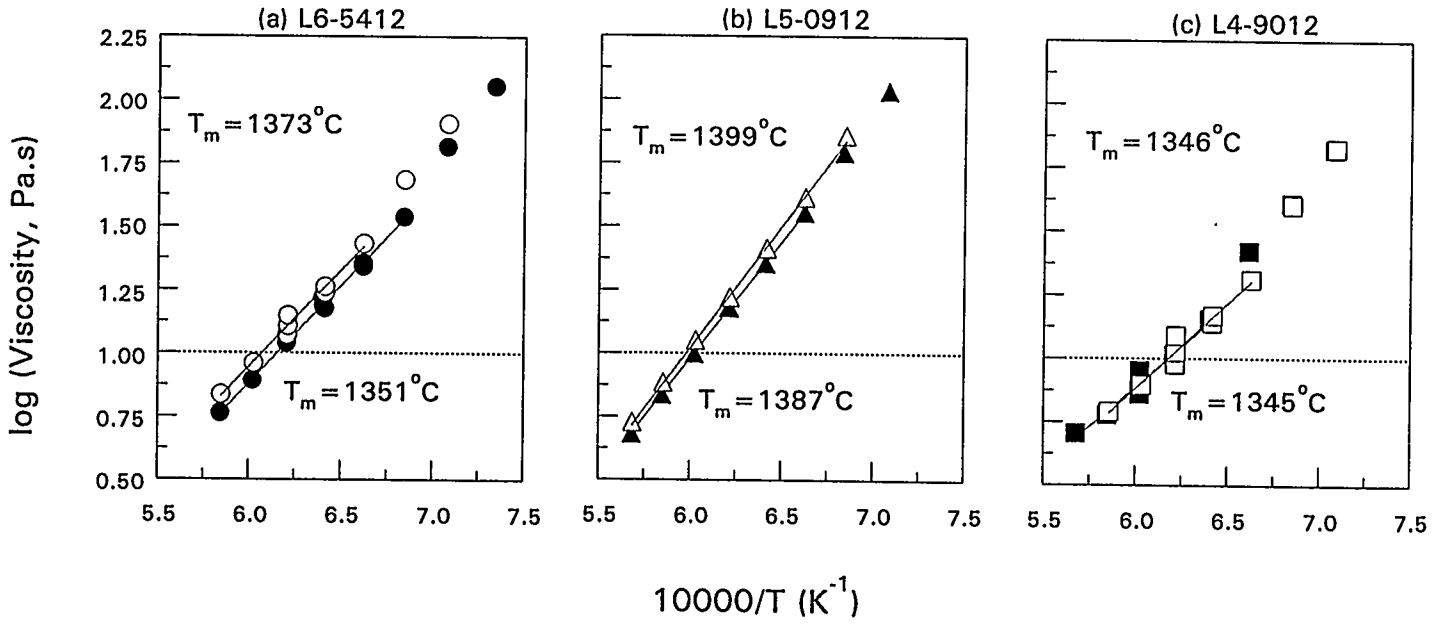

Effect of SO_3-P_2O_5 on Melt Viscosity of LLW Glasses

Decreasing

• Glass Durability

Product Consistency Test

F : Increasing
Cl, P_2O_5, SO_3, and $\underline{Cr_2O_3}$: Decreasing

Flow-Through Test

Cl : Increasing
$\underline{F}$, P_2O_5, SO_3, and Cr_2O_3 : Decreasing

(An underline is used for a component affecting the durability the most)

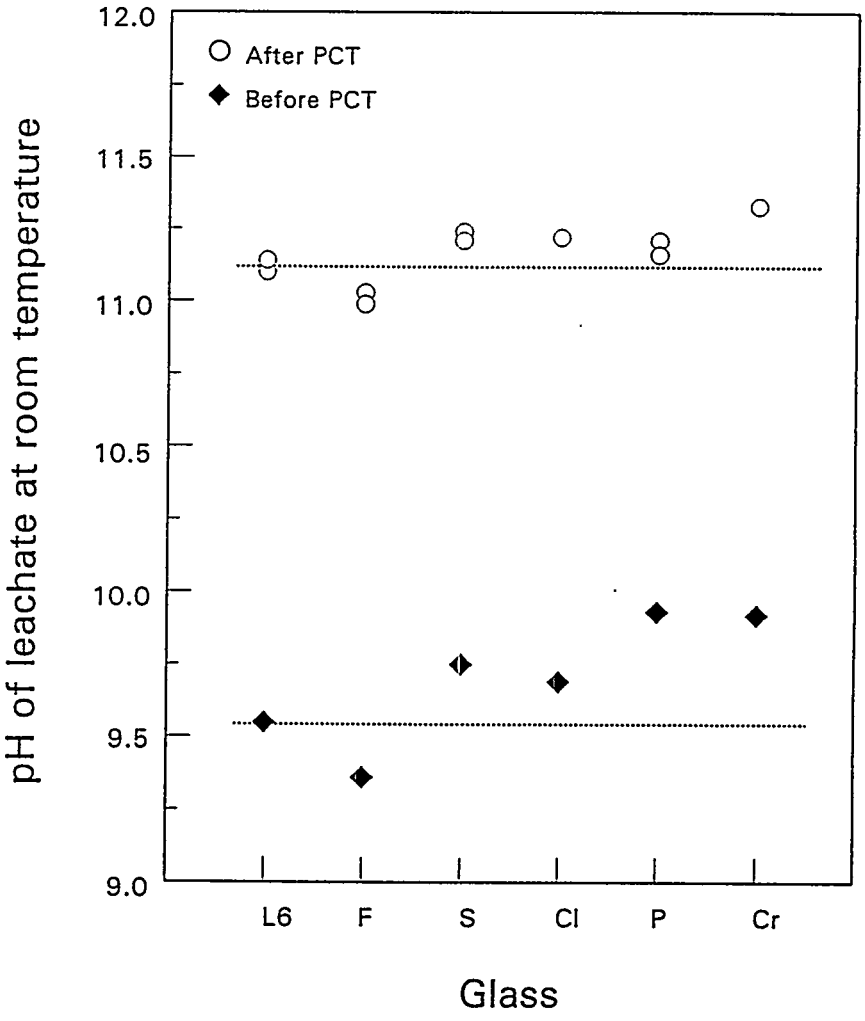
12.0
11.5
11.0
10.5
10.0
9.5
9.0
After PCT
Before PCT
pH of leachate at room temperature
L6
F
S
Cl
P
Cr
Glass

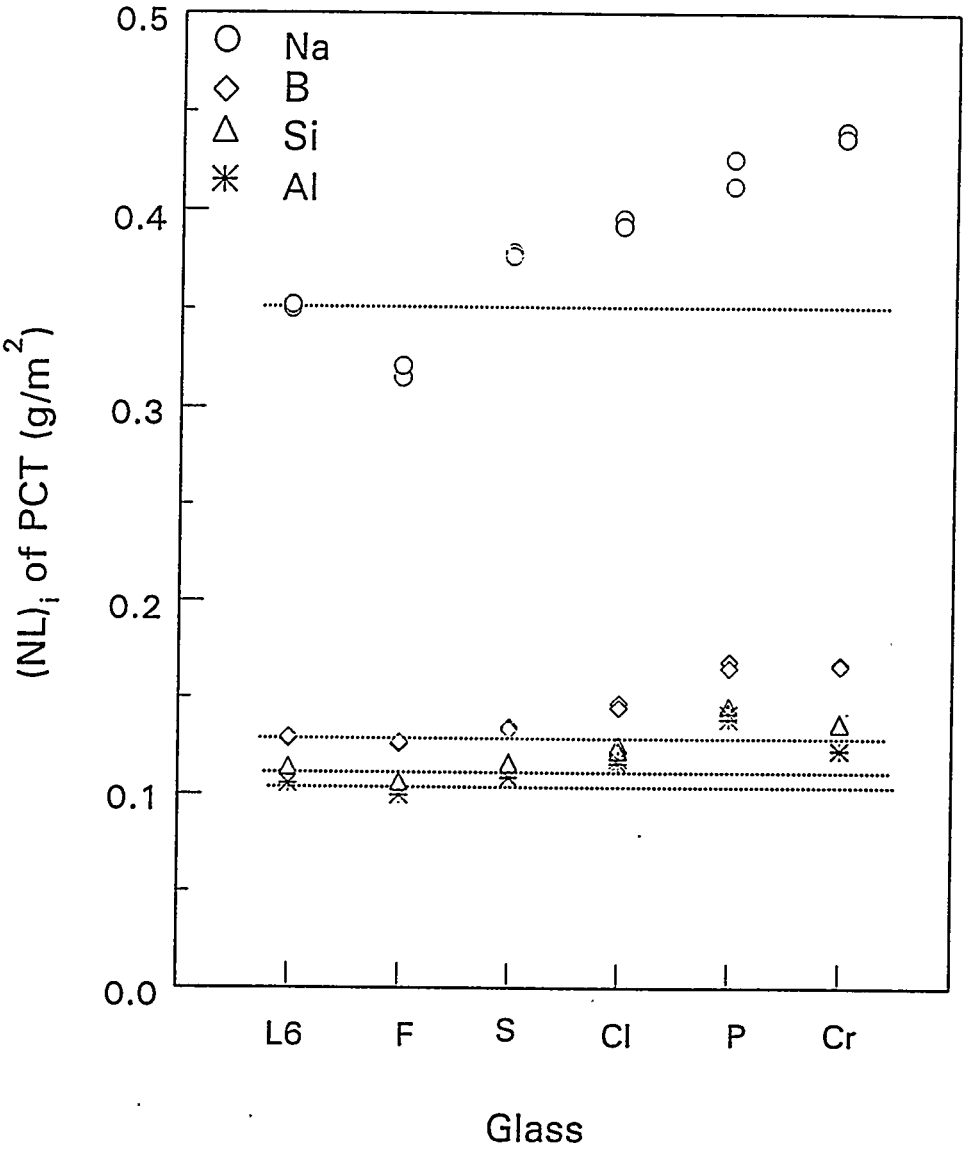
0.5
0.4
0.3
0.2
0.1
0.0
Na
B
Si
Al
(NL)i of PCT (g/m2)
L6
F
S
Cl
P
Cr
Glass

Base-line glass: L6-5412

7-day PCT (90 °C - 2000 m^{-1} - DIW)

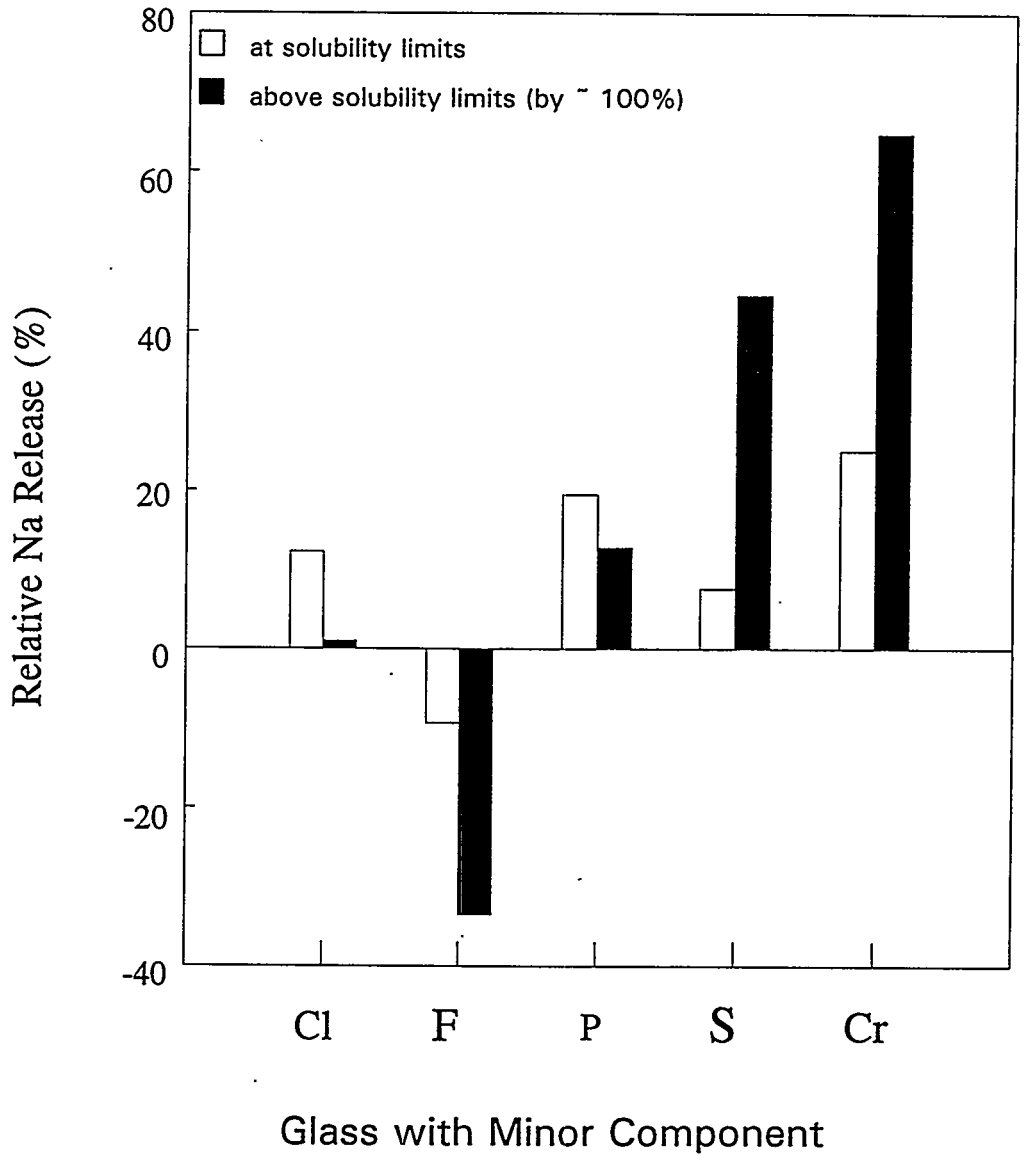

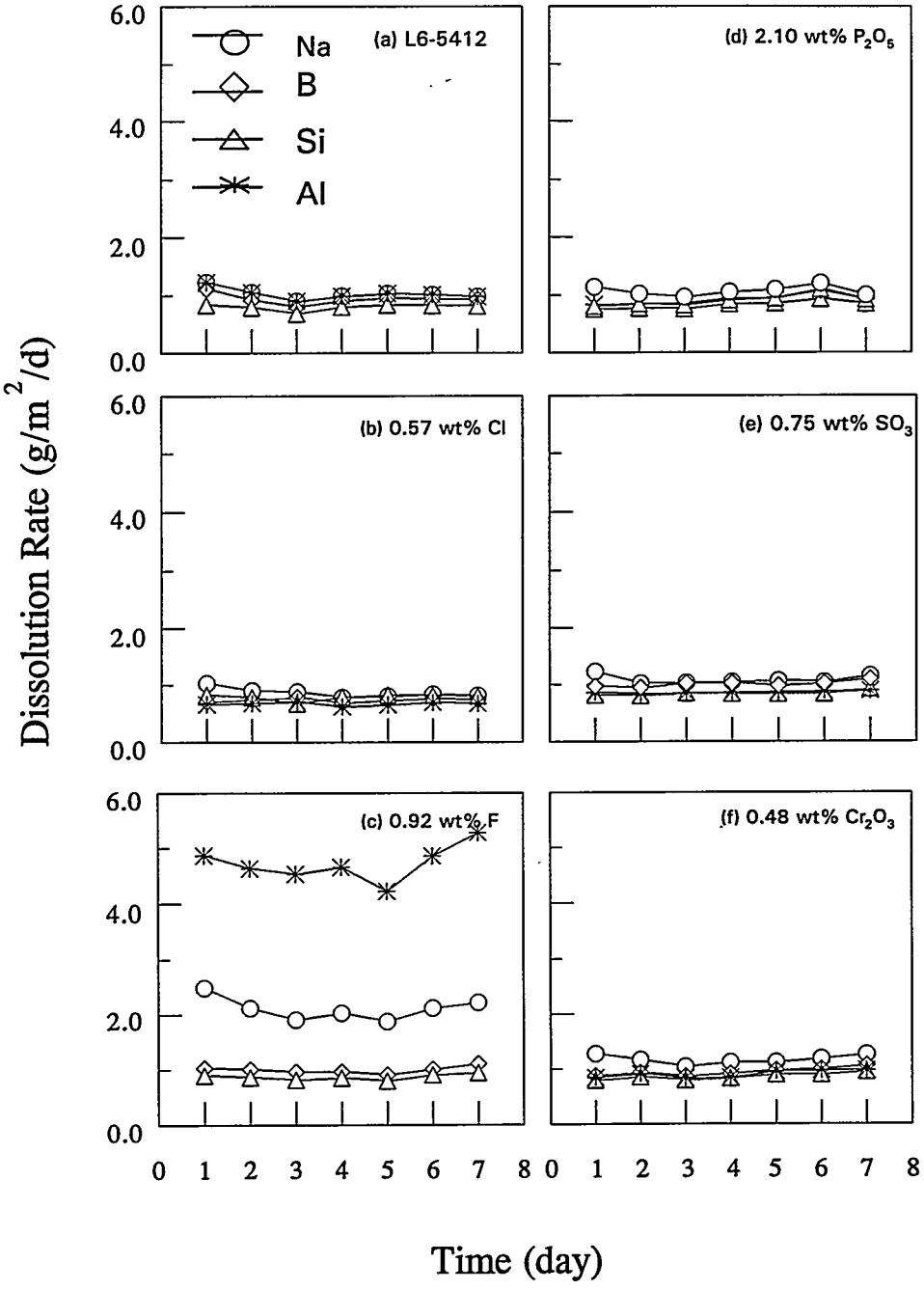
Na
B
Si
Al
(a) L6-5412
(b) 0.57 wt% Cl
(c) 0.92 wt% F
(d) 2.10 wt% P_2O_5
(e) 0.75 wt% SO_3
(f) 0.48 wt% Cr_2O_3
Dissolution Rate (g/m^2/d)
Time (day)
6.0
4.0
2.0
0.0
0 1 2 3 4 5 6 7 8

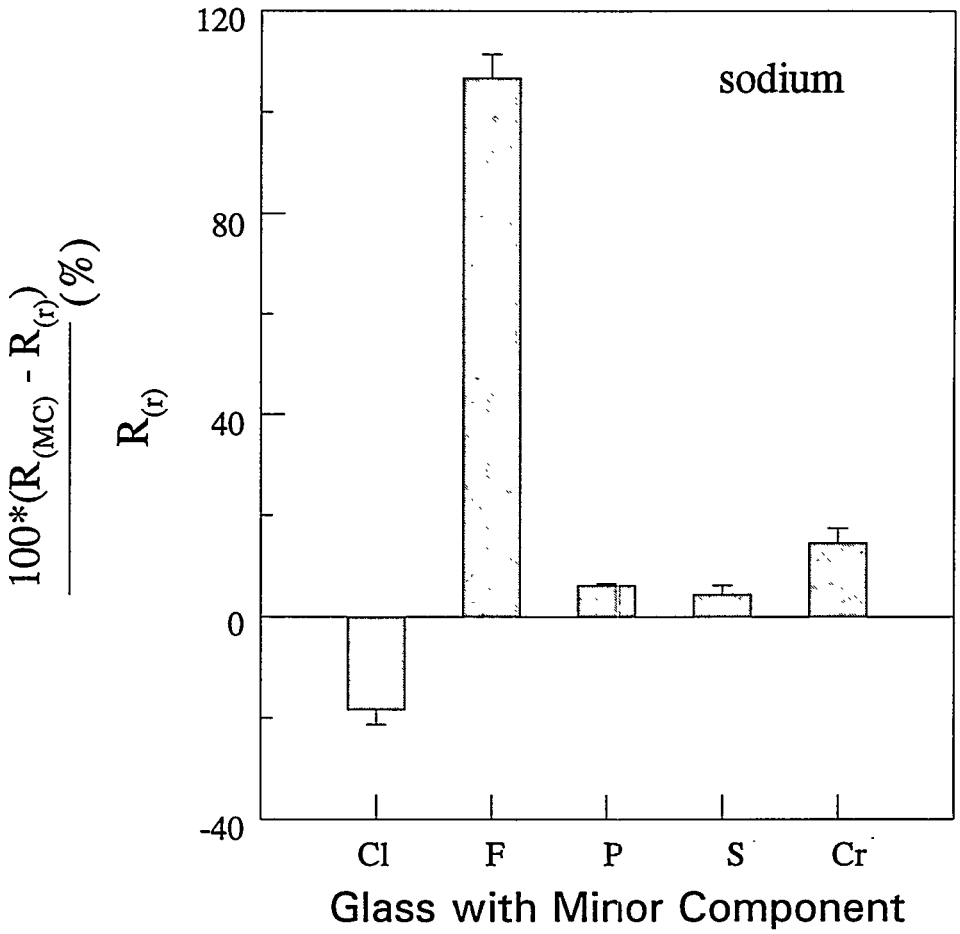
sodium
120
80
40
0
-40
Cl
F
P
S
Cr
Glass with Minor Component
100*(R(MC) - R(r)) / R(r) (%)

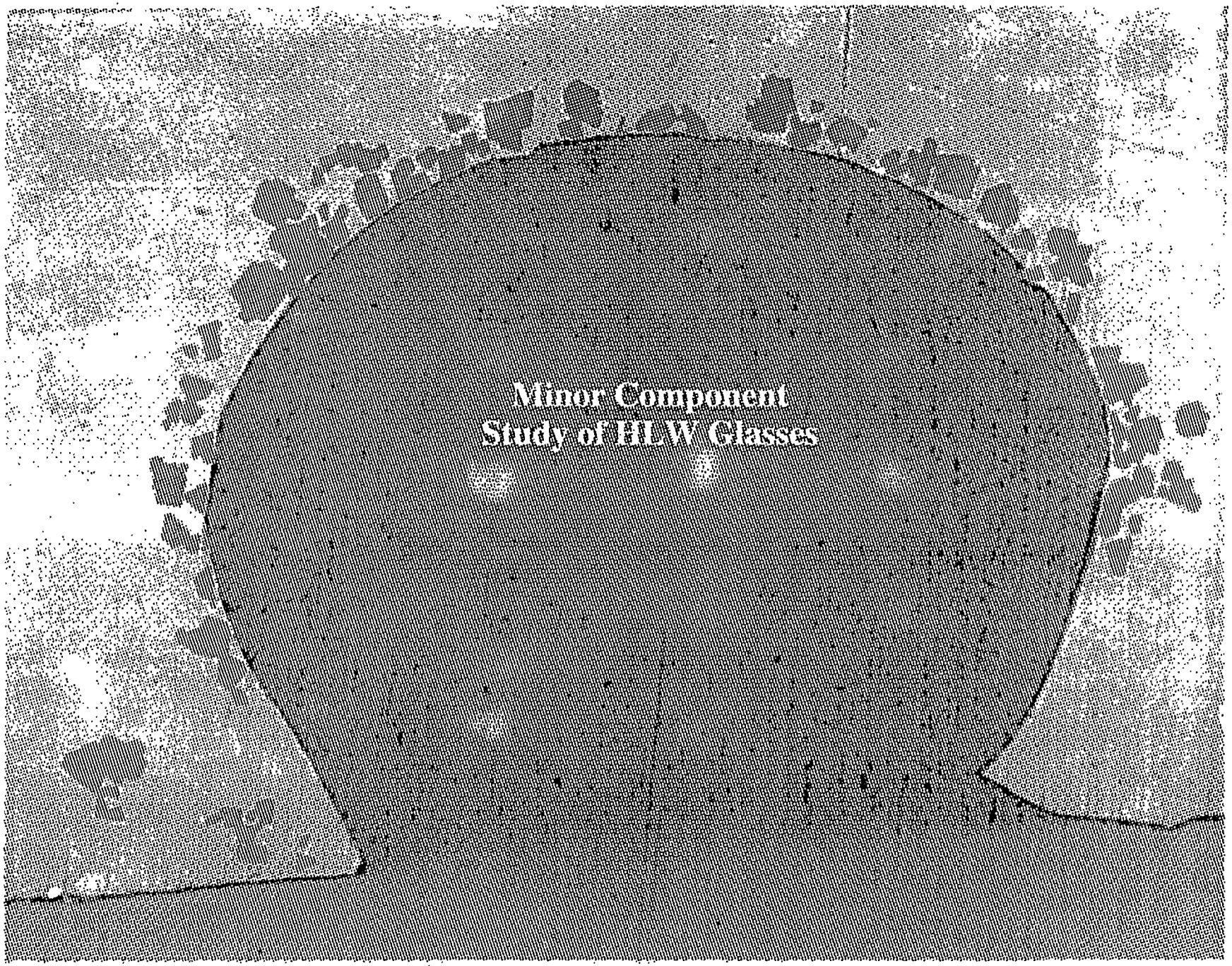
Minor Component
Study of HLW Glasses

Compositions (mol%) of PFP Glasses

Waste Loading - 40.0 wt%

Glass	PFP1	PFP2	PFP3	PFP4	PFP5	PFP6	PFP7
	(high Na2O - low B2O3)			(low Na2O - high B2O3)			
SiO2	46.27	47.90	48.46	44.19	44.78	45.65	48.72
B2O3(#)	6.46	5.53	4.36	22.66	21.35	19.40	12.55
Na2O	21.95	20.88	20.75	6.88	6.84	6.77	6.53
Li2O	3.53	3.99	4.89	4.08	5.00	6.36	11.14
CaO	1.50	1.50	1.49	1.53	1.52	1.51	1.45
MgO	0.73	0.74	0.73	0.75	0.75	0.74	0.71
Fe2O3	2.24	2.23	2.21	2.28	2.26	2.24	2.16
Al2O3	8.46	8.43	8.38	8.62	8.56	8.48	8.18
ZrO2	0.05	0.05	0.05	0.05	0.05	0.05	0.04
P2O5	2.34	2.33	2.31	2.38	2.36	2.34	2.26
SO3	0.88	0.87	0.87	0.89	0.88	0.88	0.85
Others	5.59	5.56	5.53	5.69	5.65	5.59	5.40
SUM	100.00	100.00	100.00	100.00	100.00	100.00	100.00

Boric acid, H3BO3, was used

Compositions (mol%) of WV Glasses

Glass	WV-182	WV-182Al1	WV-182Al2
	(Al2O3 increasing)		
SiO2	52.20	48.96	45.00
B2O3	13.75	13.98	14.26
Na2O	17.29	17.58	17.94
Li2O	0.10	0.10	0.10
CaO	3.68	3.74	3.82
MgO	0.36	0.36	0.37
Fe2O3	5.18	5.26	5.37
Al2O3	1.83	4.29	7.30
ZrO2	1.19	1.21	1.23
P2O5	1.34	1.36	1.39
SO3	0.18	0.18	0.19
Others	2.92	2.97	3.03
SUM	100.00	100.00	100.00

Each glass was separately spiked with 1.0, 1.5, and 2.0 wt%SO3.

- Laboratory Scale Test

☞ Batch Melting (1150 °C)

PFP glasses
Crucible : Pt-10%Rh
Time : varied, and up to 2 hr
Batch Size : ~ 200 g

WV glasses
Crucible : Al_2O_3
Time : 1 hr
Batch Size : ~ 40 g

☞ Characterizations

Optical microscopy
SEM/EDS
XRD

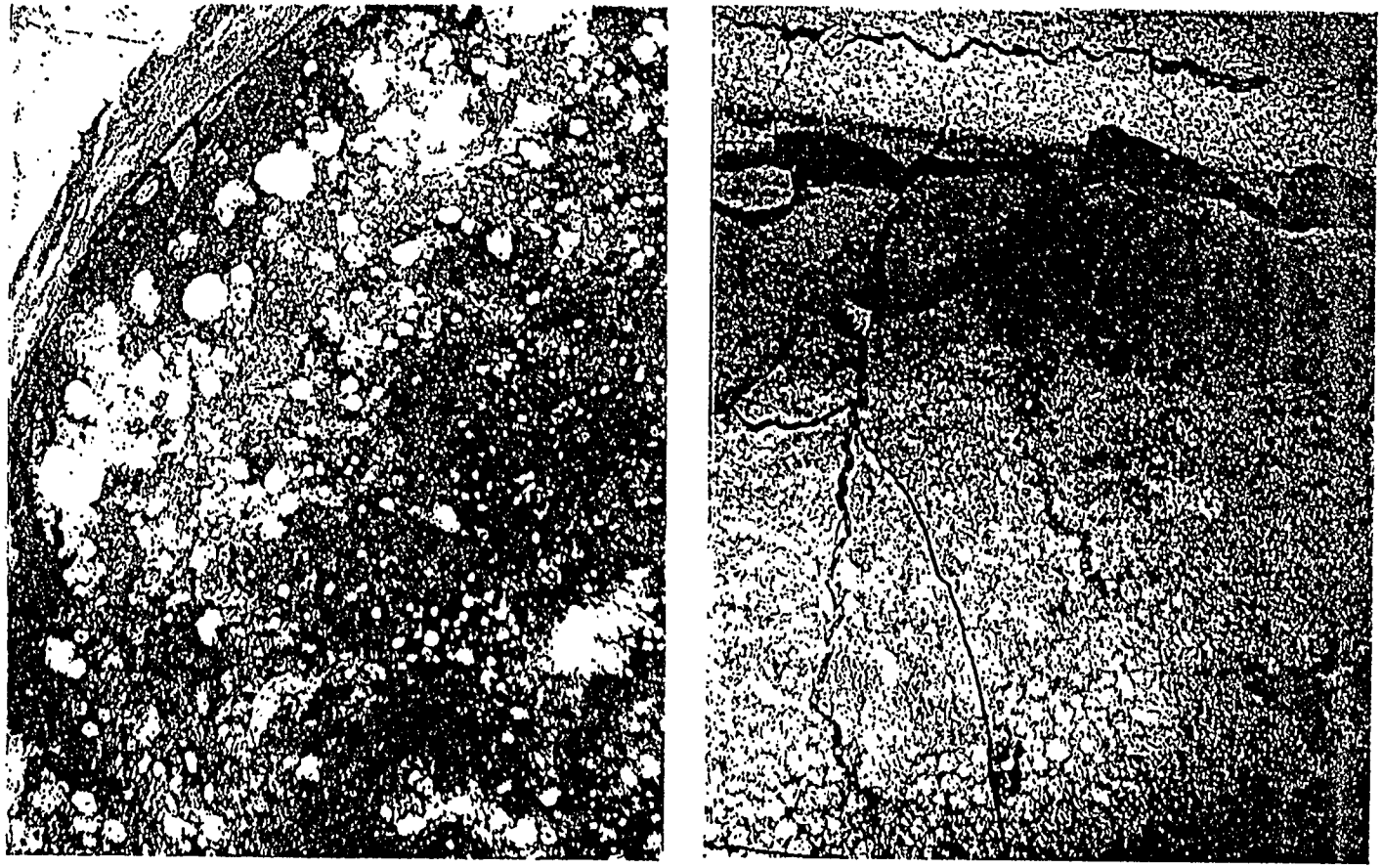

PFP 1 Glass Melt at 1150 °C

(a) 7 min (⌊——⌋ 5 mm)

(b) 60 min (⌊—⌋ 1 mm)

SEM/EDS of PFP 1 Glass Melt at 1150 °C for 7 min

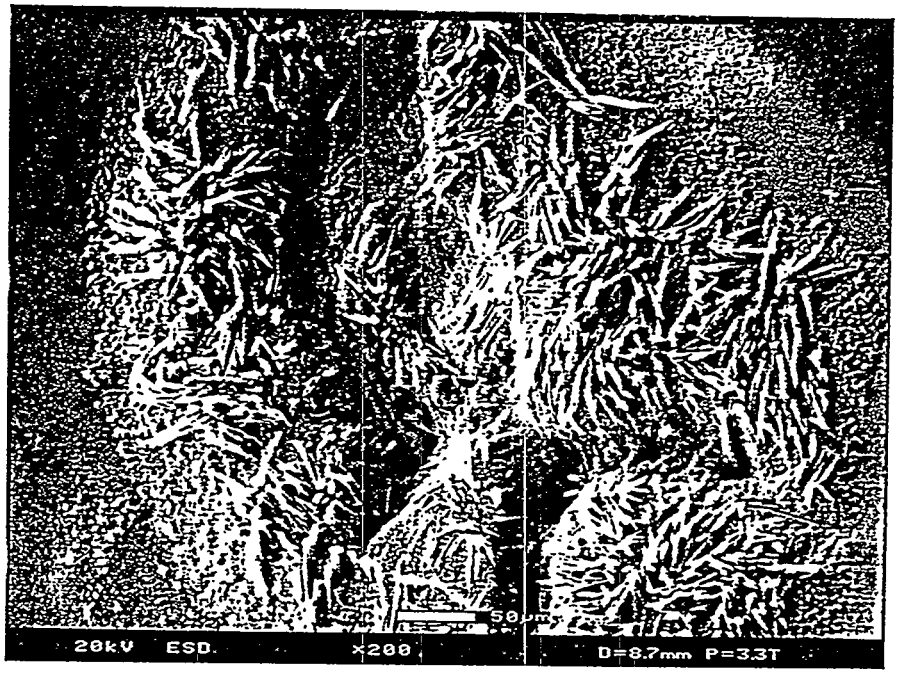

(b) area with segregated phases (Na_2SO_4 & Na_3PO_4)

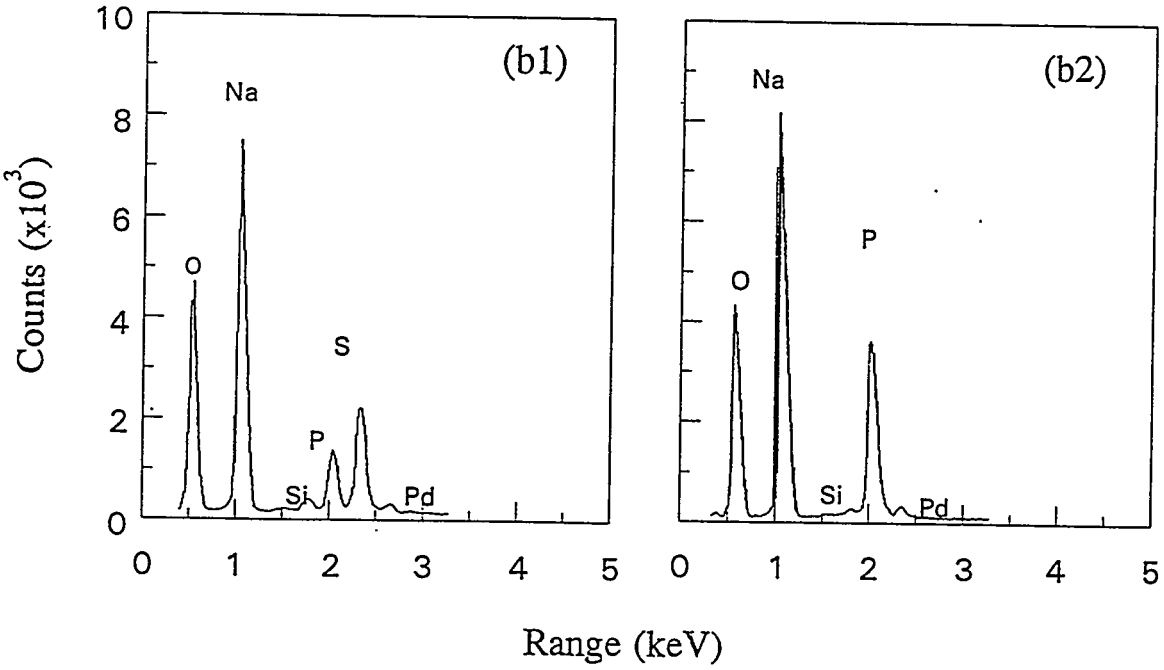

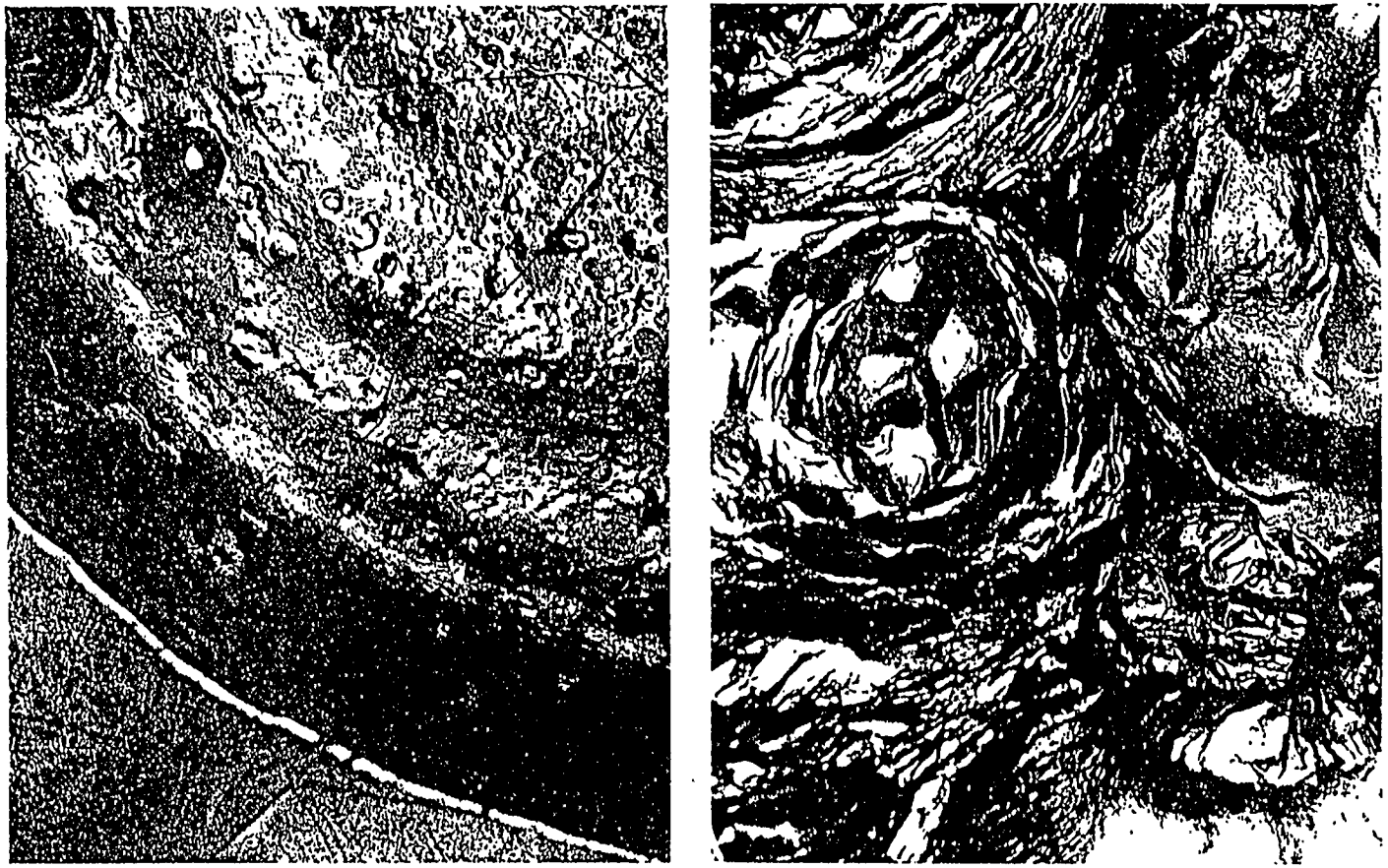

PFP Glass Melts at 1150 °C for 60 min

(a) PFP 7 (⌊——⌋ 5 mm)

(b) PFP 4 (⌊—⌋ 1 mm)

WV Glasses Spiked with 2.0 wt% SO_3

(1150 °C - 60 min)

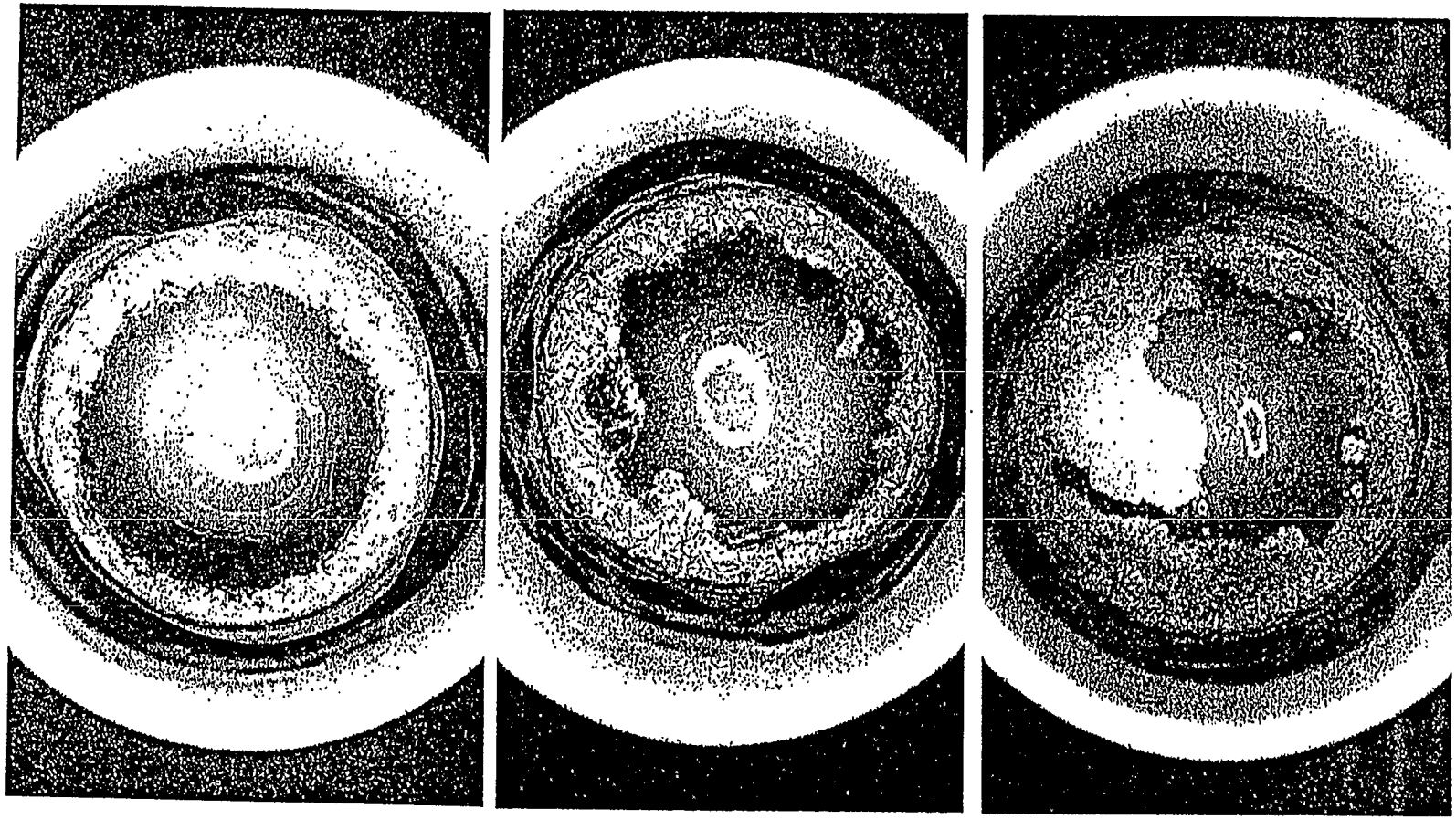

WV-182 WV-182Al1 WV-182Al2

Al_2O_3 increasing --------->

For a fixed P_2O_5 concentration

- Neither sulfate nor phosphate segregated from WV melts with lower SO_3 (about 1.0 wt%)
- Phosphate segregated from WV melts only at higher SO_3 (1.5 and 2.0 wt%)
- No phosphate segregation ocurred in PFP 4 to 7 melts (higher in H_3BO_3, but lower in Na_2O), in which sulfate segregation was suppressed.
- Phosphate segregation occured in PFP 1 to 3 melts (lower in H_3BO_3, but higher in Na_2O), in which sulfate segregation was also observed.

Phosphate segregation is promoted by the segregated sulfate phase.

Sulfate Solubility in Silicate Glass

$$\equiv Si\text{-}O\text{-}Si\equiv + 2Na^{+} : O^{2-}\ (glass) \Longleftrightarrow 2(\equiv Si\text{-}O^{-} : Na^{+})\ (glass)$$

$$SO_3\ (gas) + 2Na^{+} : O^{2-}\ (molten\ salt) \Longleftrightarrow 2Na^{+} : SO_4^{2-}\ (molten\ salt)$$

$$[SO_4^{2-}] \propto P(SO_3) * [Na^{+}]^2[\equiv S\text{-}O^{-}]^2 / [\equiv Si\text{-}O\text{-}Si\equiv]$$

(Ref: K. Papadopoulos, Phys. Chem. Glasses, 14 (1973) 60-65)

Phase segregation is a kinetic process.

- Phase segregation initiated at the early stages of batch melting
- "High S solubility" batches showed sulfate segregation

  (PFP 1 to 3 : higher in Na_2O and lower in B_2O_3)

- No difference in phase segregation was observed among PFP 1, 2, and 3 with increasing Li_2O (3.5 - 4.9 mol%)

- Effect of H_3BO_3 on Phase Segregation

Glass	B_2O_3	Na_2O	Seg.	Foam
PFP 1-3	4.4-6.5	22.0-21.0	Yes	No
WV#	~ 14.0	17.0-18.0	Yes	No
PFP 4-7	23.0-13.0	~ 7.0	No	Yes

(# Batches spiked with 1.5 and 2.0 wt% SO_3)

PFP 3 Glass Melt at 1150 °C for 60 min

(a) surface (⌊——⌋ 5 mm)

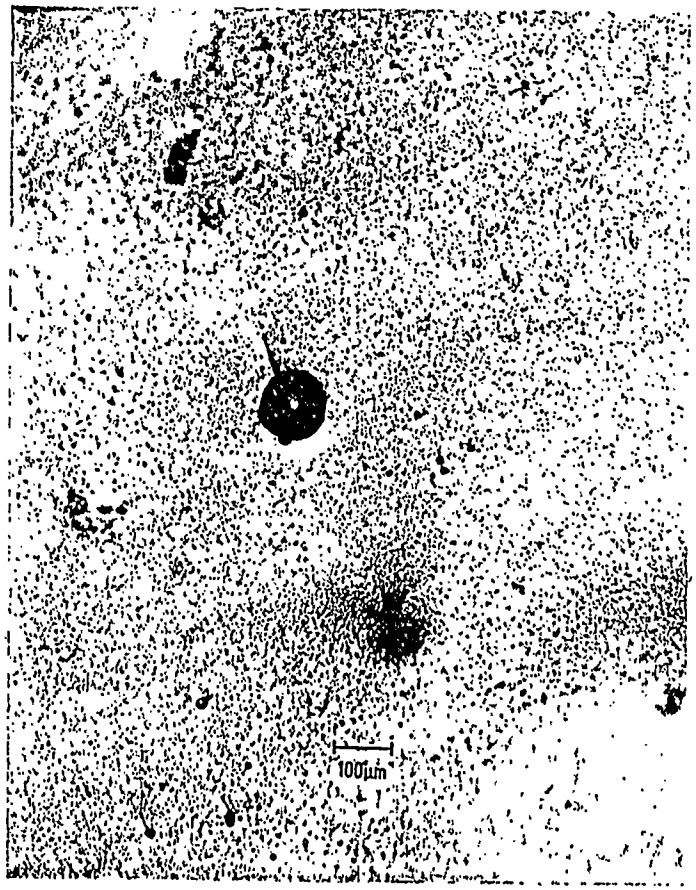

(b) bulk

PFP 5 Glass Melt at 1150 °C for 60 min

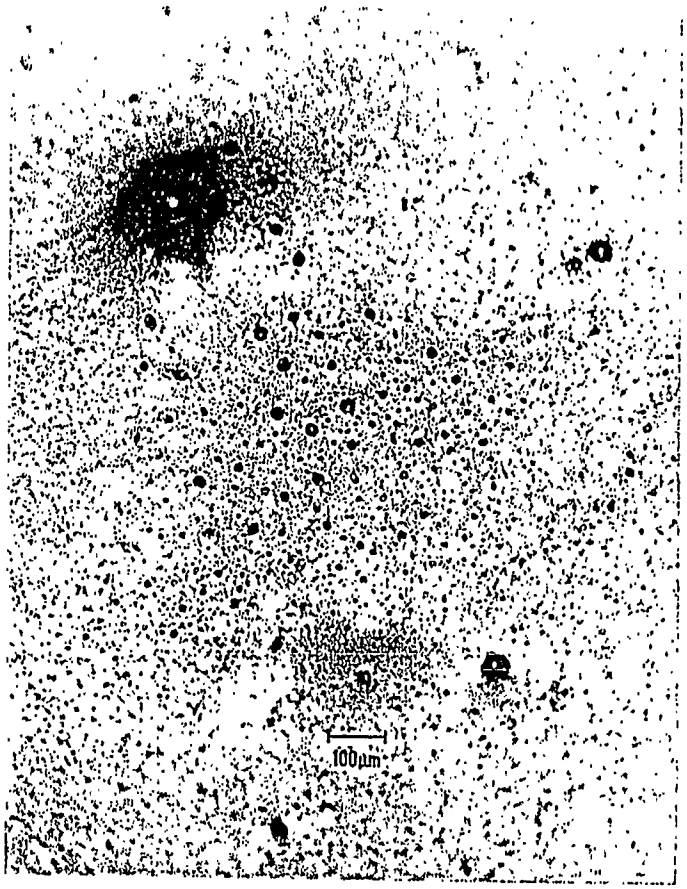

(a) surface (——— 5 mm)

(b) bulk

A link between Foaming and Segregation

- Sulfate depresses mild melt foaming
  (sulfate - foaming breaker)

Ref 1:

D.S. Kim and P.R. Hrma, "Volume Changes During Batch to Glass Conversion" Ceram. Bull. 6[6] 1039 (1990)

Ref 2:

MJ. Plodinec,"Vitrification of Savannah River Radioactive Waste Process Development Studies," USDOE Report, DP-MS-79-42, SRL, E.I. du Pont de Nemours & Co., Wilminton, DE (1987).

- Vigorous melt foaming suppresses sulfate segregation
  (H_3BO_3 - foaming agent)

Sulfate spreads on large surface area created by foam (or bubbles) and subsequently dissolves in the melt.

SUMMARY

- Phase segregation is a kinetic process, which initiated at the early stages of batch melting.
- Segregation of molten sulfate from melt promoted phosphate segregation.
- Phase segregation was suppressed by high H_3BO_3-induced vigorous melt foaming.
- Extent of phase segregation increased with an increase of Al_2O_3.

WHAT IS THE NEXT ?

MUTUAL REACTIONS BETWEEN MINOR COMPONENTS

GLASS COMPOSITION DESIGN TO MINIMIZE THE MUTUAL REACTIONS

Understanding Glass Composition Effects on Chemical Durability

Xiangdong Feng

June 27, 1995

Glass Science and Engineering Tutorial
Westinghouse Hanford Company
Richland, Washington

Glass Durability

- The ability of glass to resist corrosion, weathering, or leaching
- It is measured by durability tests and expressed as release rate of glass components or rate of weight loss, or depths of alteration

Factors Affecting Glass Durability

- Glass composition
  - Individual oxides
  - Redox
  - Charge and size
- Processing
  - Crystallization
  - Phase separation
  - Glass stress
- Testing parameters
  - Methods (PCT, flow-through, vapor-hydration)
  - SA/V
  - Leachant composition
  - Temperature

Individual Oxide Effects on Glass Durability

- SiO_2
- $Al2O_3$
- ZrO_2
- B_2O_3
- CaO
- Fe_2O_3
- Na_2O

Search for Optimized Glass Composition

- Which oxide is most effective in improving glass durability?
- Is the effect linear?
  (i.e. same improvement is expected for equal additions)
- Is the effect always consistent?
  (i.e., always positive or always negative)
- Does the redox state of the element matter?
  – Fe (II) vs. Fe(III)

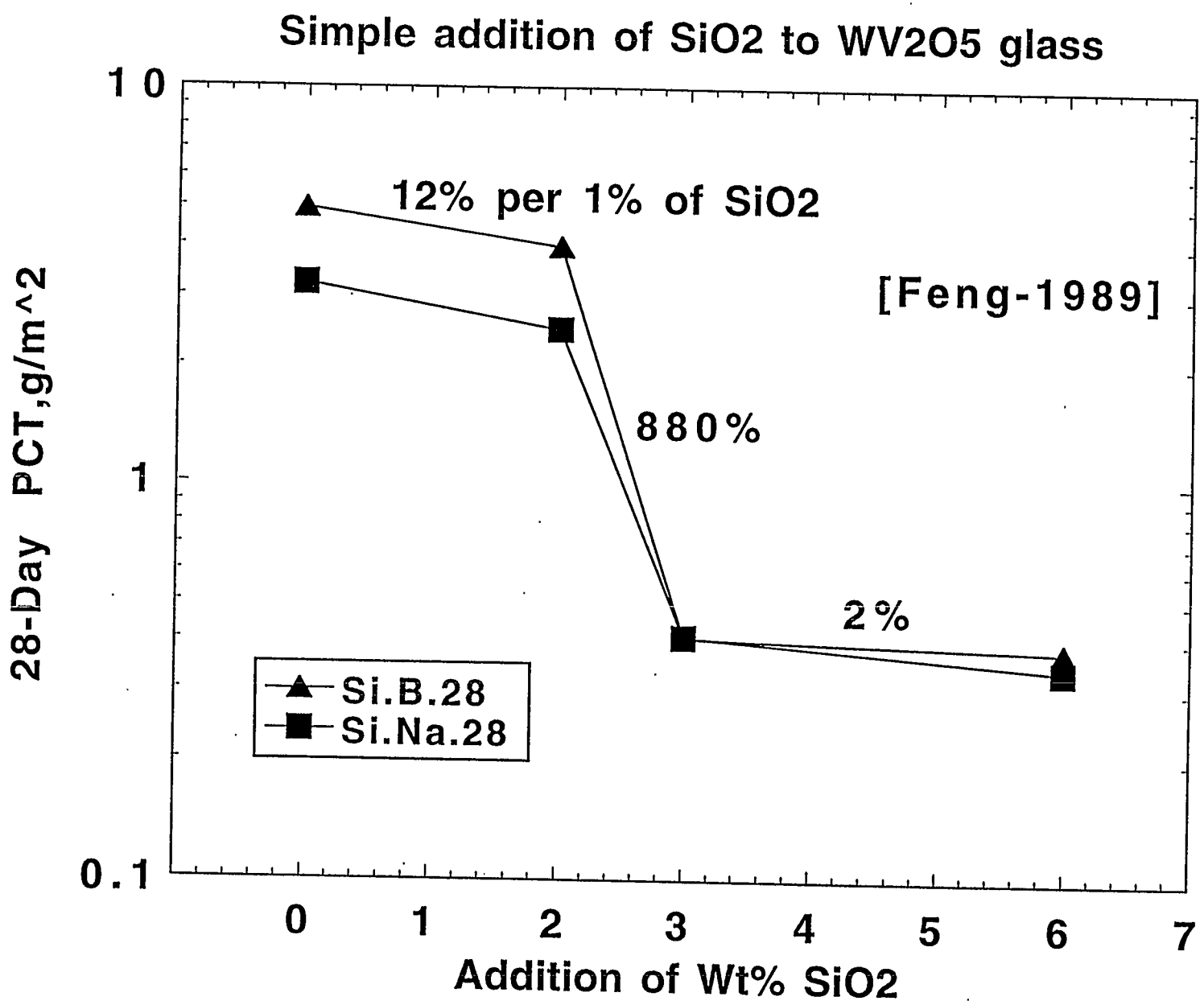
Simple addition of SiO2 to WV2O5 glass
10
1
0.1
28-Day PCT,g/m^2
12% per 1% of SiO2
[Feng-1989]
880%
2%
Si.B.28
Si.Na.28
0
1
2
3
4
5
6
7
Addition of Wt% SiO2

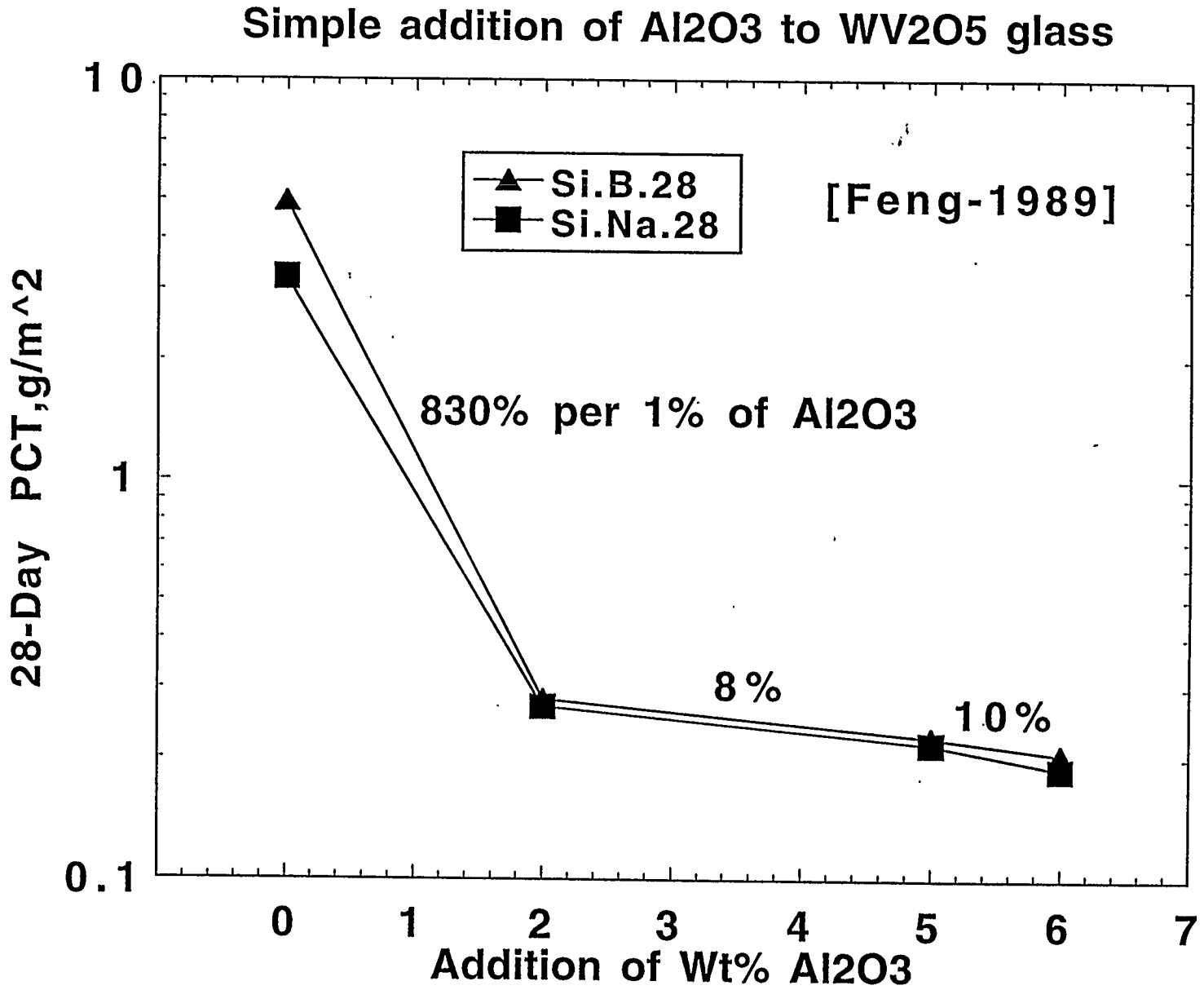
Simple addition of Al2O3 to WV2O5 glass
10
1
0.1
28-Day PCT,g/m^2
Si.B.28
Si.Na.28
[Feng-1989]
830% per 1% of Al2O3
8%
10%
0
1
2
3
4
5
6
7
Addition of Wt% Al2O3

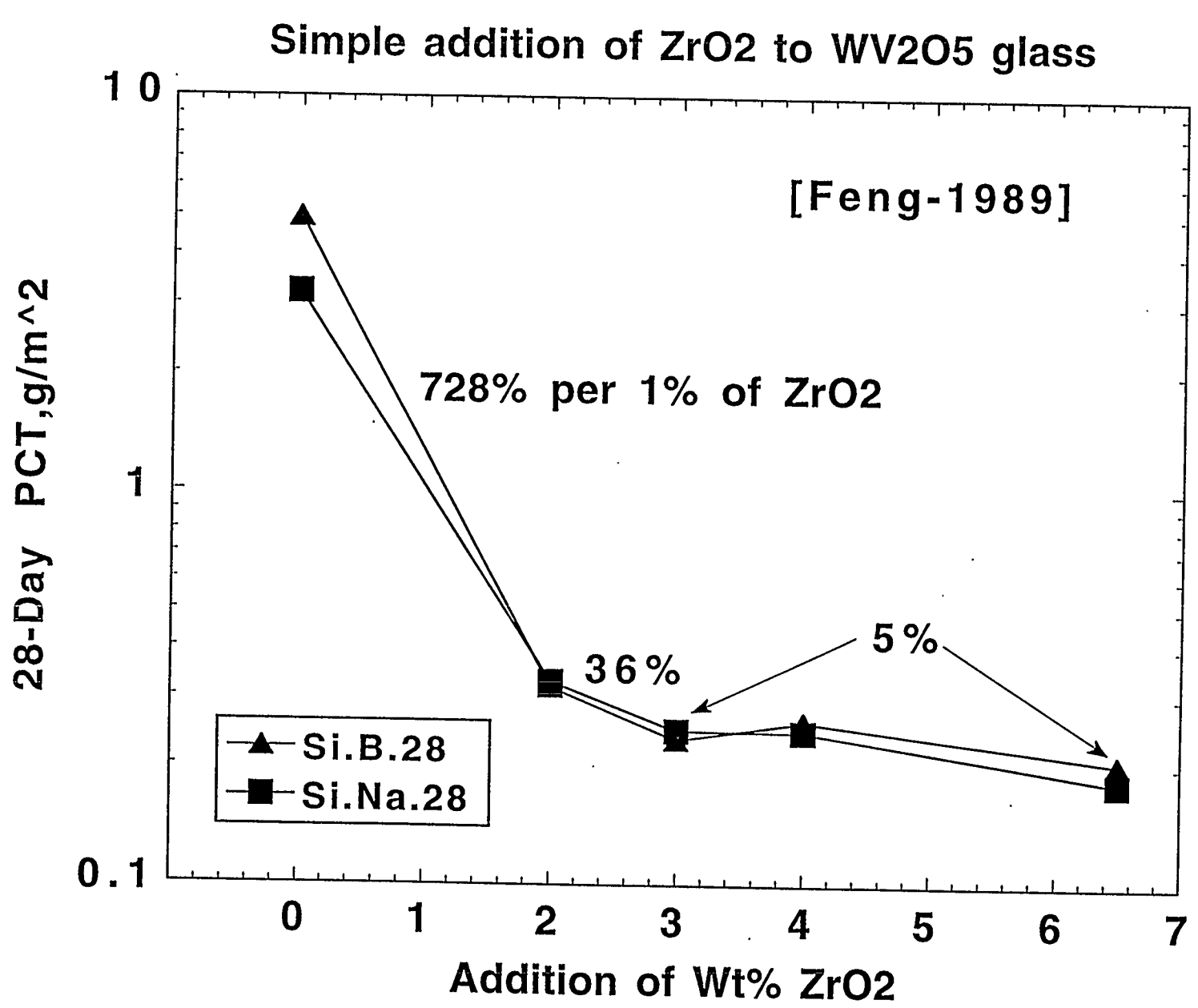
Simple addition of ZrO2 to WV2O5 glass
[Feng-1989]
728% per 1% of ZrO2
36%
5%
Si.B.28
Si.Na.28
28-Day PCT,g/m^2
10
1
0.1
0
1
2
3
4
5
6
7
Addition of Wt% ZrO2

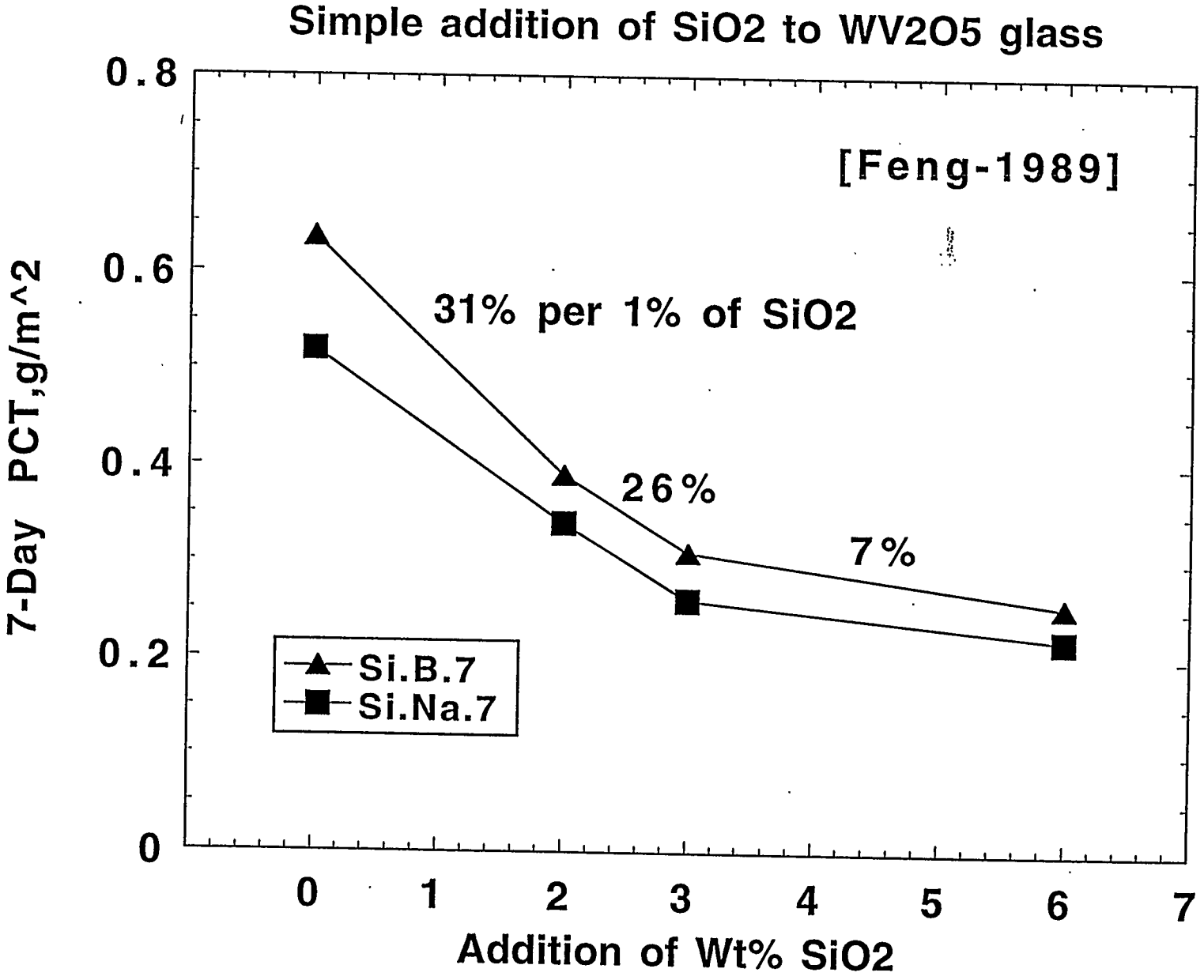
Simple addition of SiO2 to WV2O5 glass
[Feng-1989]
31% per 1% of SiO2
26%
7%
Si.B.7
Si.Na.7
7-Day PCT,g/m^2
0.8
0.6
0.4
0.2
0
0
1
2
3
4
5
6
7
Addition of Wt% SiO2

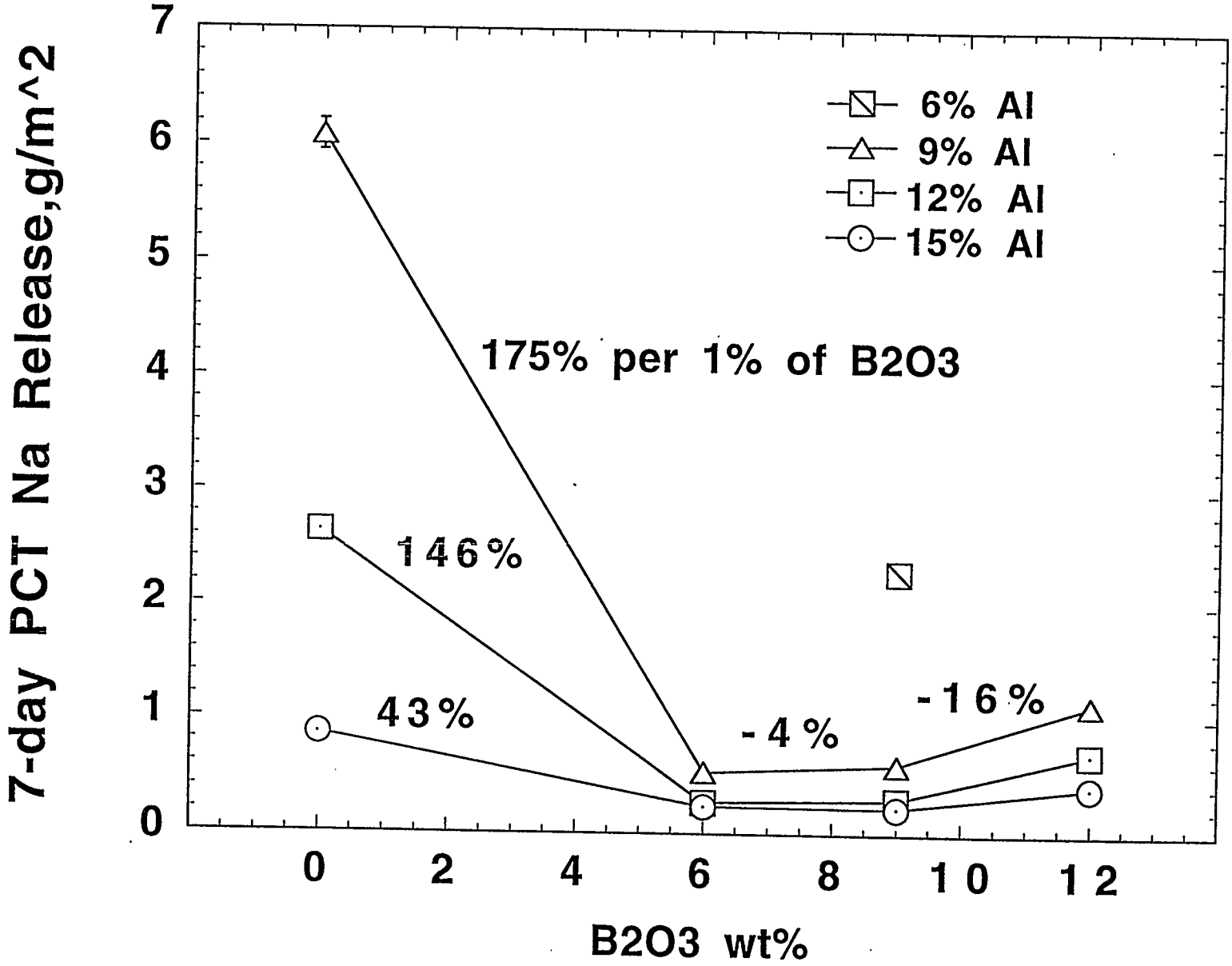
7-day PCT Na Release,g/m^2
7
6
5
4
3
2
1
0
0
2
4
6
8
10
12
B2O3 wt%
6% Al
9% Al
12% Al
15% Al
175% per 1% of B2O3
146%
43%
-4%
-16%

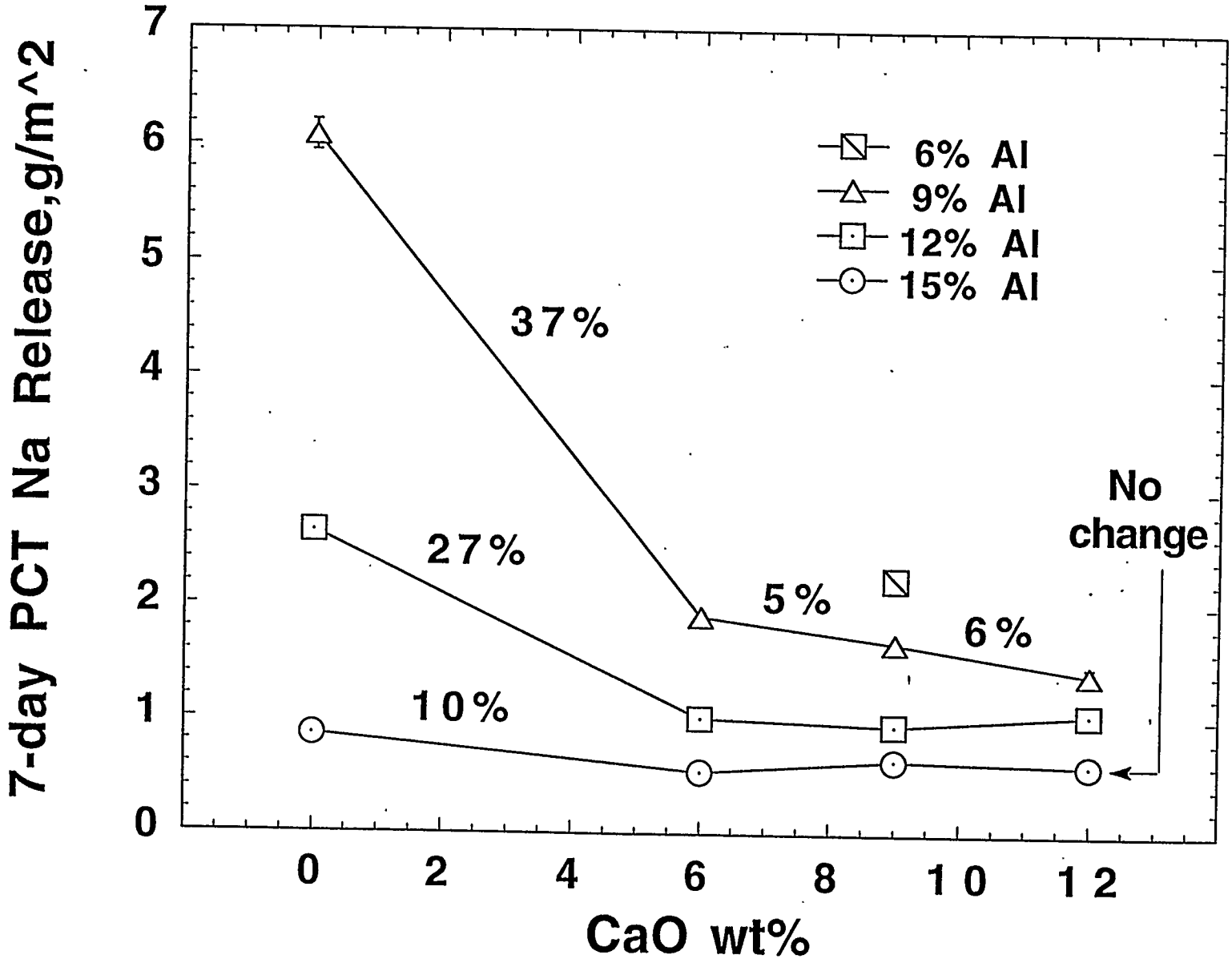
7-day PCT Na Release,g/m^2
7
6
5
4
3
2
1
0
0
2
4
6
8
10
12
CaO wt%
6% Al
9% Al
12% Al
15% Al
37%
27%
10%
5%
6%
No change

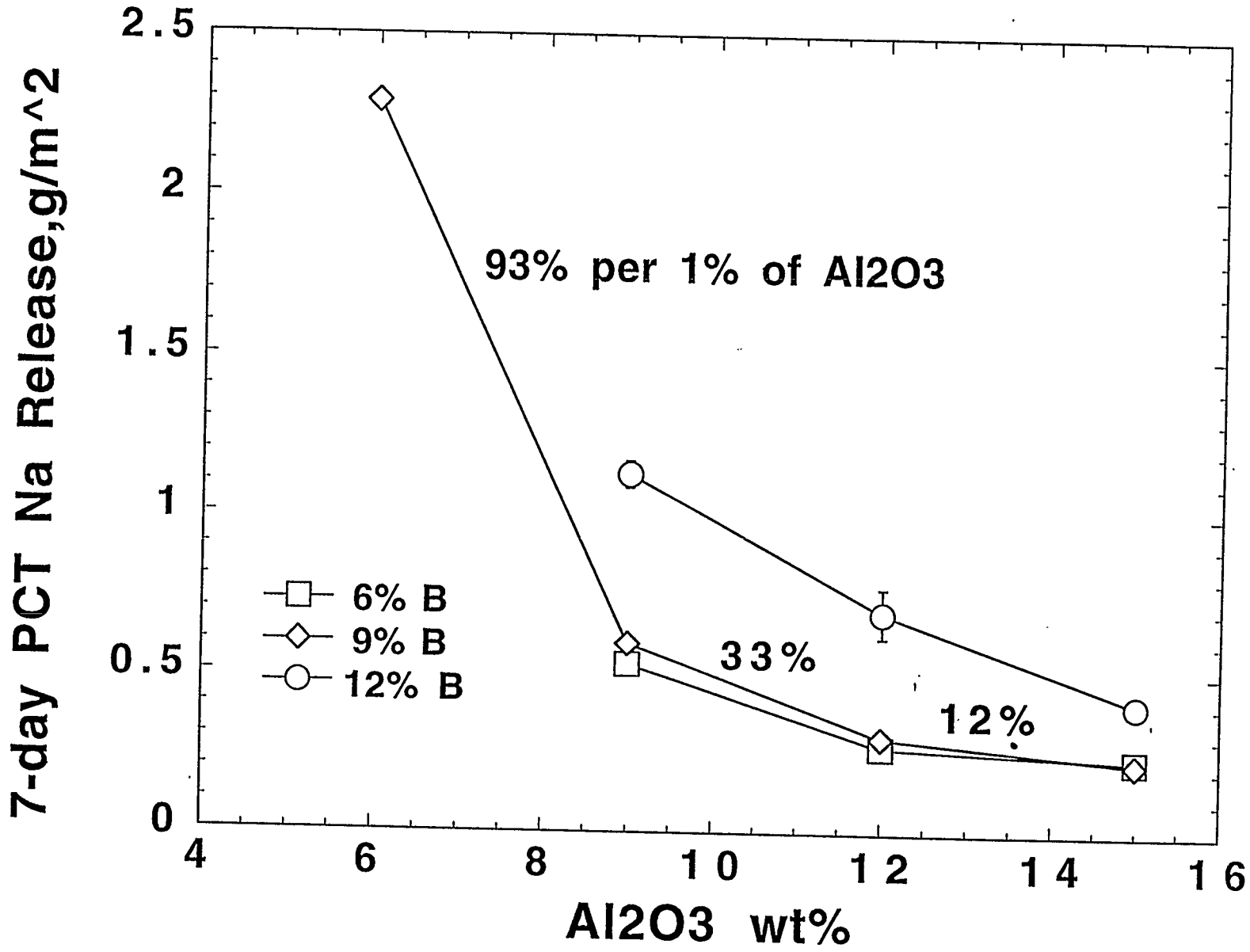
7-day PCT Na Release,g/m^2
2.5
2
1.5
1
0.5
0
4
6
8
10
12
14
16
Al2O3 wt%
93% per 1% of Al2O3
33%
12%
6% B
9% B
12% B

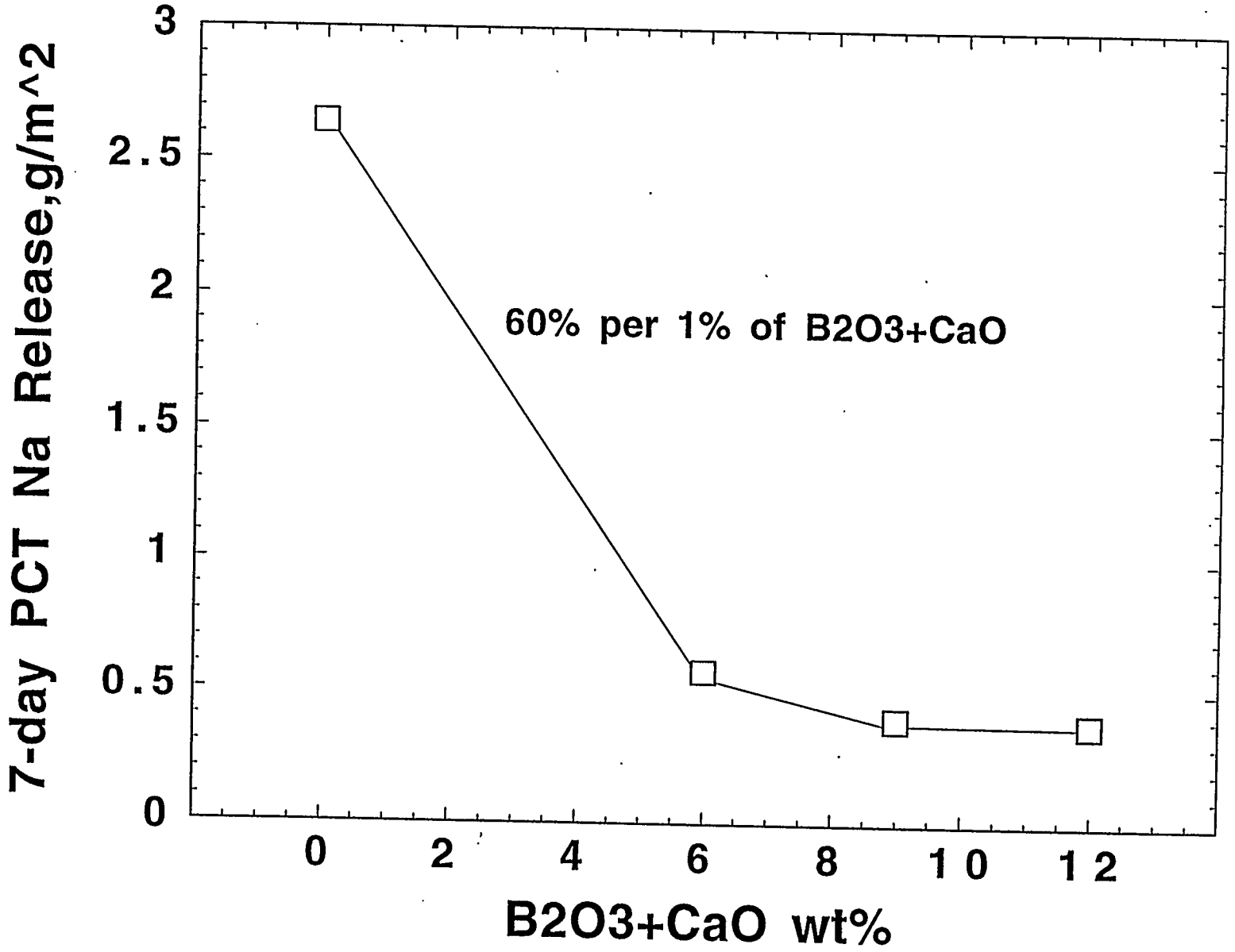
7-day PCT Na Release,g/m^2
3
2.5
2
1.5
1
0.5
0
0
2
4
6
8
10
12
B2O3+CaO wt%
60% per 1% of B2O3+CaO

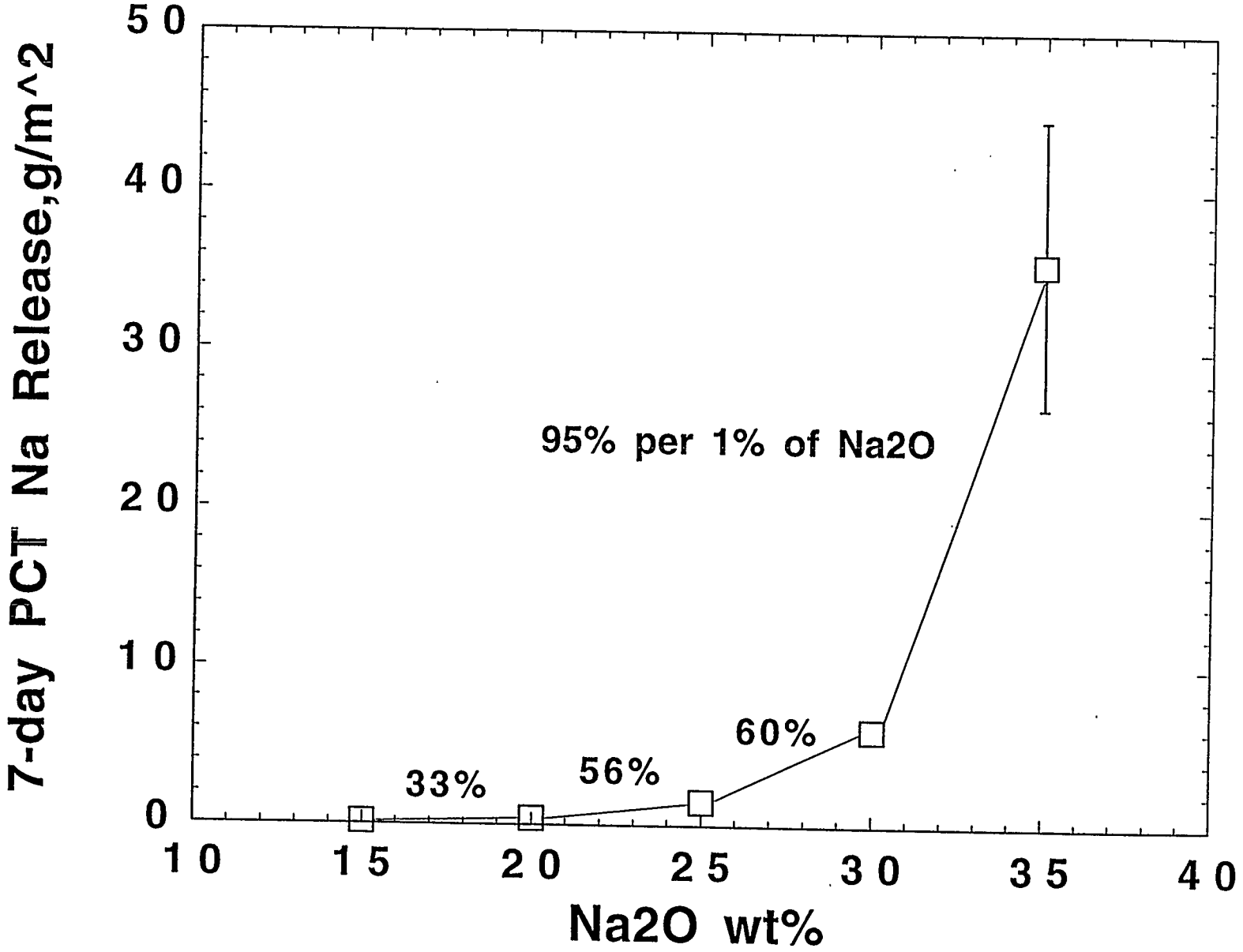
7-day PCT Na Release,g/m^2
50
40
30
20
10
0
10
15
20
25
30
35
40
Na2O wt%
95% per 1% of Na2O
33%
56%
60%

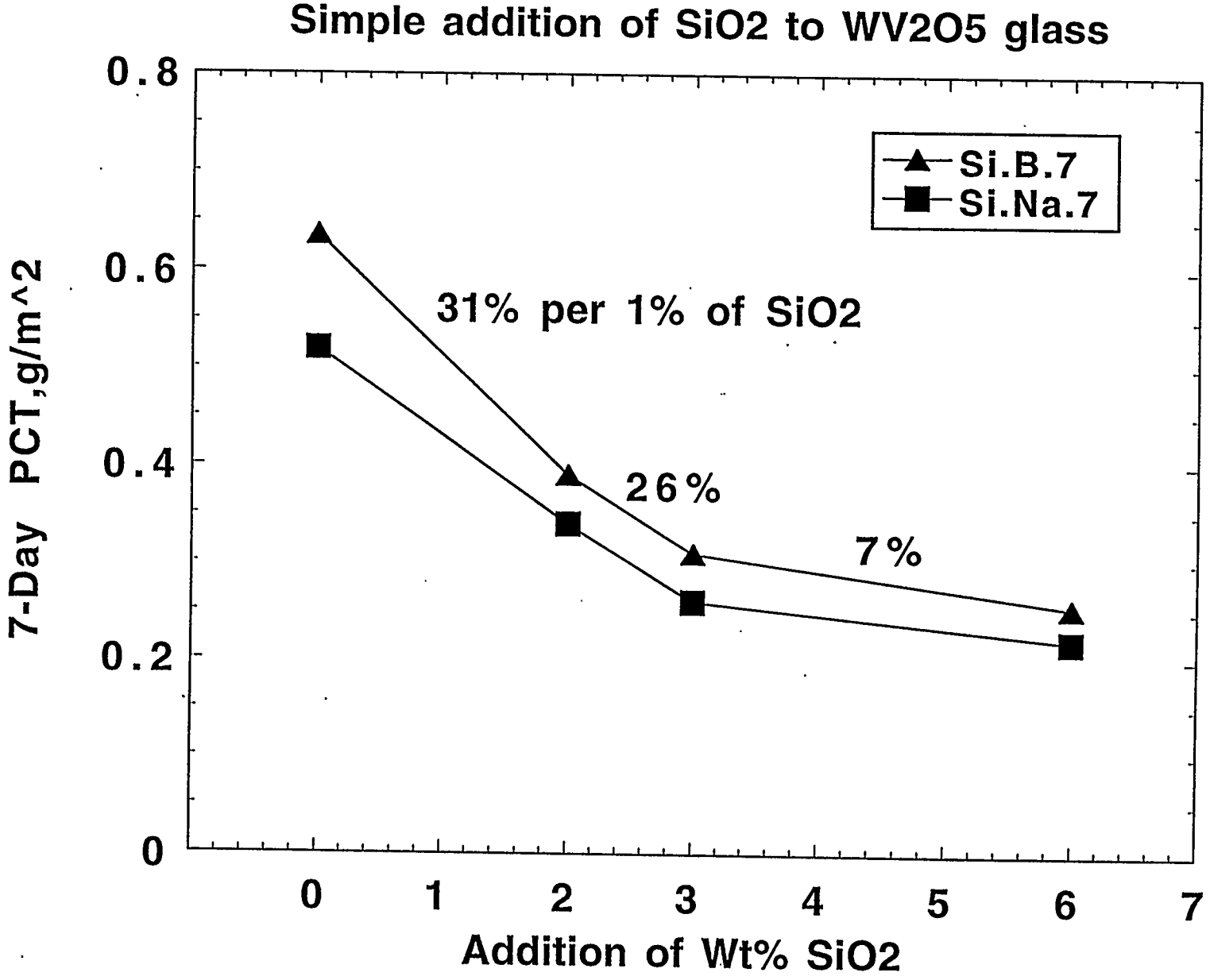
Simple addition of SiO2 to WV2O5 glass
0.8
0.6
0.4
0.2
0
7-Day PCT,g/m^2
Si.B.7
Si.Na.7
31% per 1% of SiO2
26%
7%
0
1
2
3
4
5
6
7
Addition of Wt% SiO2

The Effect of Replacing 10wt% SiO_2 with 10% Fe_2O_3 Resulted in Different Improvement in Durability in Different Glass Systems

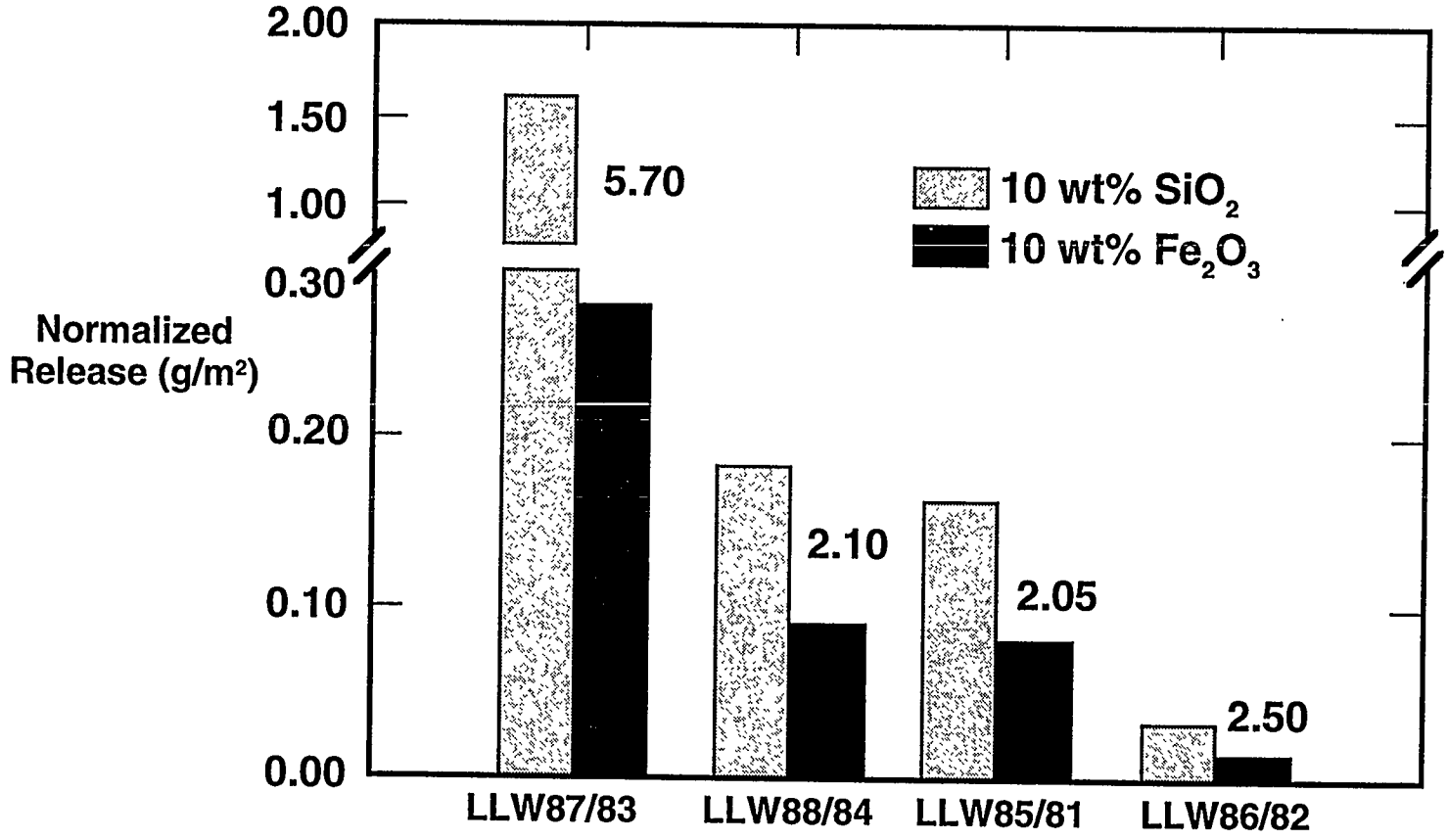

Merrill 1995

- Are these oxide effects random?
- Incomprehensible?
- Unpredictable?

6 wt% Addition to A Base Glass:
SiO2 56.78, Na2O 20.0, Al2O3 9.0,
B2O3 6.0, Others 2.22 (Total=94%)

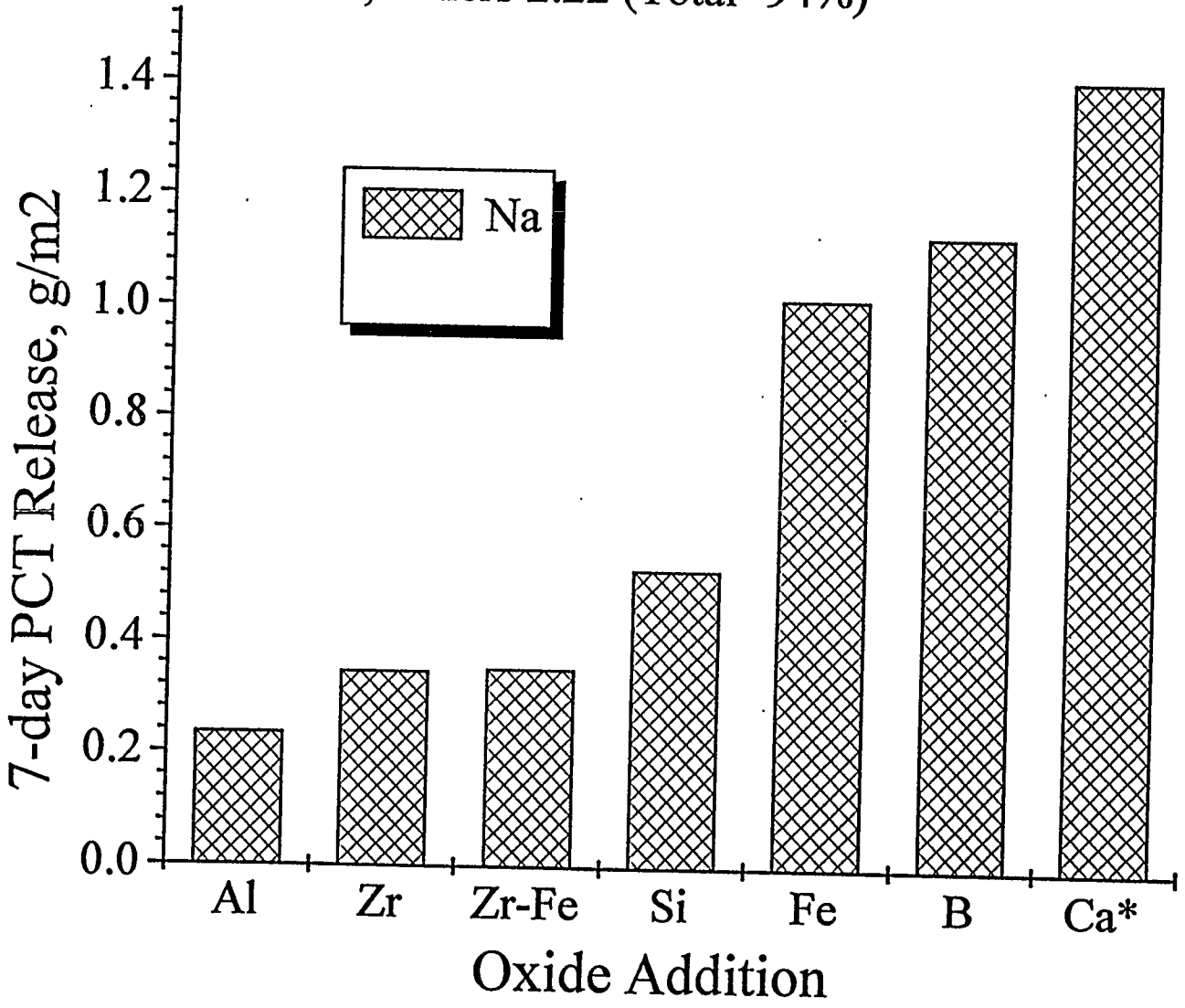

Effects on Glass Durability for Common Waste Glass Oxides

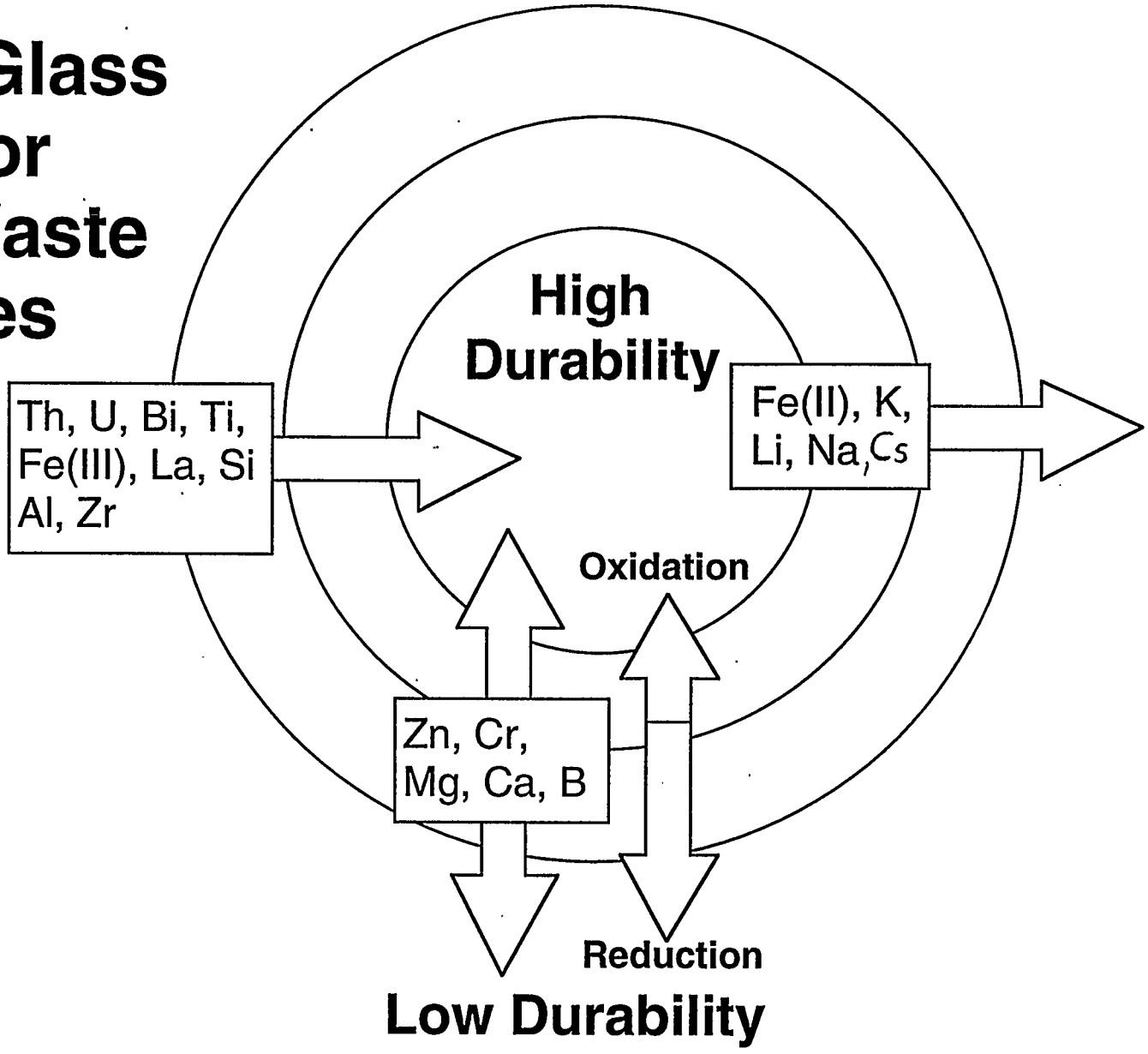

A Systematic Way to Present Data:

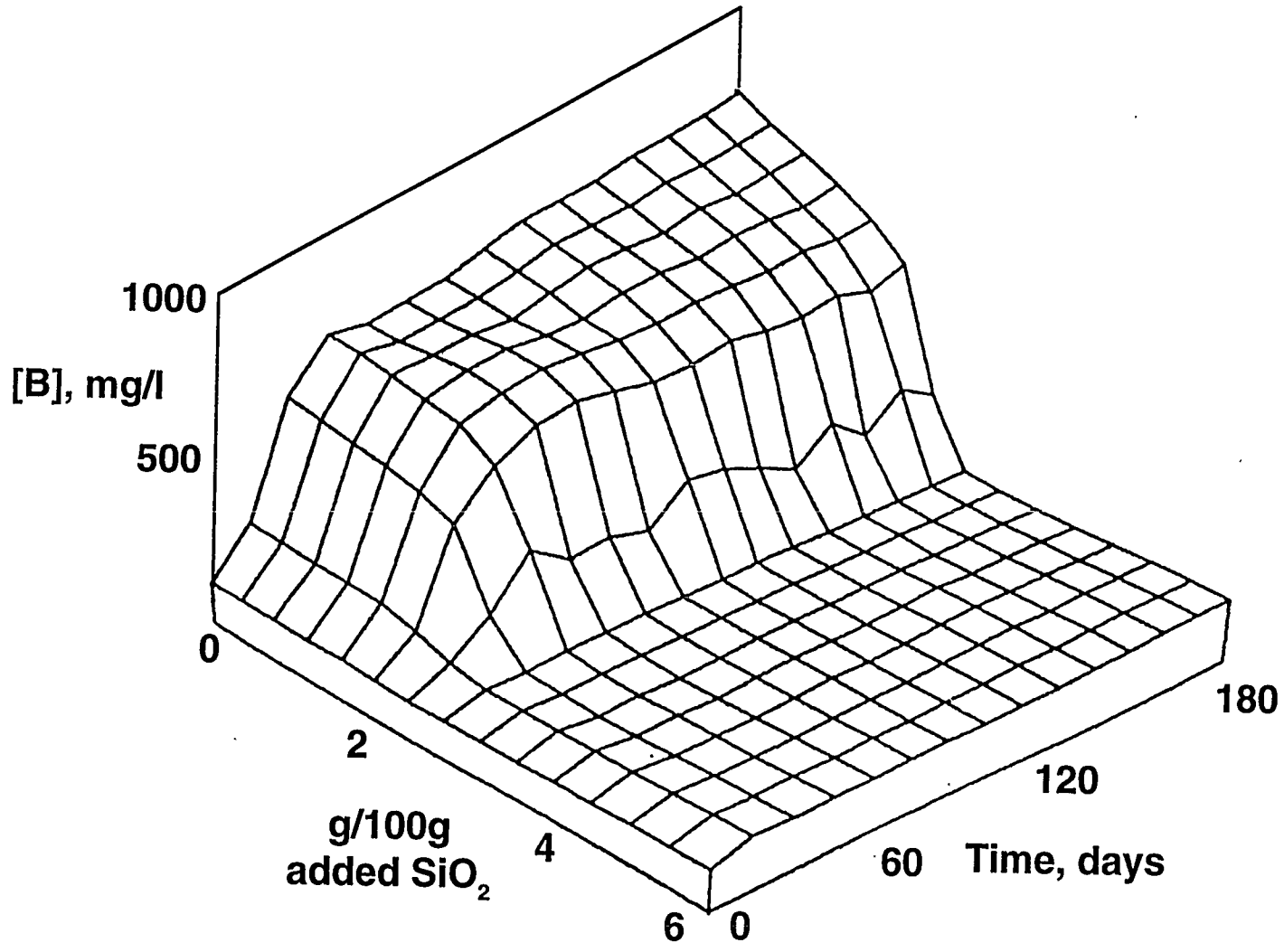

Individual Oxide Effects:

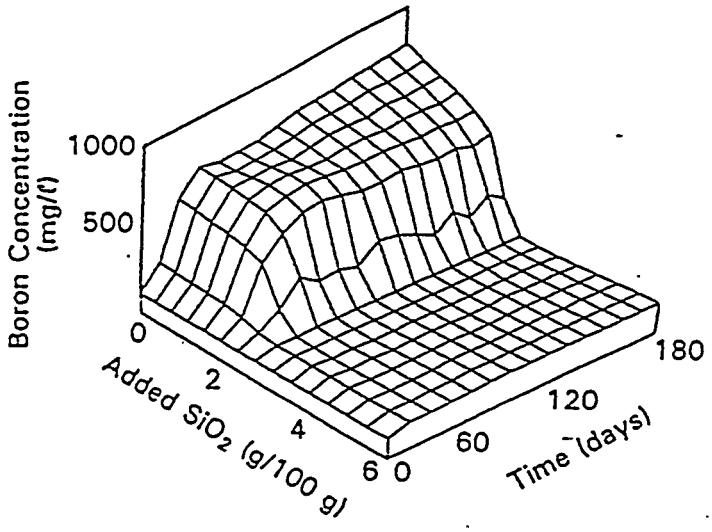

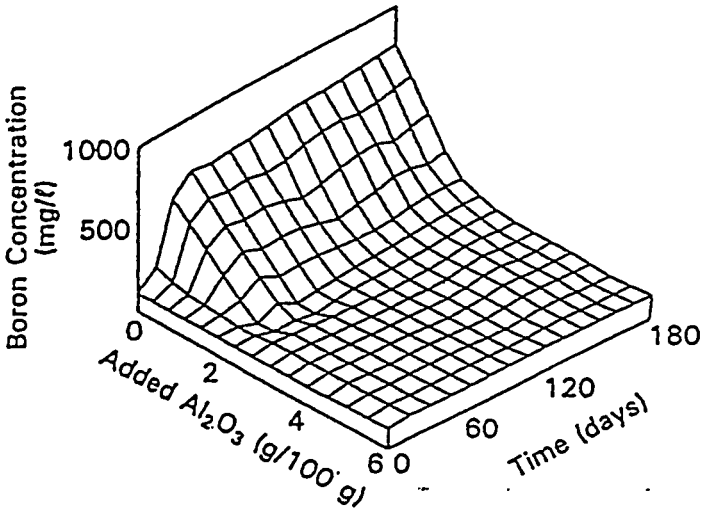

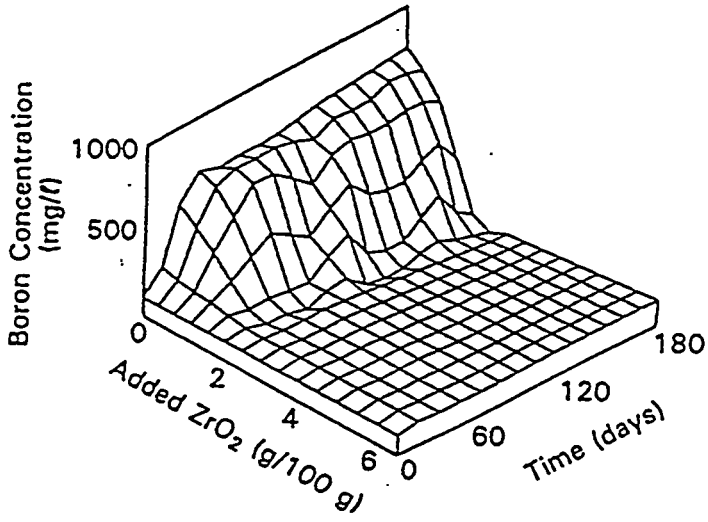

- Very non-linear

Feng et al., Nucl. Techn. (1989)

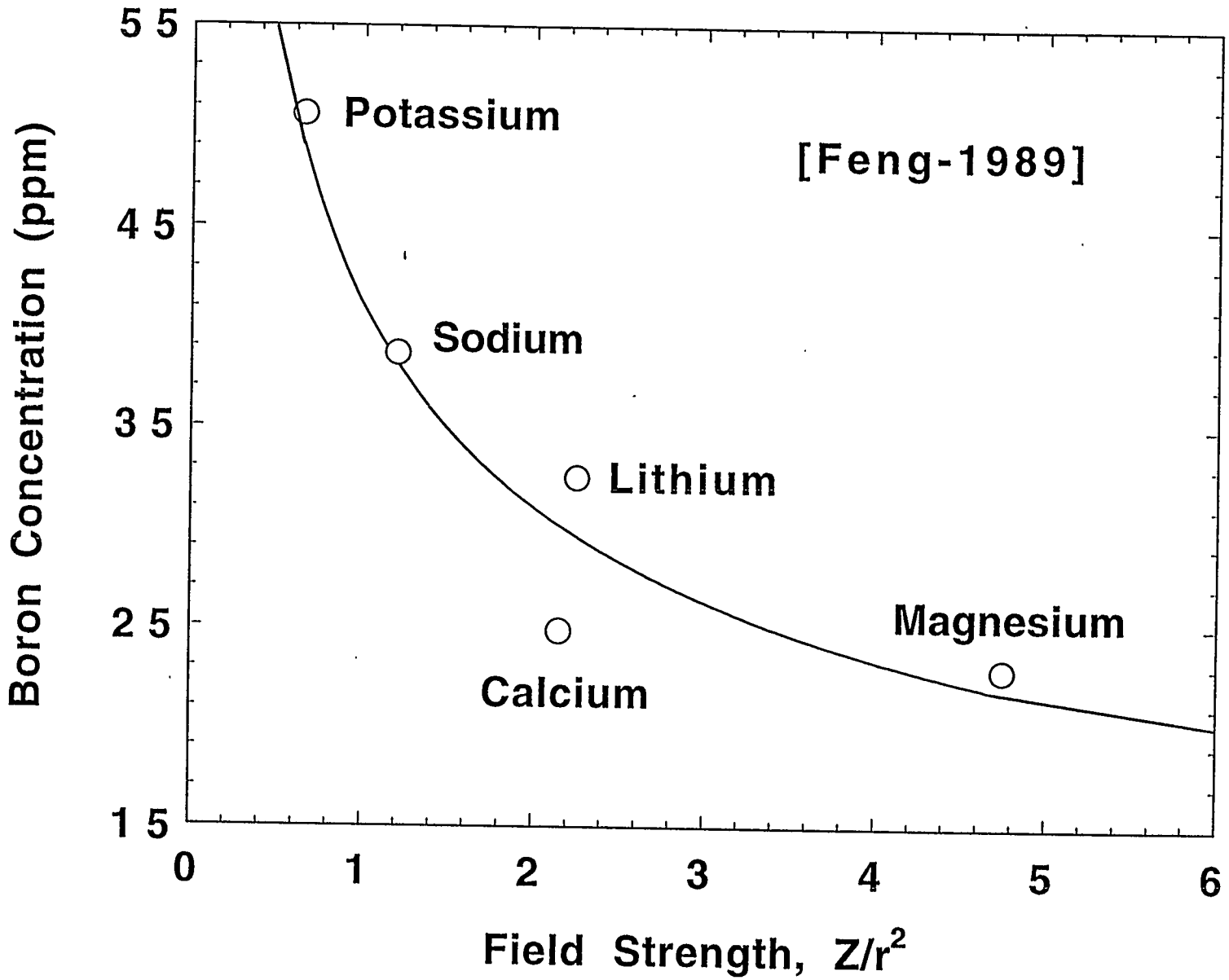
Boron Concentration (ppm)
55
45
35
25
15
0
1
2
3
4
5
6
Field Strength, Z/r2
Potassium
Sodium
Lithium
Calcium
Magnesium
[Feng-1989]

Observation of Individual Oxide Effects:

- Very non-linear
- Interactive in nature - dependence on the other components in glasses
- Very sensitive in poor durability glasses
- Insensitive in durable glasses
  - Desirable to have waste glass composition in durable glass region

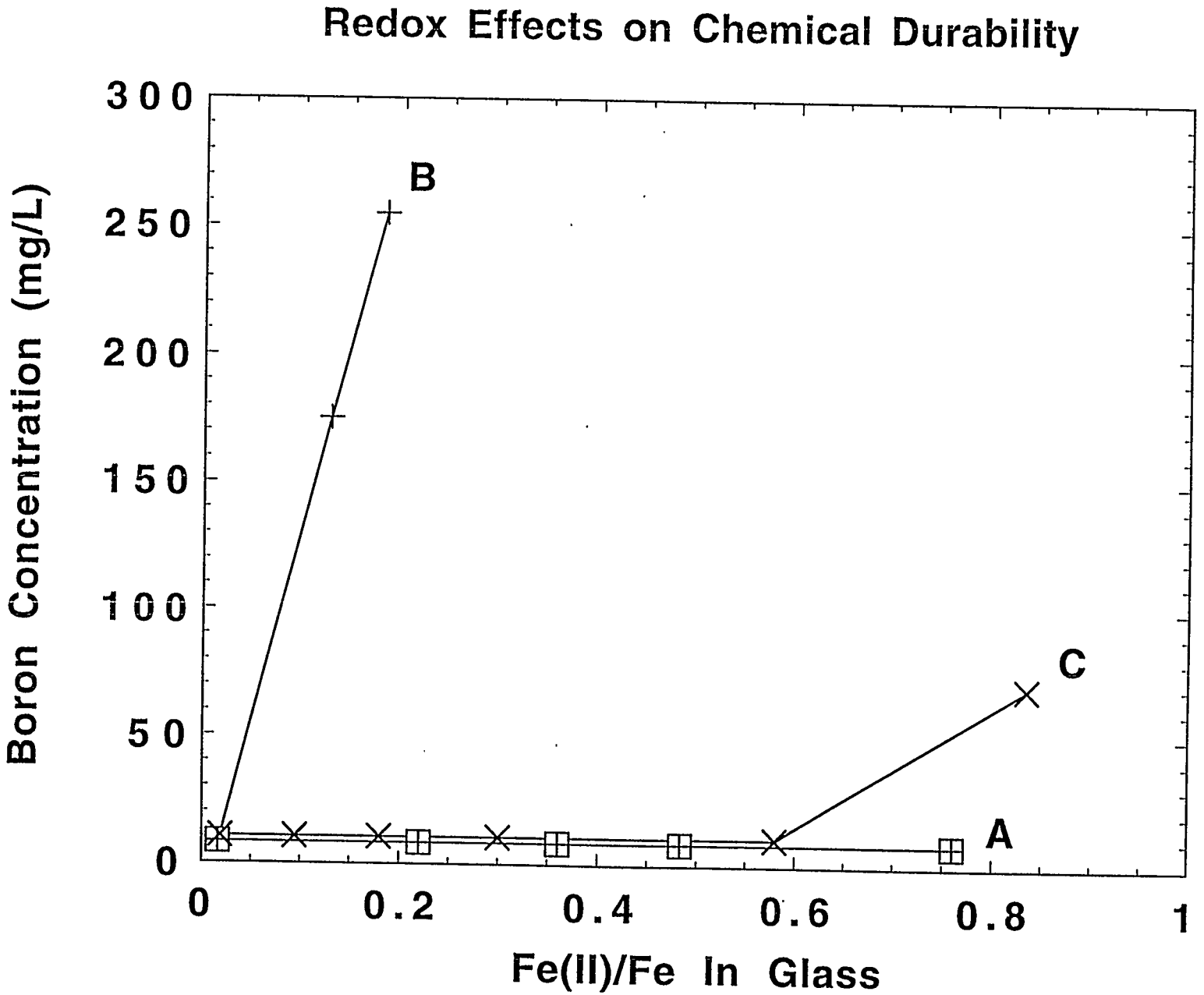
Redox Effects on Chemical Durability
Boron Concentration (mg/L)
300
250
200
150
100
50
0
0
0.2
0.4
0.6
0.8
1
Fe(II)/Fe In Glass
B
C
A

Observation of REDOX Effect on Glass Durability

- Durability decreases with reduction
- Highly composition-dependent:
  - Less sensitive for durable compositions
  - Very sensitive for poor durability ones
- Again, effects are very non-linear

Feng 1991

Why

- The addition of B_2O_3 has different effects
  - Increase durability (ID)
  - ID first, then no effect
  - Decrease durability
  - This is true also for Al_2O_3, CaO, etc.
- The effectiveness of ID is:
  - $Al_2O_3 > B_2O_3 > CaO$
- Etc.

Understanding Composition Effects

- Structural roles of individual oxides in glass:
  - Composition dependent
  - Redox dependent
- Percolation phenomenon in glasses
  - The concentration of network forming elements has to reach a critical value for a glass to belong to a durable region:
    - Glasses in durable region are sufficient in network formers and have complete network structure
    - Glasses in poor durability regions are deficient in network formers and the network of the glass is incomplete

Kinoshita 1991

Glass Chemistry

- Quartz or fused silica are very durable due to:
  - Strong bond of Si-O-Si-O-Si [BO]
  - The Si-O-Si network is continuous in 3-D

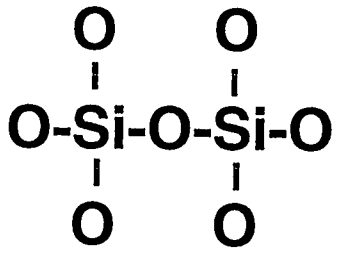

Zachariasen 1932

Addition of Alkalis to Fused Silica

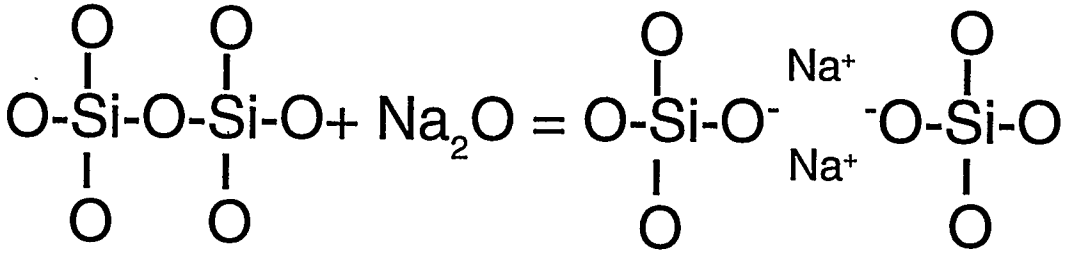

- **Break up the continuous network, i.e. destroy BO bonds**
- **Form weak Non-Bridging Oxygen (NBO) bonds**
- **Reduce durability**

Zachariasen 1932

Addition of Al_2O_3 in a SiO_2-Na_2O System

- **Reduce NBO bonds:**

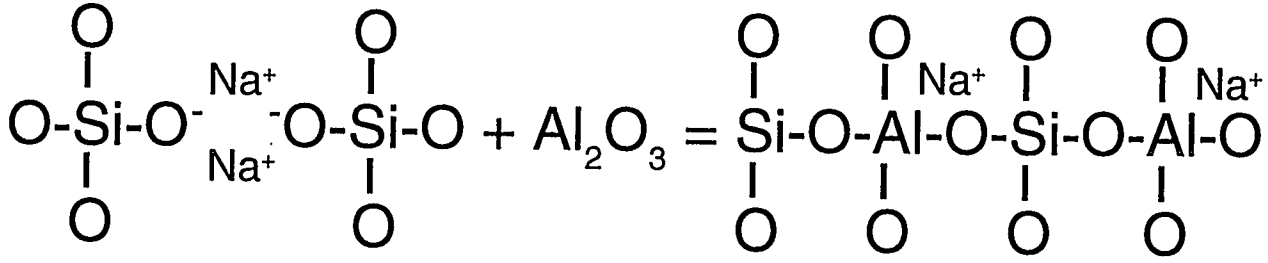

- **Increase durability**
- **Al is tetrahedrally coordinated and charge balanced by alkalis** ***(Alexander, 1986)***
- **The improvement in durability depends on available NBO bonds**
- **The above reaction is near completion**
- **Similar behavior is expected for Fe_2O_3**

Dickenson 1981, 1986

Addition of B_2O_3 in a SiO_2-Na_2O System

- **Reduce NBO bonds:**

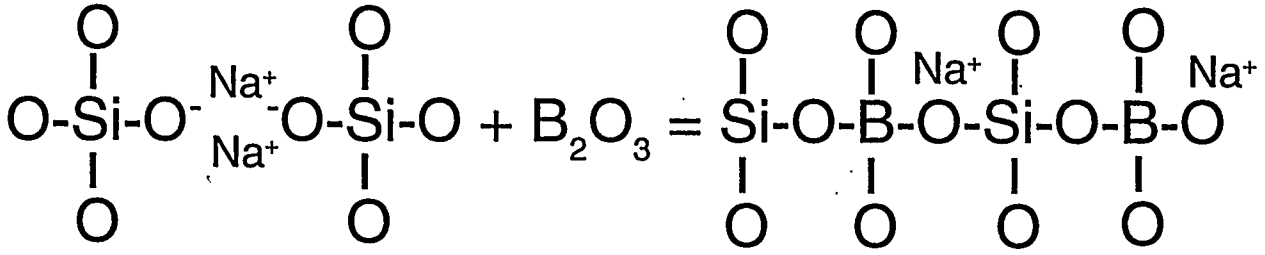

- **Increase durability**
- **Boron is tetrahedrally coordinated and charge balanced by alkalis**
- **The improvement in durability depends on available NBO bonds**
- **The above reaction is usually far from completion and is a function of contents of alkalis and silica**

Dell 1983

Addition of ZrO_2 in a SiO_2-Na_2O System

- **Reduce NBO bonds:**

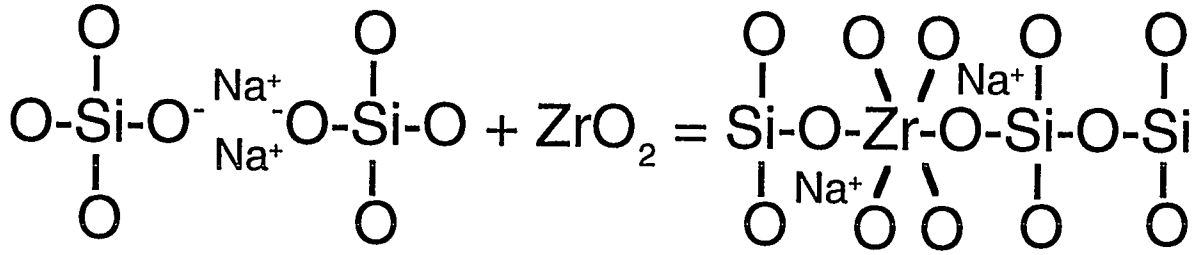

- **Increase durability**
- **Zr is in 6-coordination and stabilized by alkalis** *(Farges, 1991)*
- **The improvement in durability depends on available NBO bonds**

Addition of B_2O_3, ZrO_2, and Fe_2O_3

- Reduce NBO bonds
- Improve durability ONLY if there are NBO bonds to be reduced

Addition of CaO

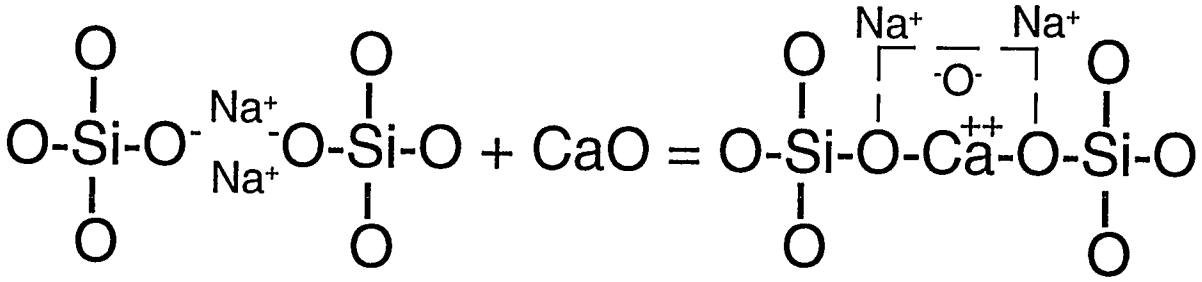

- "Reduce" NBO bonds to form a hybrid of NBO and BO, i.e., sharing NBO between alkali and alkaline earths *(Ellison 1995)*
- The -O-Ca-O- bond is not as durable as Si, Al, Zr, Fe, and other high valence -O-X-O- bonds
- Improve durability when there are NBO bonds available

The Binding Order to Alkalis

- $Al_2O_3 > ZrO_2 > Fe_2O_3 > B_2O_3 > CaO$ (SBS Model) *Feng 1988*
- This order has significant effect on the observed composition effects
- It will explain most of the non-linear behavior of composition effects

Bobkora 1983, Feng 1994, Ellison 1994

The Order of Binding Strength to Alkalis

- $Al_2O_3 > ZrO_2 > Fe_2O_3 > B_2O_3 > CaO$ (SBS Model) *Feng 1988*
- Corresponding SBS values of the oxides in networking position (Kcal/mole): 801>525>393>304>152
- This order also has significant effect on the observed composition effects
- It will explain some of the non-linear behavior of composition effects

Qualitative explanation of durability observation can be obtained through the glass structure considerations discussed above.

A Systematic Way to Present Data:

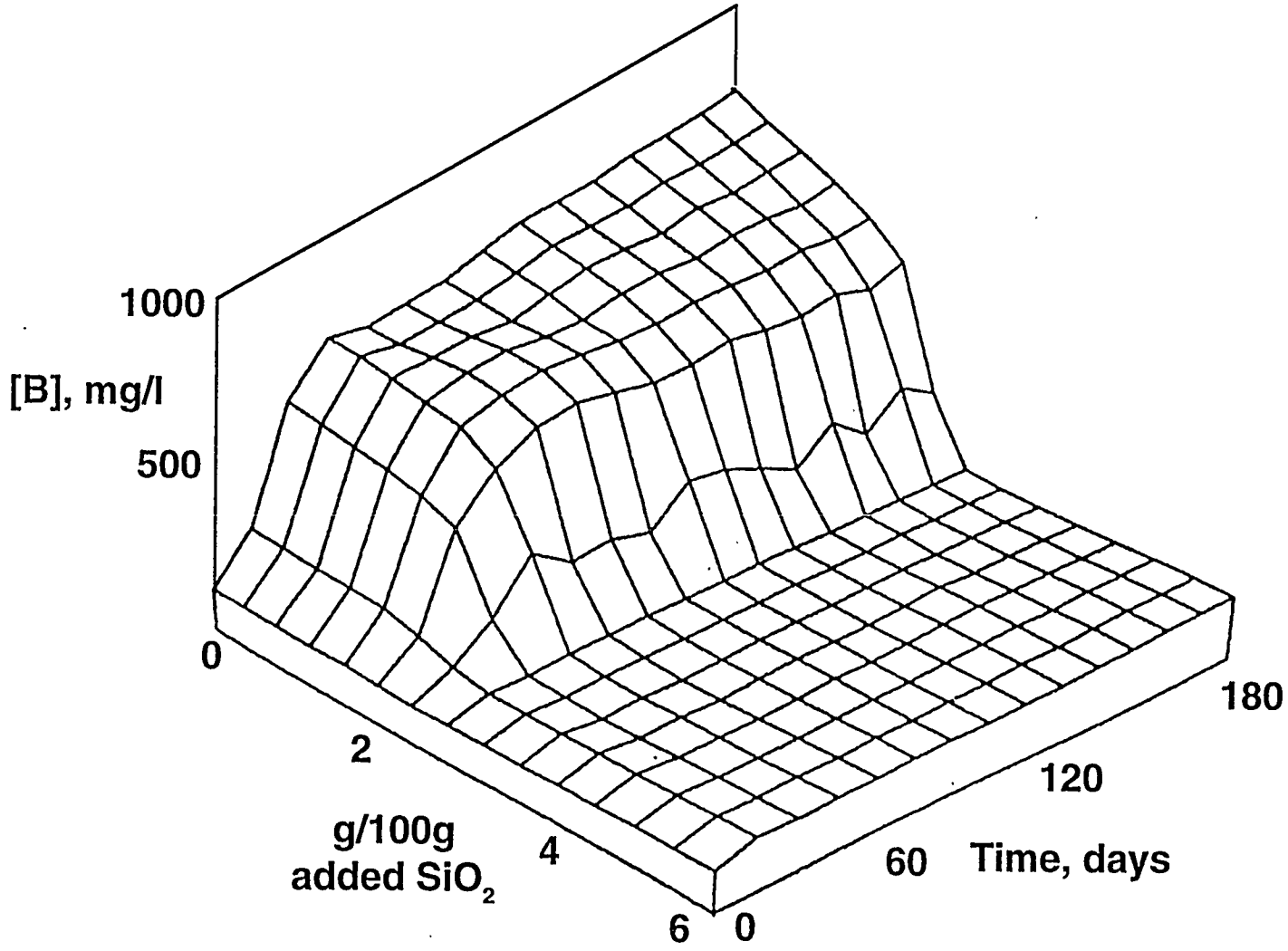

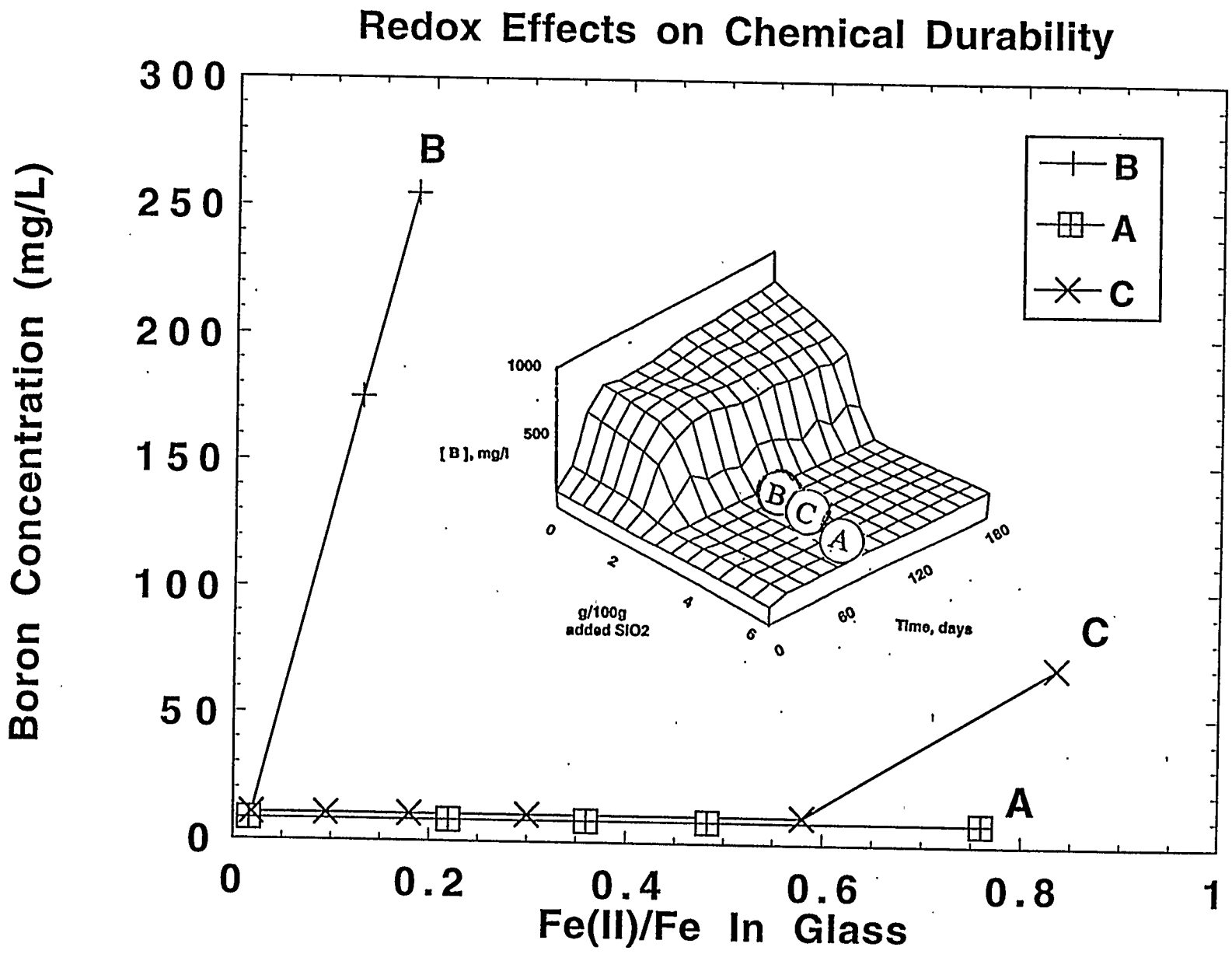
Redox Effects on Chemical Durability
Boron Concentration (mg/L)
300
250
200
150
100
50
0
0
0.2
0.4
0.6
0.8
1
Fe(II)/Fe In Glass
B
A
C
B
A
C
1000
500
[B], mg/l
0
2
4
6
g/100g
added SiO2
0
60
120
180
Time, days
B
C
A

a

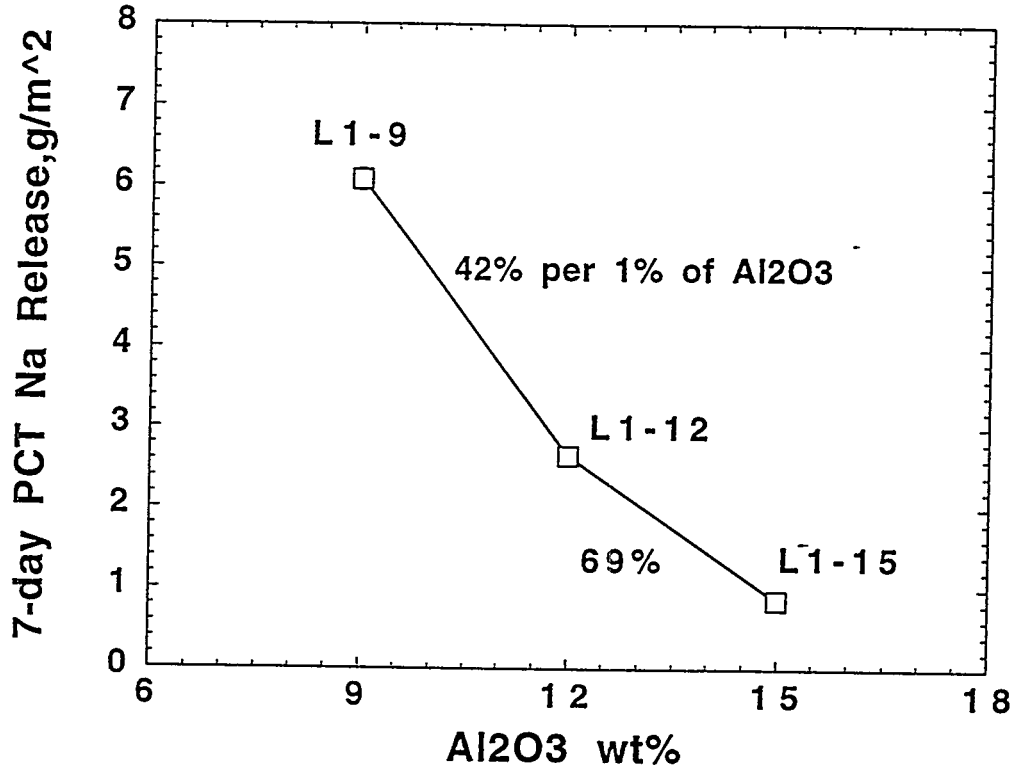
7-day PCT Na Release,g/m^2
8
7
6
5
4
3
2
1
0
L1-9
42% per 1% of Al2O3
L1-12
69%
L1-15
6
9
12
15
18
Al2O3 wt%

b

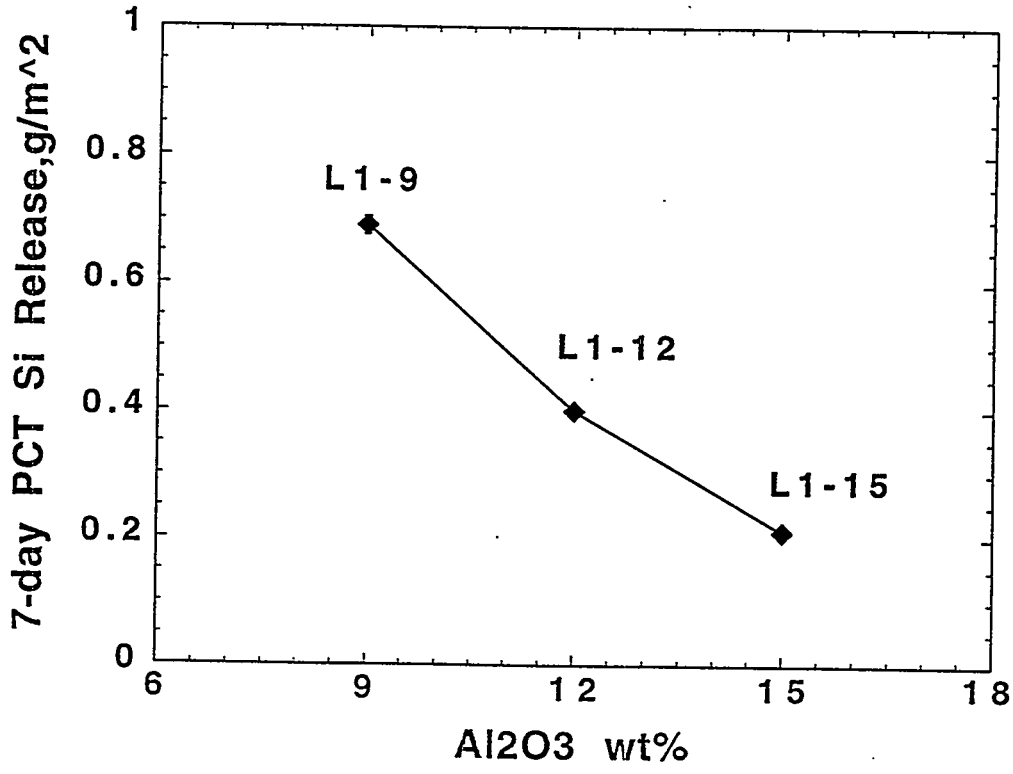
7-day PCT Si Release,g/m^2
1
0.8
0.6
0.4
0.2
0
L1-9
L1-12
L1-15
6
9
12
15
18
Al2O3 wt%

a

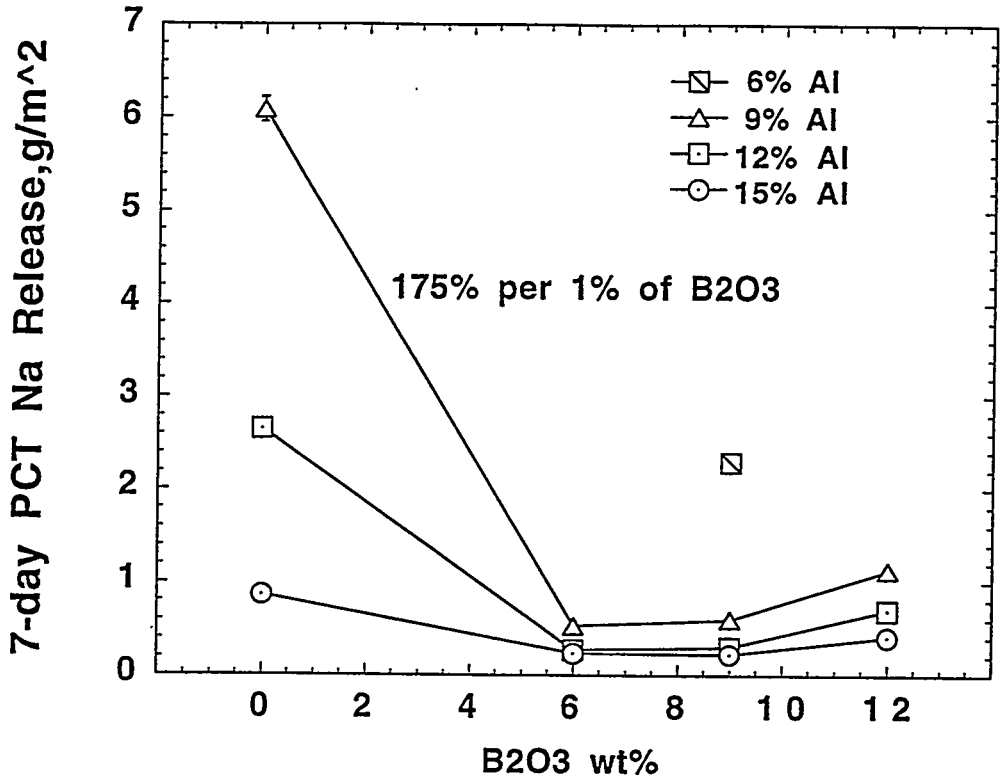
7-day PCT Na Release,g/m^2
7
6
5
4
3
2
1
0
6% Al
9% Al
12% Al
15% Al
175% per 1% of B2O3
0
2
4
6
8
10
12
B2O3 wt%

b

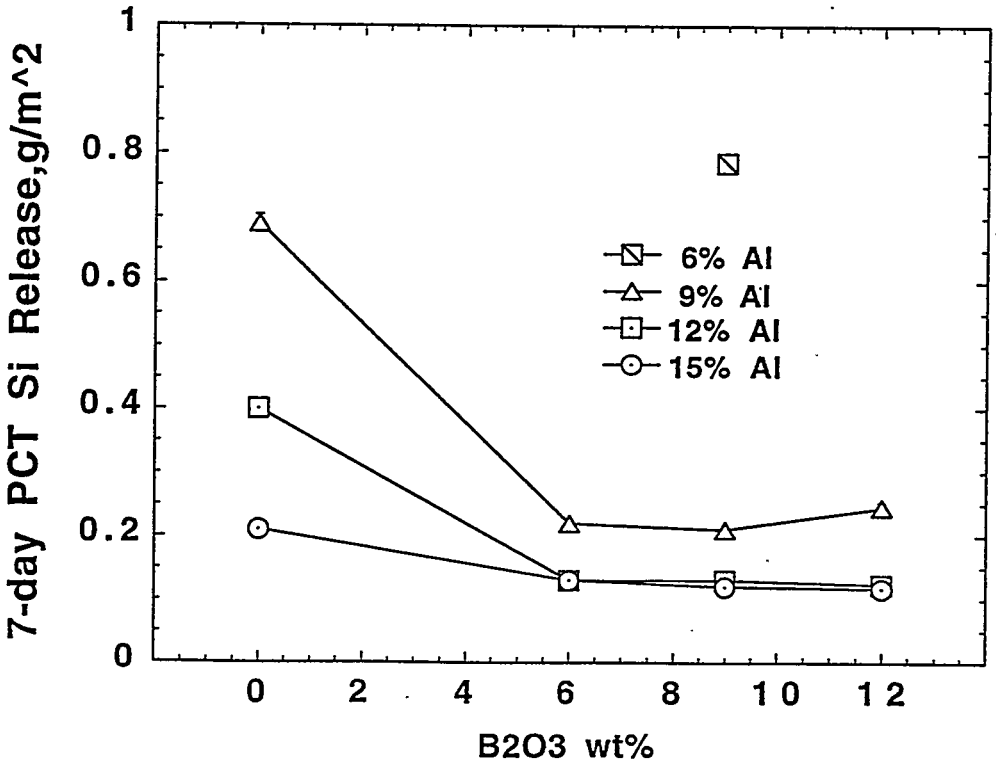
7-day PCT Si Release,g/m^2
1
0.8
0.6
0.4
0.2
0
6% Al
9% Al
12% Al
15% Al
0
2
4
6
8
10
12
B2O3 wt%

a

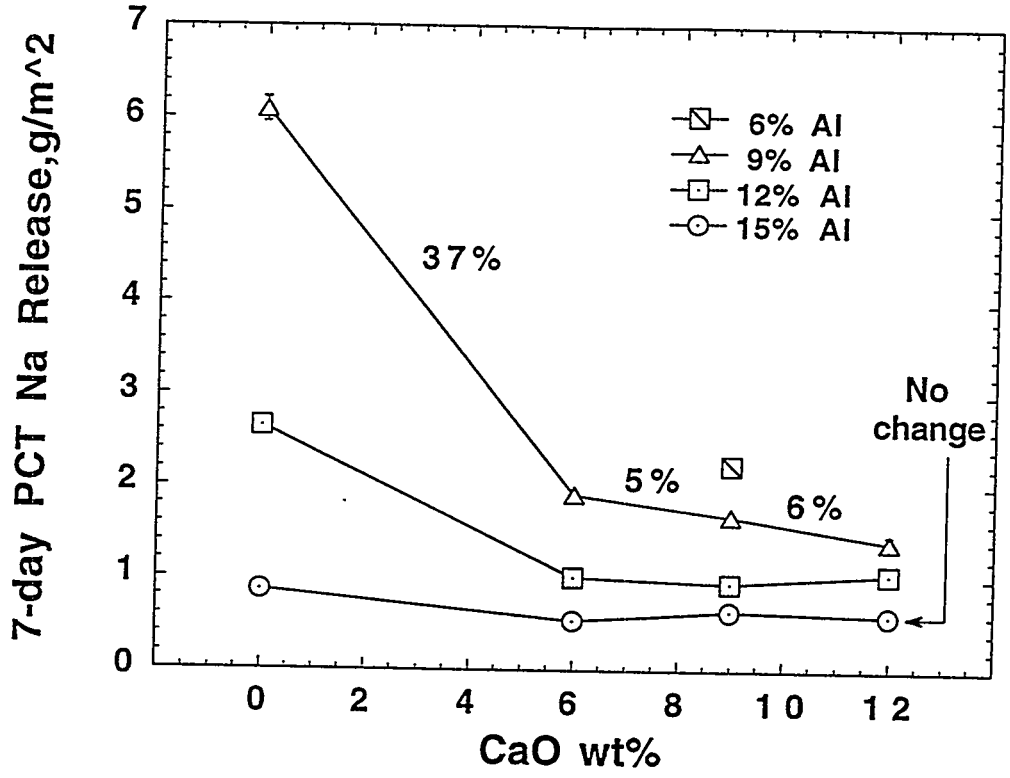
7-day PCT Na Release,g/m^2
0
1
2
3
4
5
6
7
0
2
4
6
8
10
12
CaO wt%
6% Al
9% Al
12% Al
15% Al
37%
5%
6%
No change

b

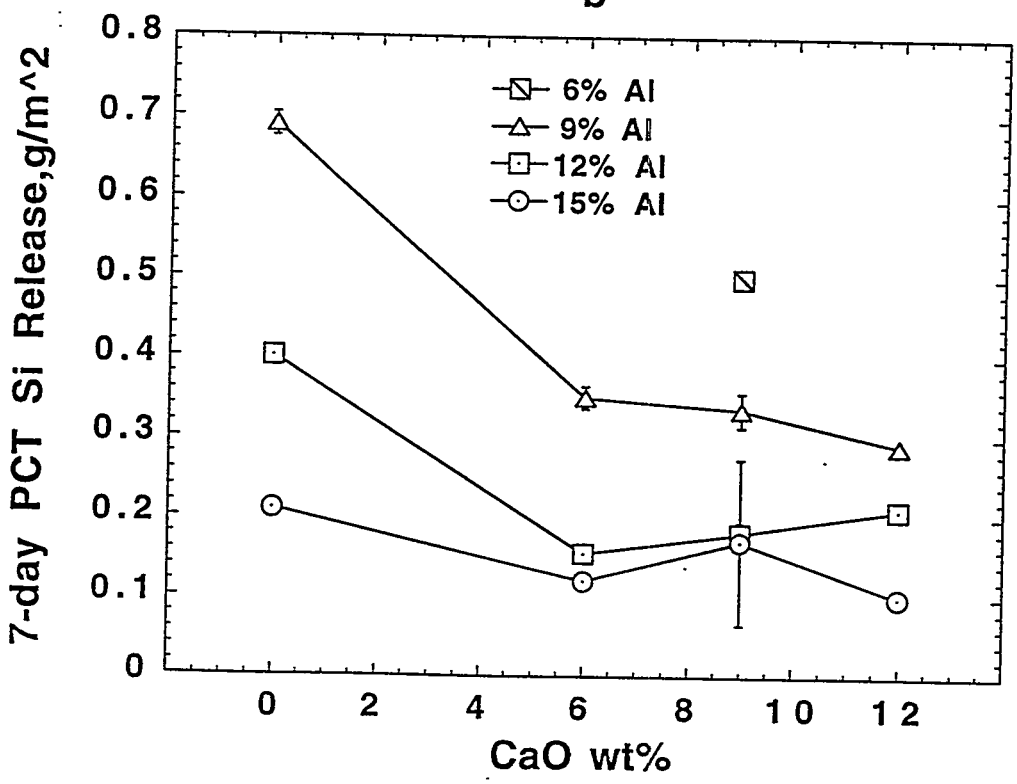
7-day PCT Si Release,g/m^2
0
0.1
0.2
0.3
0.4
0.5
0.6
0.7
0.8
0
2
4
6
8
10
12
CaO wt%
6% Al
9% Al
12% Al
15% Al

Factors Contributing to Durability

- Replace NBO by BO → Large Durability Increase (DI)
  - Extent depends on types of BO; Al-O, Zr-O, Fe-O, or B-O
- Replace a BO by a stronger BO → DI
- Extent depends on types, Al-O for Ca-O or Al-O for Zr-O
- Excess of CaO, B_2O_3, Fe_2O_3 → Reduced Durability
- Excess of Al_2O_3 and ZrO_2 dilutes BOs

For Quatitative Predictions

- A model must be able to account for the non-linear composition effects, i.e., the model index (or coefficient) for each oxide should be a function of other compounds and be able to vary from glass to glass

- A model should reflect our current understanding of glass structure and its effect on durability, the model can be improved as our understanding increases

Structural Bond Strength (SBS) Model Developed for Glass

- From composition, it predicts:
  - Chemical durability
  - Melt viscosity vs. temperature

Feng 1988, 1994, 1995

SBS Model

- Incorporates all the above structural considerations
- Focuses on the fundamental building blocks of glass:
  - O-X bond
  - Consistent with short range of order in glass
- SBS value of an oxide changes with:
  - Composition
  - Redox state
  - Temperature
- SBS model preserves the non-linear effects of oxides on durability

Basic Assumptions of SBS Model

- The chemical durability and high-temperature viscosity of an oxide waste form are determined by:
  - The binding strengths of its most fundamental building blocks: O-X_i bonds (X_i -- any element that binds to oxygen)
  - Temperature

Basic Assumptions of SBS Model (cont.)

- The binding strength (SBS value) of an oxide is a function of its structural role of X_i
- The structural roles of X_i is classified as:
  - (a) Network formers (Al_2O_3, ZrO_2, Fe_2O_3, B_2O_3, SiO_2 and other high valence cations)
  - (b) Network breakers (Na_2O, Li_2O, K_2O, Rb_2O, Cs_2O, and B_2O_3)
  - (c) Intermediates (Al_2O3, Fe_2O_3, FeO, SiO_2, CaO and other oxides not included in (a) or (b)

Basic Assumptions of SBS Model (cont.)

- The structural role of X_i is:
  - Composition dependent
  - Redox dependent
  - Temperature dependent

SBS Model Structural Role of X_i (cont.)

Composition Dependence:

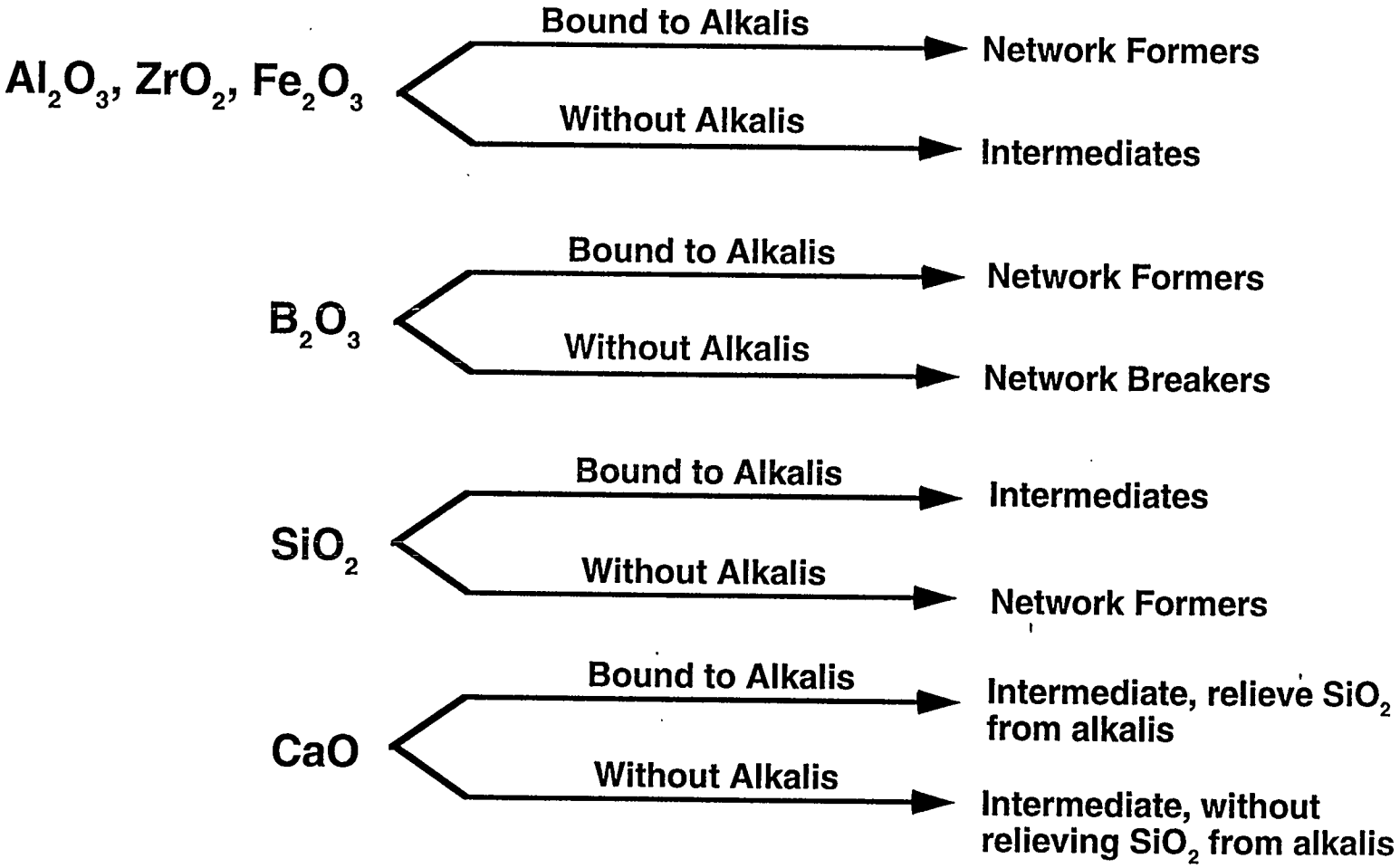

SBS Model Structural Roles of X_i

- **Redox Dependence:**

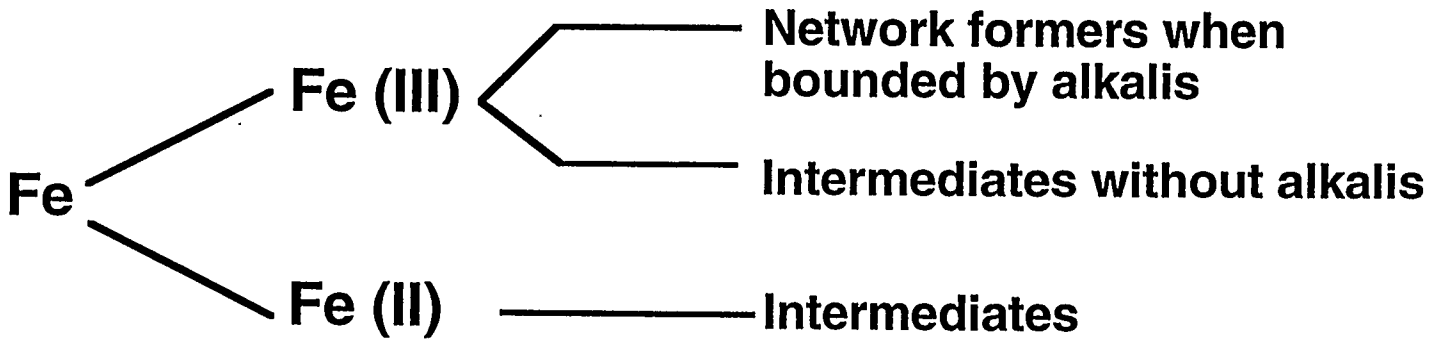

SBS Model Structural Roles of X_i

- **Temperature Dependence:**

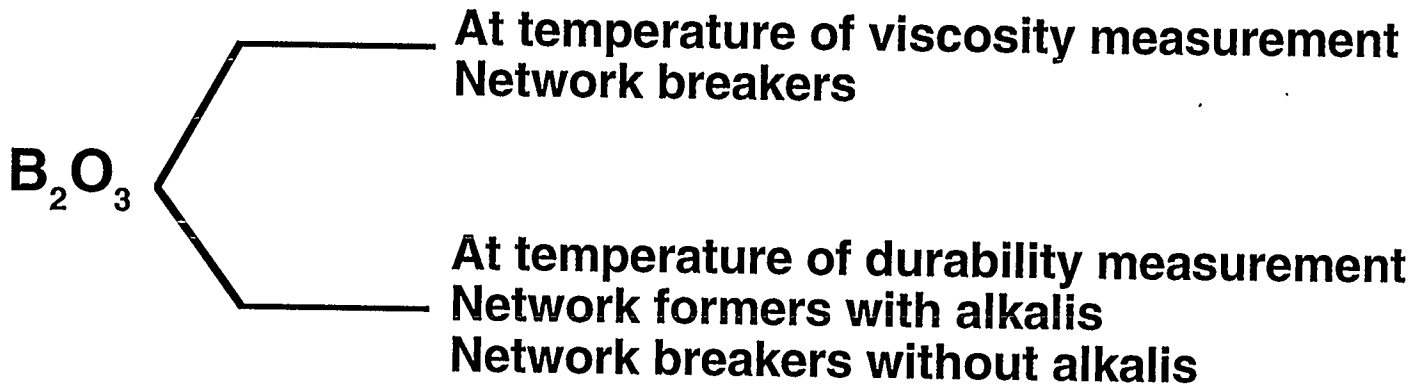

Considerations for Percolation Phenomenon in SBS Model

- **In poor durability glass composition range, the network formers are deficient and are characterized by R:**

$$R = \frac{\text{total moles of available network formers}}{\text{total alkalis}}$$

when $R \leq 0.4$, no network formers are considered

SBS Value Calculations of Each Oxide

Based on available standard enthalpy of oxide formation, ΔH_i
SBS value V_i, for oxide i

- Network formers: $V_i = 2 \cdot \Delta Hi$
- Intermediates: $V_i = \Delta Hi$
- Network breakers: $V_i = \Delta Hi - Enet$

Where Enet = average bond energy of network formers

$$E_{net} = \frac{\Sigma_i \; m_i \cdot V_i}{\Sigma_i \; a_i \cdot m_i}$$

Where m_i = number of moles of oxide i as network formers
a_i = coordination number of oxide i as network formers

SBS Model

- The total SBS value for each glass

$$V = \sum_i m_i V_i$$

where m_i = the total moles of oxide i per 100g of glass
V_i = the average SBS value of oxide i in the glass

- Correlation with durability

$$\ln[\text{durability}] = aV + b$$

where durability – measured durability for a glass
V – calculated SBS value for a glass
a and b – fitting coefficients

Structural Bond Strength Model on Glass Durability

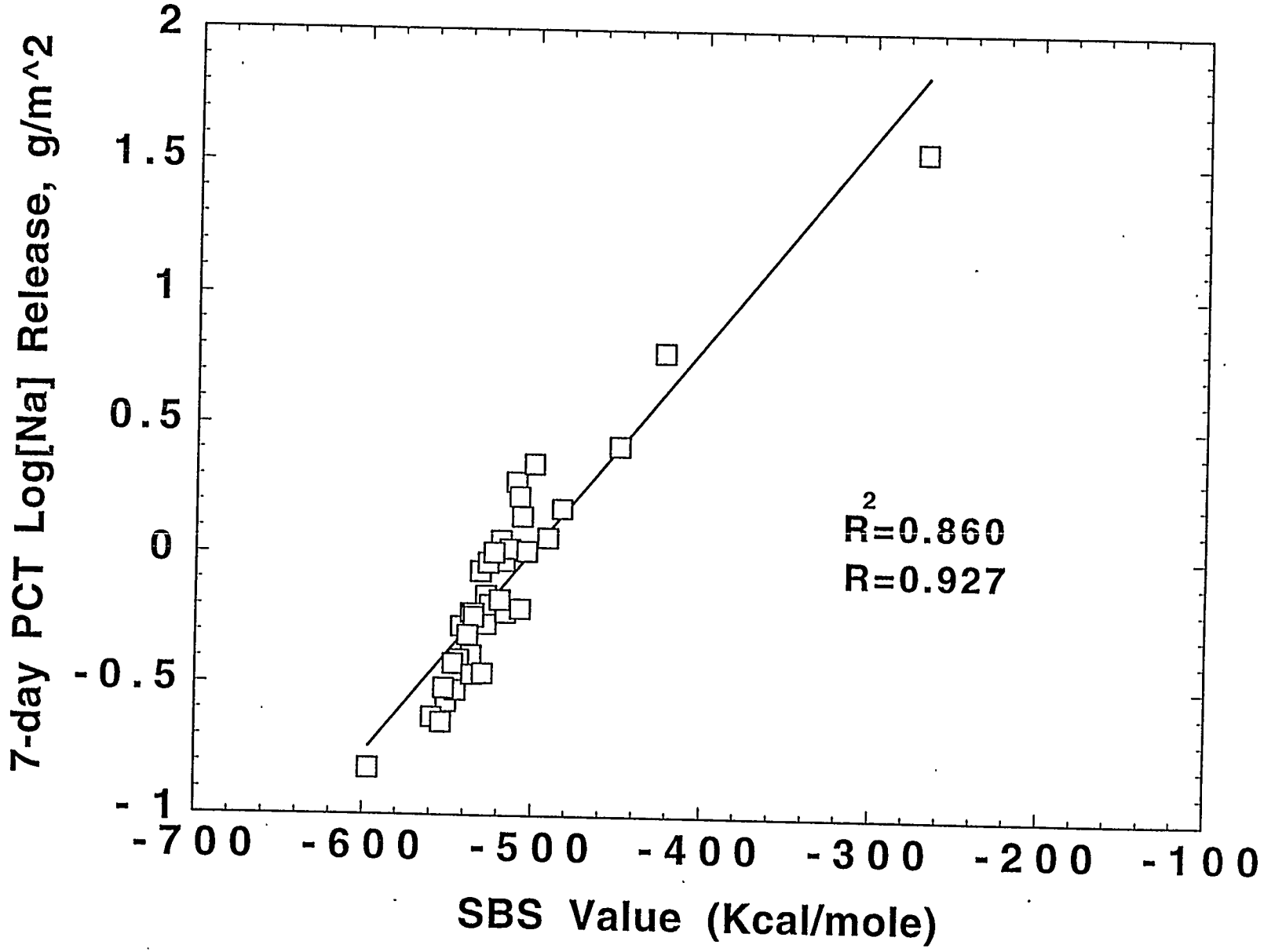

Structural Bond Strength Model on Glass Durability

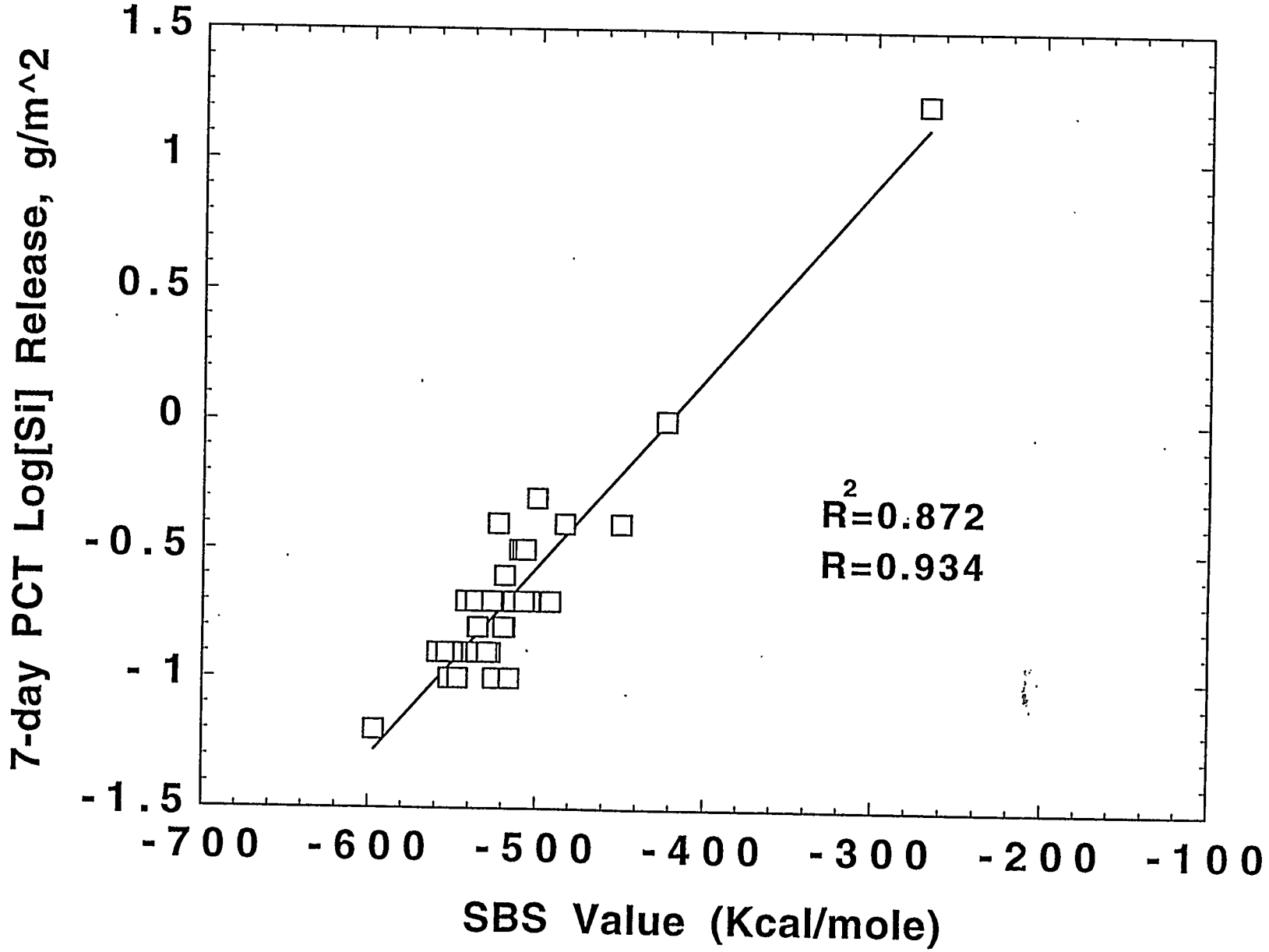

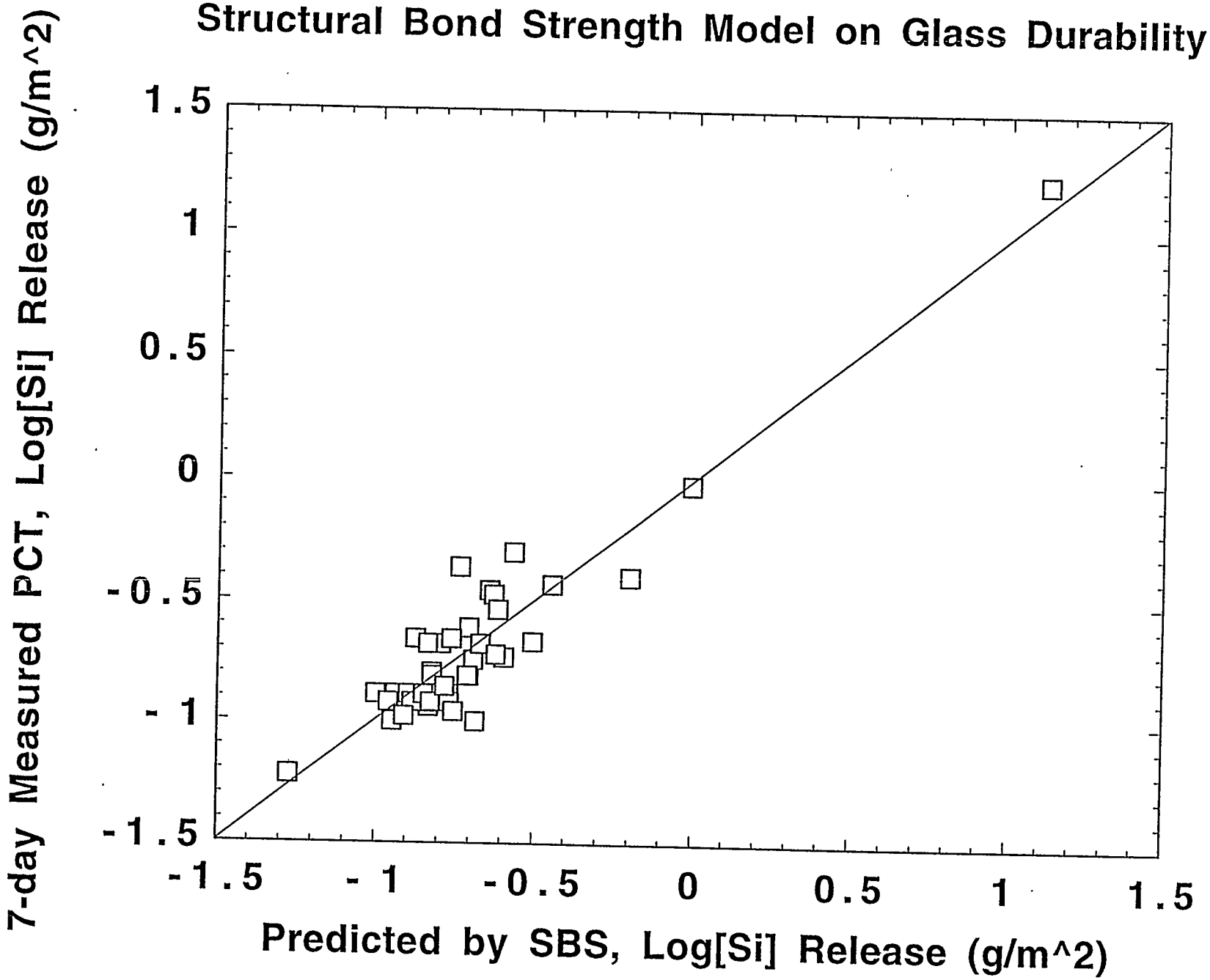
Structural Bond Strength Model on Glass Durability
7-day Measured PCT, Log[Si] Release (g/m^2)
1.5
1
0.5
0
-0.5
-1
-1.5
-1.5
-1
-0.5
0
0.5
1
1.5
Predicted by SBS, Log[Si] Release (g/m^2)

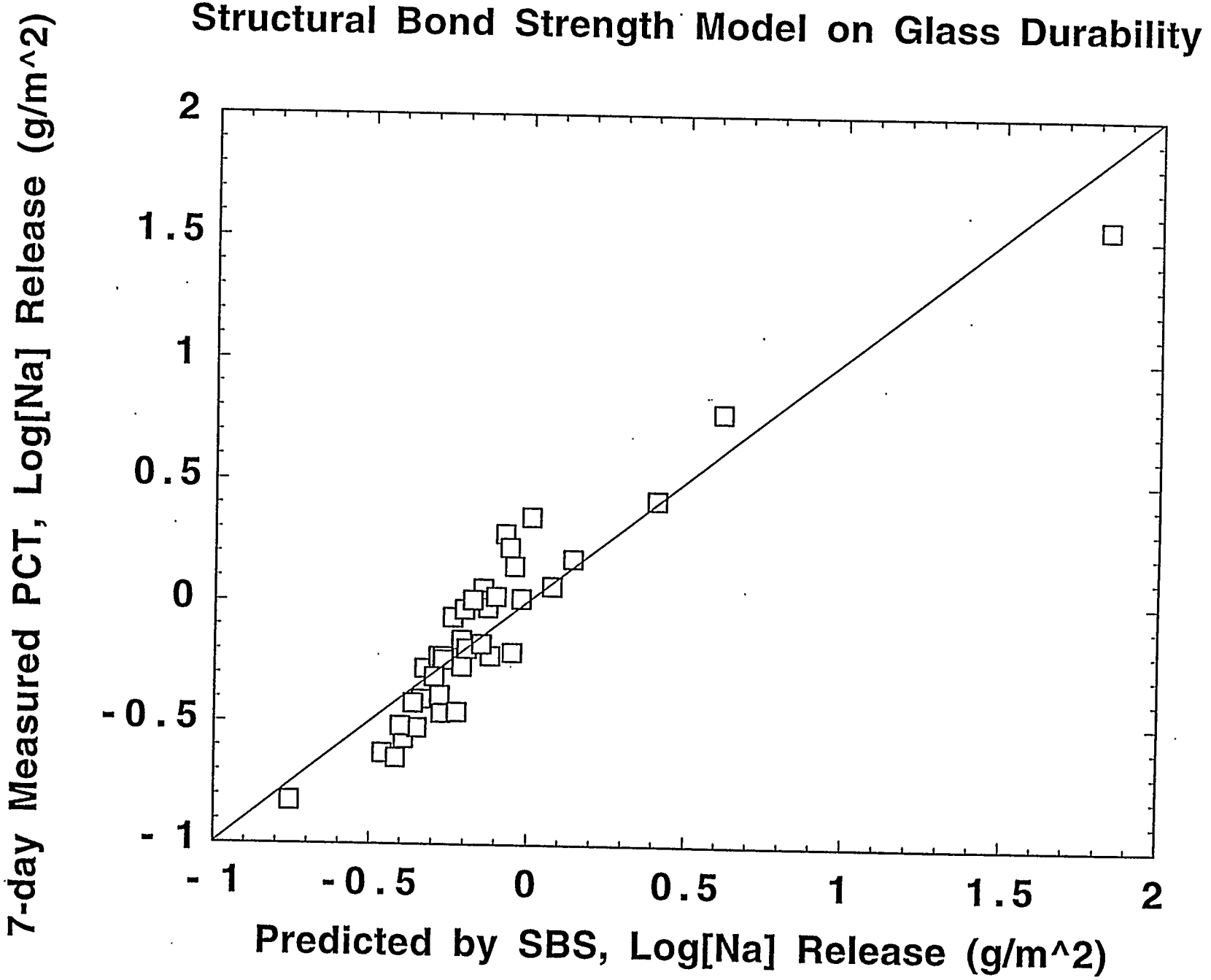
Structural Bond Strength Model on Glass Durability
7-day Measured PCT, Log[Na] Release (g/m^2)
2
1.5
1
0.5
0
-0.5
-1
-1
-0.5
0
0.5
1
1.5
2
Predicted by SBS, Log[Na] Release (g/m^2)

SBS Model Prediction of Glass
Durability at 12% Al2O3

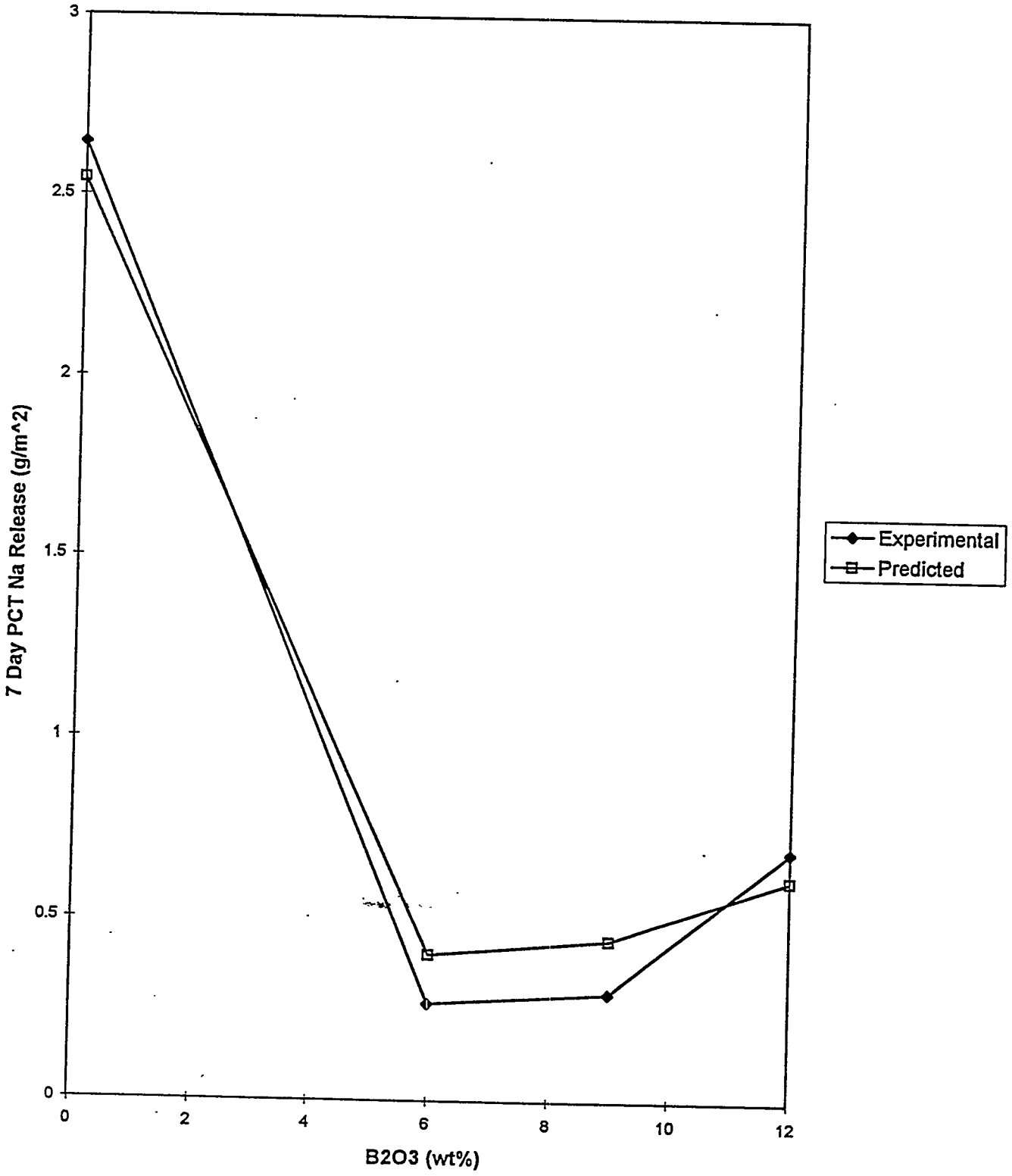

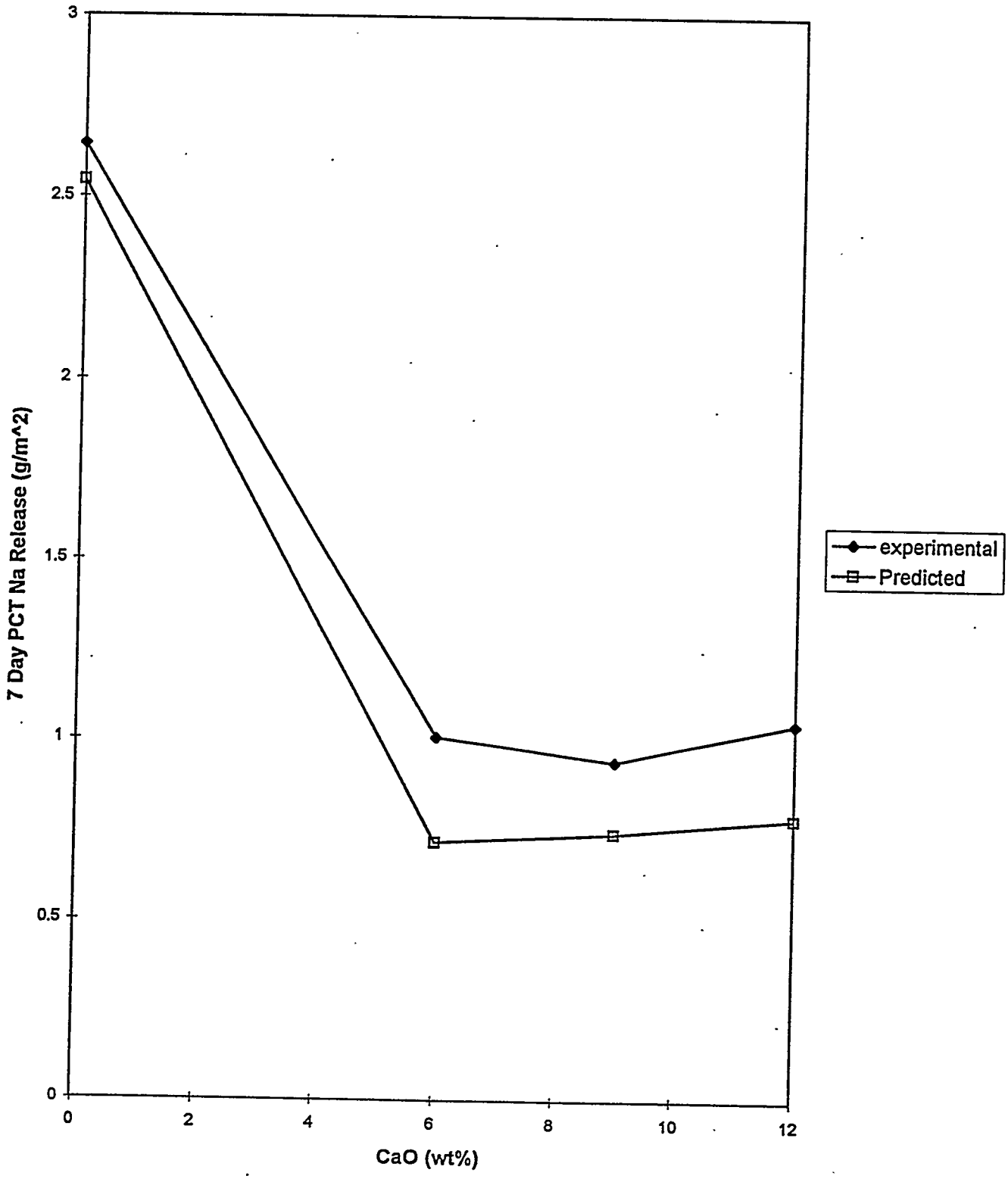
SBS Model Prediction of Glass Durability at 12% Al2O3
7 Day PCT Na Release (g/m^2)
3
2.5
2
1.5
1
0.5
0
0
2
4
6
8
10
12
CaO (wt%)
experimental
Predicted

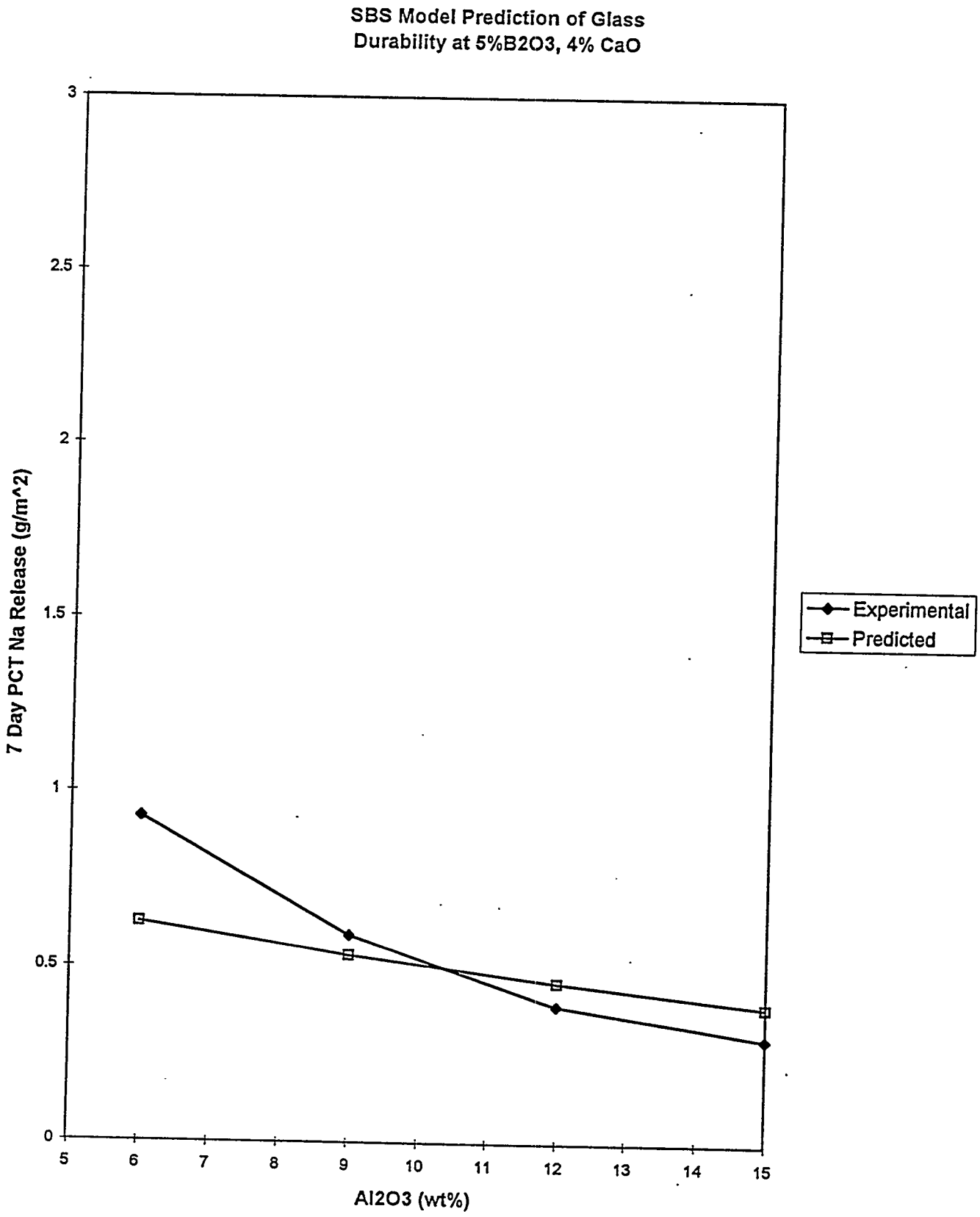
SBS Model Prediction of Glass Durability at 5%B2O3, 4% CaO
7 Day PCT Na Release (g/m^2)
3
2.5
2
1.5
1
0.5
0
5
6
7
8
9
10
11
12
13
14
15
Al2O3 (wt%)
Experimental
Predicted

SBS Model Prediction on Glass Durability- ANL Glasses (166)

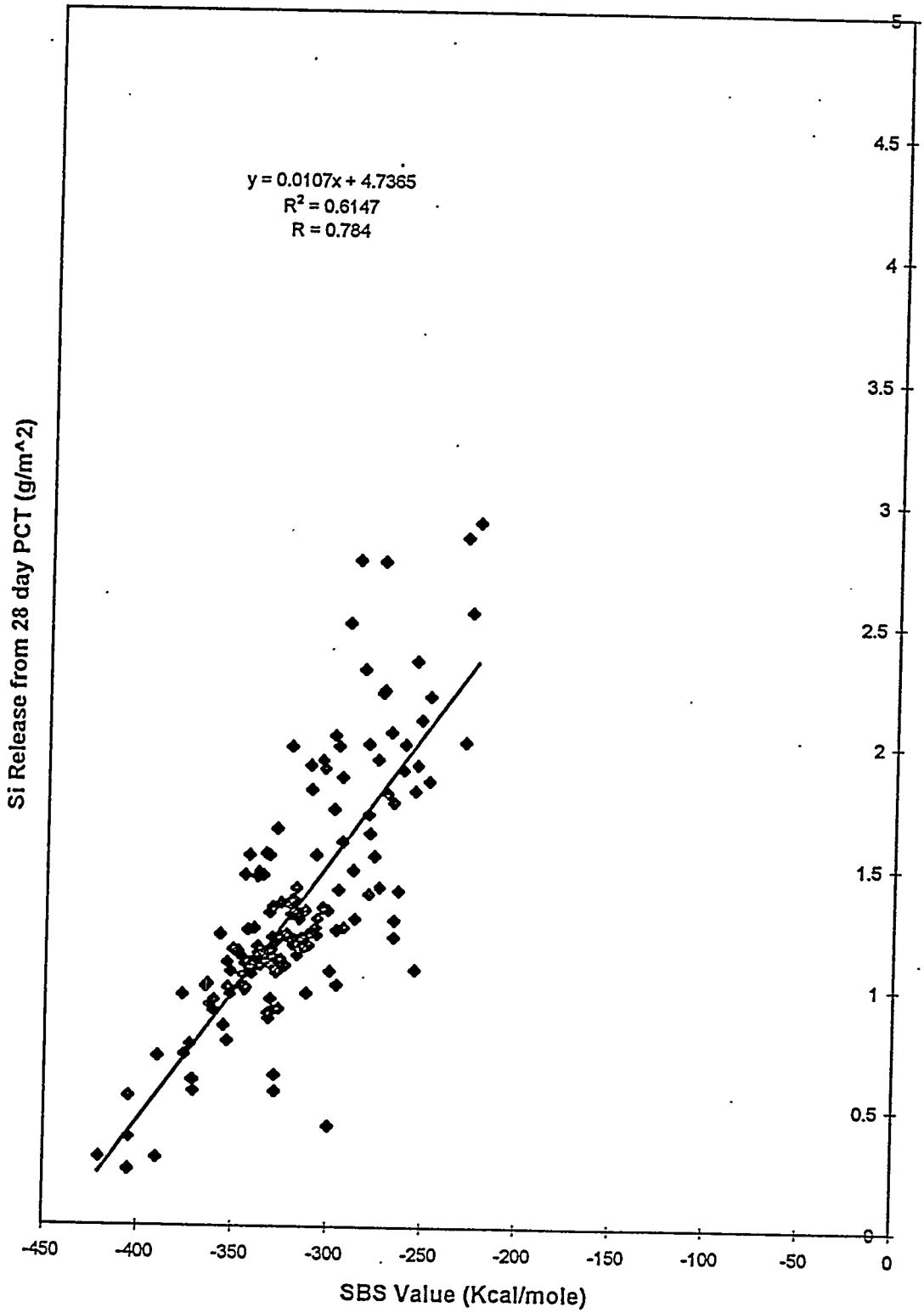

Free Energy of Hydration Model
$R = 0.59, R^2 = 0.35$

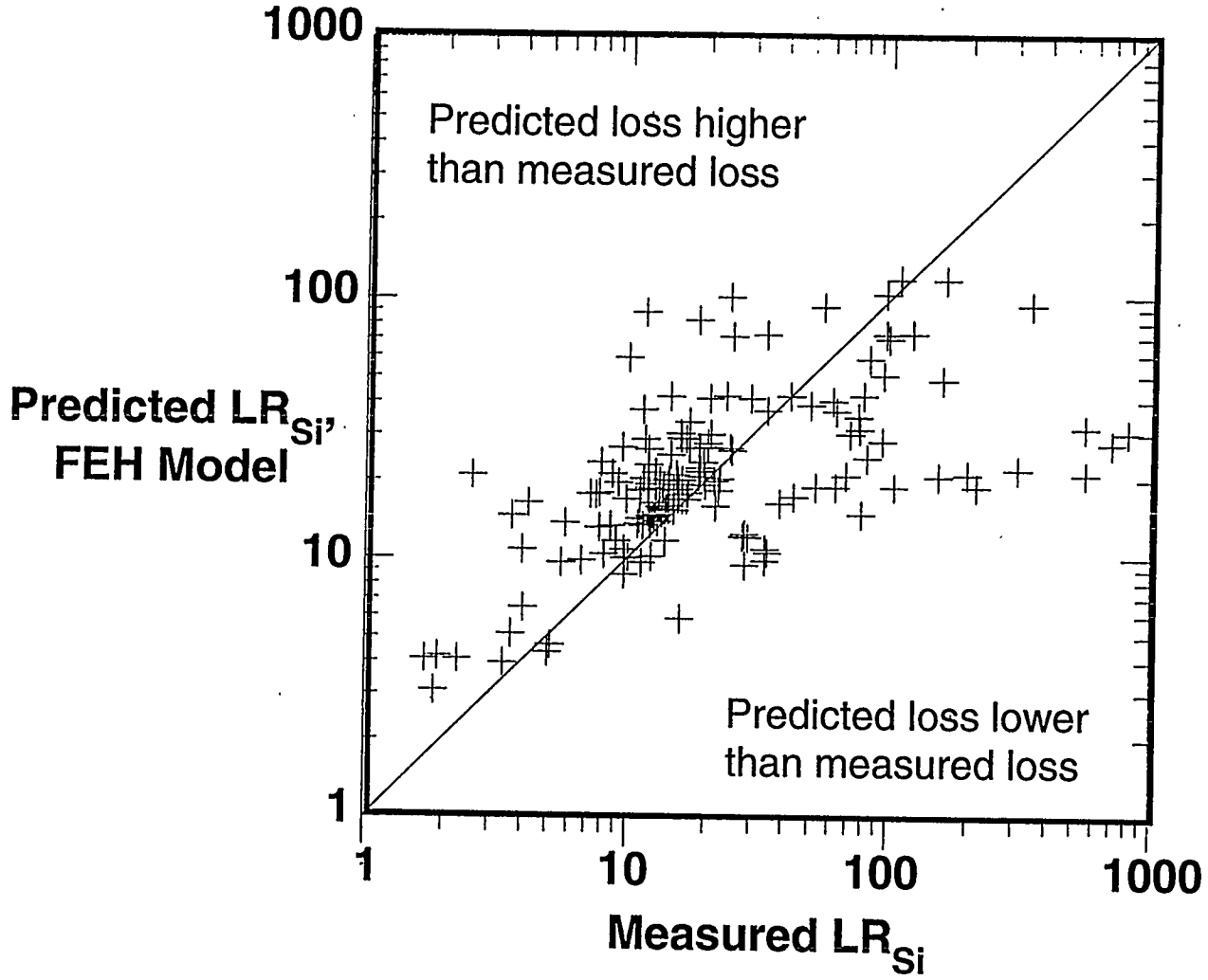

Ellison 1994

SBS Viscosity Modeling

$$\log(\eta) = \frac{B}{T} + A$$

$$A = a_o + a_1 \cdot V$$

$$B = b_o + b_1 \cdot V$$

V - SBS value in Kcal/100g

Found:

$a_o = -4.34 \pm 0.09$

$b_o = 0.0$

$a_1 = -0.00474 \pm 0.0003$

$b_1 = -23.45 \pm 0.3$

Composition Range, in Wt%, Covered by This Study

SiO_2	B_2O_3	Al_2O_3	FeO	Fe_2O_3
17-90	0-20	0-56	0-83	0-24
ZrO_2	ThO_2	UO_2	Li_2O	Na_2O
0-5.5	0-5.5	0-1	0-33	0-36
MgO	CaO	SrO	BaO	PbO
0-44	0-58	0-64	0-72	0-45
MnO	TiO_2	K_2O	P_2O_5	
0-54	0-5	0-35	0-3.5	

1671 data points on 372 glasses as 9 individual sets

EXAMPLES OF APPLICATIONS

1) 1671 data points on 372 glasses

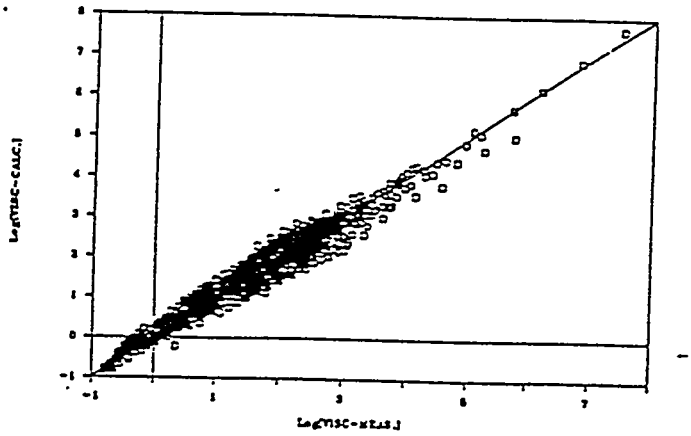

2) On NBS Soda-lime, Lead Silicate and Borosilicate glasses

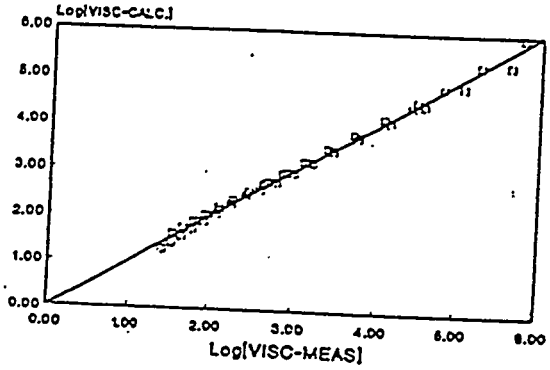

3) On Redox and Silica-Aluminate glasses

VISCOSITIES (poise)

GLASS	Fe(+3)/Fe	MEASURED	PREDICTED	TEMPERATURE
ACMITE at 1430°C:				
AC-7	0.92	20.89	19.26	1430.00
AC-1	1.00	22.91	21.34	1430.00
AC-2	0.82	15.49	17.00	1430.00
AC-3	0.52	10.23	11.99	1430.00
AC-4	0.37	9.46	10.19	1430.00
AC-5	0.25	9.48	9.00	1430.00
AC-6	0.18	9.48	8.38	1430.00
NS4F40 at 1200°C:				
F40-1	1.00	8.41	8.05	1200.00
F40-7	1.00	8.87	8.05	1200.00
F40-2	0.98	7.69	7.59	1200.00
F40-6	0.83	2.23	2.87	1200.00
F40-3	0.47	1.52	1.90	1200.00
F40-5	0.35	1.71	1.41	1200.00
F40-4	0.28	1.36	1.19	1200.00

Standard deviation = 0.057

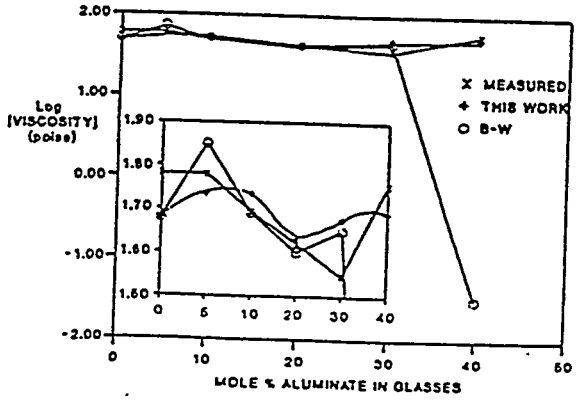

Summary of SBS Model

- A simple model based on heat of formation and structural role of oxides is developed
- This model is quite successful in representing both a wide range of compositions and detailed effects over small ranges
- It is applicable to relate waste form composition to:
  - Durability
  - Temperature dependent viscosity
- SBS model is useful for waste form optimization and it reduces the needs of crucible melts, shortens development time, and enhances the understanding of glass composition effects

Summary of Glass Composition Effects on Durability

- Individual oxide effects are:
  - Non-linear
  - Function of concentration of other components and redox states
- These composition effects can be understood in terms of
  - Structural roles in glass
  - Enthalpy of formation
  - Percolation behavior
- Models based on glass structure and chemistry can help to
  - Optimize glass compositions quickly and economically
  - Excess process control for waste glass production
  - Enhance our understanding and confidence on glass waste forms
- Past knowledge enable us to develop waste glass composition with maximum waste loading, acceptable durability, and desired processability for most of the wastes timely and economically

List of References in X. Feng's Talk on June 27, 1995

Alexander-1986

M. N. Alexander, P.I.K. Onorate, C.W. Struck, J.R. Rozen, G.W. Tasker, and D.R. Uhlmann, J. Non-Crys. Solids, 79, 137-154 (1986).

Bobkova-1983

N.M. Bobkova, O.G. Gorrodetstkaya, S.A. Yankovskay, Z.S. Tizhovka, Fizikai Hkimiya Stekla 9, 414-419 (1993)

Dell-1983

W.J. Dell, P.J. Bray, and S.Z. Xiao, J. Non-Crysta. Solids 58, 1-16 (1983).

Dickenson-1981

M.P. Dickenson and P.C. Hess, Contrib. Mineral. Petrol. 78, 352-357 (1981)

Dickenson-1986

M.P. Dickenson and P.C. Hess, Contrib. Mineral. Petrol. 92, 207-217 (1986)

Ellison-1994

A.J.G. Ellison, J.J. Mazer, and W.L. Ebert, Effects of Glass Composition on Waste Form Durability: A Critical Review, Argonne National Laboratory Report # ANL-94/28, November 1994.

Feng-1988

X. Feng and A. Barkatt, "A Structural Thermodynamic Model for Durability and Viscosity of Nuclear Waste Glasses," Scientific Basis for Nuclear Waste Management XI, Eds., M. J. Apted, and R. E. Westerman, Vol. 112, 543-554 (1988).

Feng-1989

X. Feng, I. L. Pegg, A. Barkatt, P. B. Macedo, S. J. Cucinell, and S. Lai, "Correlation between Composition Effects on Glass Durability and the Structural Role of Constituent Oxides," Nuclear Technology, Vol. 85(3), 334-345 (1989).

Feng-1990a

X. Feng, E. Saad, and I. L. Pegg, "A Model for the Viscosity of Multicomponent Glass Melts," Ceramic Transactions 9, Nuclear Waste Management III, Ed., G. B. Mellinger, 457-46 8(1990).

Feng-1990b

X. Feng, I. L. Pegg, E. Saad, S. Cucinell, and Aa. Barkatt, "Redox Effects on the Durability and Viscosity of Nuclear Waste Glasses," Ceramic Transactions 9, Nuclear Waste Management III, Ed., G. B. Mellinger, 165-174 (1990).

Feng-1994

X. Feng, D. J. Wronkiewicz, J. K. Bates, N. R. Brown, E. C. Buck, N. L. Dietz, M. Gong, and J. W. Emery, "Vitreous ceramic For Minimum Additive Waste Stabilization, Interim Program Report, May 1993 - February 1994," Argonne National Laboratory Report # ANL-94/24, 1994

Feng-1995

X. Feng and T. Metzger, "Improved Structural Bond Strength Model for Glass Durability and Viscosity," in preparation

Zachariasen-1932

W.H. Zachariasen, J. Am. Chem. Soc., 54, 3841(1932)

WASTE LOADING MAXIMIZATION

WASTE LOADING MAXIMIZATION

reduces demands on repository space, processing time, and reduces overall cost

<u>waste loading constraints</u>

- product quality (EA glass PCT standard)
- ease of processing
  - melt viscosity
  - glass crystallization

<u>waste composition</u>

Hanford Site double-shell tank/single-shell tank (DST/SST) HL simulated waste (wt %)

Na_2O	27.02	Al_2O_3	13.88	Fe_2O_3	11.75
SiO_2	10.68	Nd_2O_3	9.33	ZrO_2	7.56
P_2O_5	5.03	CeO_2	2.92	NiO	2.42
CaO	2.20	Bi_2O_3	2.09	MnO	1.59
F	0.59	Cr_2O_3	0.48	La_2O_3	0.46
SrO	0.44	PbO	0.38	SO_3	0.36
K_2O	0.24	WO_3	0.19	CdO	0.10
B_2O_3	0.08	MgO	0.08	MoO_3	0.08
RuO_2	0.05				

GLASSES FOR HIGH-TEMPERATURE MELTER (HTM)

- glass additives: addition of SiO_2 is sufficient to make a durable glass
- melting temperature (the temperature at which viscosity is 4 to 5 Pa·s): approx. 1350°C

<u>effect of crystallization</u>

- liquidus temperature: the maximum temperure at which crystalline phase can exist at quilibrium with melt
- liquidus temperature must be lower than melting temperature minus 100°C to avoid crystallization in the melter
- lab testing for melter crystallization:

  24 h heat treatment at $T = T_M$-100°C
- no crystalline phases precipitate from SST/DST blend waste glass up to W = 0.67 (HWVP limit: W = 0.25)

CRYSTALLIZATION IN CANISTER

- crystallinity can develop in the glass during cooling: the slower cooling, the more crystalline phase may precipitate
- canister centerline cooling (CCC) is the slowest cooling the glass experiences (hence, produces maximum crystallinity)
- CCC schedule:

$\partial T/\partial t = -100°C/h$	1122-872°C
$\partial T/\partial t = -29°C/h$	872-669°C
$\partial T/\partial t = -22°C/h$	669-515°C

CRYSTALLINITY IN GLASS

is acceptable if it does not decrease glass durability

- refractory components (Al_2O_3, Fe_2O_3, SiO_2, Nd_2O_3, ZrO_2, CeO_2, NiO, Cr_2O_3) are prone to crystallization
- removal of reftactory components by the precipitation of crystalline phases weakens glass matrix and increases concentration of alkali oxides (Na_2O) in residual glass; hence, glass durability is likely to be affected
- durability of Hanford Site glasses is decreased by precipitation of
  - nepheline ($NaAlSiO_4$)
  - eucriptite ($LiAlSiO_4$)
  - cristobalite (SiO_2)

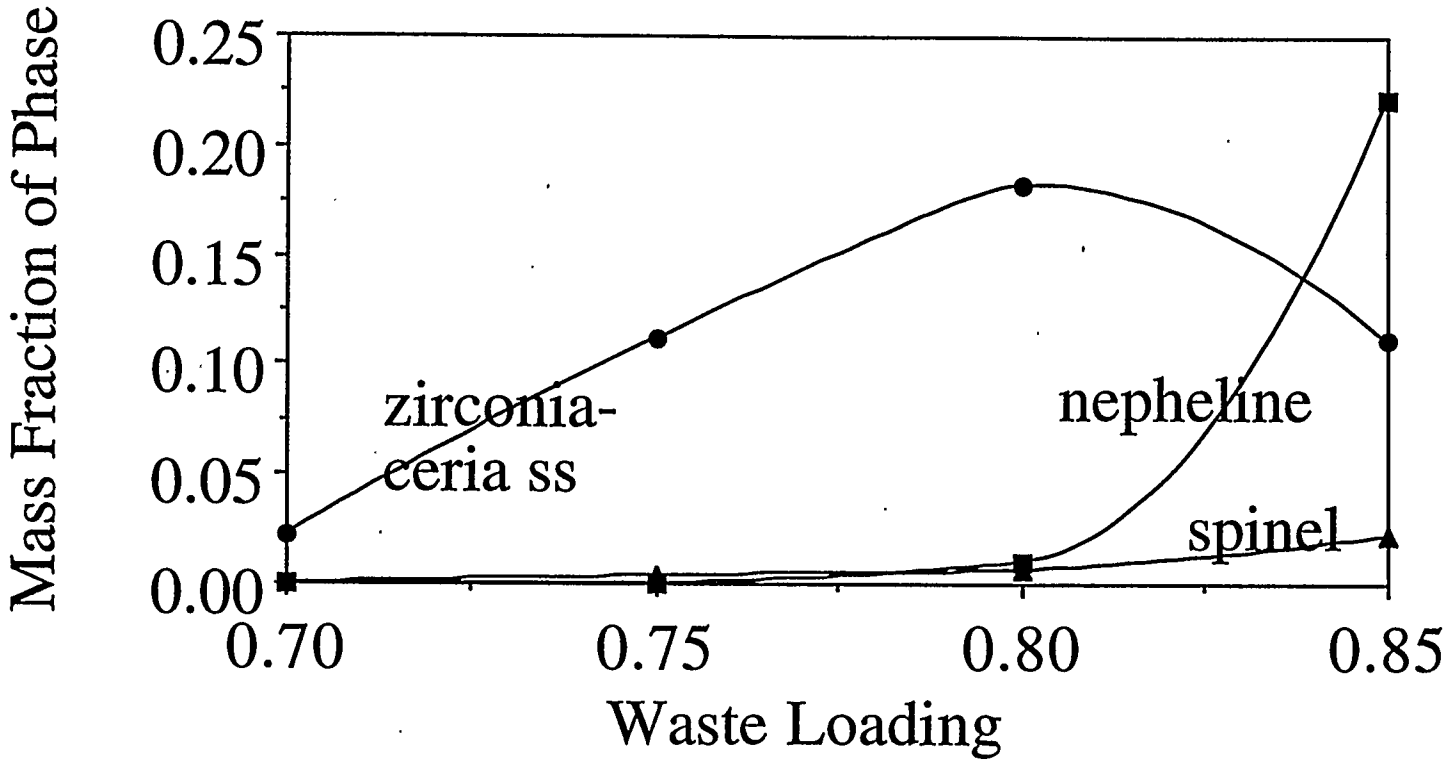

Crystallinity Versus Fraction of
Hanford All-Tank Blend HLW in Glass

ALL-BLEND SIMULATED HLW GLASS CRYSTALLINE PHASES
(from quenched melts)

<u>zirconia-containing crystals</u>
$Nd_2O_3.ZrO_2$-$Ce_2O_3.ZrO_2$ ss ($W \geq 0.7$)
<u>nepheline</u>
$Na_2O.Al_2O_3.2SiO_2$ ($W \geq 0.8$)
<u>spinel</u>
$Fe_2O_3.NiO$-$Cr_2O_3.FeO$ ss ($W \geq 0.75$)

- crystallization of nepheline ($W > 0.80$) removes SiO_2 and Al_2O_3 from residual glass and contributes to the decline in glass corrosion resistance
- both crystalline phases and amorphous phase may affect durability
- difference between the thermal expansion of the residual glass and crystals causes permanent stresses, thus affecting durability
- compositional gradients in residual glass may also impact durability

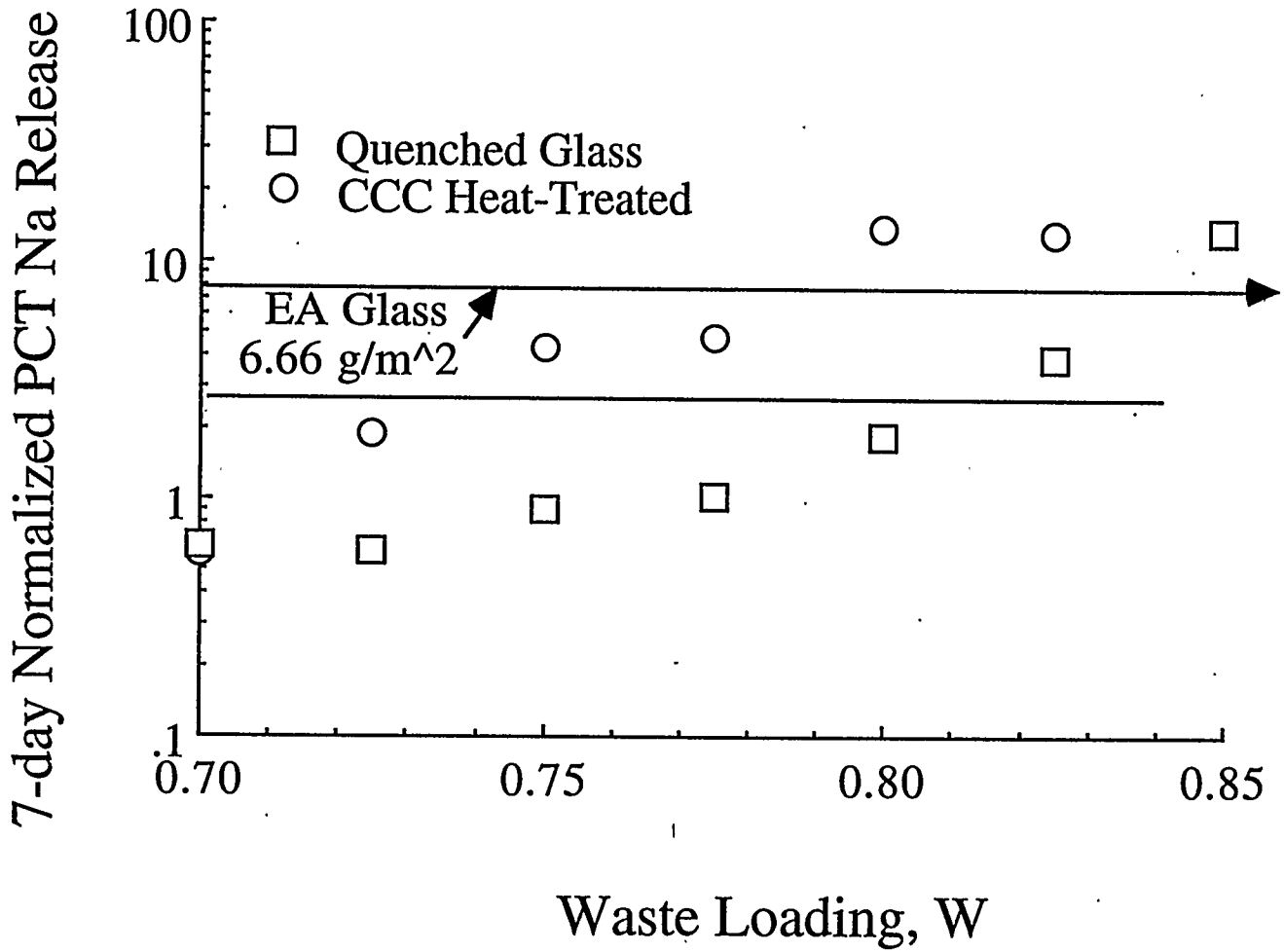
7-day Normalized PCT Na Release
100
10
1
.1
Quenched Glass
CCC Heat-Treated
EA Glass
6.66 g/m^2
0.70
0.75
0.80
0.85
Waste Loading, W

WASTE LOADING LIMITS

- fine crystallinity limit
  - fine (<10 μm) and well dispersed crystals (spinel)
  - a negligible fraction of fine crystals may settle in melter (?)

- coarse crystallinity limit
  - large (>10 μm) heavy crystals (baddeleyite)
  - large heavy crystals settle and block melter

- amorphous phase structural breakdown limit
  - Na_2O from waste eventually causes the breakdown of glass structure

WASTE LOADING FOR HANFORD SITE HLW GLASSES

- the waste loading that can be achieved for SST/DST blend without a formation of crystalline phases in the melter is 0.67 (0.25 anticipated for HWVP)
- this already high waste loading can be increased by an additional 5 to 15 %, dependent on the accepted durability, if crystallinity can be tolerated at glass melting temperatures
- although the current large scale vitrification technology does not tolerate melts with crystals, the potential for waste loading increase may stimulate future development
- for the LLW glass, the waste loading is limited by the maximum fraction of Na_2O that the glass network can accommodate while maintaining acceptable performance

Crystallization — Selected Topics

by John D. Vienna, Research Scientist, Pacific Northwest Laboratory, 372-2807

Introduction:

- Importance:

Crystalline phases precipitated in a continuous melter can cause processing problems, such as sludge formation on the melter bottom or even melter electrode shorting if the phases are highly conductive. In addition, if crystallization occurs during canister cooling, the glass durability may be strongly reduced.

For these reasons, restrictions have been placed on glass to avoid precipitation in the melter and excessive crystallization in the canister. These properties are difficult to estimate. So restrictions on composition must be conservative enough to avoid the problematic events.

- Hanford Needs:

Recent experience with Hanford HLW formulation efforts have shown that crystallinity is the factor that limits waste oxide loading in nearly every case. The ability to accurately predict these phenomena would increase the efficiency of glass formulation efforts and more importantly the overall waste oxide loading of glass produced at Hanford. This would mean a significant decrease in cleanup costs. Our current ability to predict phase transformations in waste glass is limited. To make improvements in our ability to predict these phenomena, we must develop a more complete understanding of them.

Thermodynamics (brief review):

- Gibbs Free Energy:

The free energy of a system is the energy available to do work. Gibbs free energy is defined in terms of internal energy (E), pressure (P), temperature (T), entropy (S), and enthalpy (H):

$$G = E + PV - TS = H - TS$$

The internal energy is the total energy (including kinetic and potential) of all the atoms or molecules in a system. Although E cannot be measured, ΔE can:

$$\Delta E = E_2 - E_1 = q\text{-}w$$

where q is the heat added to and w is the work done by the system. H is a measure of the heat of a system and ΔH is the heat absorbed by the system (q =

$\Delta E + P\Delta V = \Delta H$) assuming only PdV work.

ΔH can be generated by reactions, temperature change, ...

$$\Delta H = H_{prod} - H_{react}$$

$$\Delta H = H_{T_2} - H_{T_1} = \int C_P dT$$

Likewise, entropy is a measure of randomness or disorder and is given by:

$$\Delta S = S_{prod} - S_{react}$$

$$\Delta S = S_{T_2} - S_{T_1} = \frac{\Delta q_r}{T} = \int \frac{C_P}{T} dT$$

where C_P is the constant pressure heat capacity (with a temperature dependence of the form $a + bT + cT^{-2}$).

Work can be expressed in the form intensive times differential of like extensive variables:

$$dw = PdV - \sigma d\varepsilon - \gamma dA - \sum \mu_i dn_i - HdM - \ldots$$

where the mechanical, strain, surface, chemical, magnetic, and other work terms are summed. Commonly only PdV work is considered at constant pressure. However, for the purpose of phase transformations chemical work is considered. This term is a summation of chemical potentials of all components (n) in a system. Chemical potential is then defined as the partial molar free energy of a component in a system:

$$\mu_i = \left(\frac{dG}{dn_i}\right)_{P, T, n_{j \neq i}}$$

The free energy change of the system is then given as:

$$dG = VdP - SdT + \sum_i \mu_i dn_i$$

The free energy associated with mixing is given by:

$$\Delta G^M = RT\sum_i X_i \ln a_i$$

where X_i is the mole fraction and a_i is the activity of the i-th component. The activities of each component in an ideal solution are equal to the mole fractions of components. The deviation from ideality is given by the activity coefficient:

$$\gamma_i = a_i/X_i$$

For $\gamma_i > 1$, the driving force for the component to enter solution is less than that for ideal solution. Similarly, if $\gamma_i < 1$ the driving force is more than that for ideal solution.

Excess free energy (enthalpy and entropy) is the difference between the free energy and that of an ideal solution (mixture):

$$G^E = \Delta G^M - \Delta G^{M,Ideal}$$

and:

$$G^E = RT\sum_i X_i \ln \gamma_i \text{ , and } \mu_i^E = RT \ln \gamma_i$$

- Equilibrium:

Equilibrium is defined in many ways. For the purposes of this discussion it will be defined by a minimum of system free energy. This minimum is with respect to fluctuations such as kT, μ_i, n_i, etc... Such energy minimums if local (and not global) are termed meta-stable equilibriums.

When considering crystallization at constant P and T, minima in G define equilibrium. In this case reactions (such as crystallization) will proceed in the direction of negative ΔG.

The Gibb's Duhem relation yields:

$$\sum_i X_i d\mu_i = 0$$

at equilibrium and for multi-phase systems, the chemical potential of any component is equal in all phases.

- Phase Diagrams:

Developed using common tangent of free energy curves of all phases at a given temperature.

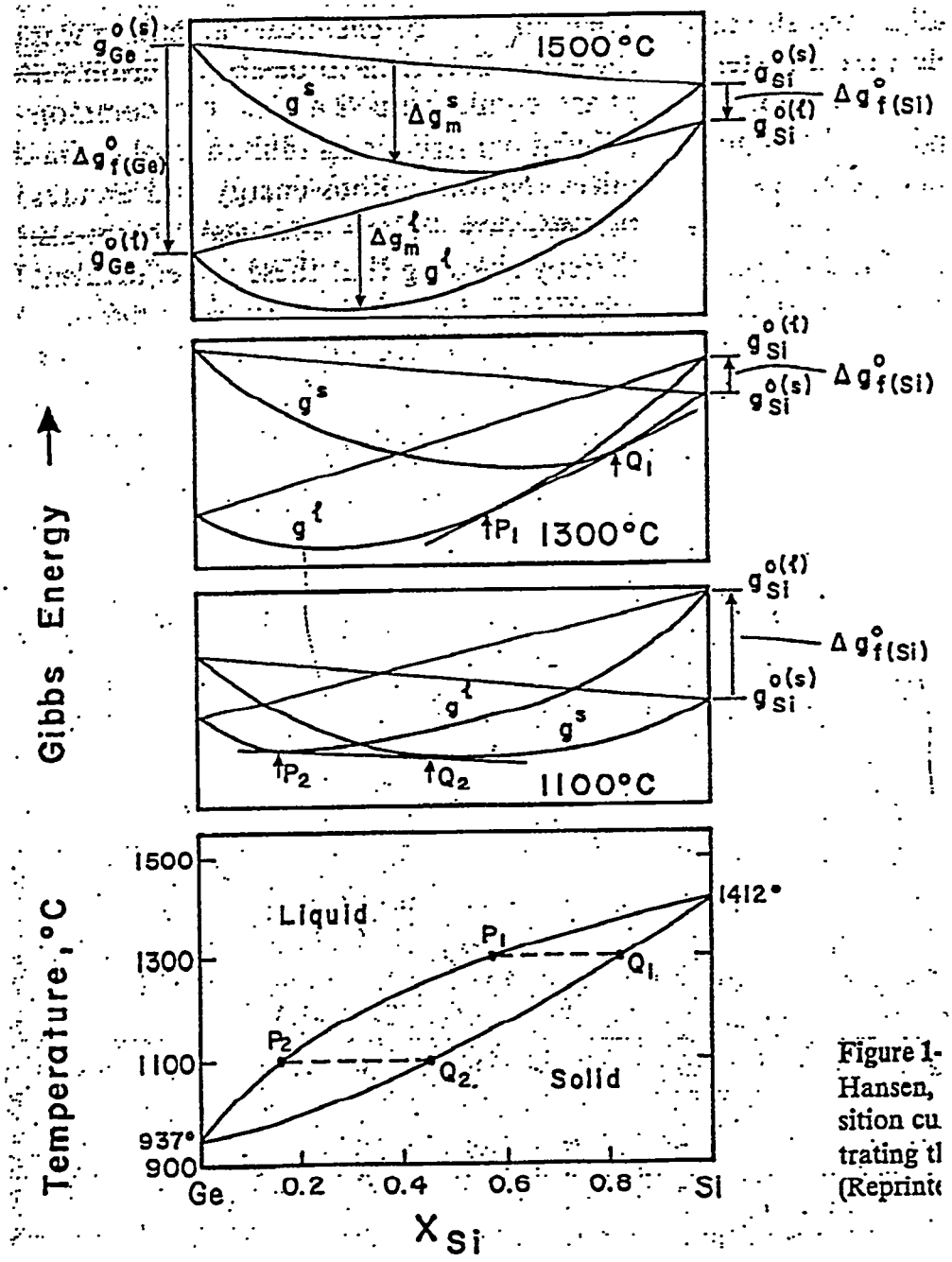

Figure 1-
Hansen,
sition cu
trating tl
(Reprint

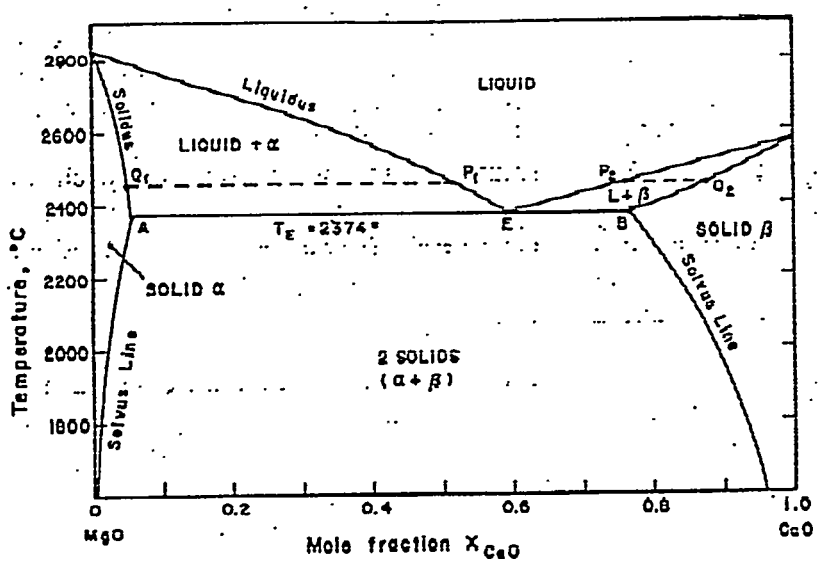

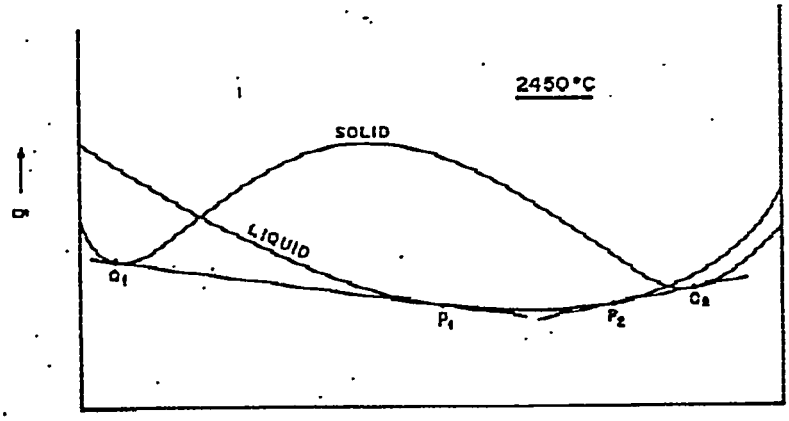

Liquidus Temperature:

- Definition:

Liquidus temperature (T_L) as seen from phase diagram is the point at which a given composition is first in equilibrium with crystal phase. In reality, there is a range of meta-stable equilibrium of liquid phase below this liquidus temperature.

Effectively, T_L is taken at the temperature of crystal precipitation. Precipitation requires there to be a finite driving force (ΔG). In addition, the additional surface work term must be considered when crystals form in (or at a surface of) a molten bath.

- Measurement:

Several methods are used to measure T_L. Factors influencing results include:

- heat treatment as dissolution or crystallization
- heat treatment crucible (Pt, SiO_2, Al_2O_3, covered, uncovered,...)
- isothermal vs gradient furnace,
- heat treatment time,
- analysis method (OM, SEM, XRD)

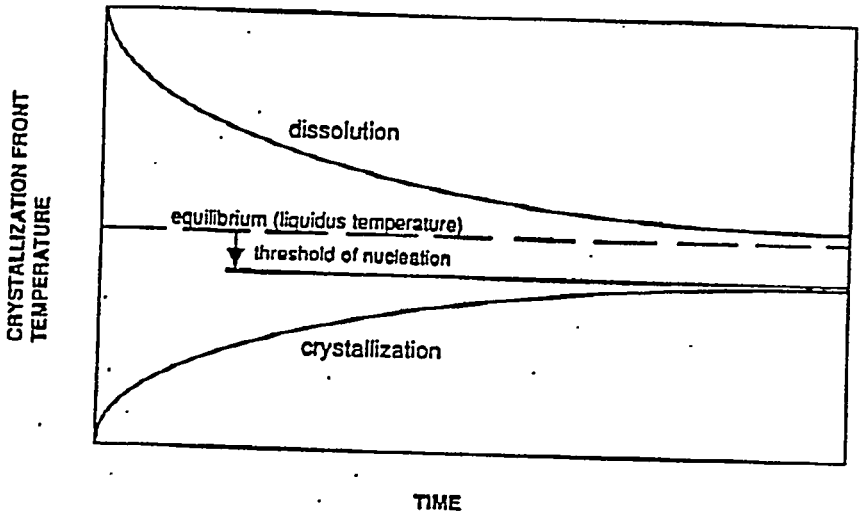

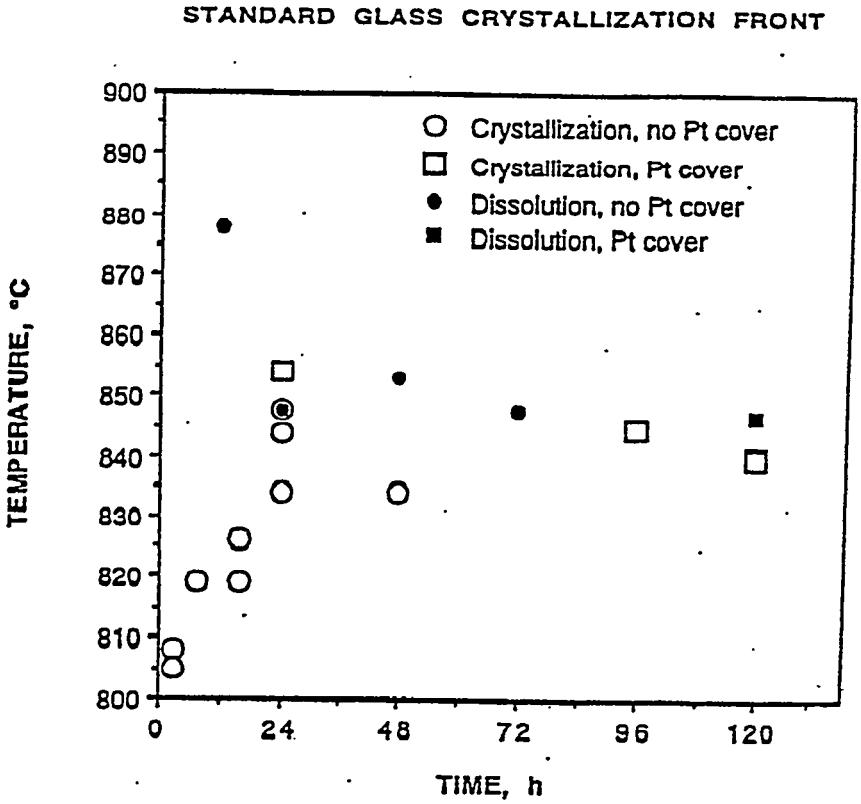

- Modelling:

Liquidus temperature is modelled using free energy estimation techniques. For a given melt composition, the free energy is estimated. That energy is then compared to the energy of crystalline phases in the melt as a function of temperature. The point at which the energy of the melt is equal to that of the crystalline phase ($\Delta G = 0$) is T_L. This generally doesn't include estimates of surface energy contributions or effects of composition fluctuations within the melt.

The regular solution theory leads to the most commonly used models of free energy of mixtures (such as glass melts). A regular solution is one which follows the simplified relationship:

$$G^E = X_A X_B(\omega - \eta T)$$

where ω and η are constants independent of temperature (they analog to excess enthalpy and entropy of mixing). Strictly, this estimation assumes substitutional solution of components with like charge, coordination, and size such that there is no configurational entropy change and bond energy is the some of nearest neighbor (NN) pairs (independent of T and composition). In this case, excess energy is due to the enthalpy of mixing, which is assumed to be the average of the change in NN bond energy.

According to the regular solution theory, the activity coefficient is given as a polynomial of composition:

$$g_A^E = X_B^2(\omega - \eta T) = RT \ln \gamma_A$$

Constant temperature estimates of excess free energy consider only ω which can be estimated by bond strength, deduced from thermodynamic data, or fit empirically.

For ionic solutions, X_i is taken as charge equivalents rather than mole fractions and second NN interactions are important. A "quasichemical model" (QCM) has been proposed as an extension of the regular solution theory for free energy prediction in oxide and salt melts.

The QCM assumes that second NN's are like charged and can segregate according in the interaction energy. A quasi-chemical reaction is written such as:

$$X_{AA} + X_{BB} \Leftrightarrow 2X_{AB}$$

with a reaction constant k given by:

$$k = \frac{X_{AB}^2}{X_{AA}\,X_{BB}} = 4\,\mathrm{Exp}\left[-\frac{2(\omega-\eta T)}{ZRT}\right]$$

The *excess energy* terms ω and η are of the form:

$$\omega_{ij} = \omega_{0(ij)} + \omega_{1(ij)}X_j + \omega_{2(ij)}X_j^2 + \omega_{3(ij)}X_j^3 + \ldots$$

where ω_{ij} are obtained from least squares fitting of binary phase diagrams. The extension of these terms to ternary and higher system requires development out of the scope of this discussion (see literature on quasichemical model).

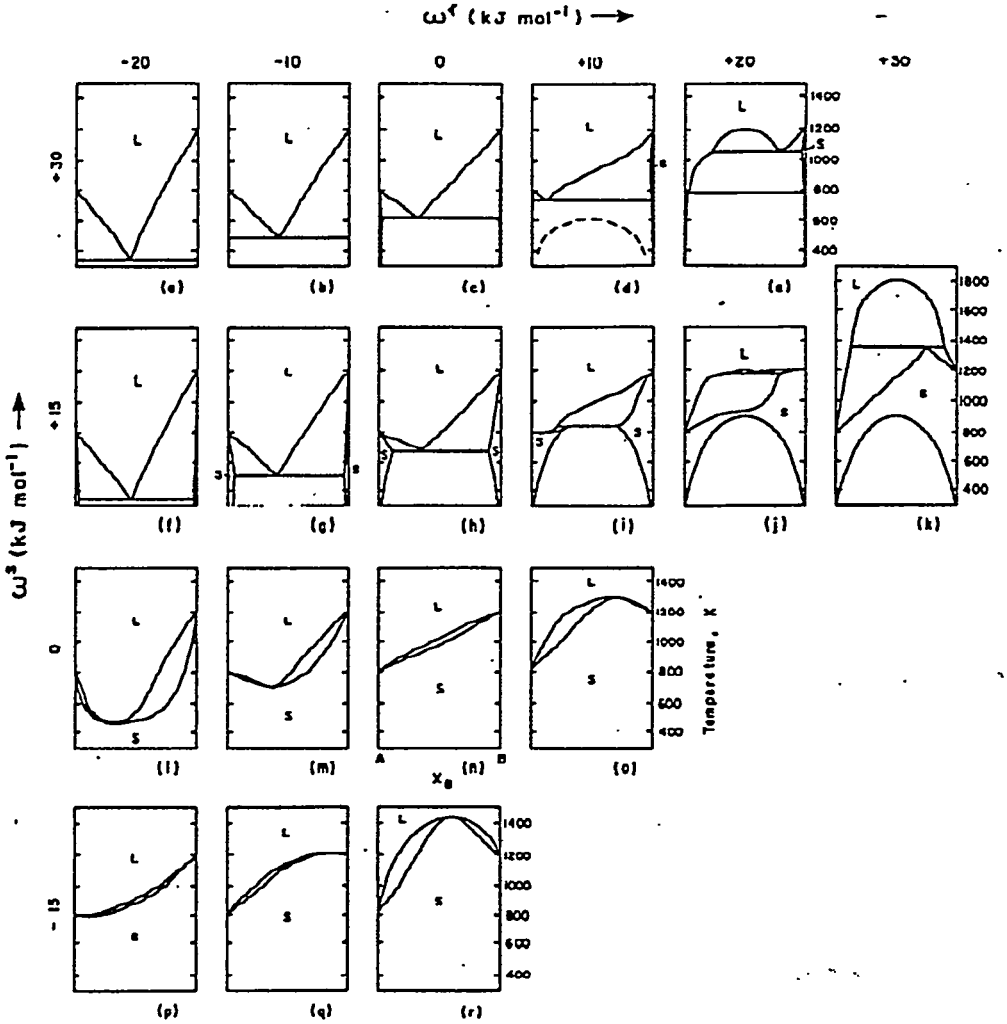

Figure 1-14. Topological changes in the phase diagram for a system A - B with regular solid and liquid phases, brought about by systematic changes in the regular solution parameters ω^0 and ω^1. Melting points of pure A and B are 800 K and 1200 K. Entropies of fusion of both A and B are 10.0 J/mol K (Pelton and Thompson, 1975). Dotted curve in panel (d) is metastable liquid-liquid miscibility gap (Reprinted from Pelton, 1983).

- Nuclear Waste Glass

The QCM has been successful in the prediction of multi-component phase diagrams of simple systems. HLW glass however contains 30+ components many of which are not commonly found in thermodynamic data or in nature for that matter. An additional complication is the effect of oxygen activity in the HLW glass melt. Transition elements such as Cr, Fe, Mn, Ce are active redox elements in the temperature and composition ranges considered.

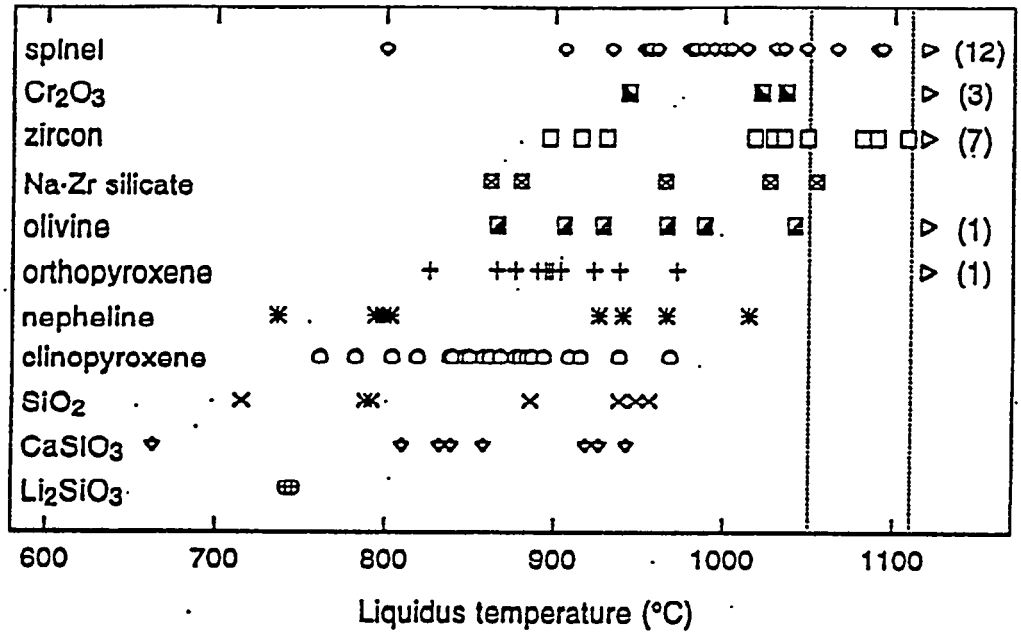

Several attempts have been made to predict T_L in HLW glass:

- concentrations of limiting components (strict single and multiple component concentrations, component ratios, tree type models, ...)
- first-order models of some major components
- preliminary QCM's

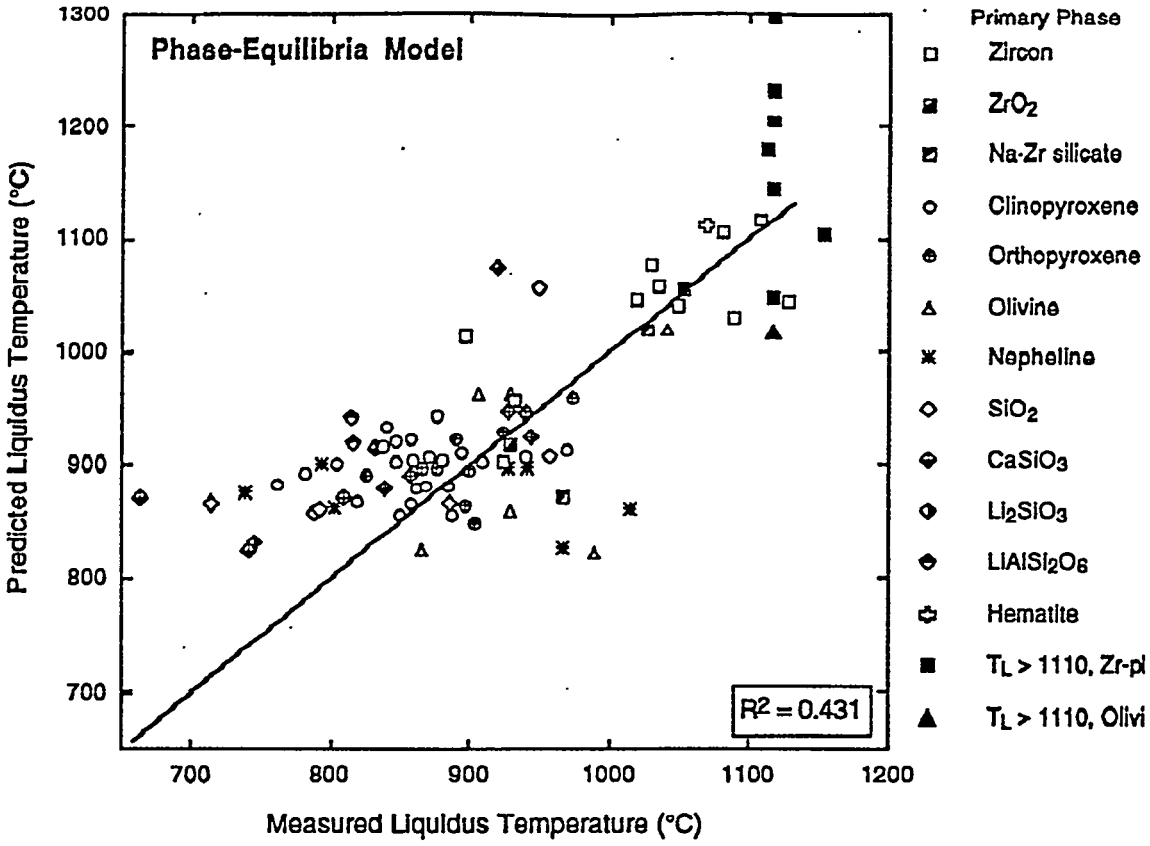
Phase-Equilibria Model
Predicted Liquidus Temperature (°C)
Measured Liquidus Temperature (°C)
1300
1200
1100
1000
900
800
700
700
800
900
1000
1100
1200
R2 = 0.431
Primary Phase
Zircon
ZrO2
Na-Zr silicate
Clinopyroxene
Orthopyroxene
Olivine
Nepheline
SiO2
CaSiO3
Li2SiO3
LiAlSi2O6
Hematite
TL > 1110, Zr-pl
TL > 1110, Olivi

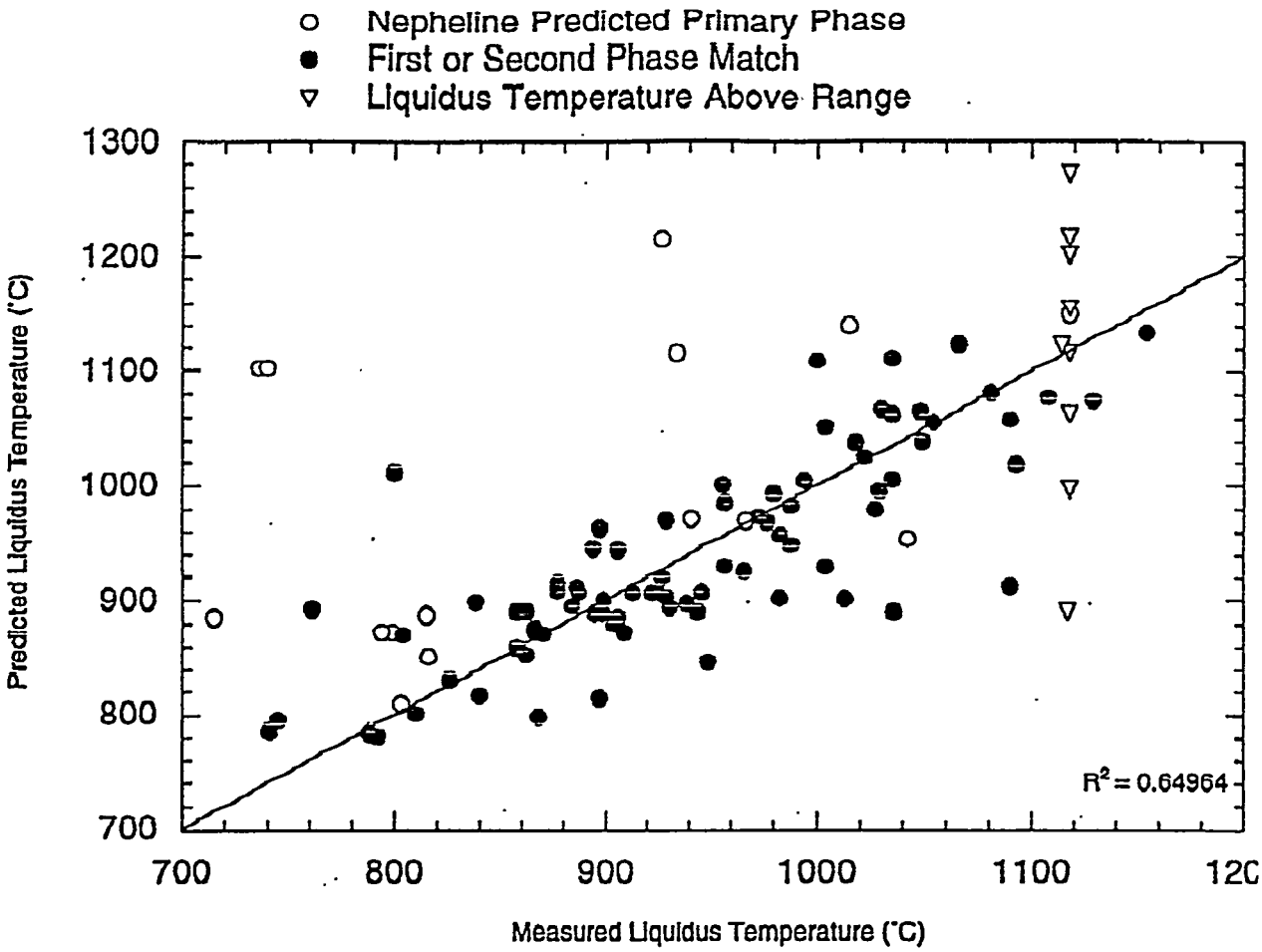

Nucleation and Growth:

- Classic Nucleation Theory

Crystallization occurs via a two stage process, nucleation and growth. Nucleation is the formation of a crystal "seed" large enough to be energetically stable. This nucleus then grows into a crystal.

Consider the formation of a spherical nucleus through random particle motion. As the nucleus forms the system free energy is lowered by:

$$\Delta G_V = 4/3\ \pi\ r^3\ \Delta g_v$$

and raised by:

$$\Delta G_S = 4\ \pi\ r^2\ \gamma$$

combining these terms leads to the following relationship between radius and

energy:

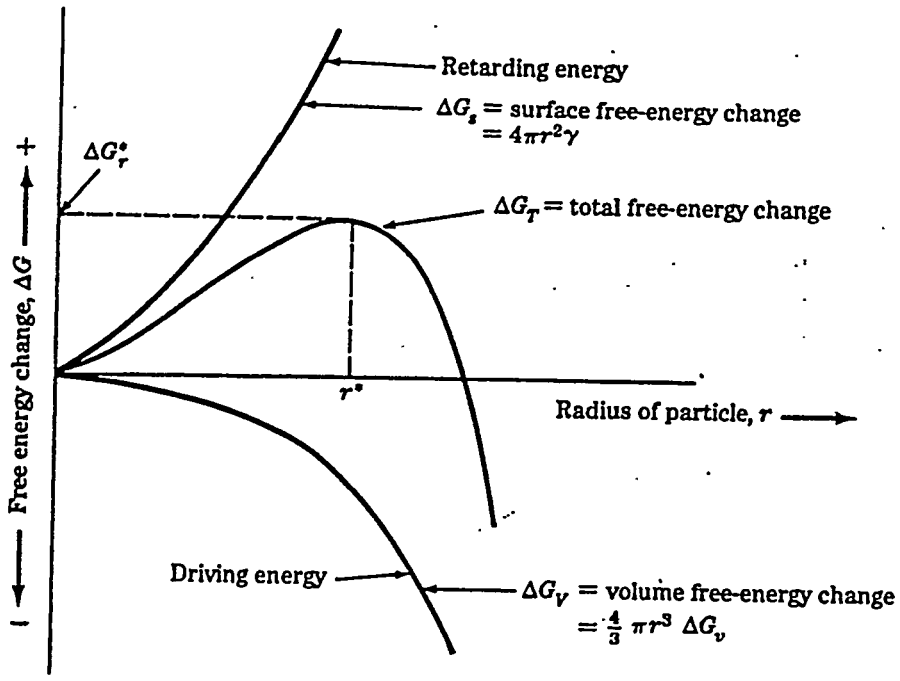

The critical radius (r*) changes with under cooling according to:

$$r^* = \frac{2\gamma T_L}{\Delta H_f \, \Delta T}$$

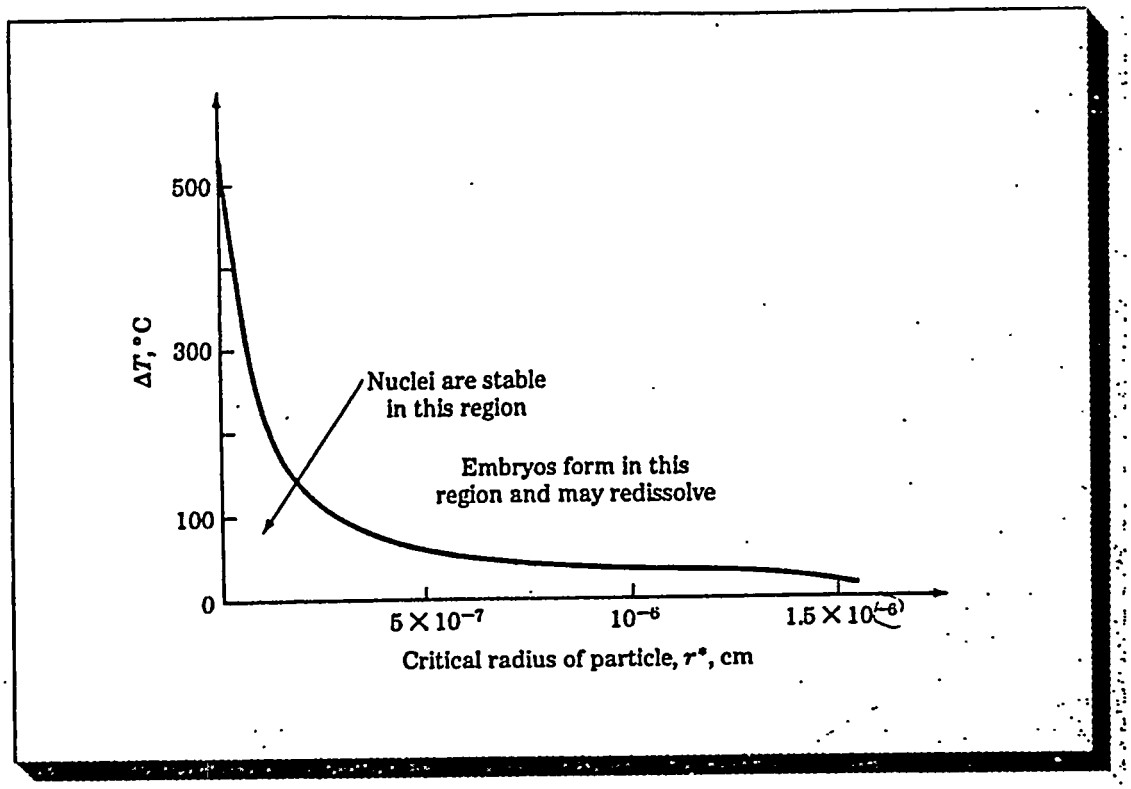

The rate of nucleation is proportional to the driving force and rate of particle motion. A commonly used equation for steady state nucleation is:

$$I^{ss} = 2\,c\,n_v \frac{kT}{\eta}\,\mathrm{Exp}\left[\frac{\Delta G_T + Q_D}{kT}\right]$$

where Q_D is the activation energy for oxygen diffusion. For transient nucleation, the Zeldovitch-Frenkel theory must be applied:

$$I = I^{ss}\left[1+2\sum_{\alpha}(-1)^{\alpha}\,\mathrm{Exp}\left(\frac{-\alpha^2 t}{\tau}\right)\right]$$

where the time constant, τ, is related to the free energy required to form a cluster of a given size and the attachment rate of atoms to the cluster.

The theory of nucleation in glass has held up very well to experimental results for simple glass systems which nucleate homogeneously. Examples of such systems are:

$BaO{\cdot}2SiO_2$
$Na_2O{\cdot}2CaO{\cdot}3SiO_2$

$CaO \cdot Al_2O_3 \cdot 2SiO_2$
$Na_2O \cdot SiO_2$
$2Na_2O \cdot CaO \cdot 3SiO_2$
$Li_2O \cdot 2SiO_2$
$CaO \cdot SiO_2$
$Li_2O \cdot SiO_2$
$Li_2O \cdot 2B_2O_3$

Homogeneous nucleation occurs in only a limited number of glass systems. Four 'rules of thumb' apply to glasses which nucleate homogeneously (Zanotto and Muller, 1991):

- Crystal composition must be close to that of glass matrix composition.
- Both cation and anion arrangements in glass are similar to those in the crystal.
- The reduced glass transition temperature (T_g/T_L) is less than 0.6 (T_g is the glass transition temperature).
- The mass density of crystal must be similar to that of glass matrix.

A majority of glass systems (including nuclear waste glass) nucleate heterogeneously on impurity particles, surfaces, and/or areas of concentration fluctuations. Heterogeneous nucleation sites lower the thermodynamic barrier (ΔG_T^*) by decreasing the surface energy associated with embryo formation. The change in thermodynamic barrier is a function of contact angle ($\emptyset$) as follows:

$$\Delta G_{T,h} = \Delta G_T \, f(\emptyset)$$

The surface factor $f(\emptyset)$ is a function of embryo shape. Given for a spherical cap geometry as:

$$f(\emptyset) = (2 + \text{Cos } \emptyset)\,(1 - \text{Cos } \emptyset)^2 / 4$$

The contact angle is related to the surface energy of the glass - surface interface (γ_{gs}), crystal or nucleus - surface interface (γ_{sc}), and the crystal - glass interface (γ_{cg}).

$$\text{Cos } \emptyset = \frac{\gamma_{gs} - \gamma_{sc}}{\gamma_{cg}}$$

- Nucleating Agents:

The above treatment assumes a flat surface or a very large radius of curvature for the substrate surface in relationship to r*. The thermodynamic barrier (ΔG_T^*) will increase if surface is concave downward (i.e. very small particle), reducing the ability to nucleate. Likewise, if the surface is concave upward (i.e. scratch or cavity), the ability to nucleate is increased. Hence, nucleation is more likely on large impurity particles.

Nucleating agents are added to glass in the manufacture of glass ceramics, and in the study of crystallization kinetics. Common agents used to nucleate crystals in glass are: Au, Ag, Ti, Pd, and Pt. In addition to nucleating agents, enhanced nucleation often occurs on interfaces of amorphous phase separation, chemical inhomogeneities, glass particle surfaces, and interfaces with crucible or melter walls.

- Nucleation in Waste Glass

Nuclear waste glass generally contains a large number of solid inclusions. These inclusions include noble metal particles, undissolved refractory oxides, and other crystals such as spinel. To predict the effects of nucleating agents on crystallization in the melter and canister, preliminary studies have been undertaken.

It was found that crystals nucleate on solid inclusions in simulated nuclear waste glass. Generally, the higher concentration of nucleation sites, the higher crystallinity in the glass after heat treatment.

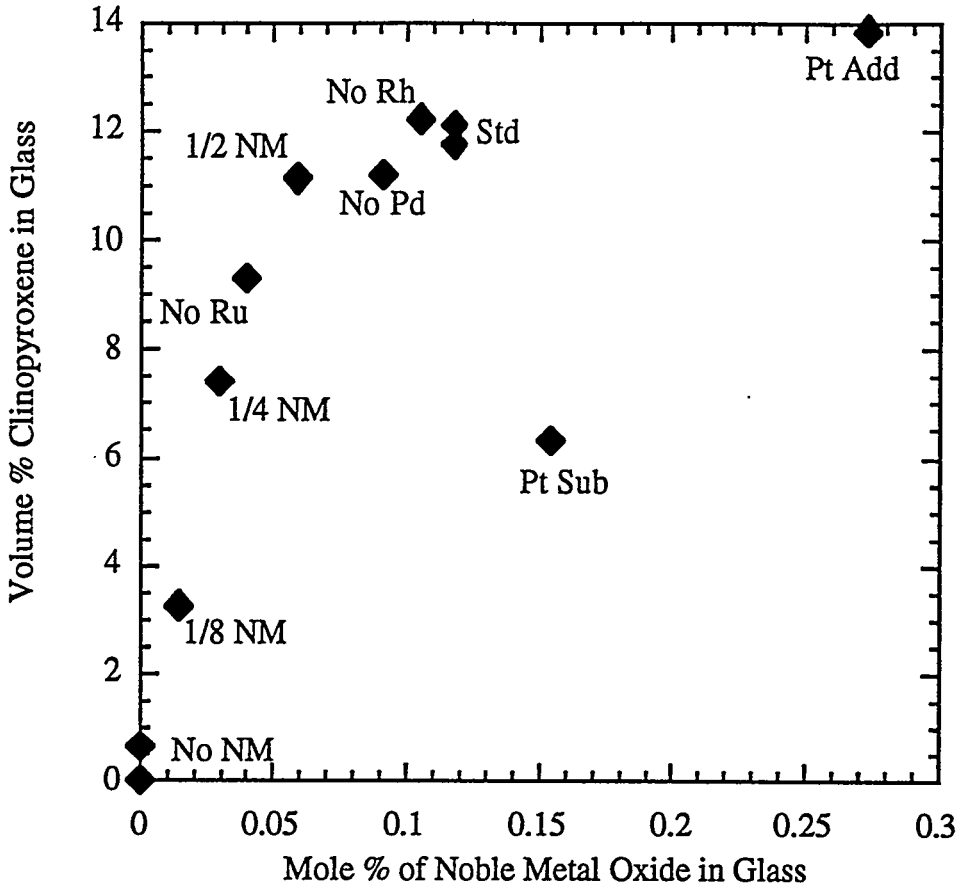

The tank waste will have varied amount of nucleating agents (such as noble metals). The size of nucleating agent agglomeration is an unknown which has been shown to change with time in the melter. These uncertainties coupled with uncertain effects of each agent causes complications in the characterization of crystallization rate in the melt.

The conservative approach is to assume a worse case scenario of unlimited nucleating sites. The above fig illustrates the effect of noble metal additions to the crystallinity of a simulated nuclear waste glass (HW39-4). As the picture shows an increase in crystallinity with increasing NM content. This increase levels off a relatively small NM concentration. Crystallinity testing can be conducted with the addition of 0.3 mole % NM's to remove the effect of nucleating sites on crystallinity.

- Growth in Waste Glass

  The growth of crystals in glass has been studied extensively for simple

glasses. When crystal composition differs significantly from glass matrix composition growth is likely controlled by diffusion of the slowest glass component (needed for crystallization) to the crystal/glass interface. The rate of diffusion controlled growth can be described as follows:

$$u = \frac{D}{\delta} \frac{C - C_e}{1 - C_e}$$

where D is the chemical inter-diffusion coefficient for the slowest species, δ is the interfacial boundary thickness, C is the concentration of that species the bulk liquid and C_e is the equilibrium (liquidus) concentration.

Reasonable agreement between this model and experimental results confirm the theory of diffusion controlled growth in many component glasses. However, direct use of this model to the prediction of crystallinity in nuclear waste glass is prevented by the inability to accurately measure δ and by the fact that changing composition in both the matrix glass and the crystal affect D.

Transformation in Waste Glass:

- Measurement:

The measurement procedures for transformation of glass to crystal include both isothermal transformation kinetics which can be measured using a gradient furnace or isotherm furnace in which samples are heat treated isothermally at several temperatures for a range of times. The samples are then characterized for crystal volume fraction using OM and SEM with image analysis and/or XRD calibrated for quantitative measurements. An example of the measured isothermal transformation of HW39-4 is shown:

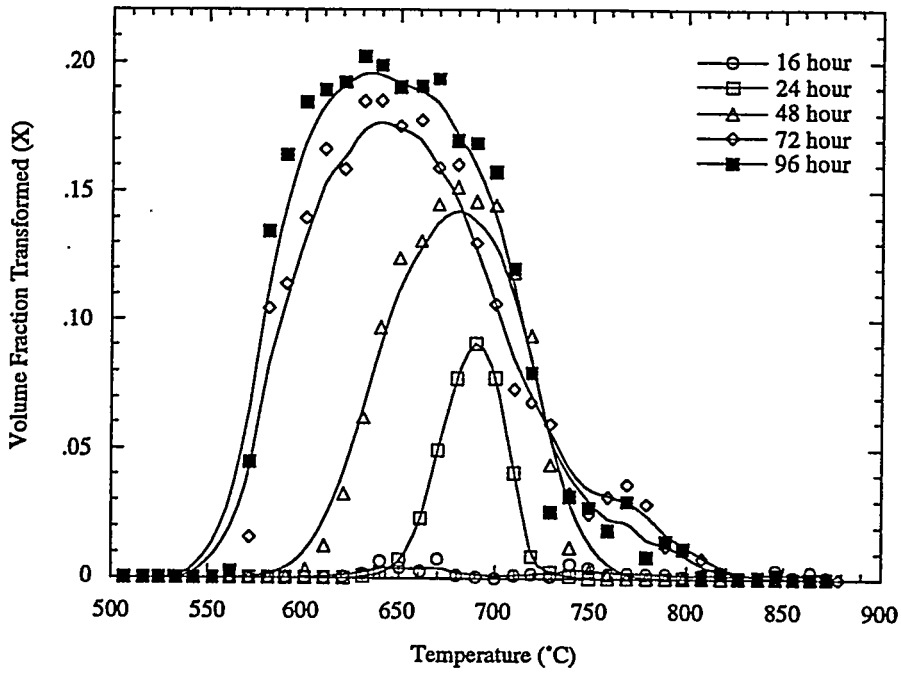

Nonisothermal transformations are measured in two common ways, the first way is to place the samples in a furnace with a scheduled heating or cooling rate. This rate can be constant (linear change in temperature with time), or logrithmic. Several samples are measured with varying rates and dwell times. Like the isothermal method, the samples are then analysed for crystal volume fraction. An example is given below:

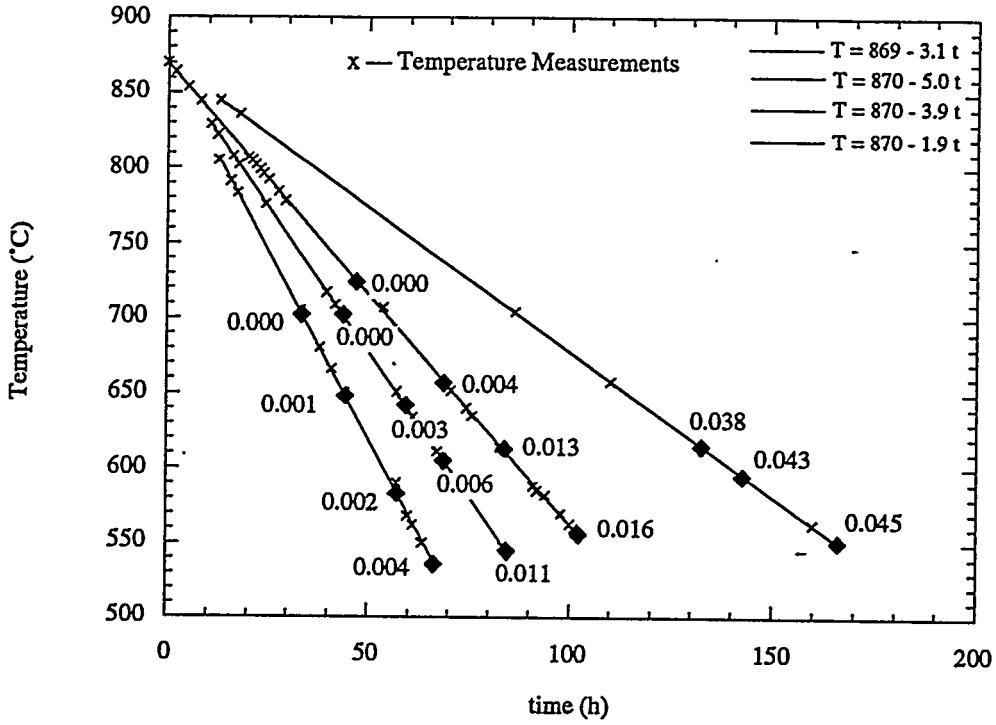

The second method to measure nonisotherm transformation kinetics entails the use of thermoanalytical devices (DSC and DTA). By this method, small samples are heated or cooled at constant rates while measuring the amount of enthalpy change in the sample. The crystallization exotherm is then characterized. The exotherm peak location and area are compared for samples with different rates. The total enthalpy (or peak area) is related to the amout of crystal formation and the peak location (measured as the temperature at the peak maximum) is related to crystallization rate.

For thourogh analysis of crystallization kinetics, the above methods should be combined. Isothermal kinetics can be used to estimate nonisothermal crystallization and vise versa for some glasses (depending on crystallization mechanisms). This will be shown in the next section.

- Modelling

Crystallization kinetic modelling generally follows the work of Johnson, Mehl, and Avrami. Johnson and Mehl developed a model based on the current theory of crystallization mechanisms to estimate the crystallization. The resulting model was successfully applied to experimental results with small volume fraction transformed but fell apart when the volume fraction increased. Avrami then modified their basic model by accounting for crystal impingement (both soft and hard impingement). The resulting model refered to as the Avrami model or

Johnson, Mehl, Avrami model is the general basis of crystallization modelling today (with some exceptions) given here for three dimmesional growth:

$$\frac{V_c}{V} = 1 - \mathrm{Exp}\left[-\int_0^t I_v\left(\int_{t'}^t u\, d\tau\right)^3 dt'\right]$$

This model cannot generally be solved analytically. Ulhmann and others give examples of numeric solutions to the model. By assuming simply activated growth and nucleation kinetics the model has been integrated for isothermal crystallization to yield:

$$\frac{V_c}{V} = 1 - e^{-(Kt)^n}$$

where K is the kinetic parameter and n is the time exponent (better known as the Avrami number). The Avrami number is related to the mechanism of crystallization as follows:

Values of 'n' for different growth and nucleation conditions

(DR MacFarelane & M Fragoulis, "Theory of devitrification in multi-component glass forming systems under diffusion control," Phys. Chem. Glass. 27[6] 1986.

	Crystallization Mechanism	
	Diffusion	Interface
Constant nucleation rate		
3-dimensional growth	5/2	4
2-dimensional growth	3/2	3
1-dimensional growth	1/2	2
Constant particle number		
3-dimensional growth	3/2	3
2-dimensional growth	2/2	2
1-dimensional growth	1/2	1
Surface nucleation	1/2	1

Although the assumptions implicit in the integrated rate equation above are very restrictive in the temperature and time dependance of K (see Uhlmann or Weinberg), the use of this model form for emperical modelling has been

successfully demonstrated and is promising for use with nuclear waste glass.

The temperature dependence of K and the transformation of this kinetic factor to nonisothermal testing is the subject of controversy. Experience has shown (see results) that K can be assumed to depend on temperature in an Arrenius mannor:

$$K = K_0 \, Exp\left(\frac{B_K}{T}\right)$$

Theoretically, the value of B combines the enthalpy of crystallization, the activation energy for viscous flow, the temperature dependance of 'jump frequency at the glass crystal interface, and several other physical factors. Practically, this value can give insight to which mechanism dominates crystallization.

K and n are commonly assumed to be time independent this is not always the case with 'real' crystallization results. These assumptions can be used to very closely estimate crystallinity.

The relationship between isothermal and non-isothermal crystallization kinetics was explored by Grange and Keifer who successfully applied an empirical approach. Assuming Arrhenian growth kinetics, several experimenters have employed non-isothermal thermoanalytic methods to describe crystallization. The following equation is used for non-isothermal kinetics following the work of MacFarlane and Fragoulis who assumed Arrhenius approximation for u and its integral, and k is independent of t.

$$\frac{V_c}{V} = 1 - Exp\left(-\left(\frac{\Theta_0}{\Theta}\right)^n Exp\left[-\frac{(n-1)B_K}{T}\right]\right)$$

where Θ_0 is a constant and Θ is the linear temperature rate.

- Results for a Simulated Nuclear Waste Glass

To calculate X_e, plots of X vs. ln(t) are constructed at each temperature. The crystal volume fractions approach the equilibrium value as ln t goes to infinity this value is given the symbol $X_{e,meas}$. The equilibrium volume fraction of crystals is related to temperature according to:

$$\frac{X_e}{X_{e0}} = 1 - Exp\left[-B_{Xe}\left(\frac{1}{T} - \frac{1}{T_L}\right)\right]$$

where the equilibrium factor (B_{Xe}) and T_L are calculated from a plot of $\ln(1-X_{e,meas})$ vs. 1/T. The observed values of 44,302 K for B_{Xe} and 1,004 K for T_L are taken from the slope and intercept of this data (assuming the occlusion of the high temperature high chromium 'shoulder'). X_{e0} is the equilibrium volume fraction of crystal at room temperature measured by the extension of the $X_{e,meas}$ data to room temperature and was determined to be 0.203. The equilibrium fraction transformed is shown in Figure 3. A thermodynamic model (FACT™) has also been used to predict X_e of acmite in HW39-4 glass.[26] The thermodynamic calculation of B_{Xe} (48,380 K) matches closely that measured, however the calculated T_L (1,148 K) is higher.

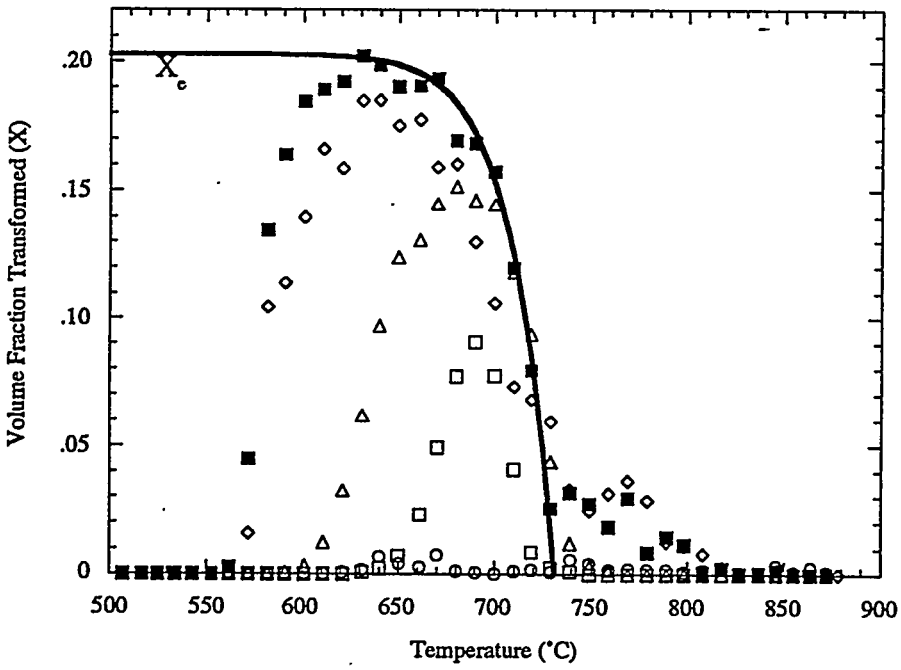

Many glasses including HW39-4 show a very distinct induction time (σ) for crystallization. This induction time is estimated by the extrapolated intercept of the linear portion of ξ vs. ln t curves as described by Weinberg.[27] Effectively σ is a combined effect of the induction time for nucleation and for growth. It was shown by Weinberg that this induction time is not uniquely determined and is dependent on experimental conditions.[26] In the case of HW39-4, σ is Arrhenian in nature (as seen in Figure 4) with a preexponential σ_0 of 1.845×10^{-3} and a temperature coefficient B_σ of 15,600 K:

$$\sigma = \sigma_0 \mathrm{Exp}\left(\frac{B_\sigma}{T}\right).$$

The relationship between σ, t', and t follows:

$$t = t' - \sigma$$

where t' is the time each sample is exposed to heat treatment temperature and t is the effective time used in Avrami equation.

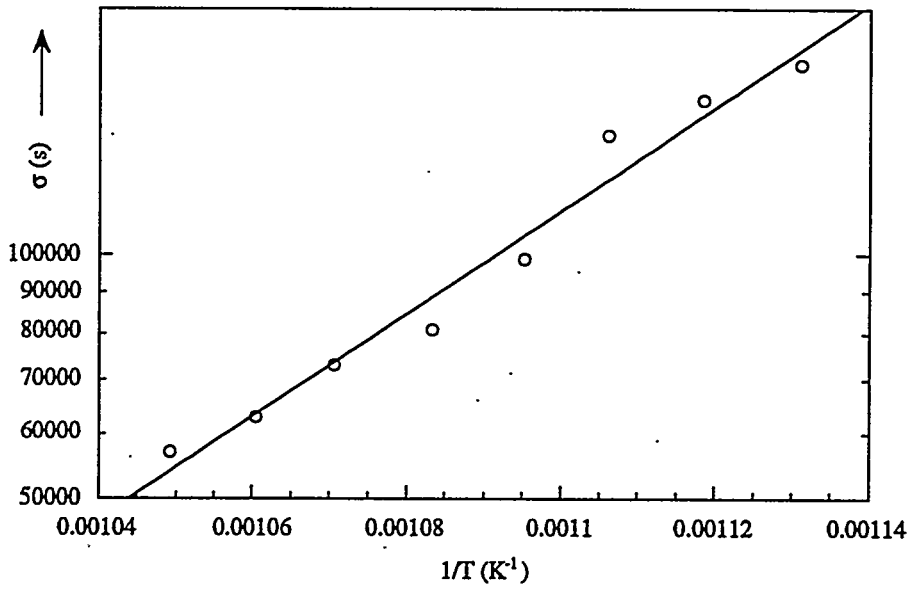

The Avrami number (n from eqns. 1, 2, and 5) is calculated from the slope of $\ln(-\ln(1-\xi))$ vs $\ln(t)$ plots at constant temperature. Using this method, an average value of 2.52 was calculated for n. Assuming three dimensional diffusion controlled growth with constant nucleation, the corresponding theoretical n value is 2.5 (this value is used in calculations shown here).

The kinetic constant (k) is then calculated from plots of $\ln(-\ln(1-\xi))$ vs 1/T at constant times. From this treatment, nB_k is given as the slope of each curve. Using 2.5 as n, b was found to be 5848.9 K and k_0 was fit by standard non-linear fit methods (using least squares of X predicted vs X measured) to be 4.92×10^{-3} s^{-1}.

The following figure shows a comparison of predicted and measured crystallinity.

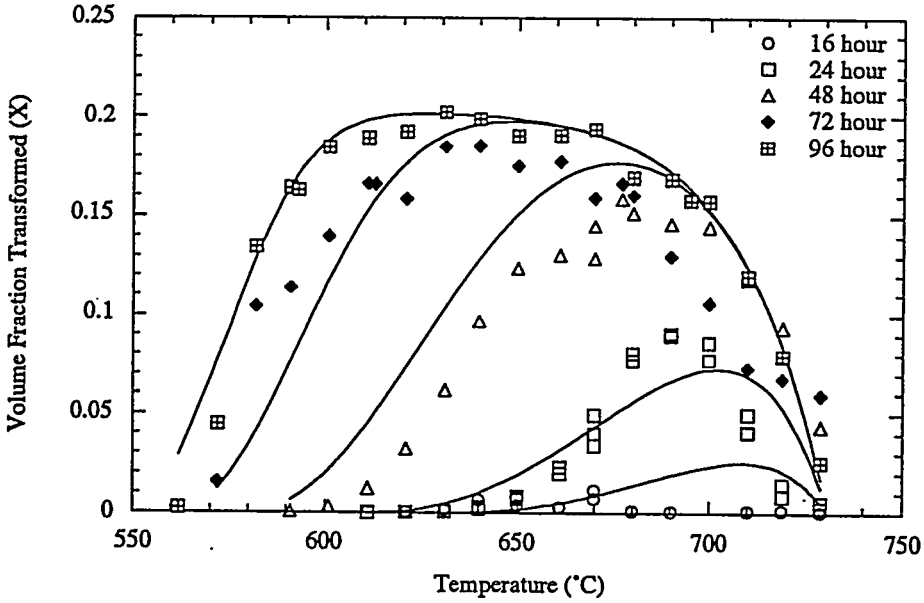

Using the characteristic temperature value (B_K) from isothermal kinetics, the non-isothermal data was fit to the nonisothermal equation. The value A is fit by standard non-linear fit methods (using least squares of X predicted vs X measured) of all non-isothermal crystallinity data. Also shown on the plot are the extreme outside boarders of predicted vs. measured X calculated from A values fit to only one non-isothermal X point at a time. From the narrow range outlined by these two lines it can be seen that kinetic parameters fit to isothermal crystallization data can be used to predict nonisothermal crystallization.

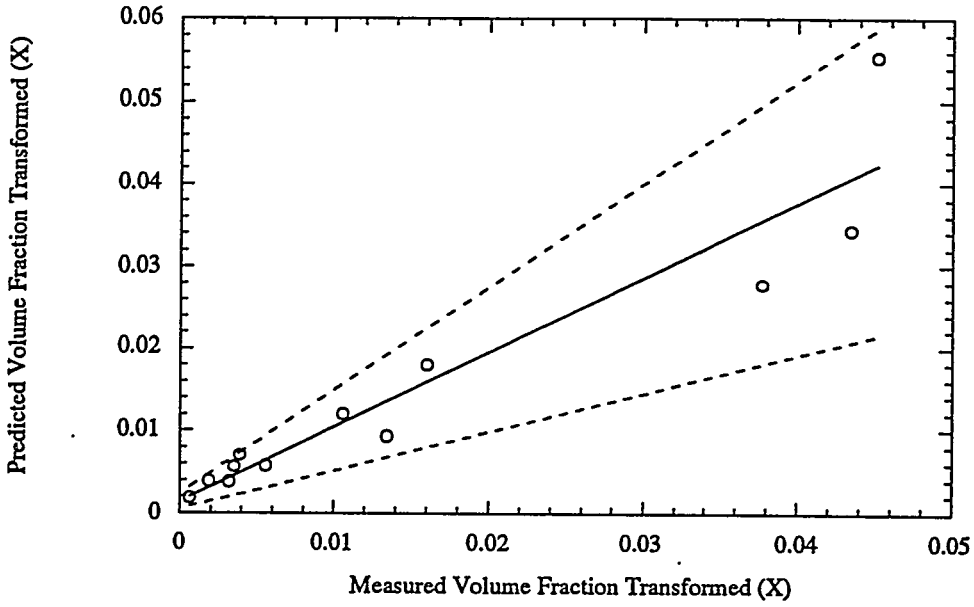

The affect of simple temperature histories (isothermal and constant cooling rate) on volume fraction of crystals can be predicted using classical model forms fit empirically to experimental data covering the representative range of time and temperature. Isothermal crystallinity data were successfully used to fit the characteristic temperature term in a non-isothermal kinetics equation. TTT diagrams were constructed from both.

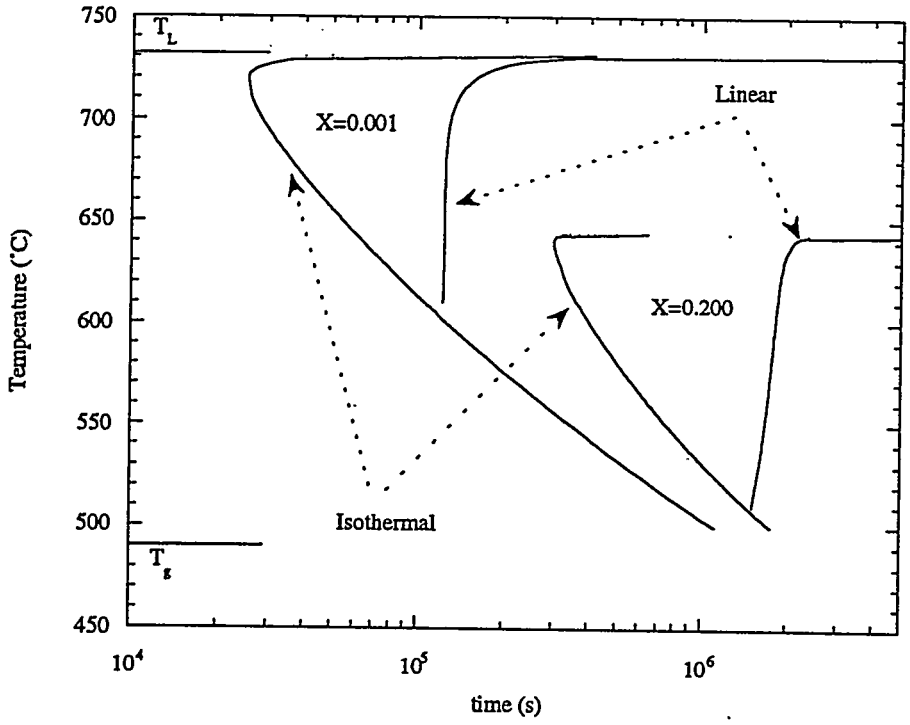

The above figure shows both isothermal and nonisothermal TTT diagrams for acmite in HW39-4 glass. This diagram can be used to estimate the amount of crystallinity in a sample heat treated for a known rate for any given time. The use of this diagram and the Avrami equation used to fit it will give quantitative crystal fractions as a function of temperature and time held at elevated temperatures either in the glass plant or in a geological repository.

Useful References:

- Thermodynamics

JW Gibbs, "The Collected Works," Green & Co. (1931).

DR Gaskell, "Introduction to Metallurgical Thermodynamics," McGraw Hill (1981).

CHP Lupis, "Chemical Thermodynamics of Materials," Prentice Hall (1983).

GM Barrow, "Physical Chemistry," McGraw Hill (1988).

LS Darken and RW Gurry, "Physical Chemistry of Metals," McGraw Hill (1953).

- Liquidus Temperature

CG Bergeron and SH Risbud, "Introduction to Phase Equilibria in Ceramics," Amcerican Ceramic Soc. (1984).

P Haasen, "Materials Science and Technology Vol 5.: Phase Transformations in Materials," VCH Publishers (1991).

K.-S. Kim and P. Hrma, "Models for Liquidus Temperature of Nuclear Waste Glasses," Ceram. Trans. 45, 327-337 (1994).

P. Hrma, G. F. Piepel, M. J. Schweiger, D. E. Smith, D.-S. Kim, P. E. Redgate, J. D. Vienna, C. A. LoPresti, D. B. Simpson, D. K. Peeler, and M. H. Langowski, "Property/Composition Relationships for Hanford High-Level Waste Glasses Melting at 1150°C," PNL-10359, Vol. 1 and 2, Pacific Northwest Laboratory, Richland, Washington (1994).

- Nucleation

JW Christian, "The Theory of Phase Transformations in Metals and Alloys," Pergamon Press (1965).

PIK Onorato and DR Uhlmann, "Nucleating Heterogeneities and Glass Formation," J. Non-Cryst. Sol. [22] 367-78 (1976).

JW Cahn and JE Hillard, "Free Energy of a Nonuniform System. III. Nucleation in a Two-Component Incompressible Fluid," J. Chem. Phys., [31] 688-99 (1959).

- Crystallization Kinetics

JW Christian, "The Theory of Phase Transformations in Metals and Alloys," Pergamon Press (1965).

J. D. Vienna, D. E. Smith, and P. Hrma, "Crystallization Kinetics in Nuclear Waste Glasses: A Modeling Approach," in preparation.

DR Uhlmann and H Yinnon, "The Formation of Glasses," in Glass Science and Technology, Vol 1, DR Uhlmann and NJ Kreidl eds., (1983).

M Weinberg and R Kapral, "Phase Transformation Kinetics in Finite Inhomogeneously Nucleated Systems," J. Chem Phys., [91] 7147-52 (1989).

JH Simmons, DR Uhlmann, and GH Beall, "Nucleation and Crystallization in

Glasses," American Ceramic Society (1982).

STATISTICAL APPROACH TO GLASS DEVELOPMENT

Greg Piepel & Trish Redgate

Pacific Northwest Laboratory
Richland, Washington

presented at tutorial
"Waste Glass Technology for Hanford"
June 27-28, 1995

OUTLINE

- ★ Statistics and its roles
- ★ Statistics in glass development
- ★ Experimental design
- ★ Data analysis and property modeling
- ★ Accounting for uncertainty
- ★ Summary

STATISTICS

- ★ The science and art of collecting and analyzing data to make inferences in the presence of uncertainty or variability

- ★ This presentation focuses on application of statistics to glass development

- ★ Statistics also has roles in other areas such as: ***waste characterization, pretreatment and blending, feed specifications, waste form qualification, and vitrification plant operation & control,*** but not discussed here

VARIATIONS IN WASTE AND GLASS COMPOSITIONS

- ★ Waste feed compositions to HLW melter will vary considerably
- ★ Glass compositions for different waste types will vary considerably
- ★ For a given waste type, composition of glass will vary due to variations in feed and processing

COMPOSITION AND GLASS PROPERTIES

★ Changes in glass composition affect glass properties, e.g.

-- viscosity

-- electrical conductivity

-- liquidus temperature

-- solubility, crystallinity, and phase behavior

-- chemical durability

GLASS DEVELOPMENT

- ★ HLW glass systems are complex, and existing theory and knowledge are not sufficient for predicting glass properties as functions of composition (and temperature, where appropriate)

- ★ Need to perform experiments and collect data to understand and relate glass properties to composition and temperature

GLASS DEVELOPMENT APPROACH

- ★ If waste types to be processed in melter were already "known", ideal approach would be to develop an "optimal" glass composition for each waste type

- ★ Waste types not yet "known", and glass compositions expected to vary

- ★ ***Composition Variation Study (CVS)*** or ***composition envelope*** approach used to provide basis for developing glasses over a region of possible glass compositions

GLASS DEVELOPMENT APPROACH (cont.)

Until waste types determined, strategy is to:

- ★ Use CVS/composition envelope approach to study region(s) of potential glass compositions

- ★ Formulate glasses for and perform some studies on selected "best-guess-at-this-time" waste compositions

GLASS DEVELOPMENT APPROACH (cont.)

When waste types determined:

- ★ Use "global CVS" results to select preliminary glass formulation for a waste type

- ★ Perform "mini CVS" around preliminary glass formulation to confirm or fine-tune formulation and property models from "global CVS"

STATISTICS & GLASS DEVELOPMENT

- ★ Statistical ***experimental design*** selects glass compositions to efficiently study dependence of glass properties on composition

- ★ Statistical ***graphics*** and ***data analysis*** help interpret results given data uncertainty

- ★ Statistical ***model development*** techniques provide for predicting glass properties for compositions and temperatures not experimentally tested

STATISTICS & GLASS DEVELOPMENT (cont.)

- ★ Glass property models and corresponding uncertainty expressions can be used to formulate (with high confidence) glasses with desired/acceptable properties

- ★ Glass property models and uncertainty expressions can be used for other purposes besides glass development (e.g., waste pretreatment and blending, plant operation and control, waste form qualification)

MIXTURE EXPERIMENTS

- ★ A ***mixture experiment*** involves mixing components in various proportions and studying the effects of changing composition on properties of interest

- ★ Proportions of mixture components sum to 1 (or percentages to 100%)

- ★ Techniques for experimental design, data analysis, and modeling of mixture data in statistics literature since late 1950s

EXPERIMENTAL DESIGN STEPS

- ★ Select components to experimentally vary that will vary in waste glasses and affect glass properties

- ★ Specify composition region of interest
  - -- Lower and upper bounds on components
  - -- Property constraints implemented via property models
  - -- Multicomponent constraints ***as necessary*** to eliminate undesirable combinations of components

EXPERIMENTAL DESIGN STEPS (cont.)

★ Statistically select compositions to:

-- adequately cover the (boundary and interior of) composition region of interest

-- study component or other variable effects of particular interest

-- support developing property models to minimize uncertainty of predictions

★ Compositions selected via special software for statistical ***mixture experiment design*** and ***optimal experimental design***

EXPERIMENTAL DESIGN (cont.)

- ★ Varying components ***many/all-at-a-time*** provides information about "average" effect of each component and information about interactions of components

- ★ Varying components ***one-at-a-time*** from a base composition provides information about the specific effects of components when added to or subtracted from the base composition

CVS (LTM) EXPERIMENTAL DESIGN

- ★ Designed in 5 phases, with results of earlier phases used to design later phases
- ★ 147 glasses, including 14 replicates
- ★ CVS-I a 10-component screening study and 4 phases of CVS-II with same components
- ★ Boundary and interior compositions
- ★ Many-at-a-time, one-at-a-time, and special interest compositions

CVS (LTM) COMPONENT BOUNDS

Component	Mass Fraction Bounds	
	Lower	Upper
SiO_2	.42	.57
B_2O_3	.05	.20
Na_2O	.05	.20
Li_2O	.01	.07
CaO	0	.10
MgO	0	.08
Fe_2O_3	0	.15
Al_2O_3	0	.17
ZrO_2	0	.13
Others	.01	.10

Also different property and multicomponent constraints were applied in the 5 phases

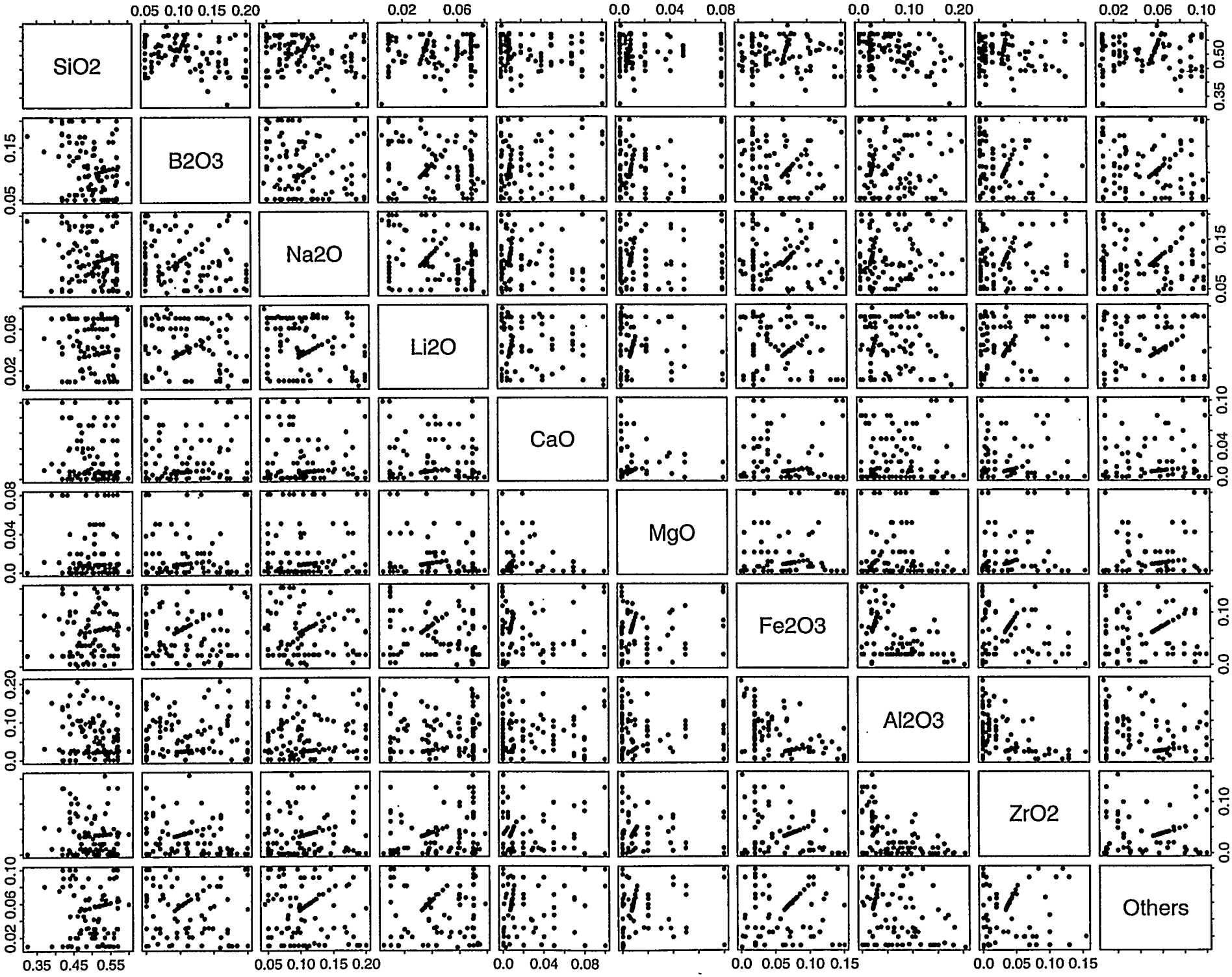
SiO2
B2O3
Na2O
Li2O
CaO
MgO
Fe2O3
Al2O3
ZrO2
Others

STATISTICAL DATA ANALYSES

- ★ Assess outlying/influential data
- ★ Compare target and analyzed glass compositions
- ★ Quantify experimental uncertainty using replicate data
- ★ Develop and validate property models and uncertainty expressions
- ★ Compare empirical & semi-empirical models

GLASS PROPERTY MODELING

- ★ Ideally, would prefer mechanistic models based on glass theory/structure/knowledge
- ★ However, waste glasses are complex systems with many components, and the theory and knowledge is insufficient to yield such mechanistic models
- ★ Consider empirical and semi-empirical models

EMPIRICAL VS. SEMI-EMPIRICAL MODELS

- ★ Empirical--Polynomials (Taylor series) or other functional forms used to approximate true property-composition response surface with coefficients determined by data

- ★ Semi-empirical--Usually a two-coefficient line relating the property to an index function of composition (index coefficients based on theory or structural assumptions)

- ★ Both model types are fitted to data, typically via least squares regression

MIXTURE MODELS

★ **First- and second-order mixture models**

$$f(\textit{Property}) = \sum_{i=1}^{10} b_i x_i$$

$$f(\textit{Property}) = \sum_{i=1}^{10} b_i x_i + \textit{selected terms}$$

$$\textit{of} \sum_{i<j}^{10}\sum b_{ij} x_i x_j + \sum_{i=1}^{10} b_{ii} x_i^2$$

★ **Second-order terms handle curvature and interactive effects of components**

MODEL GOODNESS-OF-FIT

★ R^2 = proportion of variation in property data accounted for by the model

$0 \leq R^2 \leq 1$, with closer to 1 better.
Generally, want $R^2 > .85 - .95$

★ "Predicted versus measured" plots

★ Statistical lack-of-fit and validation tests

-- Test LOF vs. experimental variation

-- Validate models using data not used to develop them

MIXTURE MODELS FOR LTM CVS

- ★ First- and second-order mixture models fitted for durability (PCT and MCC-1), viscosity, electrical conductivity, transition temperature, liquidus temperature, etc.

- ★ Later sections of tutorial will show results, including comparison of empirical mixture to semi-empirical free energy of hydration models for PCT durability

- ★ A few examples here, however

1ST-ORDER MODEL, CVS η_{1150} DATA

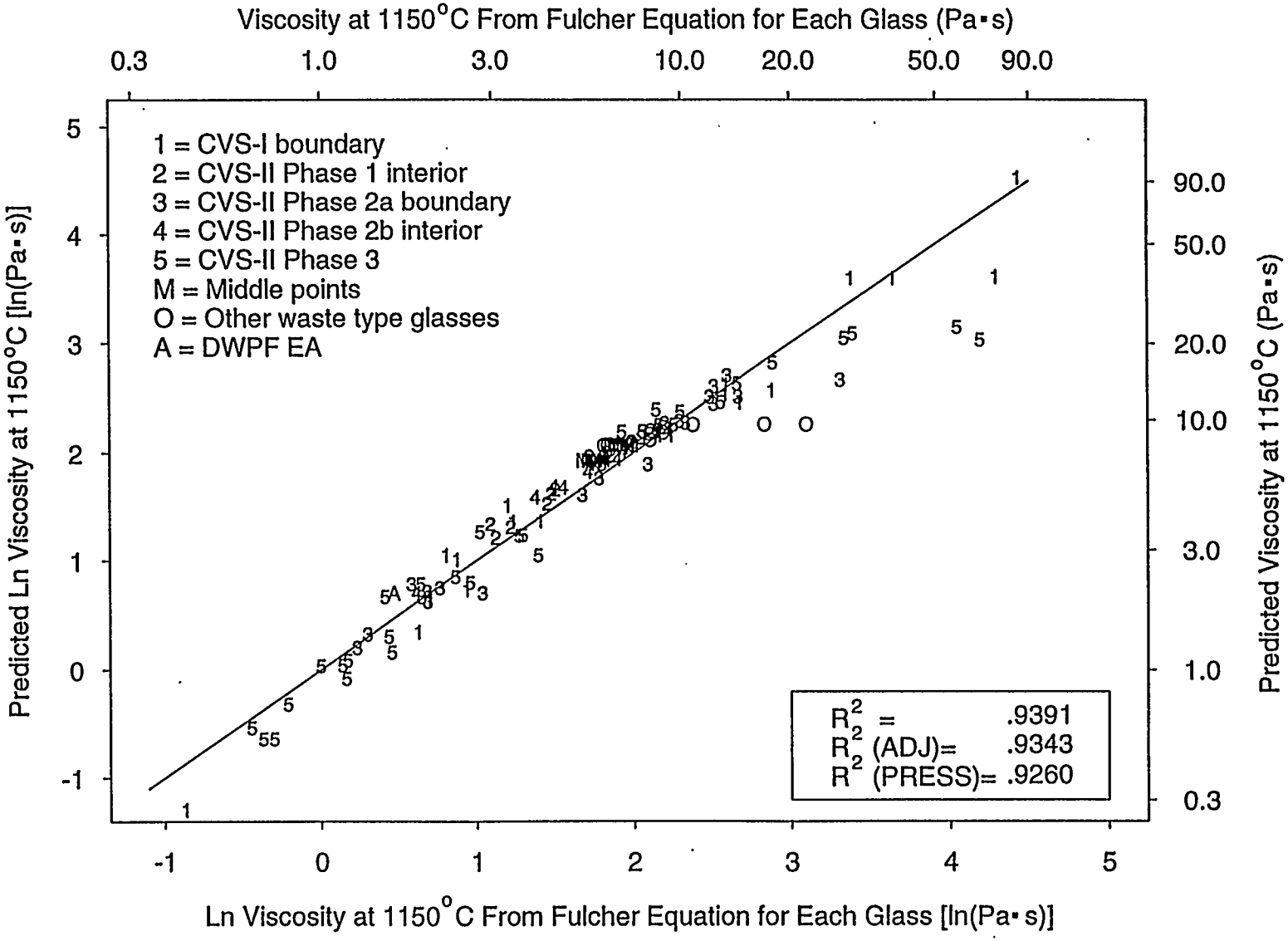

2ND-ORDER MODEL, CVS η_{1150} DATA

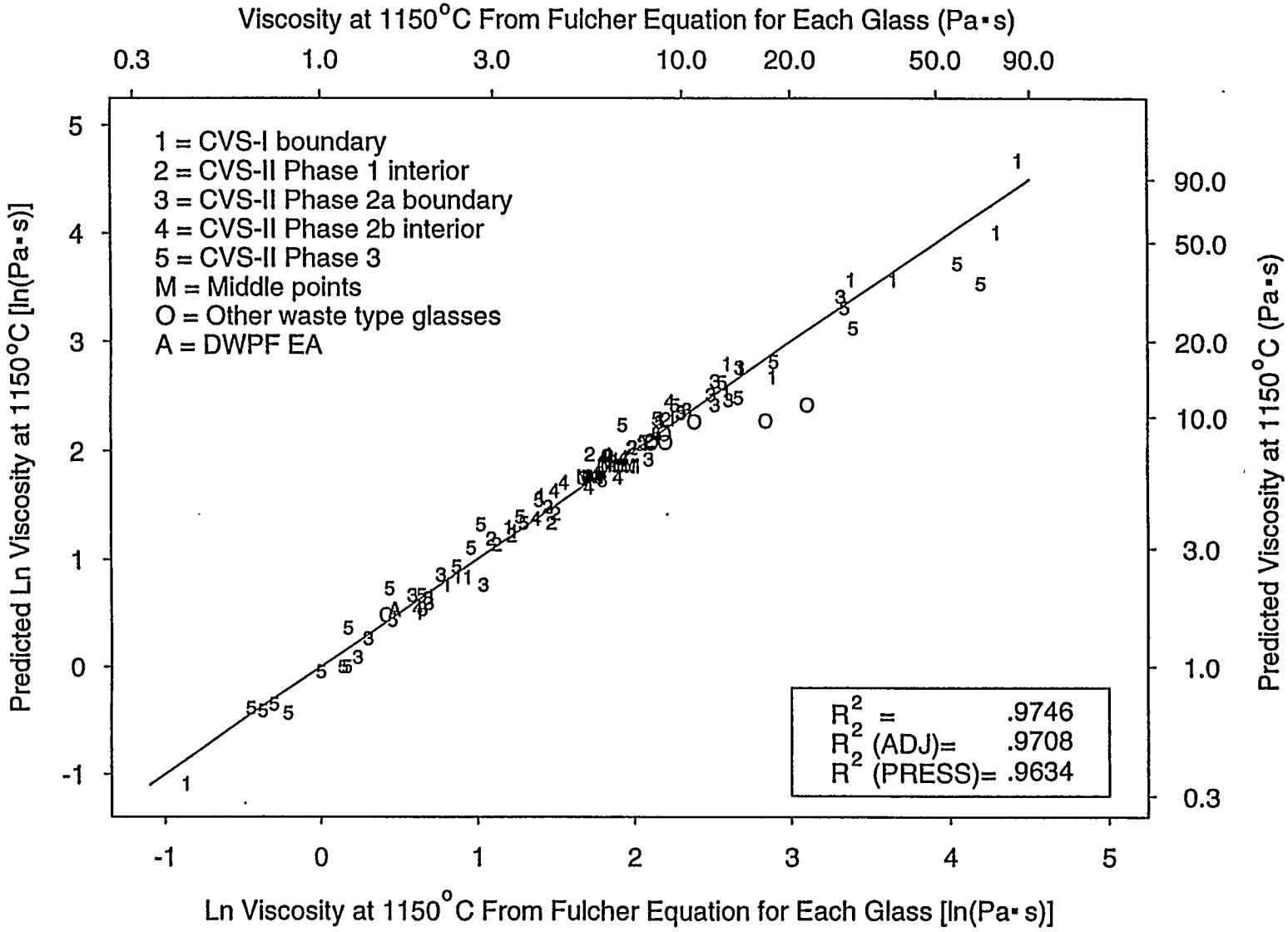

COMPONENT EFFECTS, 1ST-ORDER η_{1150}

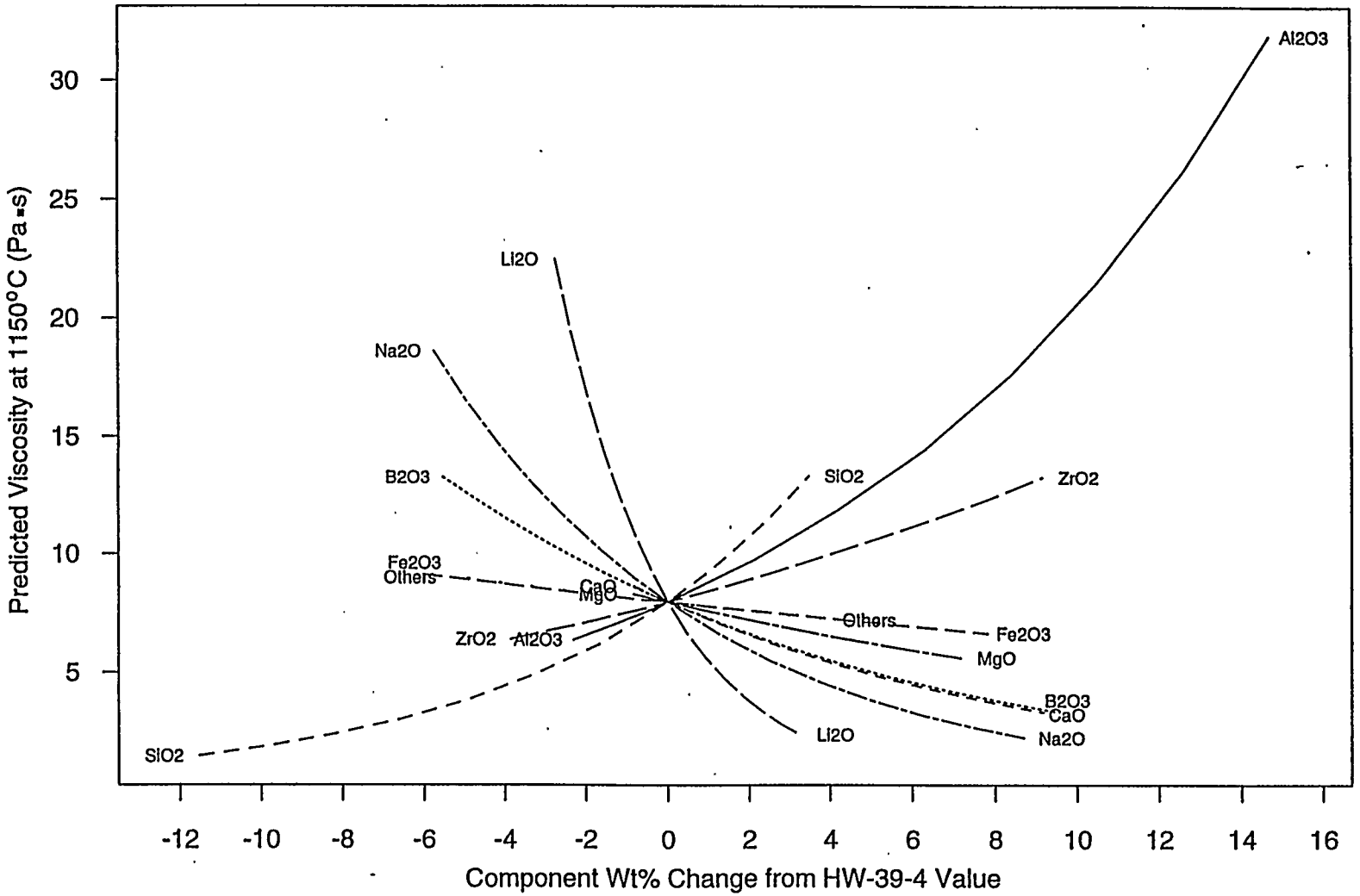

VALIDATION OF 1ST-ORDER η_{1150} MODEL, HISTORICAL DATA

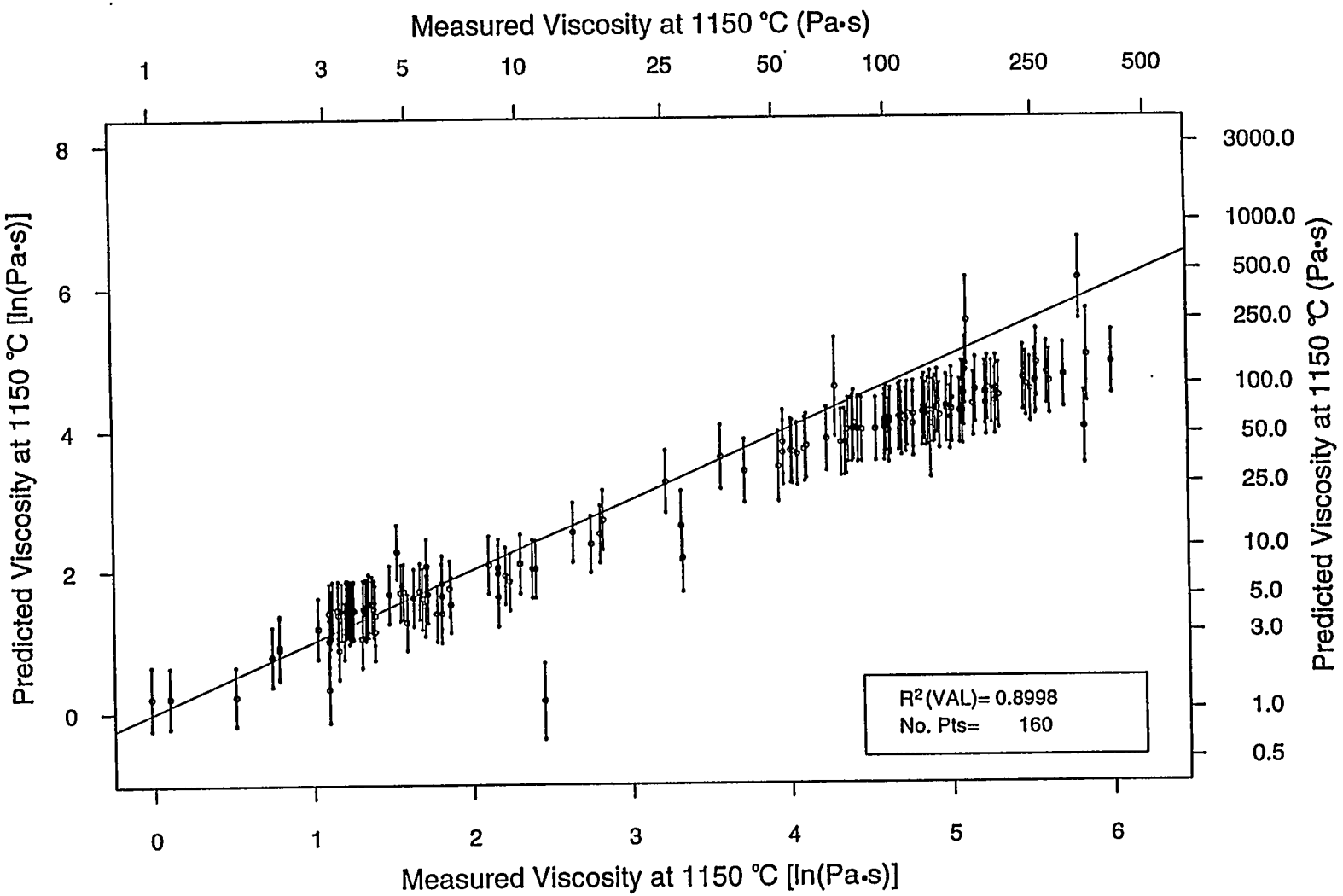

TREE MODELS

- ★ Do not require assuming a particular model form
- ★ Do require sufficient data to build the tree model
- ★ Can be used for continuous or categorical response variables (properties)
- ★ Can perform much better than parametric models when the property-composition relationship is complex

TREE MODEL, T_L < OR > 1050°C

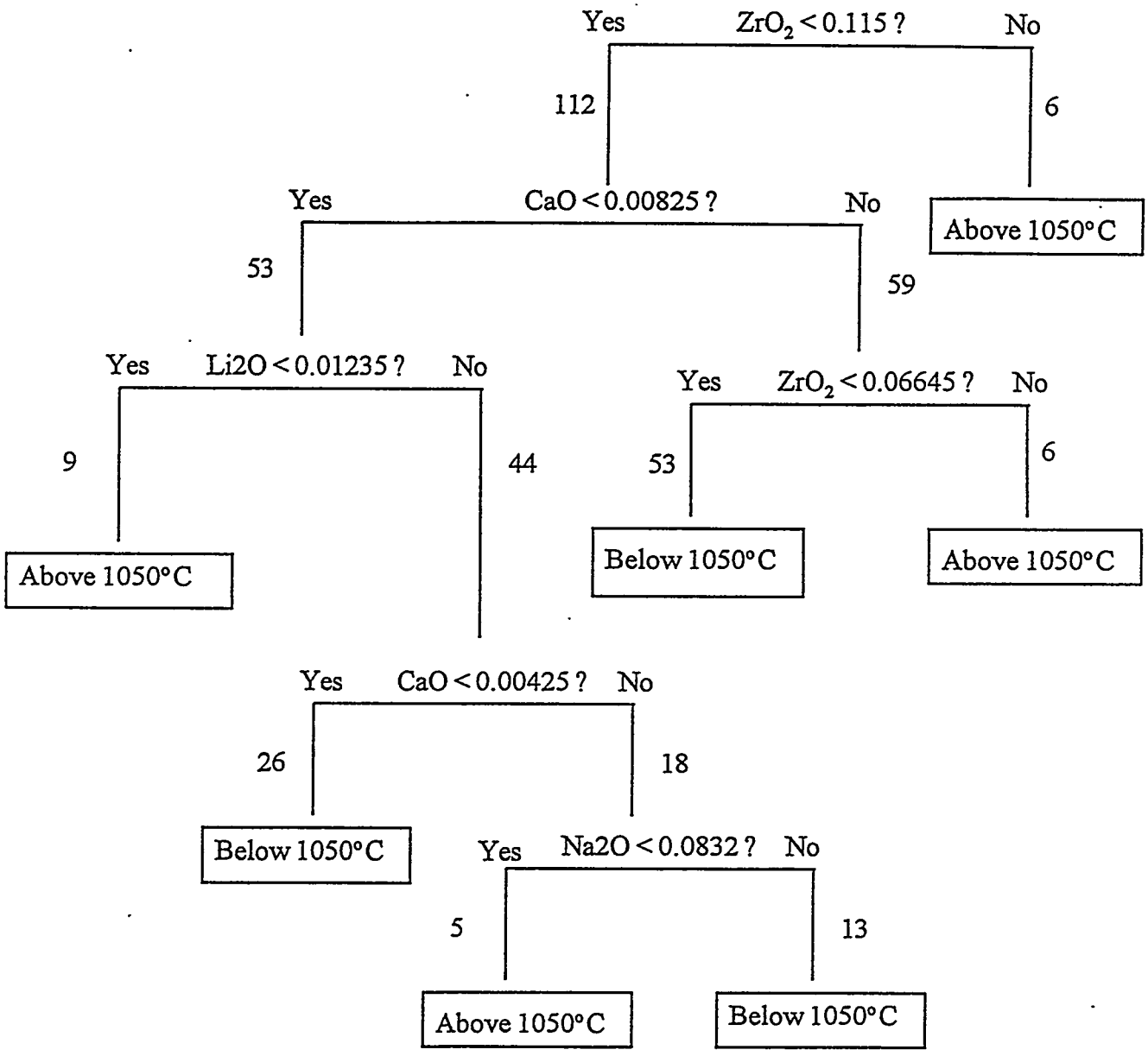

Mis-classification rate = 11%

ACCOUNTING FOR UNCERTAINTY

- ★ Statistical design provides for efficiently and correctly assessing effects of experimental variables (e.g., composition) in the presence of uncertainty

- ★ Statistical data analyses account for uncertainty in determining significance of experimental effects

ACCOUNTING FOR UNCERTAINTY (cont.)

★ Statistical intervals (e.g., confidence or prediction intervals) on property model predictions

$$\text{Interval} = \hat{y} \pm K * sd(\hat{y})$$

account for data and model uncertainty in assessing glass acceptability

★ Statistical intervals useful in glass development and many other areas

SUMMARY

Statistical experimental design, data analysis, and property modeling techniques applied in glass development work yield data and other results that serve as fundamental "building blocks" for:

-- glass formulation/optimization

-- other purposes (e.g., pretreatment and blending, feed specifications, waste form qualification, and vitrification plant operation & control)

MODEL COMPARISONS:

EMPIRICAL MIXTURE & FREE ENERGY OF HYDRATION MODELS

Greg Piepel & Trish Redgate

Pacific Northwest Laboratory
Richland, Washington

presented at tutorial
"Waste Glass Technology for Hanford"
June 27-28, 1995

OUTLINE

- Background -- Glass Durability
- Empirical Mixture and Free Energy Model Forms
- Comparison of Empirical Mixture & Free Energy Models
- Data Sets
- Results
- Summary

Background -- Glass Durability

- DOE-EM WAPS 1.3 Product Consistency Specification requires final waste form to be judged on the Product Consistency Test (PCT) of the glass

- Acceptable waste glass must be more durable than waste glass identified in the DWPF Environmental Assessment (EA)

- Need to evaluate glass durability before glass is vitrified

Background -- Glass Durability (cont)

- Achieved by modeling glass durability as a function of composition
- SRTC developed Free Energy of Hydration Model
- PNL has tried several model forms and chose to use Empirical Mixture Models
- PNL and SRTC working jointly to understand differences between models

Empirical Mixture Models

First-Order: $$\ln(NR) = \sum_{i=1}^{q} b_i x_i$$

where,

ln(NR) = natural logarithm of a normalized elemental release,

x_i = mole fraction of i-th glass component such that $x_1 + x_2 + x_3 + \ldots + x_q = 1$,

b_i's = coefficients estimated from data.

Empirical Mixture Models (cont)

Second-Order:

$$\ln(NR) = \sum_{i=1}^{10} b_i x_i + \textit{selected terms}$$

$$\textit{of} \sum_{i<j}^{10} \sum b_{ij} x_i x_j + \sum_{i=1}^{10} b_{ii} x_i^2$$

- Second-order terms handle curvature and interactive effects of components

***Free Energy of Hydration Model*:**

$$\ln(NR) = a + b\left\{\sum_{i \neq SiO_2} (\Delta G_i)\, x_i + (\Delta G_{SiO_2})\left[x_{SiO_2} - \sum_{i \in S} x_i\right]\right\}$$

where,

ln(NR) = natural logarithm of a normalized elemental release from the Product Consistency Test (PCT),

x_i = mole fraction of i-th glass component such that $x_1 + x_2 + x_3 + \ldots + x_q = 1$,

ΔG_i = free energy of hydration value for i-th glass component,

a , b = coefficients determined empirically by fitting model.

Comparison of Mixture and Free Energy Models

Free Energy Model can be re-written as:

$$\ln(NR) = \sum_{i \notin S} [a + b(\Delta G_i)] x_i + \sum_{i \in S} [a + b(\Delta G_i - \Delta G_{SiO_2})] x_i$$

$$= \sum_{i \notin S} c_i x_i + \sum_{i \in S} d_i x_i$$

this is the same general form as First-Order Mixture Model:

$$\ln(NR) = \sum_{i=1}^{q} b_i x_i$$

Comparison of Mixture and Free Energy Models (cont)

- The b_i coefficient for each component in First-Order Mixture Model can be compared with c_i or d_i from Free Energy of Hydration Model.

Main Difference:

- *Free Energy of Hydration* uses assumed/calculated free energy of hydrations for each component.

- *Empirical Mixture* estimates the component of free energy of hydration values using data for composition region.

Data Sets

Composition Variation Study (CVS) Glasses:

- 147 simulated glass compositions in five phases

- Varied 10 components: SiO_2, B_2O_3, Na_2O, Li_2O, CaO, MgO, Fe_2O_3, Al_2O_3, ZrO_2 and Others (all remaining waste components)

- 123 compositions from first four phases used in following modeling work

Data Sets (cont)

SRTC / DWPF Homogeneous & Inhomogeneous Glasses:

- Homogeneous: no crystalline species & no liquid-liquid phase separation -- 137 glasses including 43 replicates

- Inhomogeneous: crystallinity or phase separation--28 glasses

- SRTC data covers a smaller composition region than CVS data

Model Fitting Results

$$R^2 = 1 - \frac{\sum_{i=1}^{n} (y_i - \hat{y}_i)^2}{\sum_{i=1}^{n} (y_i - \bar{y})^2}$$

- Unitless number between 0 and 1.
- Proportion of variation in ln(NR) release values for data set which is accounted for by a model fitted to the data set.
- Focus on ln(Boron Release in g/m^2).

Model Fitting Results (cont)

Data Set Used in Fit	Model Form	R^2
CVS	Free Energy of Hydration	.3316
	First-Order Mixture	.8057
SRTC Homogeneous	Free Energy of Hydration	.7659
	First-Order Mixture	.9703
SRTC Inhomogeneous	Free Energy of Hydration	.8924
	First-Order Mixture	.9868

Free Energy of Hydration Model Fitted to CVS Data

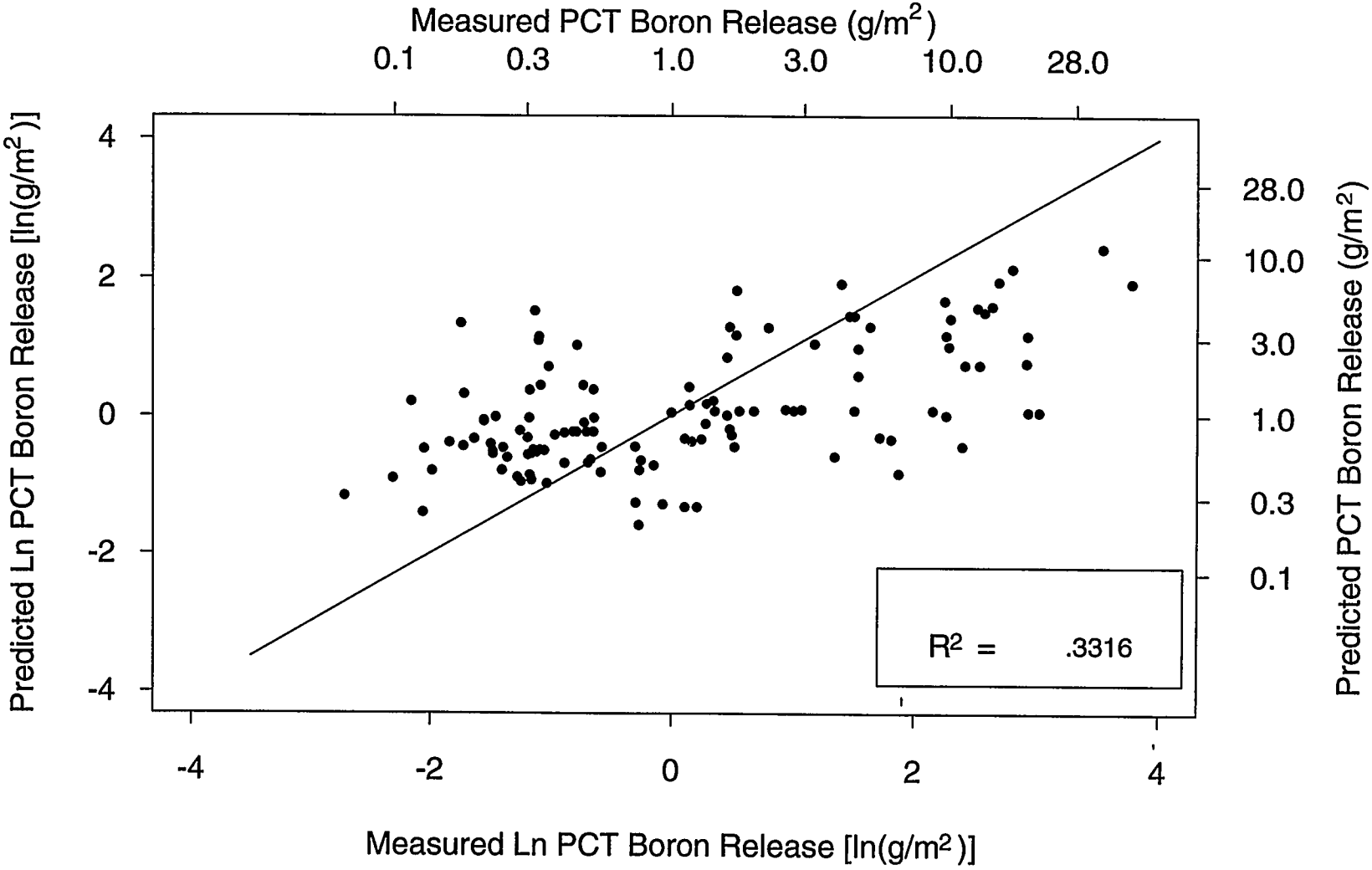

First-Order Mixture Model Fitted to CVS Data

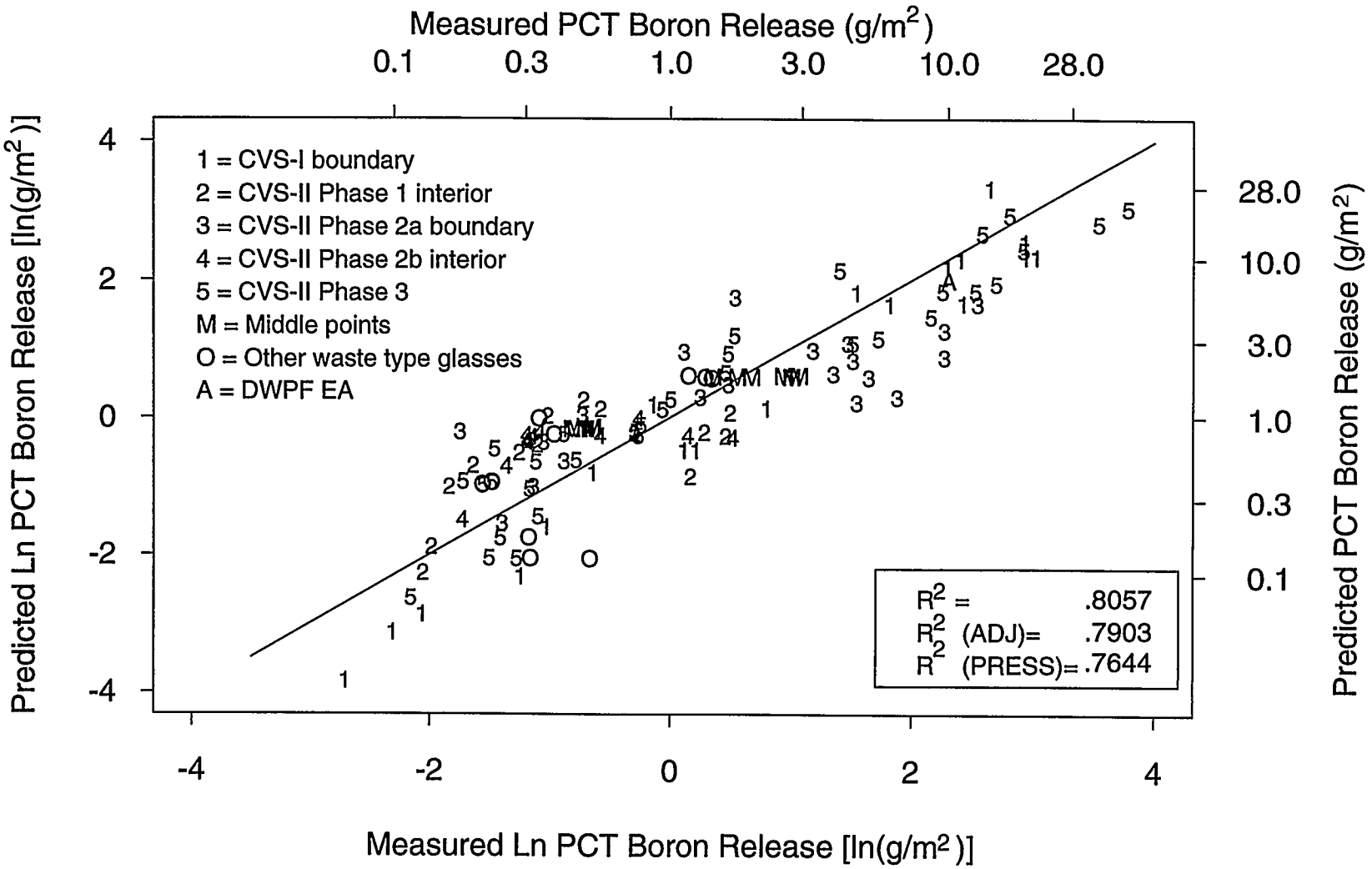

Free Energy of Hydration Model Fitted to SRTC Data

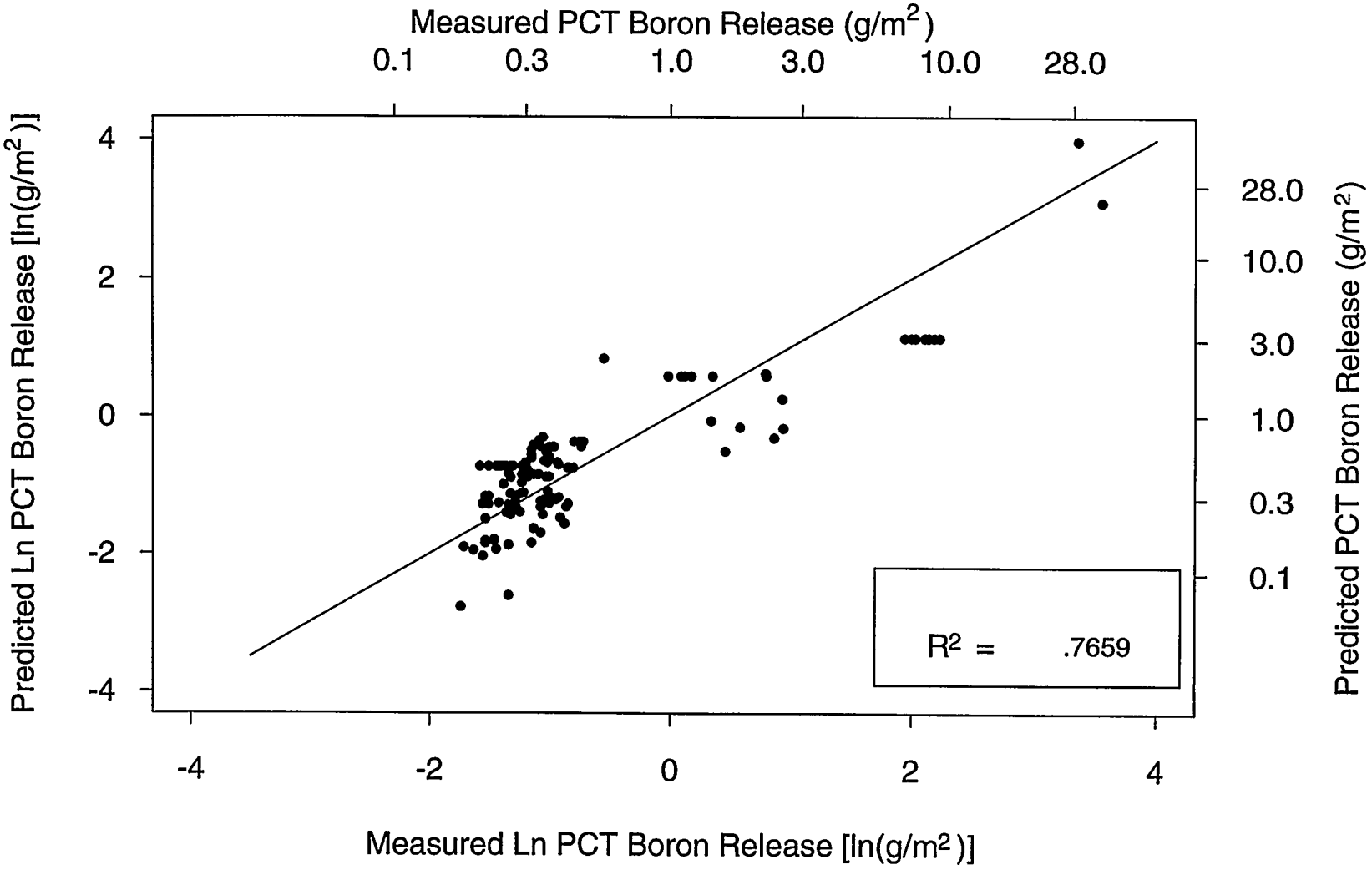

First-Order Mixture Model Fitted to SRTC Data

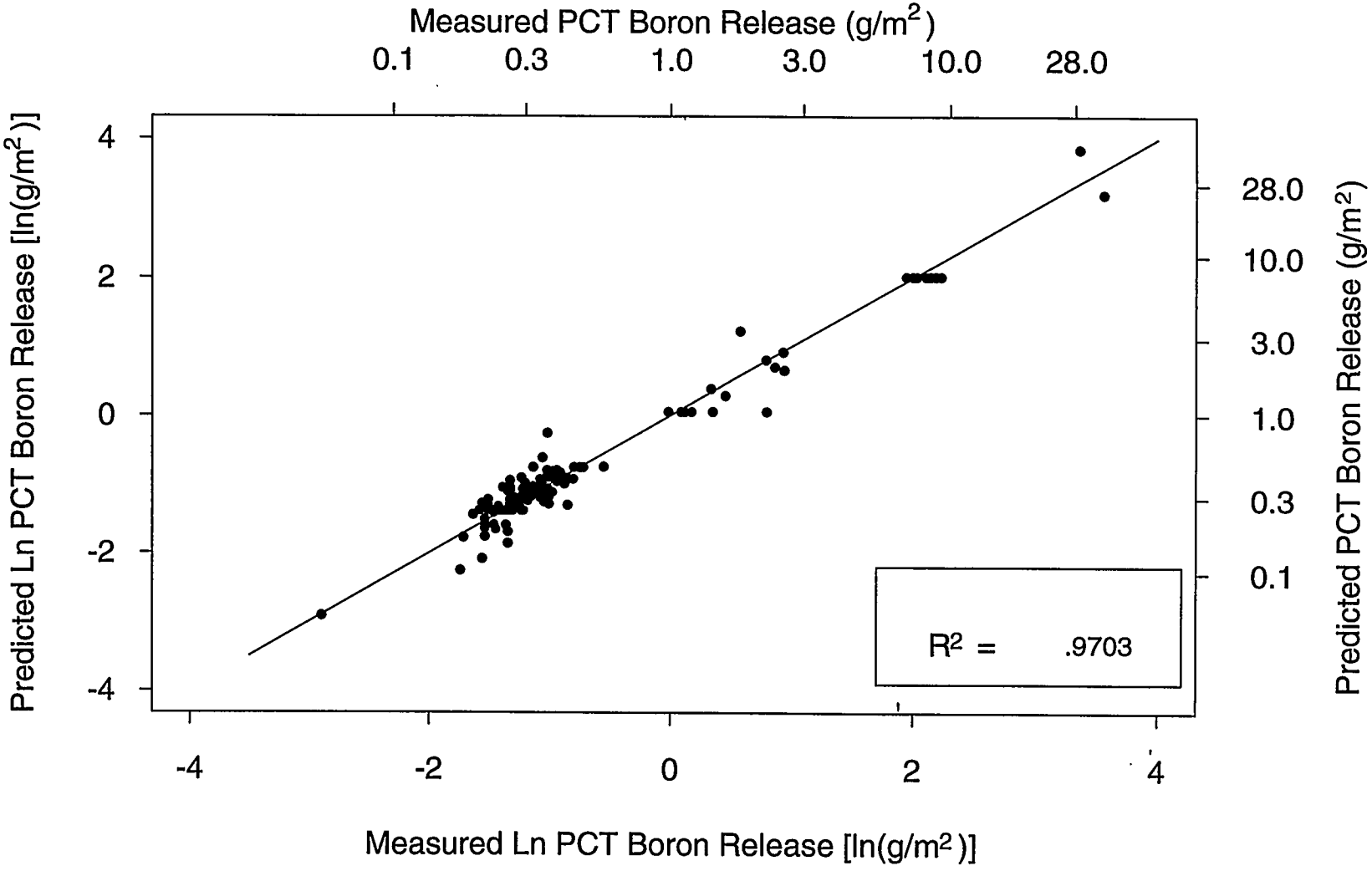

Coefficients for Models Using CVS Data

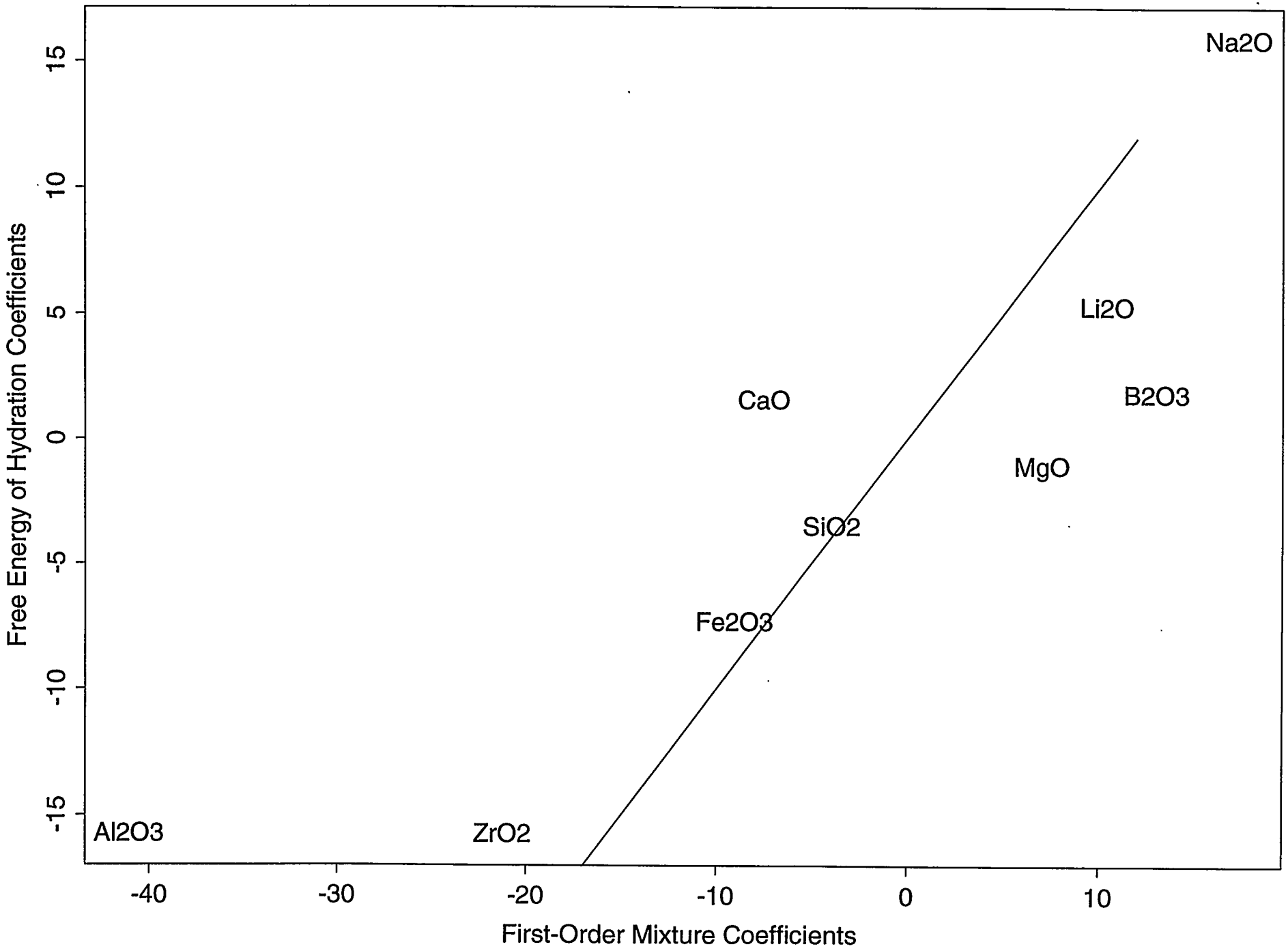

Summary

- Free Energy of Hydration Model performs well for SRTC data, but not for CVS data
- First-Order Mixture Model performs well for CVS and SRTC data
- CVS data covers a larger composition region
- Both First-Order Mixture and Free Energy of Hydration cannot account for nonlinear and interactive effects of components
- Second-Order Mixture Models and other nonlinear model forms (e.g., Tree Models) are being investigated at PNL
- Investigation of differences between models will continue jointly with PNL and SRTC

HANFORD LOW-LEVEL WASTE GLASS: STRUCTURE AND CHEMISTRY

John G. Darab, Hong Li, John C. Linehan*, Dean W. Matson, Shiv K. Sharma** and Peter A. Smith
Materials Sciences Department
Pacific Northwest Laboratory
Richland, WA 99352

Robert K. MacCrone
Materials Engineering Department
Rensselaer Polytechnic Institute
Troy, NY 12181

** Chemical Sciences Department*
*** On leave from Hawaii Institute of Geophysics, University of Hawaii, Honolulu, HI*

Pacific Northwest Laboratory

OUTLINE

~ What is glass?

~ Glass structure and chemistry

~ Why do we want to study the structure and chemistry of glass?

~ How do we go about studying glass structure and chemistry?

~ Case studies of glass structure and chemistry

WHAT IS GLASS?

Structural and Chemical Definition

~ Concept of "motif"

- motif for designing fabric, wall paper, etc.

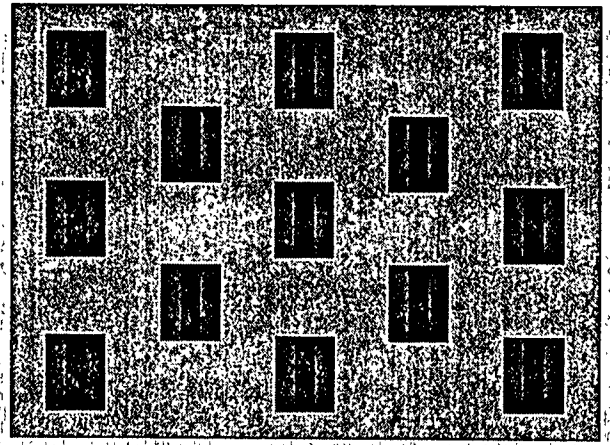

Ordered arrangement
of motif- "crystalline"

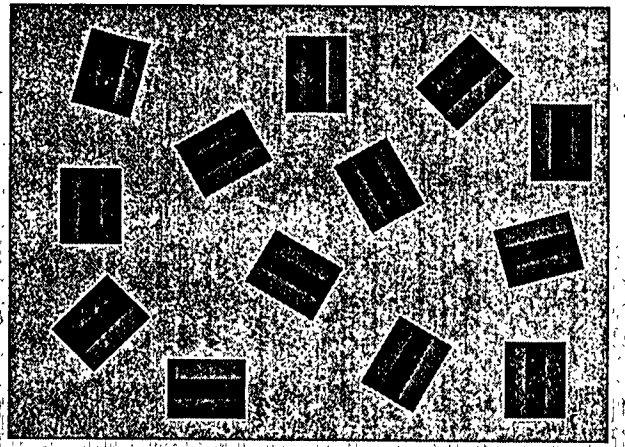

Random arrangement
of motif- "amorphous"

Pacific Northwest Laboratory

WHAT IS GLASS?

Example: Silicon Dioxide (SiO_2, Silica)

~ Concept of "motif"

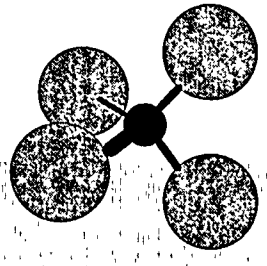

structural and chemical motif:

● **Si**

● **O**

Si is tetrahedrally coordinated to four **O** forming the *orthosilicate* monomer

~ Ordered arrangement of orthosilicate motif- crystalline SiO_2.

~ Random arrangement of orthosilicate motif- amorphous SiO_2.

Pacific Northwest Laboratory

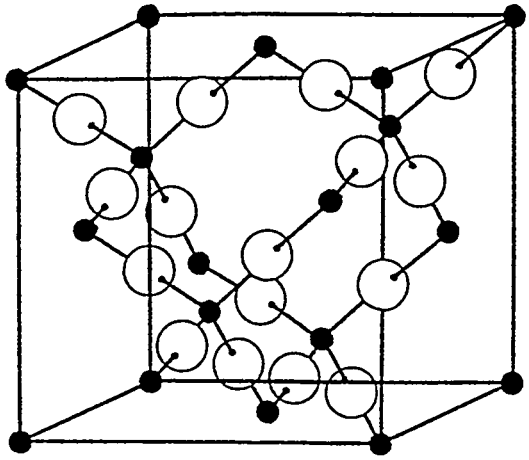

Fig. 1 The crystal structure of high cristobalite, showing the organization of tetrahedral units of silicon (black dots) and oxygen (O). Reprinted from Ref. 6a with permission from Elsevier.

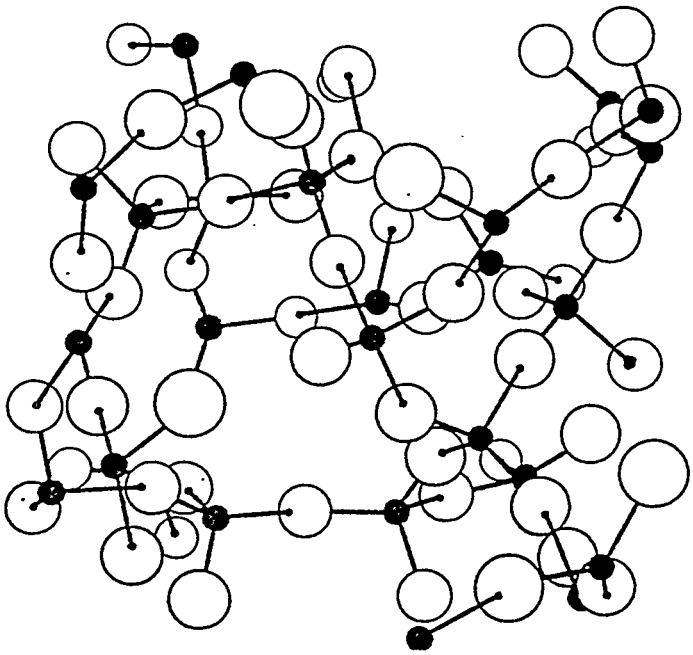

Fig. 2 A schematic diagram of vitreous silica, showing silica tetrahedra linked at corners to form a random network with rings and cages. Reprinted from Ref. 6a with permission from Elsevier.

WHAT IS GLASS?

Summary

~ Glass lacks order at long-range (greater than 20 atoms). *Random arrangement of motif or motifs.*

~ Glass exhibits order at short-range (central atom and its nearest neighbors). *The nature of a motif does not change significantly from site-to-site.*

~ Some order at intermediate-range (2-20 atoms) may also exist in certain glasses.

GLASS STRUCTURE AND CHEMISTRY
Silica Glass (SiO_2)

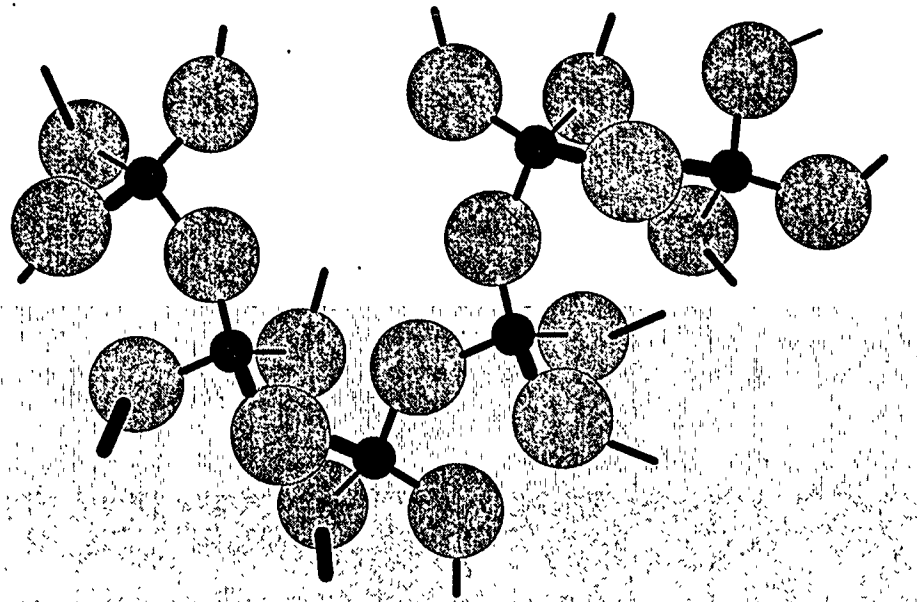

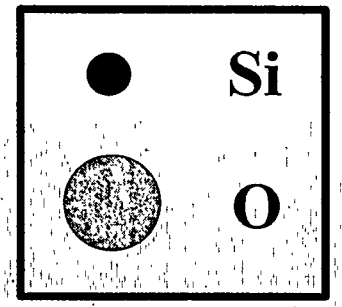

~ All SiO_4 tetrahedra are linked to each other through corner-shairing **O**.

*~ All **Si** atoms occupy Q4 sites. All **O** atoms are bridging **(BO)**. No non-bridging **O (NBO)** are present.*

Pacific Northwest Laboratory

GLASS STRUCTURE AND CHEMISTRY
Sodium Silicate Glass (Na_2O-SiO_2)

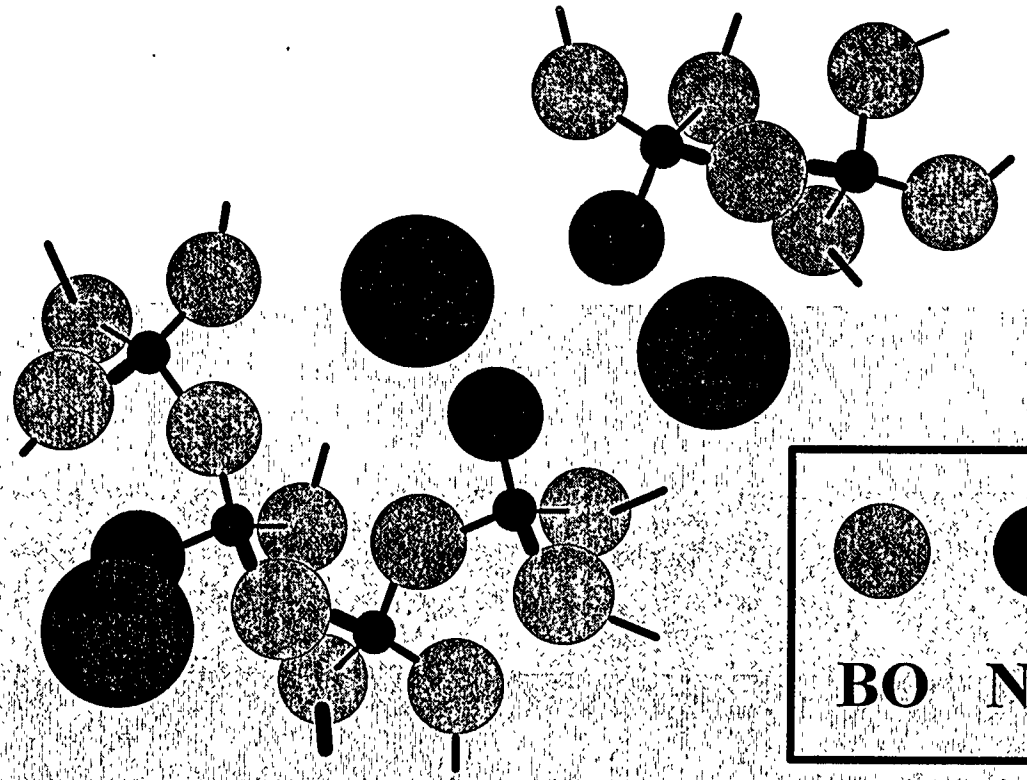

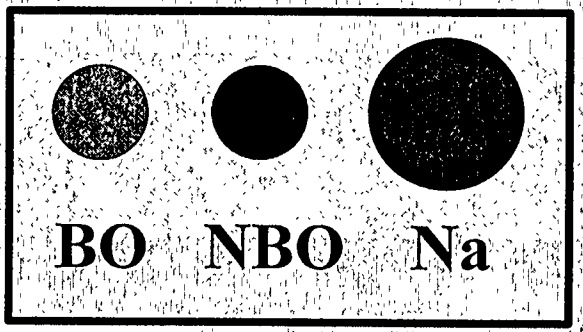

~ Some **Si** atoms occupy Q4 sites (4-**BO**), others occupy *Q3 sites* (3-**BO**, 1-**NBO**).

Pacific Northwest Laboratory

GLASS STRUCTURE AND CHEMISTRY
Sodium Borosilicate Glass (Na_2O-B_2O_3-SiO_2)

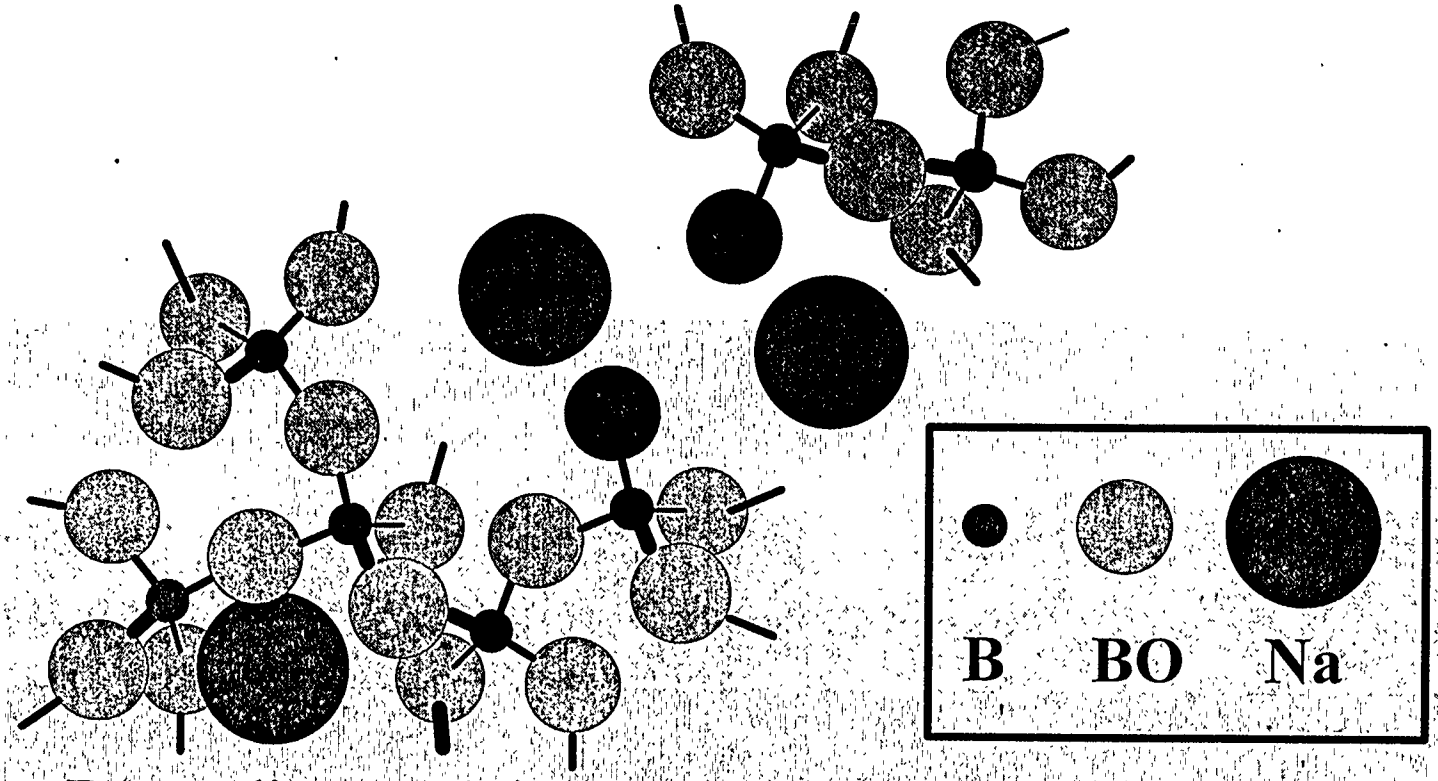

~ Depending on the amount of **Na**, **B** (and **Al**) can occupy network forming tetrahedral sites.

Pacific Northwest Laboratory

Oxide-equivalent compositions of glasses studied in this work.

Oxide	LD6-5510 CBC (wt%)	L4-9012 CBC (wt%)	L6-5412 CBC (wt%)	L6-5412 TMF (wt%)	L6-5412 MCF (wt%)
SiO_2	56.79	56.78	56.78	56.83	58.08
Na_2O	20.00	20.00	20.00	20.02	20.45
B_2O_3	5.00	9.00	5.00	5.00	5.11
CaO	5.00		4.00	4.00	4.09
Al_2O_3	10.00	12.00	12.00	12.01	12.27
Others*	3.21	2.22	2.22	2.14	0.00
Total	100.00	100.00	100.00	100.00	100.00
*Others					
Cl	0.36	0.09	0.09	0.09	
F	0.31	0.21	0.21	0.21	
I	0.14				
Cr_2O_3	0.04	0.04	0.04		
Fe_2O_3	0.005	0.005	0.005		
MoO_3	0.16				
K_2O	1.51	0.33	0.33	0.33	
MnO	0.002	0.007	0.007		
MgO	0.003				
P_2O_5	0.19	1.19	1.19	1.19	
SO_3	0.22	0.32	0.32	0.32	
Bi_2O_3		0.014	0.014		
ZrO_2		0.005	0.005		
SrO	0.12				
Cs_2O	0.15				
Total	3.21	2.217	2.217	2.140	0.00

GLASS STRUCTURE AND CHEMISTRY

Hanford Low-Level Waste Glass-Major Components

Component	Structural & Chemical Issues
SiO_2	Distribution of Q4, Q3, & Q2 sites.
Al_2O_3	Distribution of 4-coord. network former & 6-coord. network intermediate sites.
B_2O_3	Distribution of 4-coord. network former & 3-coord. network intermediate sites.
Na_2O, CaO	Intermediate-range interactions?

GLASS STRUCTURE AND CHEMISTRY

Hanford Low-Level Waste Glass-Minor Components

Component	Structural & Chemical Issues
Cr_2O_3	Distribution of 4-coord. network former & 6-coord. network intermediate sites. Oxidation state.
F, Cl, I	Bridging or non-bridging substituition for **O**?
SO_3	Network former, modifier or intermediate? Oxidation state.
P_2O_5	Network former or intermediate?
TcO_2/ReO_2	Network former or intermediate? Oxidation state.
All, Cs_2O	Intermediate-range interactions?

WHY STUDY GLASS STRUCTURE AND CHEMISTRY?

A Few Things Structure and Chemistry Influence in Glass and Glass Manufacture:

~ Durability

~ Melt viscosity

~ Volatility

~ Optical, magnetic, and electronic properties

METHODS OF STUDYING GLASS STRUCTURE AND CHEMISTRY

~ **Electron Paramagnetic Resonance (EPR) spectroscopy.** Measures transitions between electronic spin states made degenerate in energy by the application of an external magnetic field. Resonance position (g) is sensitive to local chemistry and symmetry around molecules possessing an electronic angular momentum. Interactions of the electron(s) with nuclei possessing nuclear spins as well gives additional information.

~ **Raman spectroscopy.** Measures atomic level vibrational modes induced by an incident laser pulse. Sensitive to structure and chemistry. High temperature measurements (up to 1400C) are possible.

~ **UV/Vis optical absorption spectroscopy.** Measures electronic transitions between d-orbitals. Absorption position (1/cm) sensitive to structure and chemistry.

METHODS OF STUDYING GLASS STRUCTURE AND CHEMISTRY

~ **Magic Angle Spinning Nuclear Magnetic Resonance (MAS NMR) spectroscopy.** Measures transitions between nuclear spin states made degenerate in energy by the application of an external magnetic field. Resonance position (ppm from a reference material) is sensitive to local chemistry around nuclei possessing a nuclear spin. Element sensitive.

~ **X-ray Absorption Near Edge Spectroscopy (XANES).** Measures transitions between core electrons (1s, 2p) and the continuum state. Absorption edge position (2-20 keV) is sensitive to oxidation state and local chemistry. Element sensitive.

~ **X-ray Absorption Fine Structure Spectroscopy (XAFS).** Oscillations in absorption above the transition energy gives information about the number and distance of nearest neighbors around the central atom. Element sensitive.

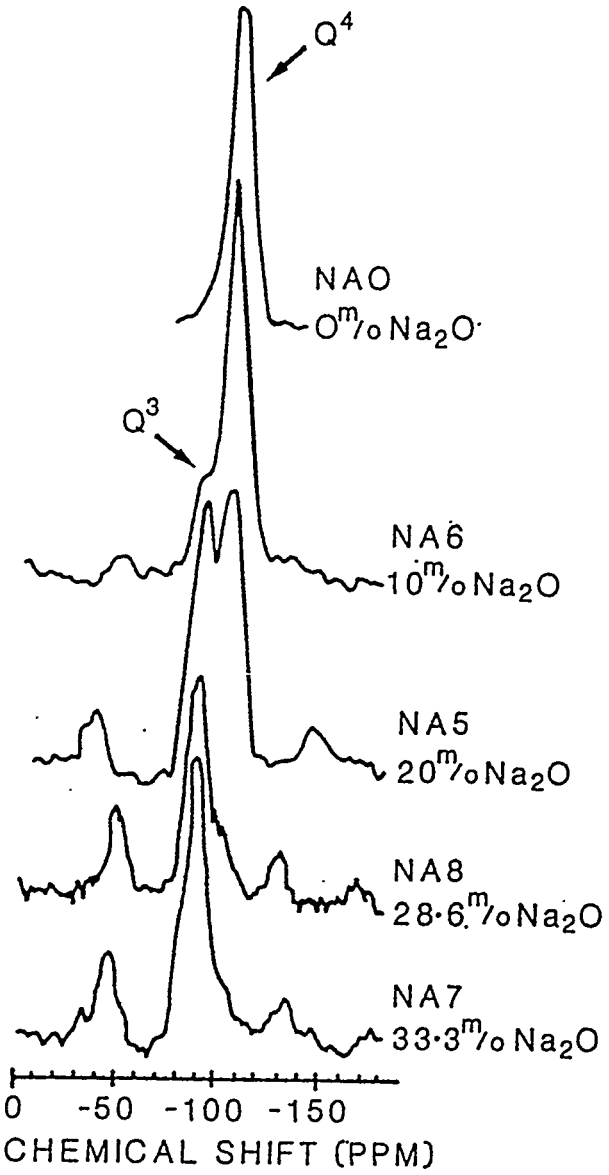

Figure 34. ^{29}Si MAS NMR spectra of glasses in the Na_2O - SiO_2 system. Note the presence of peaks for Si-sites with Q^4 (-111 ppm) and Q^3 (-95 ppm) polymerizations. After Dupree et al. (1984).

LD6-5510 SI29 MAS NMR

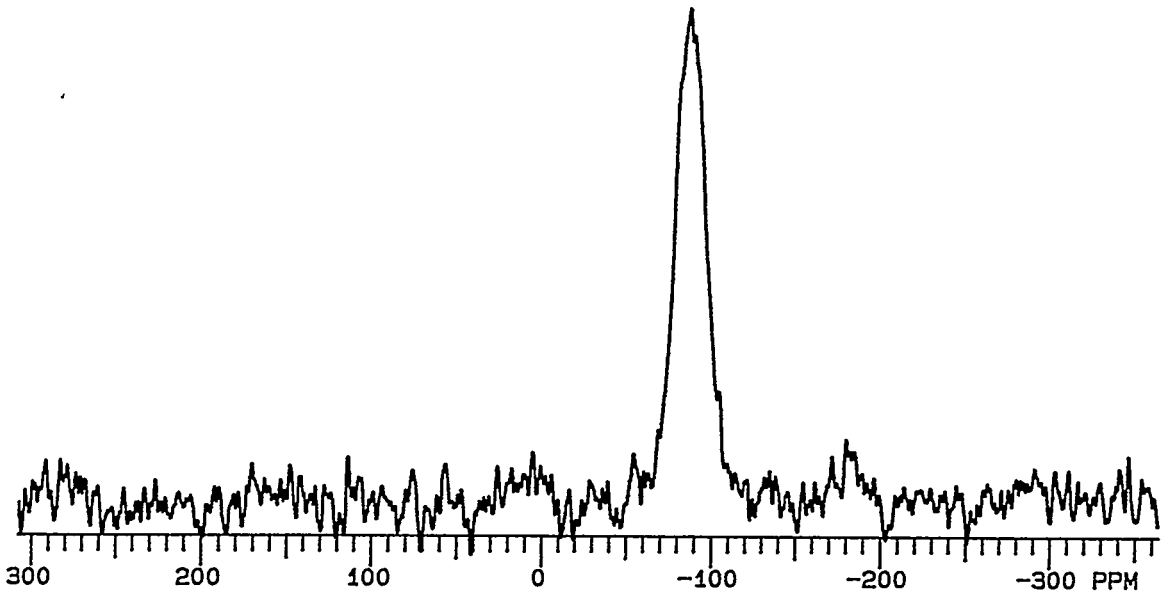

GLASS CHARACTERIZATION
Si-29 MAS NMR

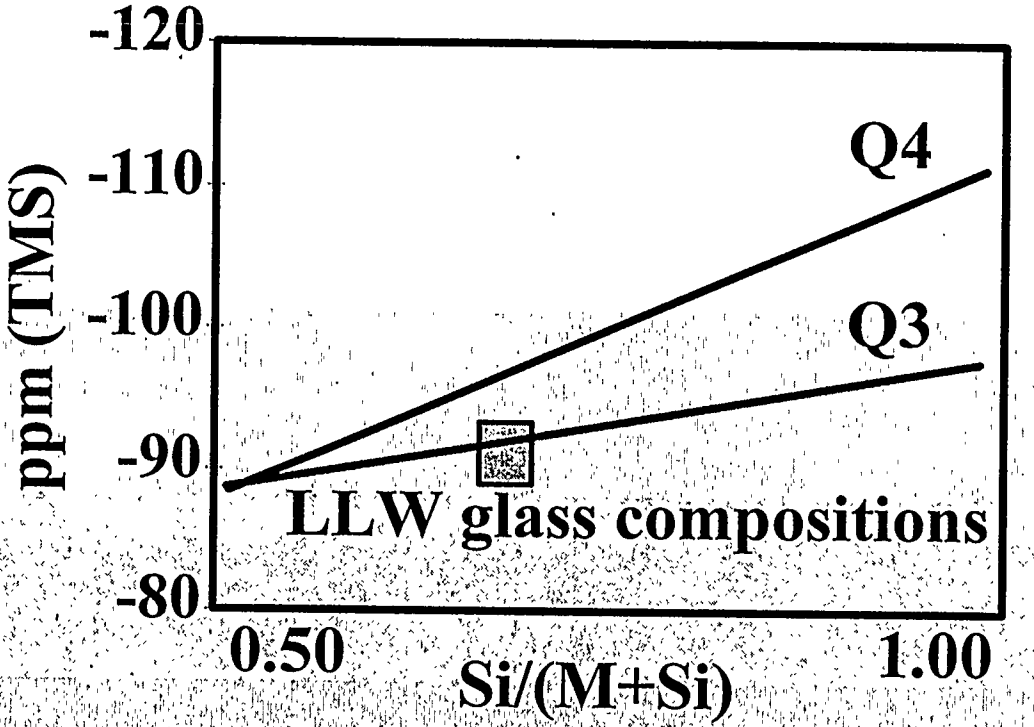

~ Red and blue lines summarize literature data.

~ Box represents data obtained from LLW glasses.

Pacific Northwest Laboratory

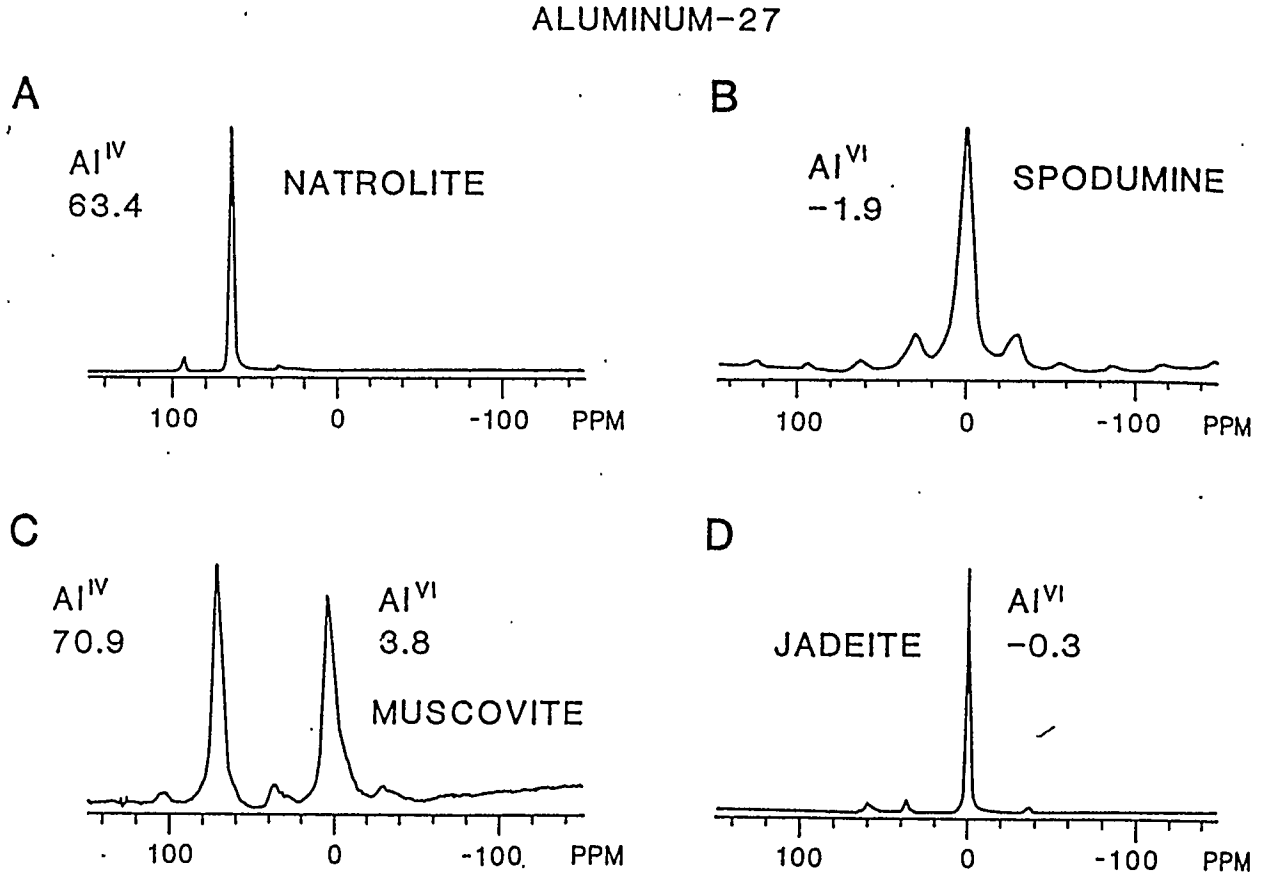

Figure 14. ^{27}Al MAS NMR spectra of aluminosilicate crystals, showing the excellent resolution of signals for Al^{IV} and Al^{VI}. Al^{IV} falls in the range +50 to +80 ppm, and Al^{VI} in the range -10 to +20 ppm at $H_0 = 11.7T$. Al^{V} falls in the range of about +30 to +40 ppm.

LD6-5510 AL27 MAS NMR

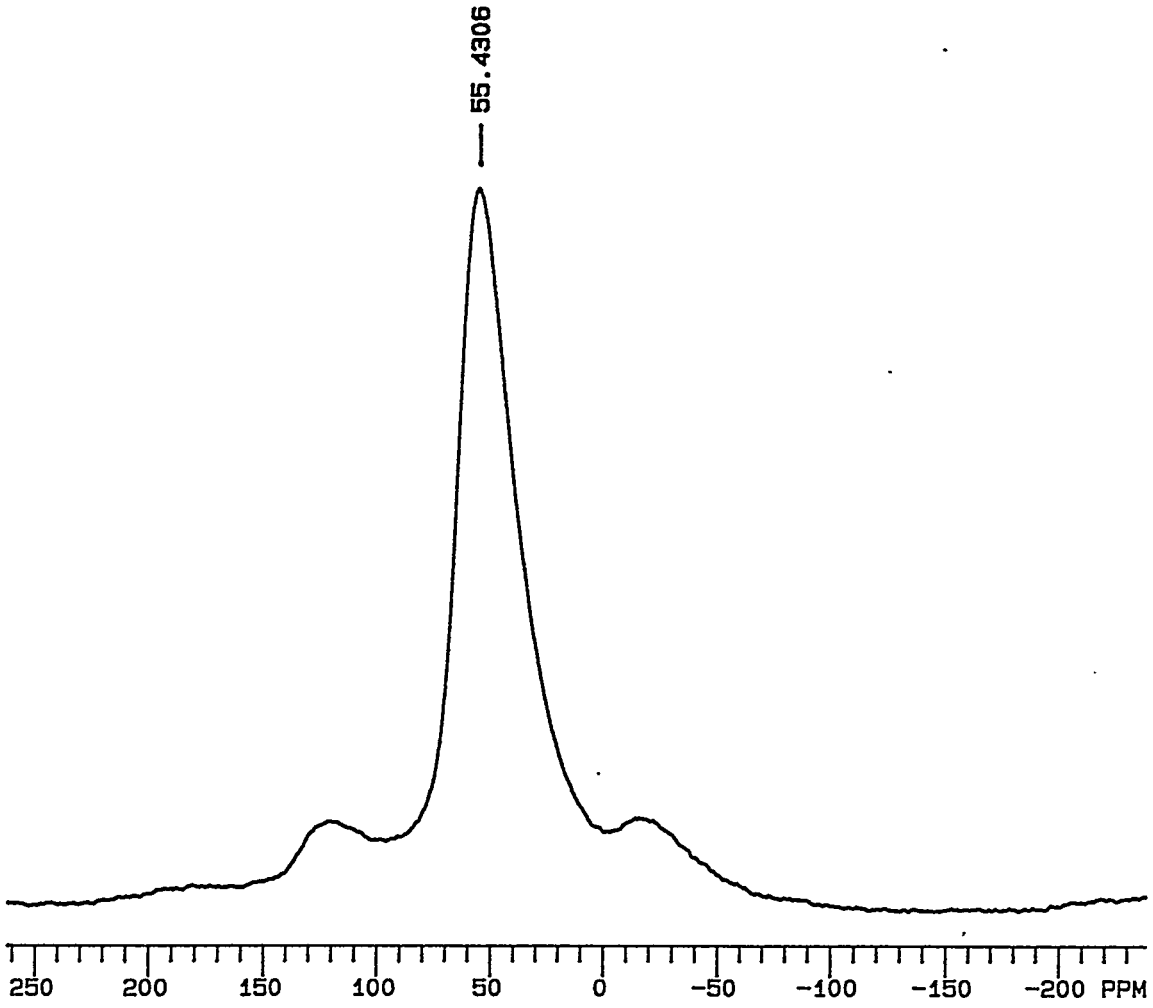

GLASS CHARACTERIZATION
Al-27 MAS NMR

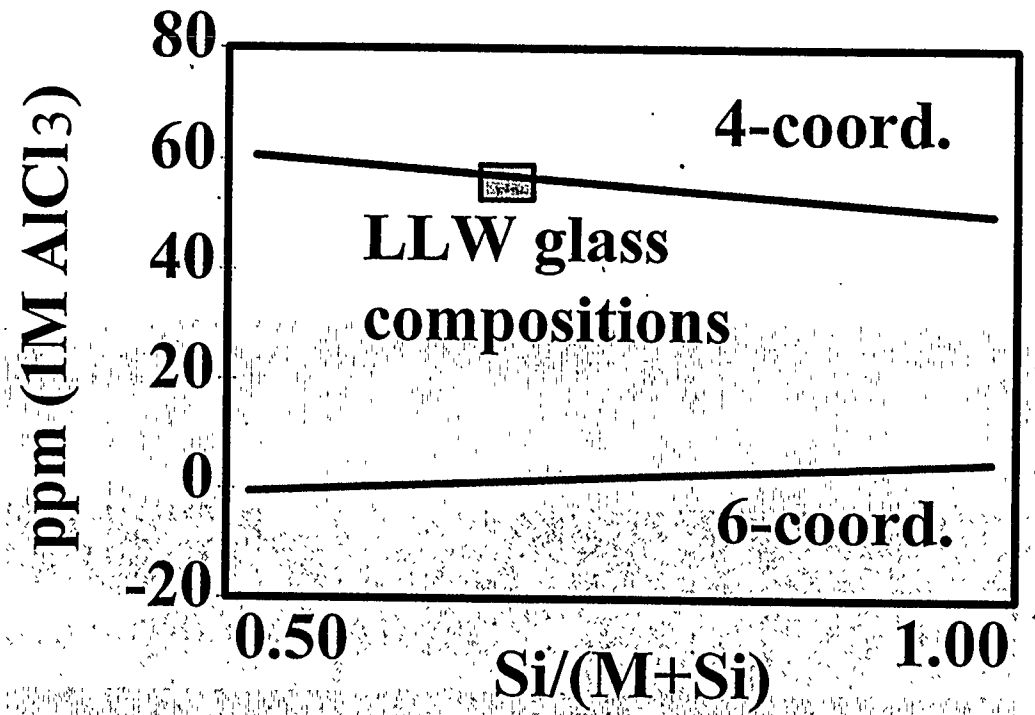

~ Red and blue lines summarize literature data.

~ Box represents data obtained from LLW glasses.

Pacific Northwest Laboratory

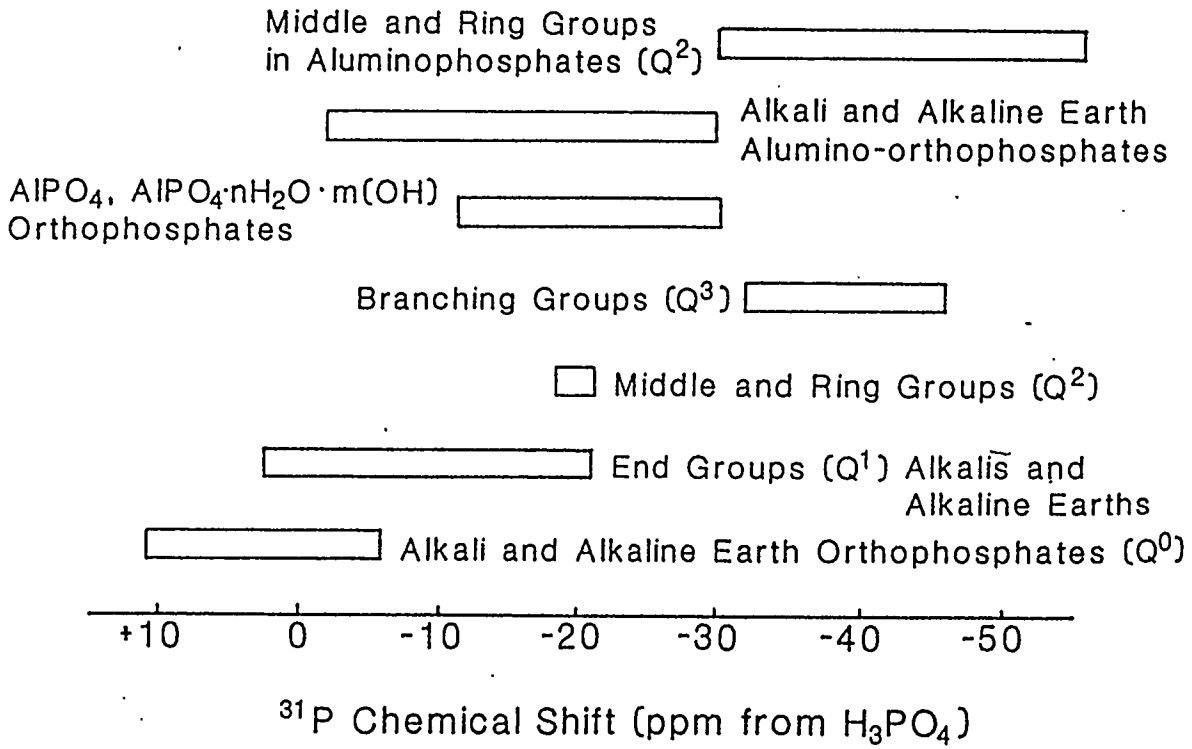

Figure 13. Ranges of ^{31}P chemical shifts in crystalline phosphate phases. Modified from Turner et al. (1986b).

L4-9012 W/S AND P ADD., P31 MAS NMR

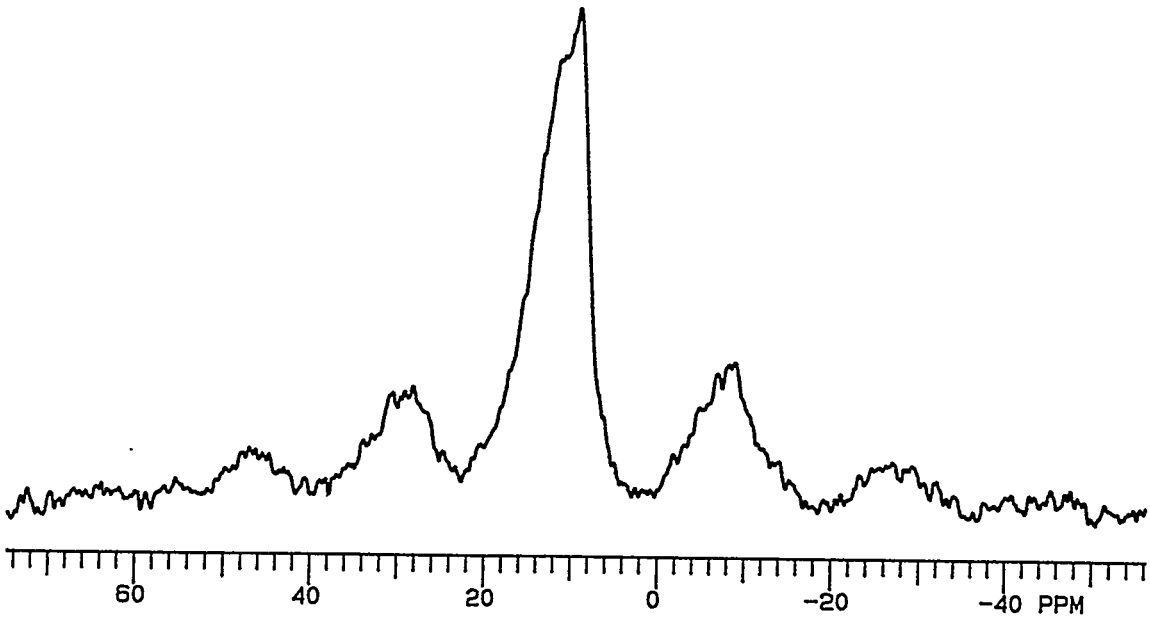

L6-5412 CS133 MAS NMR

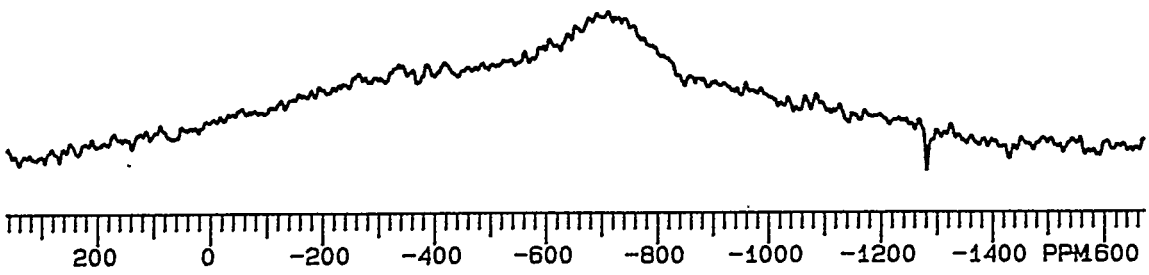

GLASS CHARACTERIZATION

Summary of MAS NMR Results obtained from LLW Glasses to Date

Component	Structural & Chemical Assignment
SiO_2	Mixture of Q3 and Q4 sites.
Al_2O_3	All sites are 4-coord. network formers.
B_2O_3	All sites are 4-coord. network formers.
Cs_2O	Broad distribution of environments.
ReO_2	Difficult nucleus to detect - no resonance detected at ca. 2 wt% loading of ReO_2.
P_2O_5	Varying number of sites, all of which are orthophosphate (PO_4) groups. No P-O-P polymer units detected.

Cr K-Edge Features of Simulated Hanford L6-5412 Based Low-Level Waste Glasses Batched from Various Amounts of Cr_2O_3.

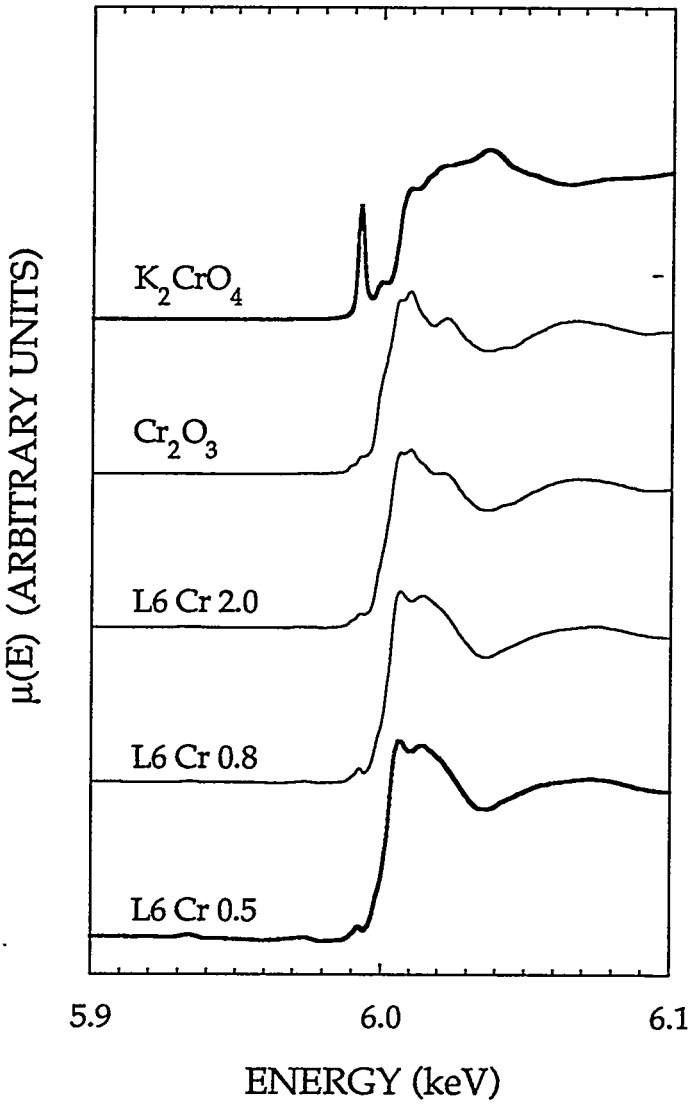

~ Edge energy is sensitive to oxidation state.
~ Pre-edge feature is sensitive to coordination symmetry and oxidation state.

Cr K-Edge and XAFS of K_2CrO_4.

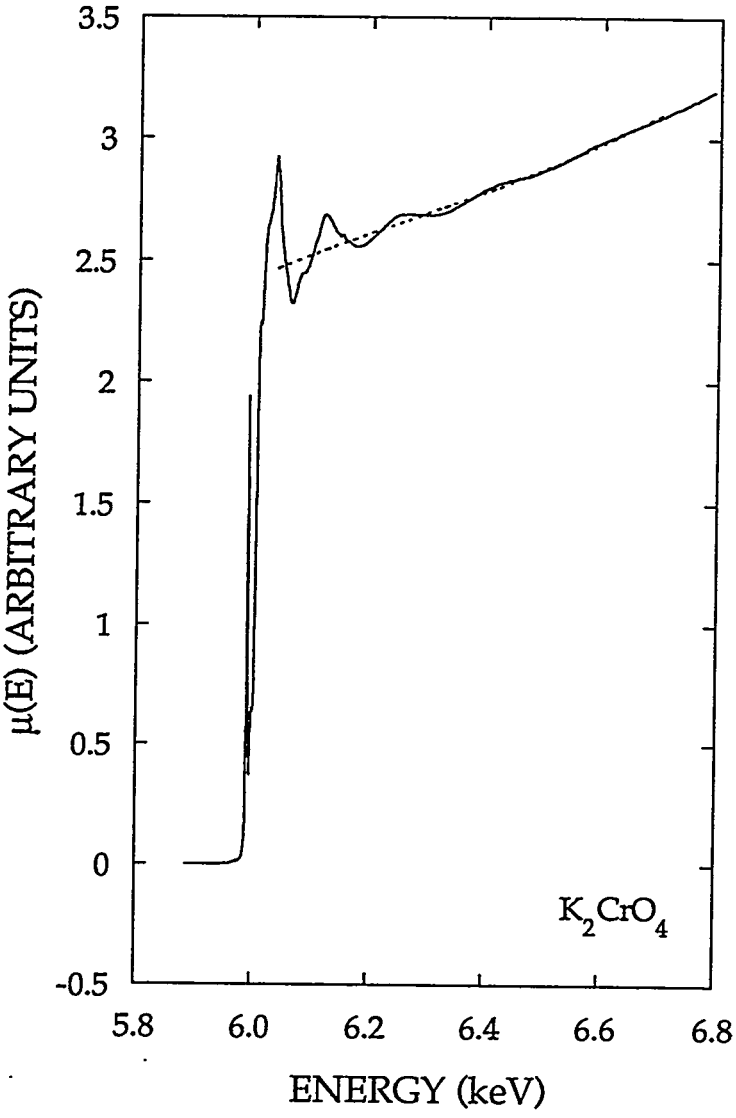

~ X-ray absorption coefficient, $\mu(E)$
~ Edge energy, E_0 (= 6008 eV for K_2CrO_4)
~ Background X-ray absorption coefficient (dashed line), $\mu_0(E)$
~ XAFS region starts ≈30eV above E_0.

Extracted XAFS Data for K_2CrO_4.

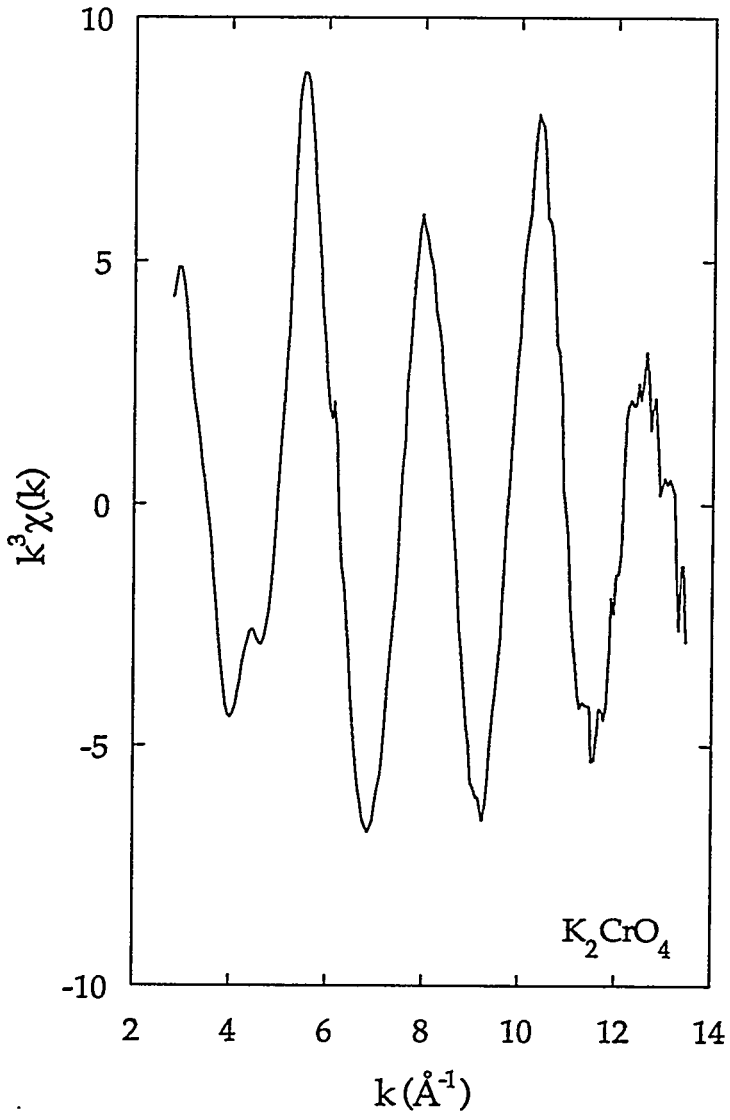

~ XAFS, $\chi(k)$, is obtained from $\chi(E)$, which equals $[\mu(E) - \mu_0(E)]/\mu_0(E)$.

~ Wave vector, k, equals $\{[2m(E - E_0)]/h^2\}^{1/2}$.

~ The amplitude and phase of $\chi(k)$ are related to the number and distance of the nearest neighbors (NN).

Extracted $\chi(k)$ Data for Simulated Hanford L6-5412 Based Low-Level Waste Glass Batched from 0.5wt% Cr_2O_3.

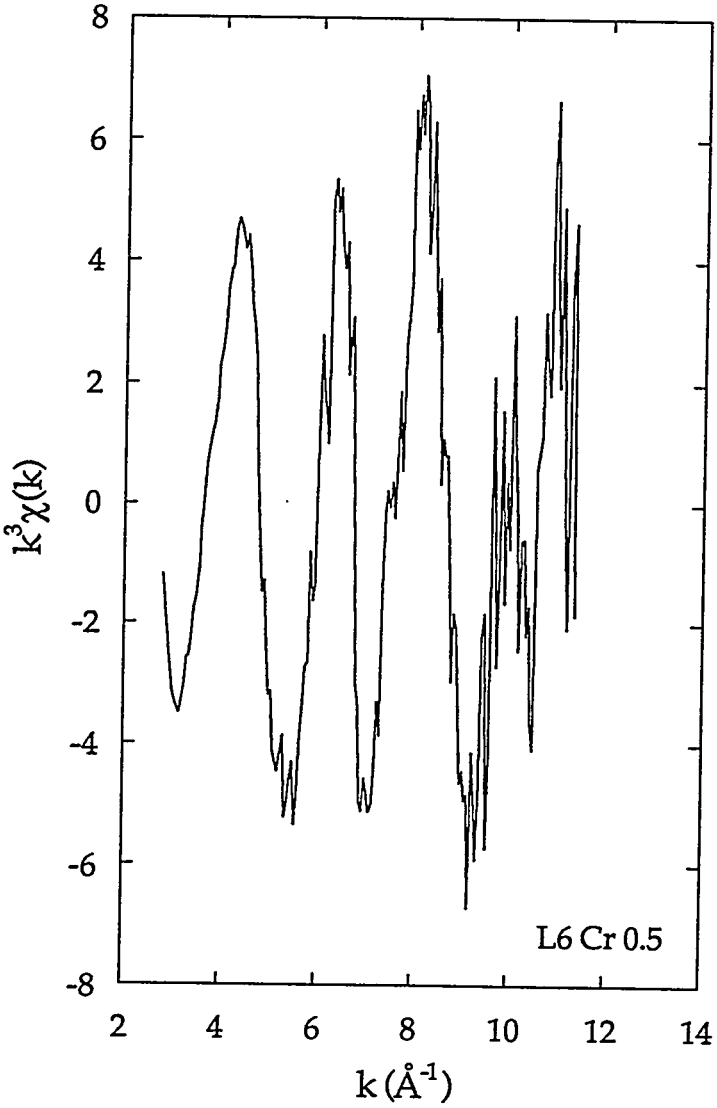

~ Fourier transformation of $\chi(k)$ gives a radial structure plot.

Radial Structure Plots of Cr in Simulated Hanford L6-5412 Based Low-Level Waste Glasses Batched from Various Amounts of Cr_2O_3.

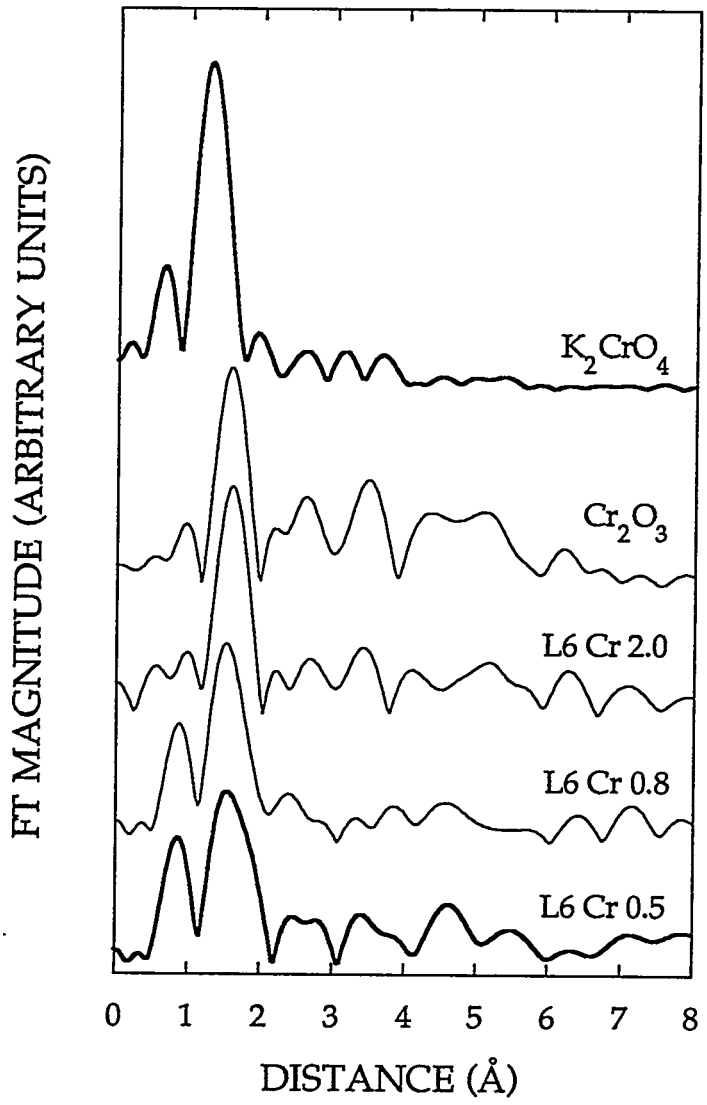

~ The peak at about 1-2 Å is due to the "shell" of first NNs.

~ The peak at <1 Å is an artifact caused by the background subtraction.

NN Shell Phase Difference and Amplitude Ratio Results For Simulated Hanford Based LLW Glasses using K_2CrO_4 as a Standard.

COMPOUND	N	R(Å)
K_2CrO_4	4.00	1.700
L6 Cr 2.0	5.3	2.01
L6 Cr 0.8	5.7	2.00
L6 Cr 0.5	5.8	2.01
L4 Cr 1.0	5.2	1.99

Fit of Back Fourier Transformed NN Shell of Simulated Hanford L6-5412 Based LLW 0.5wt% Cr_2O_3 Glass Using Two Coordination Environments.

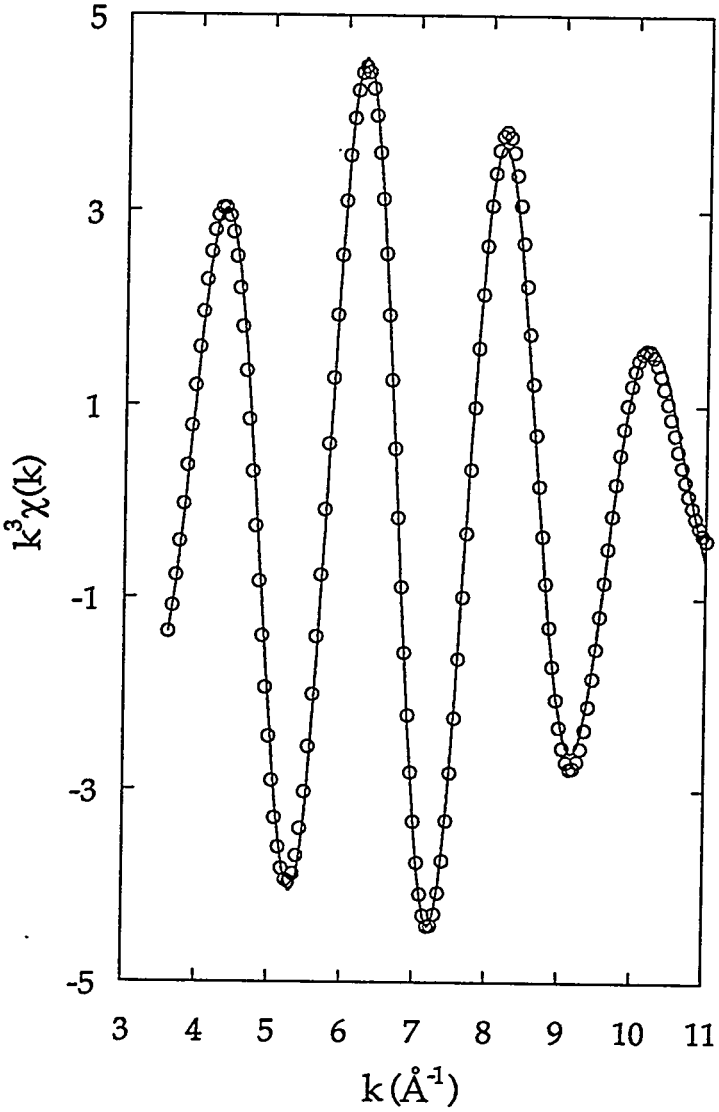

Site 1: N_1=4.8 @ R_1=2.11Å
Site 2: N_2=1.5 @ R_2=2.06Å
Mean : N_T=6.3 @ R_M=2.08Å

Correlation between S K-Edge Chemical Shifts and S Formal Oxidation State for Various Inorganic Sulfur-Oxygen Compounds.

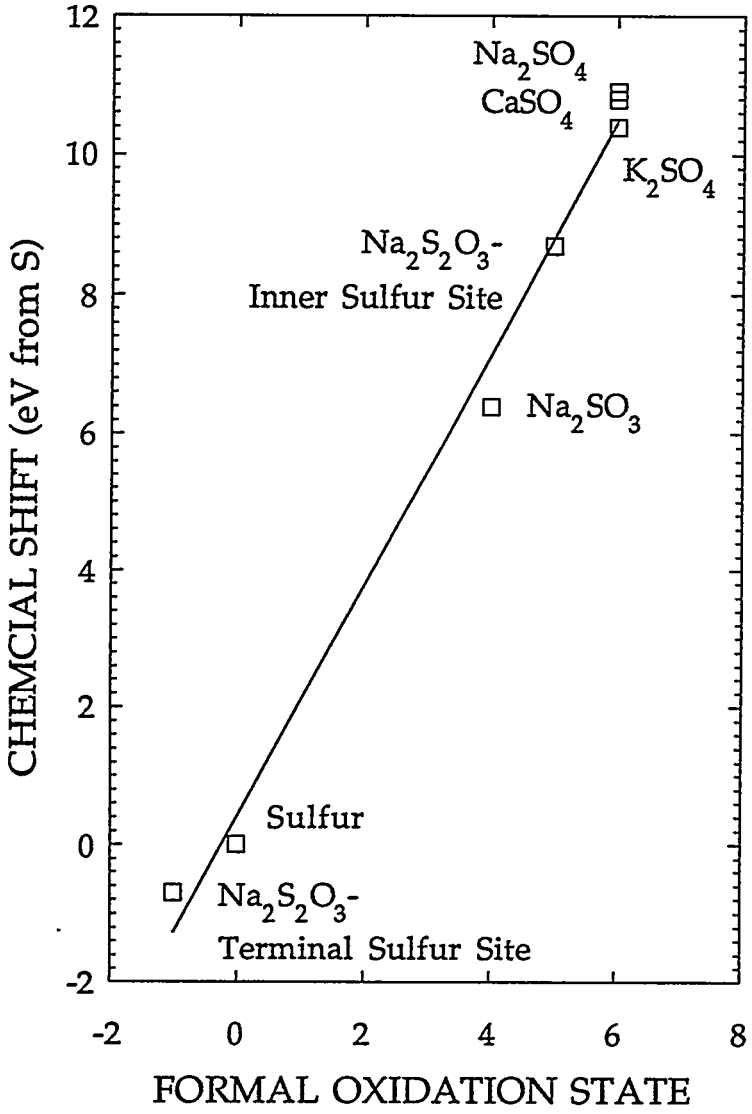

~ Sulfur chemical shift in LLW glasses ≈ 10.8eV

Cl First Derivative K-Edge Features of Simulated Hanford L6-5412 Based Low-Level Waste Glasses Batched from Various Amounts of NaCl.

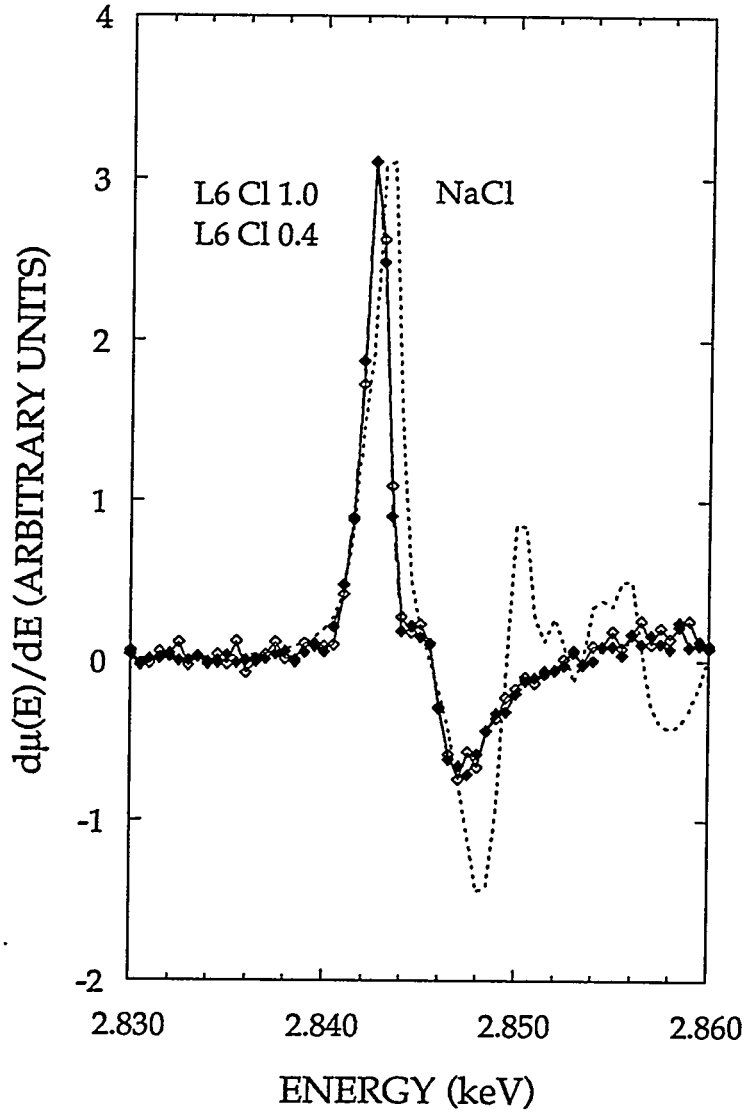

~ Oxidation state of Cl in L6-5412 glasses ≈ -1?

GLASS CHARACTERIZATION

Summary of XAFS and XANES Results obtained from LLW Glasses to Date

Component	Structural & Chemical Assignment
Cr_2O_3	Majority of sites (>95%) are 6-fold Cr(III). A small number of sites (<5%) are 4-fold Cr(VI).
SO_3	Sulfur is in +6 oxidation state as sulfate (SO_4) groups.
Cl	Chlorine is in -1 oxidation state?

Corrosion of Electrodes and Refractories in Waste Vitrification Technology

To
Westinghouse Hanford Company
June 27-28, 1995

By
S. K. Sundaram*
Coauthors: D. A. Lamar, G. L. Smith, and P. A. Smith
Pacific Northwest Laboratories
Richland, Washington

* Supported by AWU, NW under Grant DE-FG06-89ER-75522 or DE-FG06-92RL-12451 with the U. S. Department of Energy.

PNL

Outline

- Melter Technology
- Big Picture
- Electrode Corrosion
  - Testing
  - Materials
  - Glasses
  - Corrosion Rates
  - Summary
- Refractory Corrosion
  - Testing
  - Materials
  - Glasses
  - Corrosion Rates
  - Summary
- Future Trend

Melter Technology Chronological Review

Melter	Electrode Corrosion (mils/day)	Refractory Corrosion (mils/day)
Engineering Scale Ceramic Melter(1976)	Nickel-chrome alloy 2.4-27.3 wt%	Monofrax E
Calcined Fed Melter (CFM, SRL) (1983)	Inconel 690 rods 0.50	Monofrax K3 2 .76
Small Cyl. Melter-2 (SCM-2, SRL)(1983)	Inconel 690 0.07-1.51	
Large Scale Melter (SRL)(1984)	Inconel 690 0.54	Monofrax K3 2 .70
Pilost-Scale Field Test (PSFT, PNL)(1984)	Graphite Molybdenum 11.34-48.03 nominal-pitting	
Small Cyl. Melter (SCM, SRL)(1985)	Inconel 690 0.27-1.50	Monofrax K3 1.81-5.53
Penberthy joule-heated melter (MRC)(1985)	High purity iron	Fused cast AZS 0.19
Large Slurry Fed Melter (LSFM, SRL)(1985)	Inconel 690 0.30, 0.12-0.20(thermo-well, 3 02 days)	Monofrax K3 0.98
Pilot Scale Ceramic Mleter (PSCM,PNL)(1986)	Inconel 690 (6.8%)	Monofrax K3 0.52 Melt line 0.26 Half-down
Liquid Fed Ceramic Melter (LFCM, PNL)(1986)	Inconel 690 0.12	Monofrax K3 0.92
Joule Ceramic Melter (JCM, Harwell, UK)(1986)	Inconel 690 4.2-14.6%	Monofrax K3
Cogema Vitrification (French)(1986)	Inconel (melt containment)	
Liquid Active Waste (Russian)(1990)	SnO_2 with Monel(70%Ni-30%Cu) or 70%Ni-15-17% Cr-Balance Ti) 0.38-0.76	XAU,1.1-1.5 Bakor-33 ,3.8-5.3 Chamotte,7.6-9.5
PSCM,PNL (1990)	Inconel 690	
EhP-500 Radiactive Melter (USSR)(1990)	Molybdenum	Aluminozircon Bakor-30
Joule Heated Melter (JHM, INEL)(1992)	Molybdenum Serious oxidation	Monofrax K3 1.3 , Monofrax E 0.3
1994-95		
Terra-Vit (PNL)	Graphite	
DC Arc (PNL-EPI-MIT)	Graphite	
Research Scale Melter (RSM,PNL)	Inconel 690	Monofrax K3
SSHTM, PNL	Refractory oxide Monofrax K3	
HTM, PNL	Refractory oxide Monofrax K3 Molybdenum	

PNL

Big Picture

Low temperature vitrification (<1200°C):

Electrode	**Inconel 690, No protection**
	Corrosion rates 0-7.2 mils/day
Refractory	**Monofrax K3**
	Corrosion rates 0.9-6.0 mils/day

High temperature vitrification

Electrode	**Mo, Ta, Cr, Cr-Al_2O_3, SnO_2,**
	Pt-10%Rh, refractory oxide,
	Protection?
	Corrosion rate?
Refractory	**Monofrax K3, C1215Z**
	Corrosion rate?

PNL

Effect of Temperature on Corrosion

REFRACTORIES:

- Temperature dependence (Arrhenius equation): Corrosion rate = A exp(-E/RT)
  - Corrosion rate doubles for each 50-100°C increase in interface temperature (T_i). (Trier, 1987)
  - Glass fluidity doubles for each 50-100°C increase in T_i.

- Flow raises T_i enhancing corrosion

- Corrosion rate is roughly proportional to glass fluidity, for a refractory corroded by various glasses of the same chemical family. (Woolley, 1989)

ELECTRODES:

- Oxidation of metal
  - Kinetics: Linear, $x = k_L t$; Logarithmic, $x = k_e \log (at + 1)$; Inverse logarithmic, $1/x = b - k_i \log t$; Parabolic, $x^2 = (k_p/2)t$; Cubic, $x^3 = k't$. (x = thickness or mass of oxide, t = time)
  - Protecting/non-protecting

- High temperature creep: logarithmic relationship between stress and creep rate as a function of temperature

- Alloying/eutectic formation

PNL

Electrode Corrosion Test Methods

Static/Dynamic Isothermal

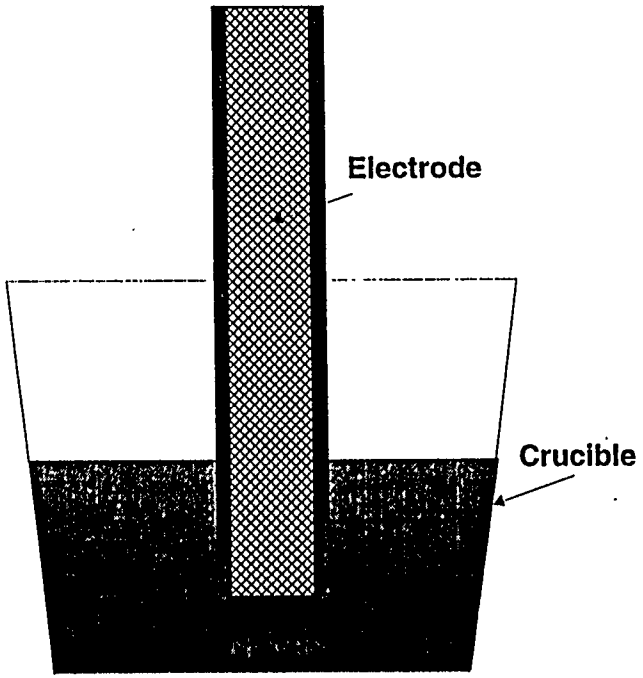

Powered Electrode Test

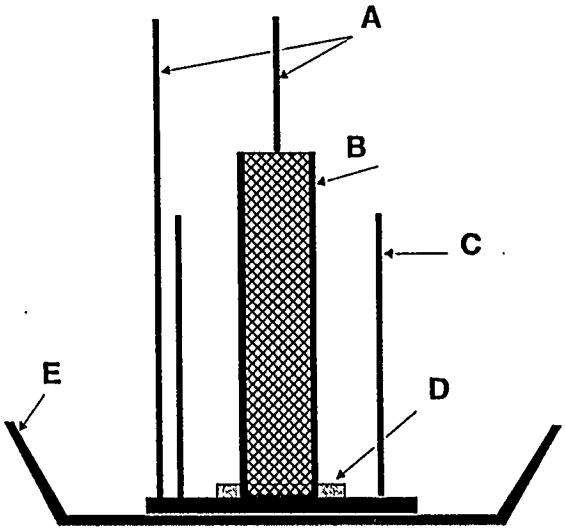

A - Leads from power supply to speciment and crucible (inconel welding rod).

B - Electrode Specimen

C - Crucible made of same material as specimen

D - Alumina insulating disk to prevent shorting and eliminate end effects of current

E - Alumina over flow basin

Service Test

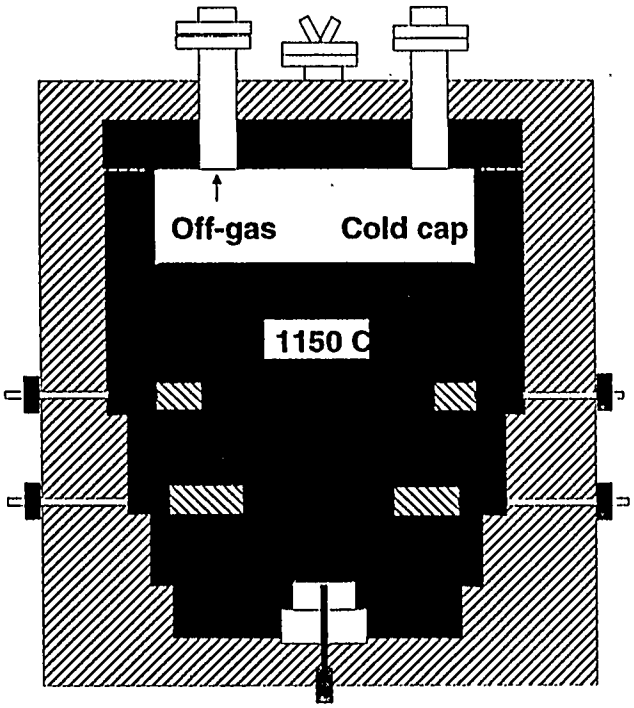

PNL

Electrochemical Corrosion Testing

(ASTM G5-87 & G3-89)

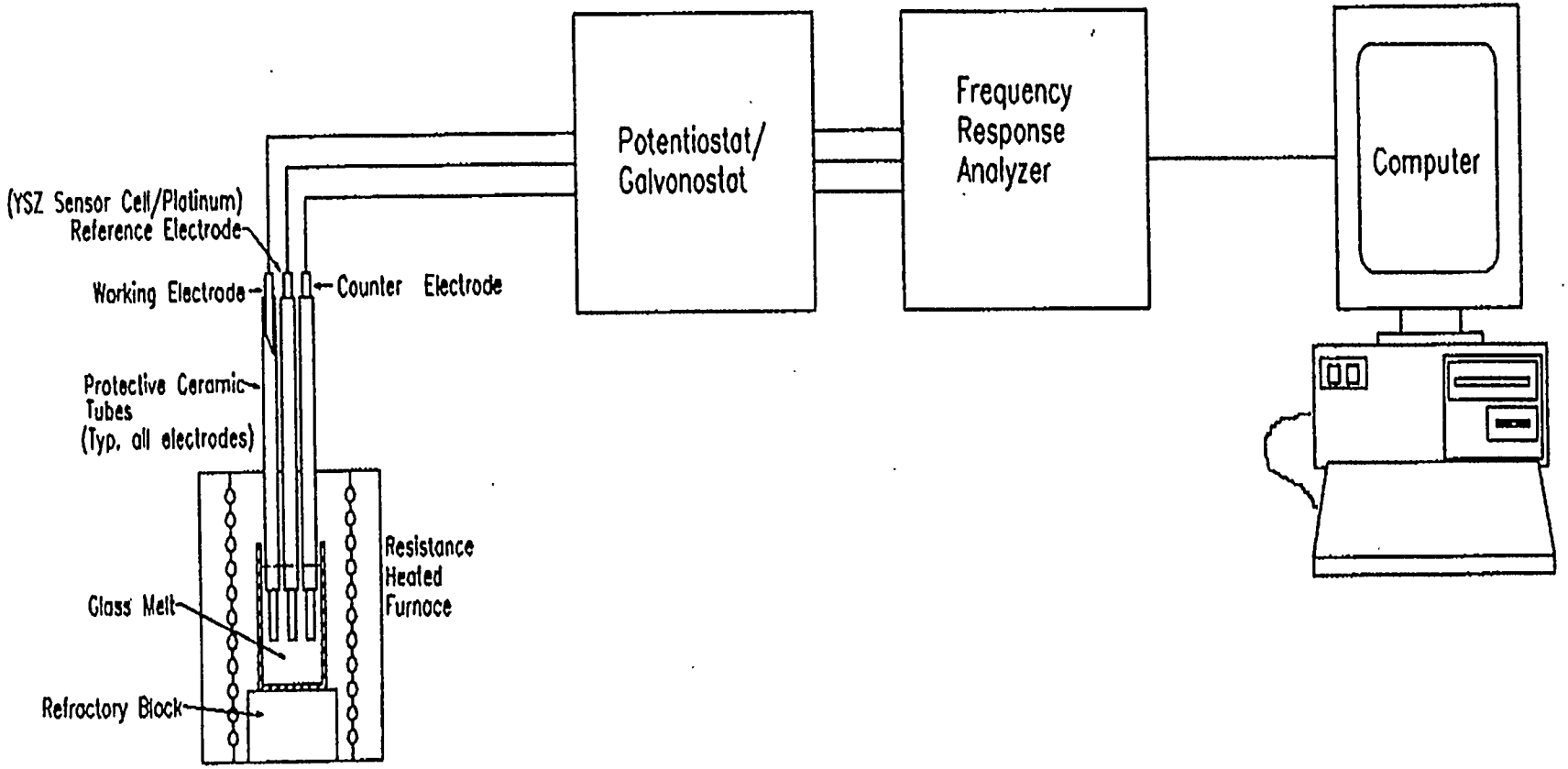

Electrochemical corrosion rate

Protection potential (cathodic/anodic)

PNL

Electrochemical Corrosion

	Aqueous Corrosion	Molten Glass Corrosion
Electrolyte	Aqueous solution	Molten glass
Electrodes	Working, counter, and Reference	Working, counter Reference
Reference (common)	Calomel, Hydrogen	Oxygen, noble element
Anodic reactions	$Zn \longrightarrow Zn^{2+} + 2e^-$ $Al \longrightarrow Al^{3+} + 3e^-$	$Mo \longrightarrow Mo^{4+} + 4e^-$ $Ta \longrightarrow Ta^{5+} + 5e^-$
Cathodic reactions	$H^+ \longrightarrow 1/2H_2 - e^-$ $Cu^{2+} \longrightarrow Cu - 2e^-$	$O_2^- \longrightarrow 2e^- + 1/2O_2$ $Fe^{3+} \longrightarrow Fe^{2+} - e^-$
Key factor	pH	p_{O2}

PNL

Theoretical Background

Typical Potentiodynamic Scan

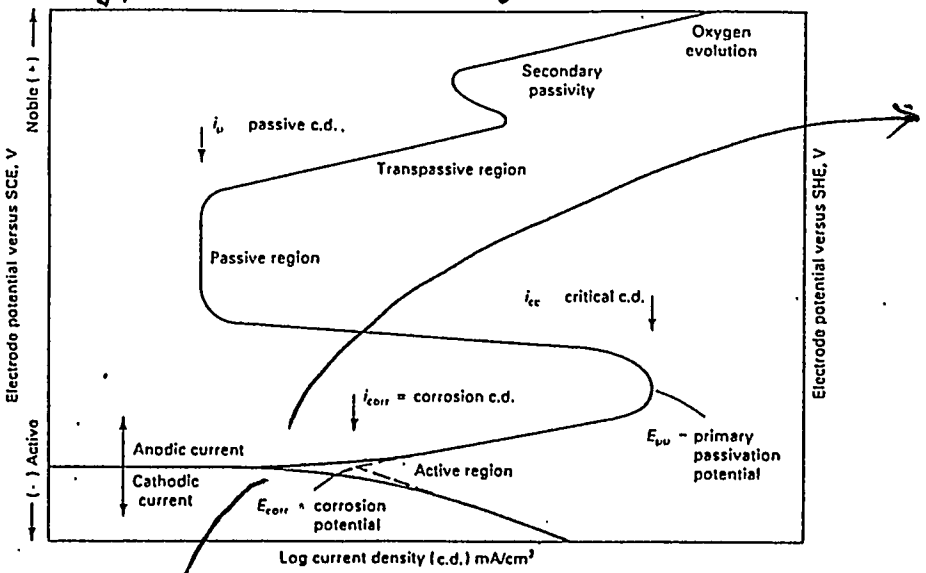

R_p Fit

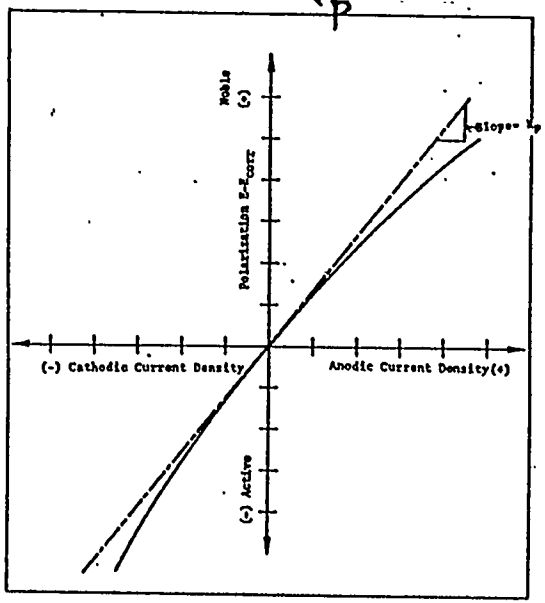

In determination of the corrosion rate of a material, linear plots are used in the determination of the polarization resistance (R_p), which is defined as the slope of a potential-current density plot at the corrosion potential (E_{corr}) and the corrosion current density (i_{corr}), and β_a and β_c are the anodic and cathodic Tafel slopes, respectively.

$$\left[\frac{d\Delta E}{di}\right]_{\Delta E \to 0} = R_p = \frac{\beta_a \beta_c}{2.303(\beta_a + \beta_c) i_{Corr}}$$

Upon rearranging this equation the corrosion current density can be solved for as,

$$i_{Corr} = \left(\frac{1}{2.3 \cdot R_p}\right)\left(\frac{\beta_a \cdot \beta_c}{\beta_a + \beta_c}\right)$$

Finally, knowledge of R_p and Tafel slopes permit direct determination of the corrosion rate at any instant in time as follows:

$$\text{Corrosion rate (mm/year)} = \frac{3.27 \times 10^3 \cdot i_{Corr} \cdot E.W.}{d}$$

where E.W. is the equivalent weight of the material in grams and d is the metal or alloy density in grams/cc.

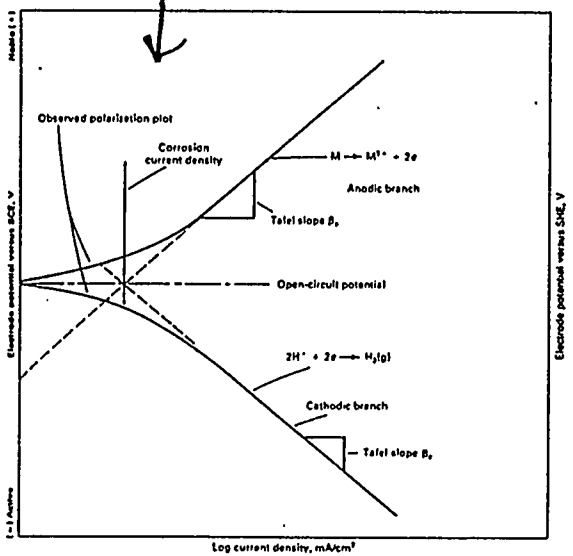

Tafel Fit

PNL

Nominal Composition of Alloys Used for Electrode Corrosion Testing

Material		wt% Elements Cr	Ni	Fe	C	Mo	Others
304L SS		20	9	Balance	0.03		
310		25	20	Balance	0.25		
330		18	35	47			
347		17	9	Balance	0.15		
410		12		Balance	0.15		
446		25	75				
Inconel	600	15.5	76	8			
	601	23	60	14	0.15		1.4 Al
	617	22	54			9	1 Al, 12.5 Co
	625	21	61	2.5		9	3.7 Nb and Ta
	671	48	50				0.35 Ti
	690	30	60	10			
Incoloy	801	20	32	44			1.13
	802	21	32	46			
Hastelloy	C-4	18	Balance	3	0.02	17	0.7 Ti, 1 Mn
	X	22	Balance	18	0.1	9	1 W, 2 Co
Haynes	188	24	24	3	0.2		31 Co,16 W, 1.2 Mn, 0.4 La
	25	21	10	3			54 Co, 15 W
Teledyne Allcorr		31	56			10	2 W,0.25 Ti, 0.25 Al
UCAR LT-1		77					22 Al_2O_3

Other materials: Ti, Ta, Pt, Mo, SnO_2, TiB_2, Cr

Corbett, Bickford, and Morrison (1986).

PNL

Glass Compositions Used for Electrode Corrosion Testing

wt% Oxides

Compound	SBS	SBSR	SBSF	ABS	SLS
SiO_2	35-58	40-55	38.6	63	70.5
Al_2O_3	1-11	0.1-3.6	5.9	17.3	
B_2O_3	9-14	5.8-7.8	9.4	10	
P_2O_5		2.3-3.6	1.3	5.8	
Fe_2O_3, Cr_2O_3, Bi_2O_3	0.2-5.8	12.6-15.2			0.02,(1.28)
CaO, MgO, ZnO	0.4-3.6	2-5.2	0.03		11.6,-,-
Na_2O, K_2O, Li_2O	2-14	1-15	0.03-16	0.4-0.9	8.7,7.7,-
SO_3		0.1			0.2
F^- (CaF_2)		1.8	18.3	2	
TiO_2	0.9-6	1.1	6.7		
ZrO_2	2.5-5.3	0.1	5		
RE Oxide	0.3-15	0.4-4			

SBS = Sodium Boro Silicate
SBSR = Sodium Boro Silicate (with R_2O_3)
SBSF = Sodium Boro Silicate (with F)
ABS = Alumino Boro Silicate
SLS = Soda-Lime-Silicate, container glass composition, SRM 710 from NIST
(R_2O_3)

PNL

Corrosion of Electrode Materials in Various Glasses

Static "C 621" Type Isothermal Testing (1050-1400°C, 7 days)
(Corrosion* in mils/day)

Electrode	T°C	SBS		SBSR		SBSF		ABS	
		ML	IM	ML	IM	ML	IM	ML	IM
Molybdenum	1200		0		0-1.93				
	1300		0		1.14-2.13				
	1400		0-0.08		0.75-3.66				
Inconel 690	1050	0	0.16-0.20	0-1.14	0	0.51	0	0.59	0
	1150	0.16-0.20	0-0.28	0.08-0.28	0	0.16	0.08	0.28	0
	1200	0	0	0-1.14	0-0.47				
	1300	0.83-1.34	0	2.68-7.24	1.02-6.10				
Inconel 601	1050	0.71	0.2-0.59	0.16-0.51	0-0.20	0.28	0.20	0.51	0.20
	1150	1.06-1.65	0.51-1.30	0-0.16	0	0.28	0	0.59	0
SnO_2	1050	0.35	0.16-0.35	0.20-0.59	0.08-0.20	0.20	0.16	0.35	0.35
	1150	0.59	0	0.59-0.71	0-0.59	0.43	0.28	0.59	0
	1200	0.71-2.24	0.39-0.98	1.85-4.45	0.43-1.34				
	1300	1.93-3.19	0.71-1.38	3.5-5.75	2.44-2.91				
	1400	3.98-5.75	1.38-3.90	10.98	3.15-5.20				
304-L-SS	1050	2.01-2.28	0.35-2.72	0.35-0.51	0-0.08	2.01	0.79	1.85	0.08
	1150	6.93-7.99	3.43-3.94	1.22-3.07	0.43-0.71	3.94	1.85	1.65	0.35

ML =Melt Line
IM - In-Melt

* Data from: M. R. ELmore (1979) and R. A. Palmer (1980).

PNL

Corrosion of Electrode Materials in Various Glasses

Powered Electrode Testing, 5A/inch²*
(Corrosion in mils/day)

Electrode	T°C	SBS		SBSR		ABS		SLS
		ML	IM	ML	IM	ML	IM	IM
304-L SS	1050	3.54	3.54					
Inconel 601	1050	0.71	0.71					
Inconel 690	1050	0.16-0.43	0.08-0.35	0.08	0			
Nickel-base alloy**		Sodium Calcium Silicate Glass with Fe & S, 1150°C, 0.3 A/cm², 31 hours				0.82		
Chromium-base alloy**		Sodium Calcium Silicate Glass with Fe & S, 1150°C, 0.3 A/cm², 80 hours				0.23		
SnO_2**		Sodium Alumino Phosphate Glass with Fe & S, 1150°C, 1.0 A/cm², 100 hours				0.45		
Molybdenum***		Soda Lime Silicate Glass, 1430°C, 1 A/cm²						1.37
		Soda Lime Silicate Glass + 0.4 mol% Sb_2O_3, 1430°C, 1A/cm²						3.01
		Soda Lime Silicate Glass + 2 mol% Fe_2O_3, 1430°C, 1A/cm²						5.48
		(Lead Glass, 1350°C, 1A/cm²)						(29.2)
		(Lead Glass, 1350°C + 1 mol% Sb_2O_3, 1A/cm²)						(42.04)

ML =Melt Line
IM - In-Melt
*Data from M. R. Elmore (1979).
**Data from A. S. Polyakov et.al. (1989).
***Data from C. Russel et. al. (1989).

PNL

Corrosion Rate (melt line) vs. Chromium Content

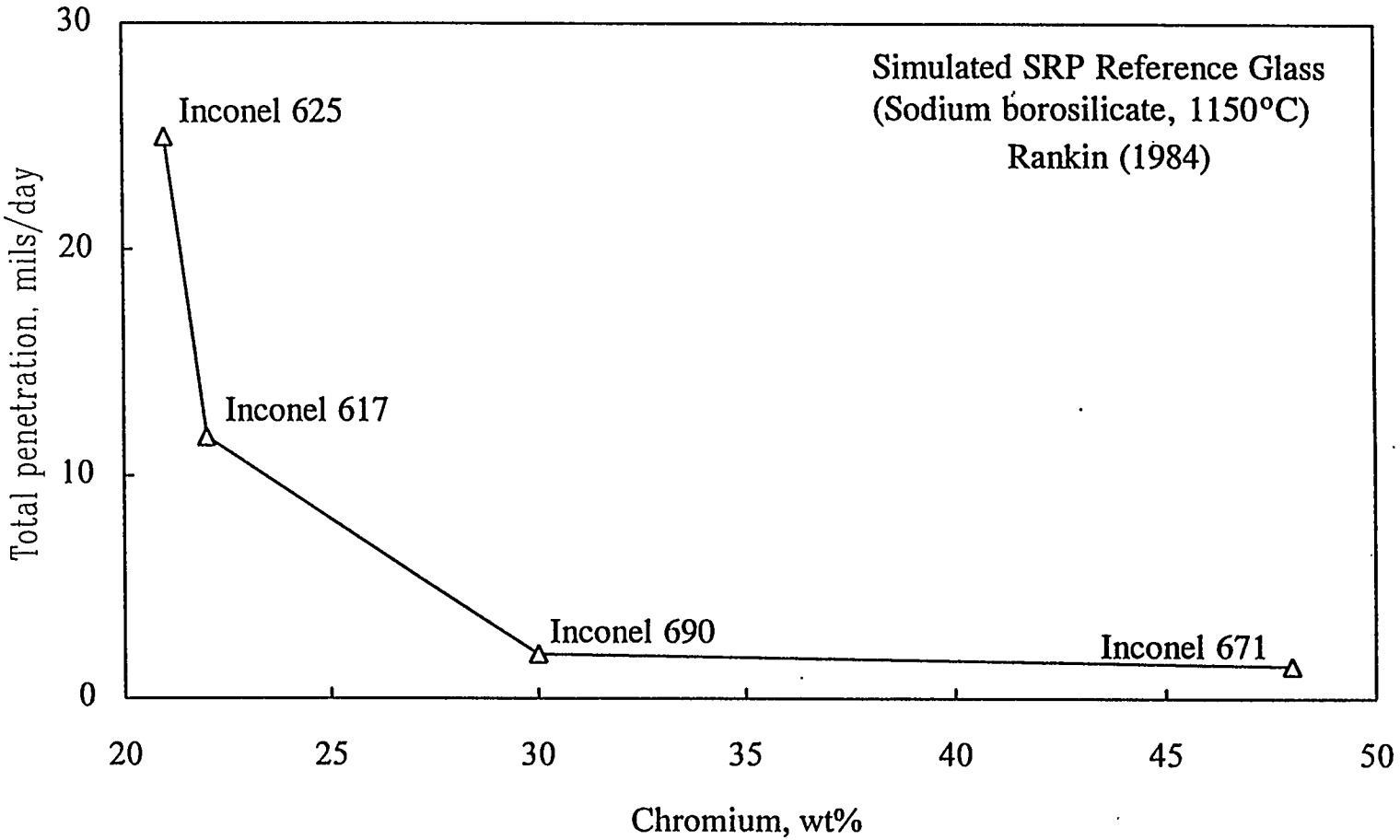

- Inconel 671 is slightly more corrosion resistant than Inconel 690 (melting range, 1343-1377°C), but has lower melting range (1307-1409°C) and is scarce.

PNL

Corrosion Mechanism of Inconel 690

- Rankin, SRL (1981)

  Selective penetration of elements of the molten glass such as Ti, Al, and C along the grain boundaries of Inconel 690.

- Barnes et.al, PNL (1982)

  Innermost chromium-depleted Inconel 690.
  Intermediate layer of mixed spinels, $(Mn,Ni)(Cr,Fe)2O_4$.
  Outermost layer of $(Fe,Ni)Cr_2O_4$ and Cr_2O_3.
  Al, C, Cr, and Ti phases at the grain boundaries.
  Noncontinuous voids to depths of 1-3 microns due to faster chromium diffusion to the reaction zone than the alloy could fill the voids.
  Vacancies coalesce at crystal imperfections.
  Subsurface void formation (Kirkendall effect).

Corrosion of Inconel 690 in Mixed Molten Salts

``Catastrophic Sulfidation of Inconel 690 in PAMELA Melter''

Bickford et.al (1986)

- 46 coupons partially submerged in various mixtures of sodium/sulfur salts, redox agents, and reagents simulating deposits found in melters. 3 levels of testing.

  Variables: Oxidation state of Na_2SO_4, Halide content, Oxidation state of molybdenum, Saturation of nickel oxide, and alkali fluxing.

  Weight loss of Inconel 690 = 1-04-100% (in various mixed molten salts)

  Alloys containing 30% or more chromium (Inconel 690 and 671) survived the tests. All others failed by rapid oxidation, sulfidation, or breakaway corrosion.

- To prevent sulfidation-
  Avoid accumulation of molten salts
  Keep alloys below the critical temperature (~650°C for nickel-based alloys)

Marra et.al (1994)

- Extensive degradation in the metal alloys by a combination of attack by the chloride and sulfate. The chloride breaks down the protective oxide film on the alloy allowing subsequent sufidation of the exposed metal.

•Inconel MA-758 (mechanically alloyed)?

PNL

Molybdenum - Potentiodynamic Scans

(Pt counter electrode, Pt reference electrode, 1400 °C 0.5 mV/sec)

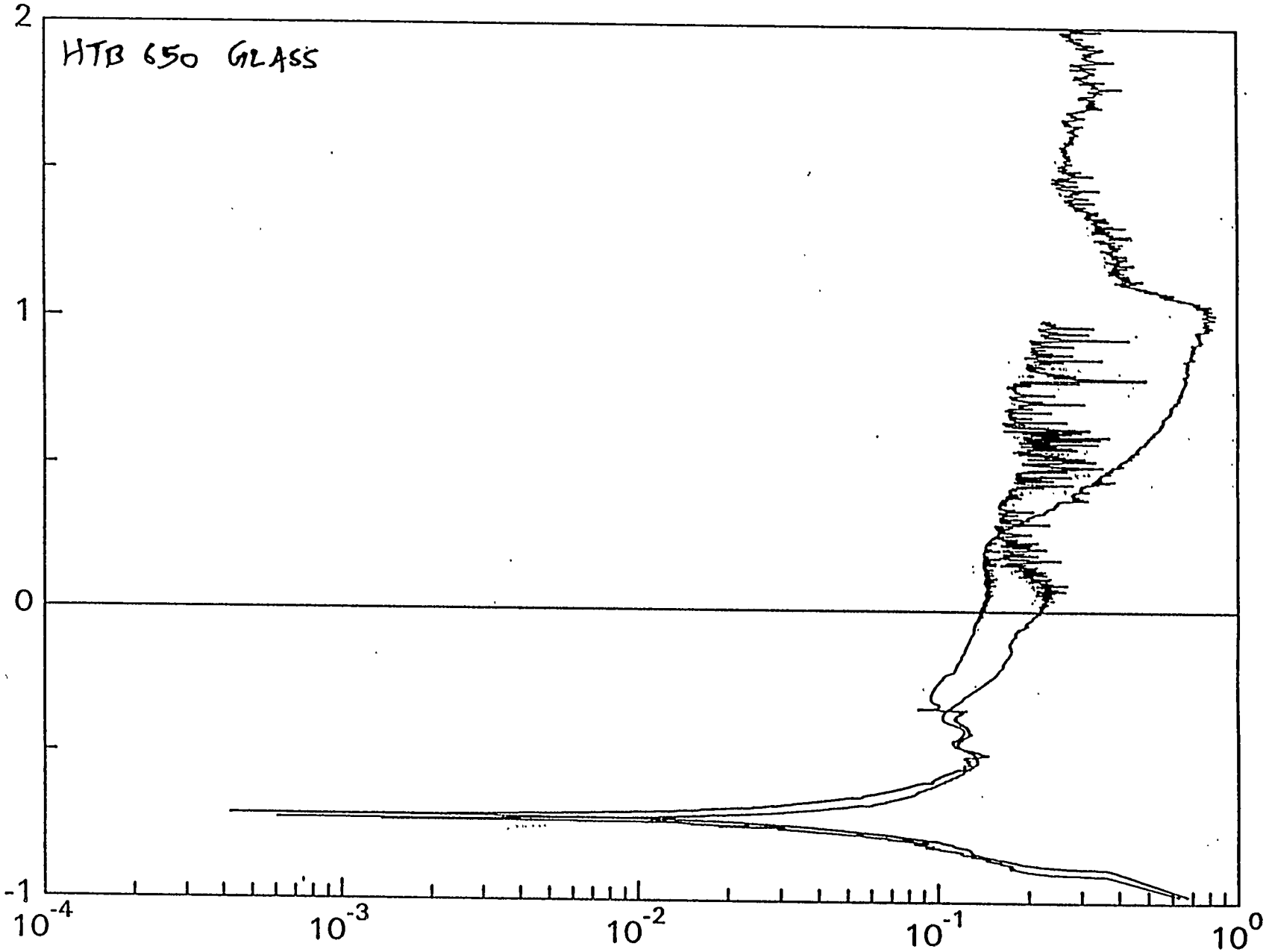

PNL

Molybdenum - Tafel Fit

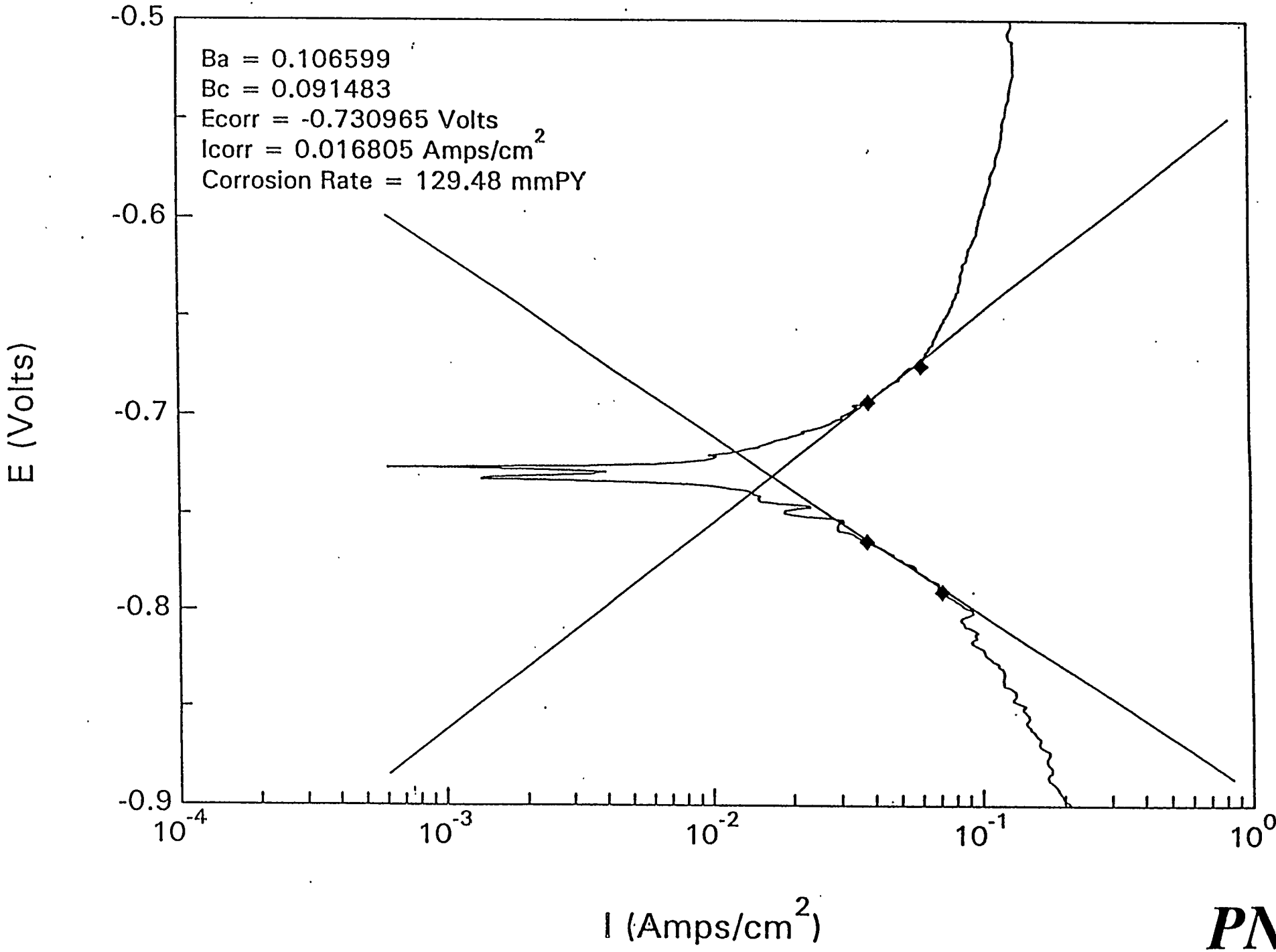

PNL

Molybdenum - Polarization Resistance (R_p) Fit

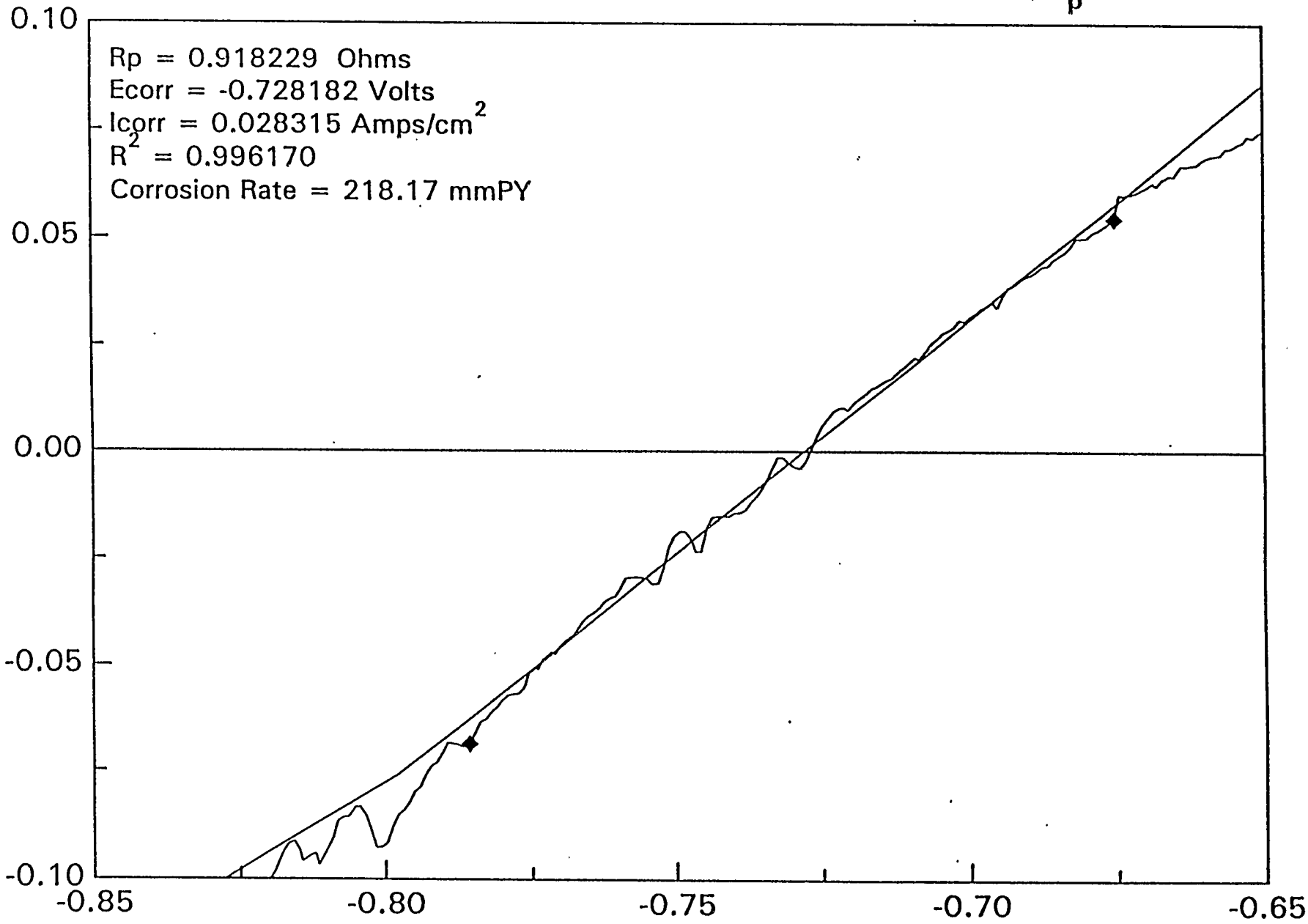

PNL

Molybdenum - Nyquist Plot

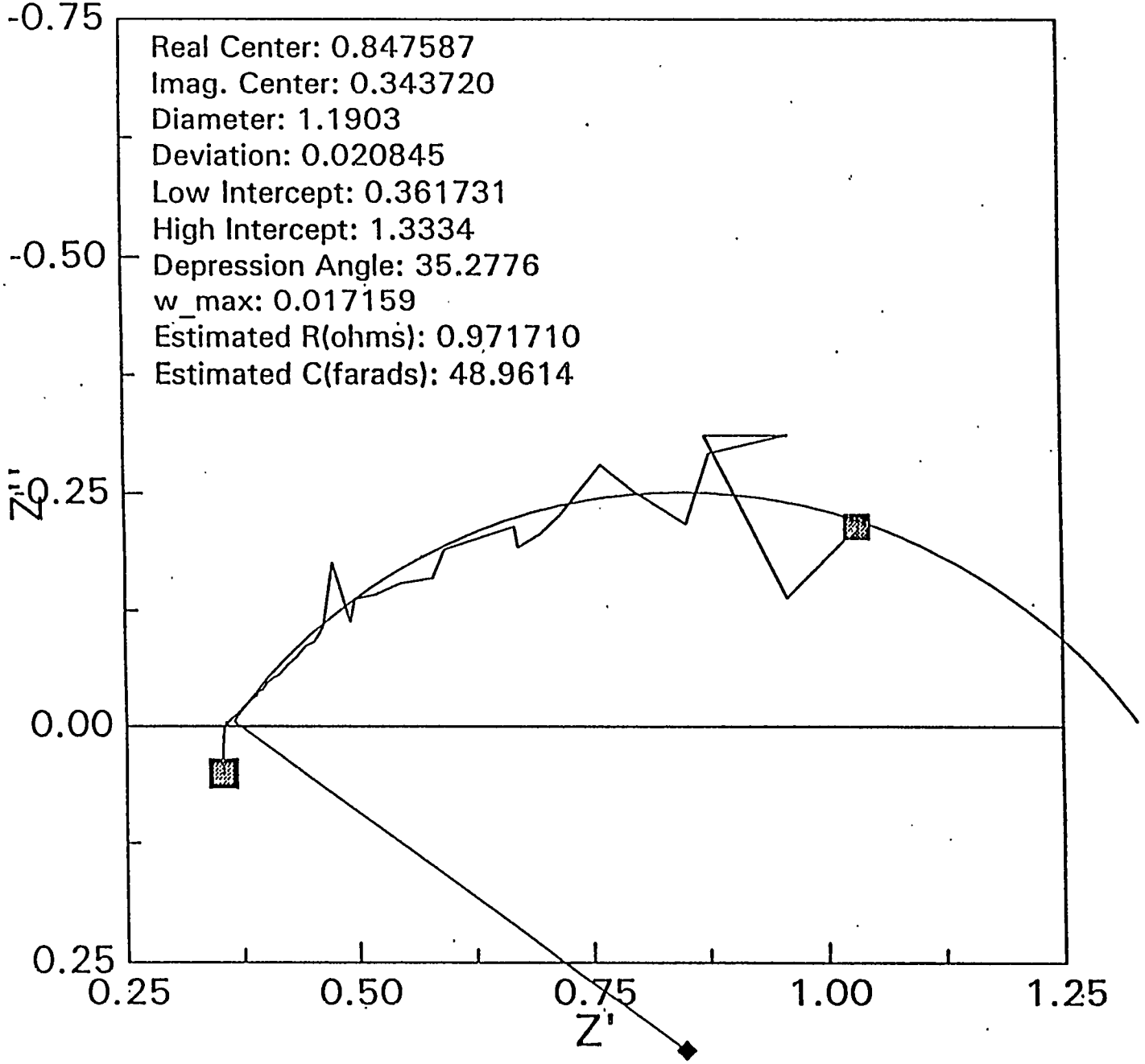

PNL

Tantalum - Potentiodynamic Scans

(Pt counter electrode, YSZ oxygen reference electrode, 1400 °C)

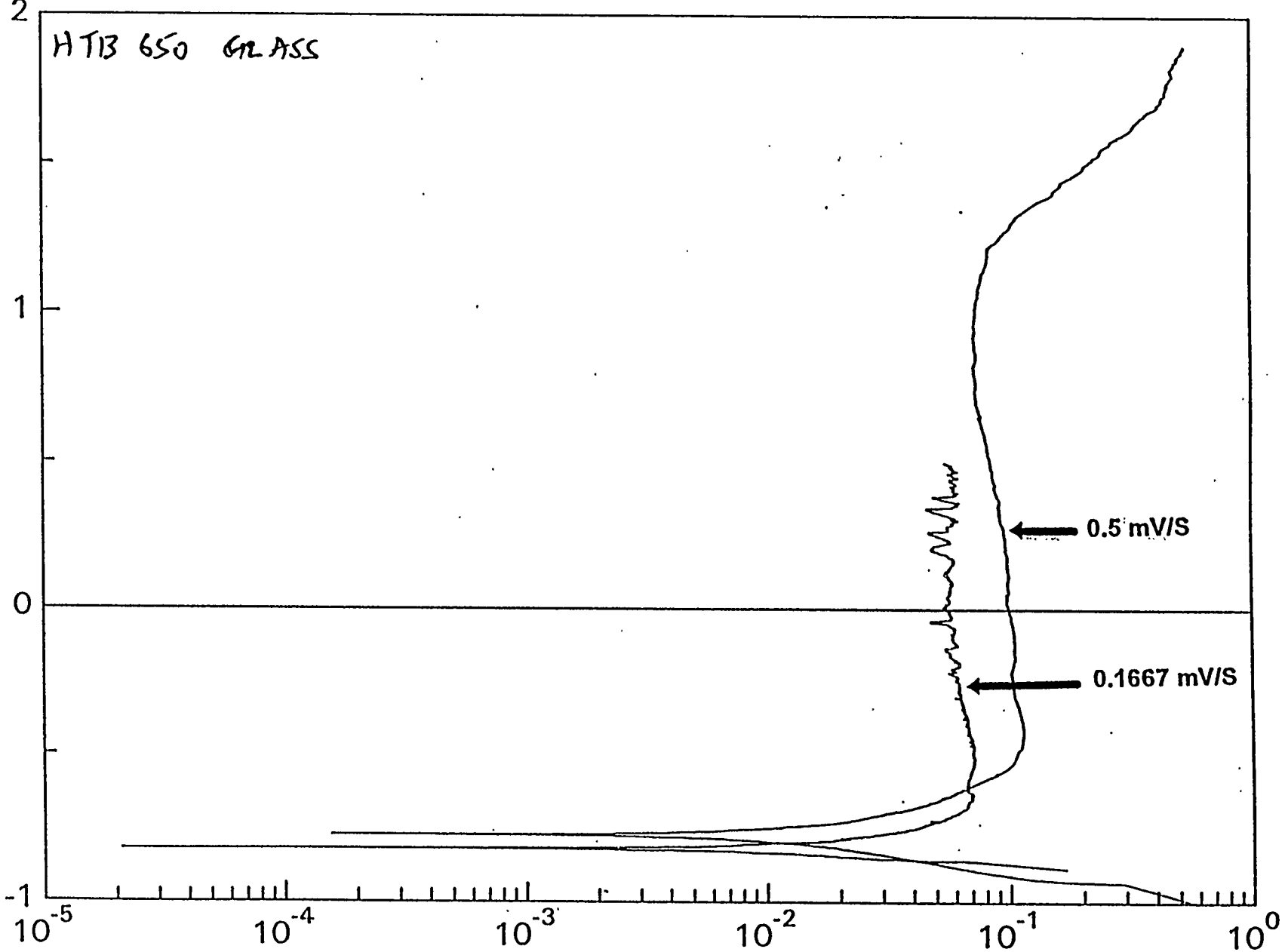

PNL

Tantalum - Nyquist Plot

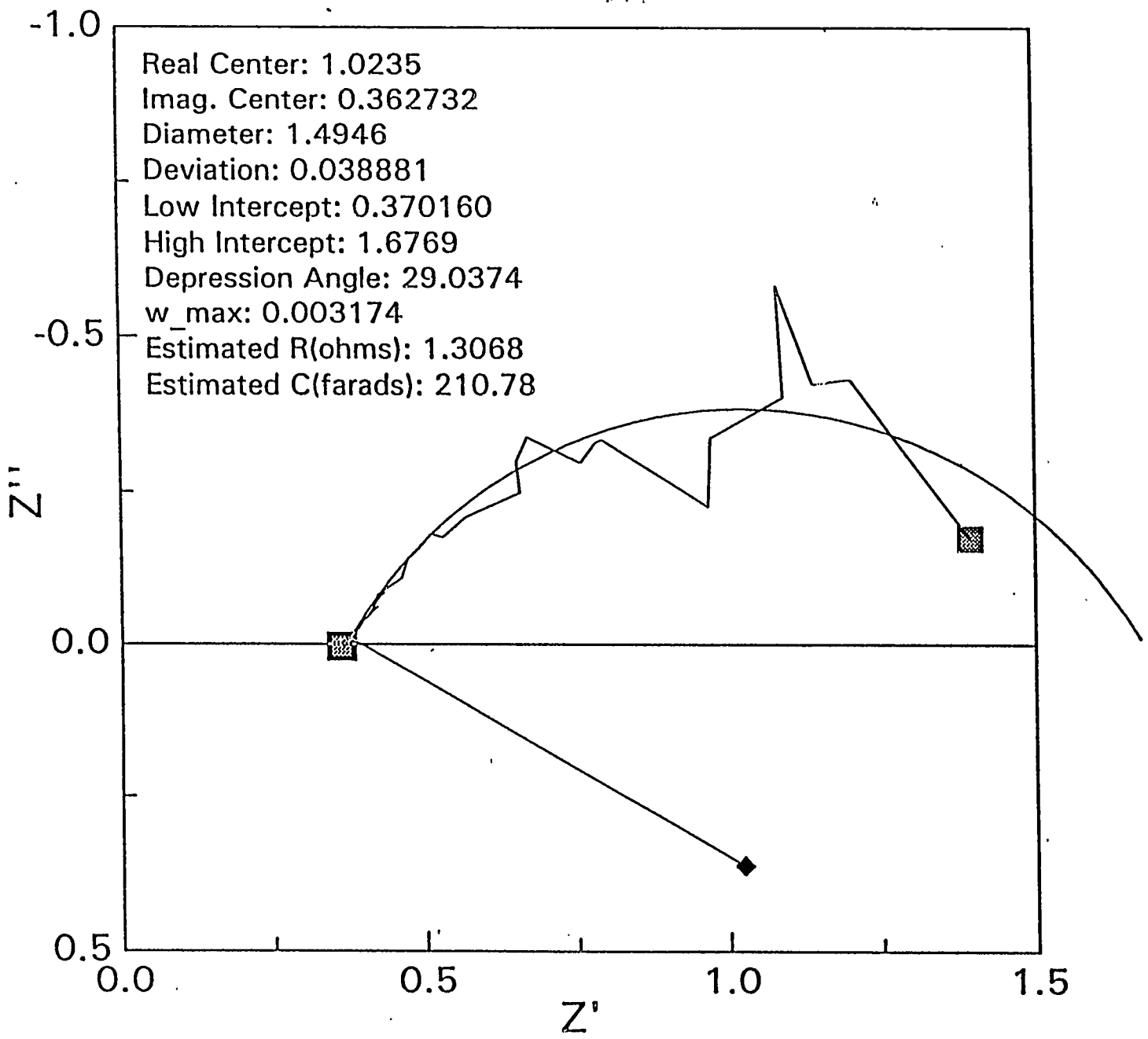

PNL

Electrochemical Corrosion Rates (HTB 650,1400°C)

	Corrosion Rate (mils/year)			
	Tantalum		Molybdenum	
	Data	Corrected*	Data	Corrected*
Tafel Fit	1149	1049	5098	3700
R_p Fit (Stern-Geary Approximation)	5061	3061	8589	4495

* R_p from impedance data.

PNL

Results

Static Corrosion of Molybdenum in Conventional and Simulant Glass
(LD6-5510, 1300°C)

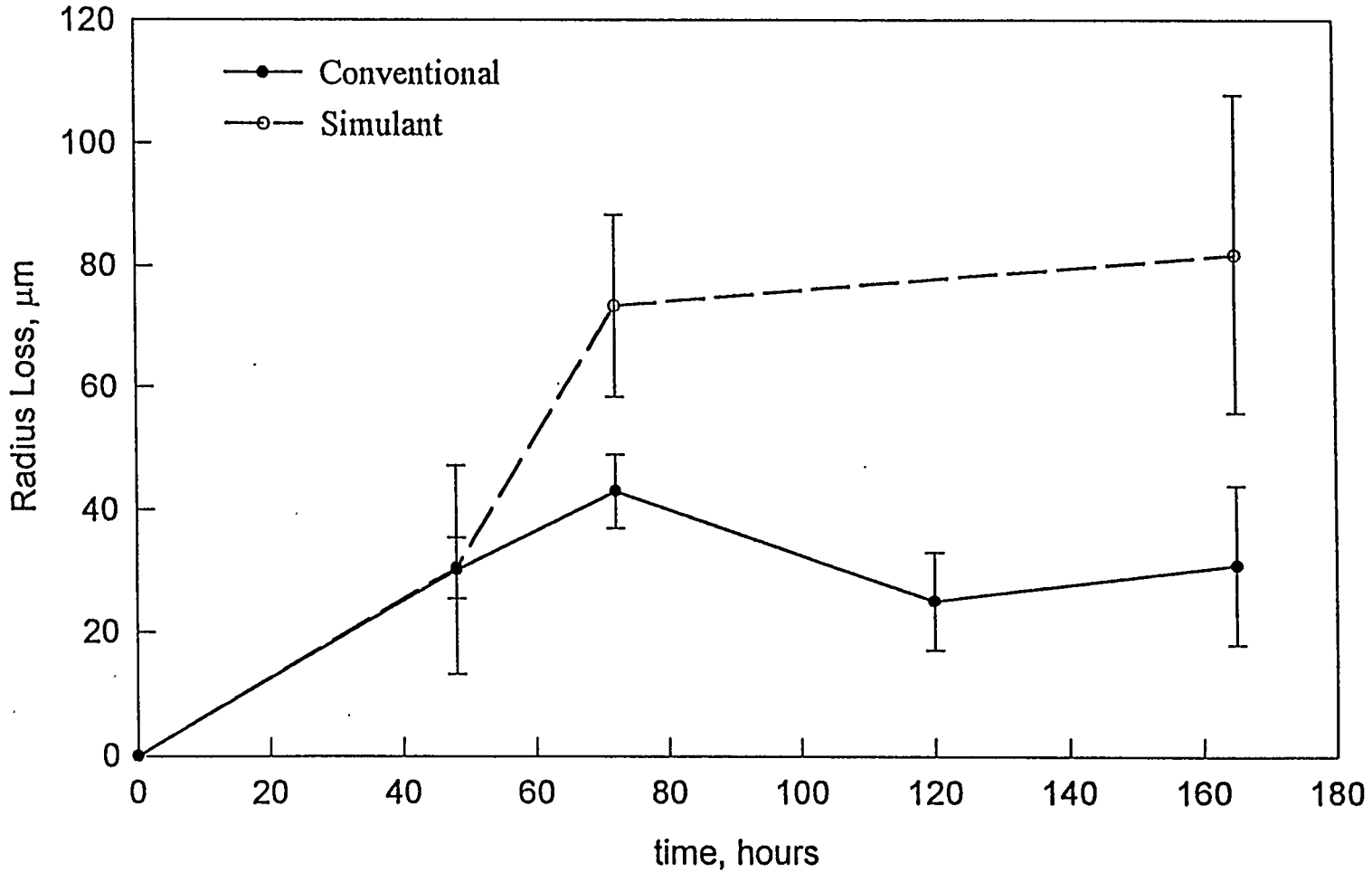

PNL

Summary

- Electrode corrosion rate is dependent on the following parameters:
  - Temperature
  - Viscosity (Lower the viscosity, higher the corrosion)
  - Current density
  - Reducible ions present in the melt (redox equilibrium).
  - Molten salts present in the plenum/melt
- High chromium content of Inconel alloys :
  - Higher corrosion resistance
    - resistant to basic fluxing
    - low solubility in waste glasses
  - Higher Melting temperature
  - Lower workability and higher brittleness ($>$ 50 wt%)

  Inconel 690 is the most used electrode materials ($<$1200°C)
- High salt levels increase corrosion rates.
  - Sulfates: S
  - Molybdates: Na, NH_4
  - Oxides: Na, Ni
  - Halides: Cl, F

PNL

Summary (contd.)

- Corrosion mechanisms of Inconel 690:
  - Selective penetration of Ti, Al, and C (from the melt) along grain boundaries
  - Vacancy coalescence and subsurface void formation (Kirkendall effect)
- Catastrophic sulfidation of Inconel 690:
  - Oxidation state of Na_2SO_4
  - Halide content
  - Avoid accumulation of molten salts
- In HTB 650 glass melt at 1400°C:
  - Molybdenum corrodes more than tantalum.
  - Tantalum passivating electrode - Protection
  - Molybdenum non-passivating electrode
- In LD6-5510 glass melt at 1300°C:
  - Molybdenum corrodes up to 72 hours and then the corrosion rate tends to ``flatten''
  - Maximum corrosion is ~50μm in conventional melt
  - and ~ 100μm, in simulant melt.

PNL

Glass-Contact Refractory Corrosion Test Methods

Static Isothermal

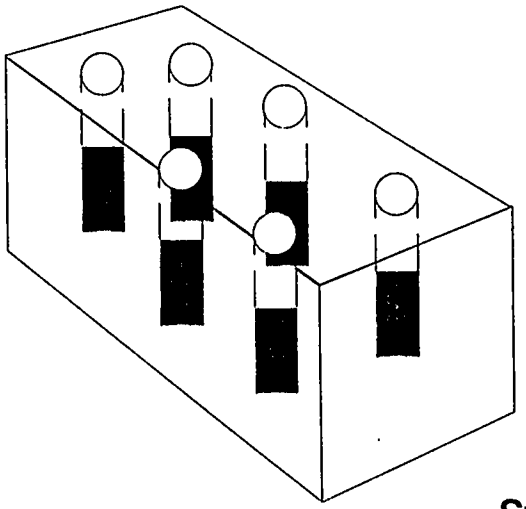

Sample Coupon/Service Test

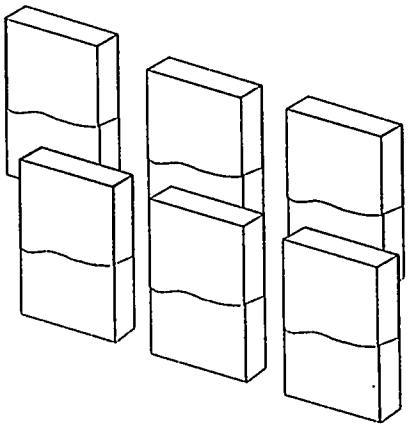

Service Test

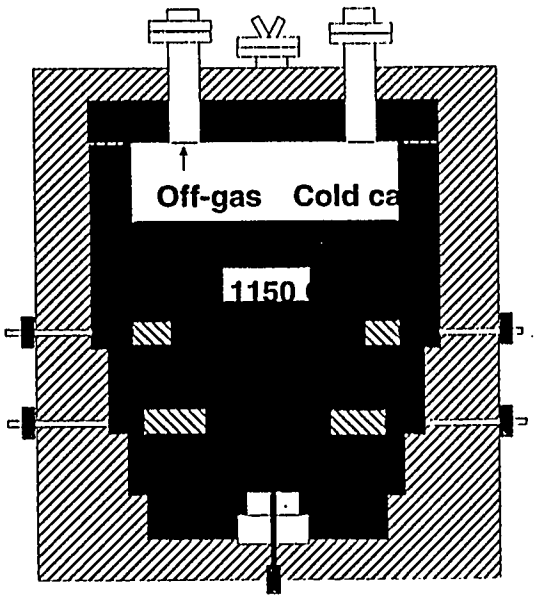

Static Isothermal

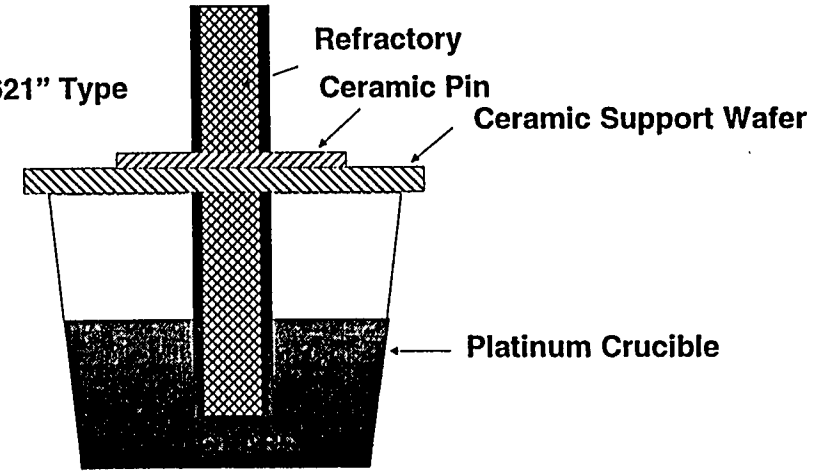

PNL

Theoretical Background

Primary mechanism:

Dissolution of refractory components (DIFFUSION)

- the phase-boundary reaction rate
- materials transfer
  - molecular diffusion
  - natural convection
  - forced convection

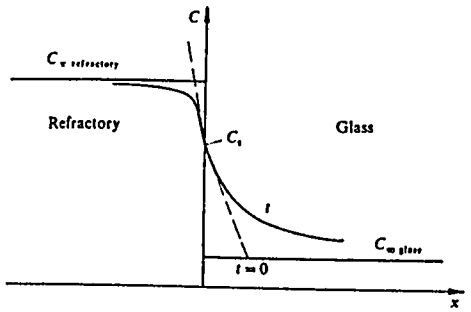

Schematic Concentration Profile

Concentration gradient -

$$\left(\frac{\partial c}{\partial x}\right)_{x=0} = -\frac{c_{G,\infty}}{\sqrt{\pi D t}} = \frac{c_{G,\infty}}{\delta_N}$$

δ_N ← Boundary layer thickness

D: Diffusion coefficient; t: time

(c_s at phase boundary set 0)

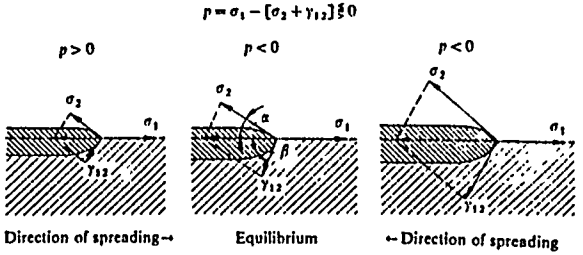

Spreading Pressure

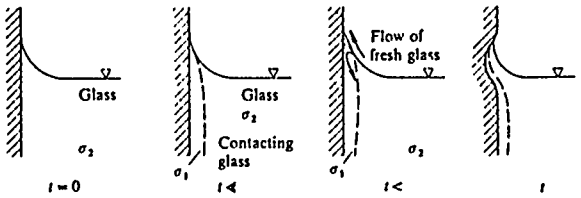

Progress of Flux Line Corrosion

How to reduce corrosion?

- reduce σ (surface tension)
- reduce density difference between glass and dissolved refractory material
- increase viscosity of the dissolved phase
- reduce c_s, saturation concentration
- increase c_∞, concentration of effective component in glass.

PNL

Ranked Glass-Contact Refractories from Corrosion Testing Studies

wt% Oxides

Refractory	Al_2O_3	ZrO_2	SiO_2	Cr_2O_3	Fe_2O_3	TiO_2	P_2O_5	MgO	$Na_2O + K_2O$
Dyko CR95WA				96		4			
C1215	Trace		Trace	92.7	0.4	3.8		Trace	Trace
1780				93	0.4	3.8		Trace	Trace
Monofrax	4		1.6	77.7	7.9			8.7	0.1
Monofrax K3	60.4		1.77	27.26	4.21			6.05	0.31
XAU-30	(26.8)	(27.5)	(15)	(27)	(1.65)				(1.15)
SEPR2161	31.5	26	13	26					
SEPRS2161	31	28	13	16					
Stannex	No data available: expected to be close to pure SnO_2								
SEPR1711	45.9	40.3	12.3		0.08	0.02			0.8
Bakor-33	(45.5)	(41)	(12.2)						(1.0)
Serv-M	89.7		0.5	9.8	0.5		1		0.4
Ruby	89.5		0.1	9.5	0.1			0.5	
Chamotte	(50.6)	(32.5)	(15.6)						(1.1)
Iso-Z-265	No data available: expected to be close to pure $ZrSiO_4$								
X13181	59	26	14.5						0.5
Iso-alumina	No data available: expected to be close to pure Al_2O_3								
SERPJurgal M	95		1.2			Trace			35
Iso-mullite	No data available: expected to be close to pure $Al_6Si_2O_{13}$								

PNL

Glass Compositions Used for Refractory Corrosion Testing

wt% Oxides

Compound	BSG	IEB	TSG	ASG	SLSG	AshG
SiO_2	25-58	35-57	47	53	70.5	29-41
Al_2O_3	0-10	8-17	9	21		1-2
B_2O_3	9-22					7-10
Fe_2O_3, Cr_2O_3, MnO	0-20	10-35			0.02,(1.28)	
CaO, MgO, ZnO	0-6	0-18	14	12	11.6,-,-	16-26
Na_2O, K_2O, Li_2O	8-23	0-7	6	9	8.7,7.7,-	11-17
SO_3	0-1				0.2	
TiO_2	0-1		18			13-22
ZrO_2	0-3	0-14	1			
Waste Component	0-30	0-20+	5	5	0	30-50
Temp. 2-10 Pa s(°C)	1400-1000	(1500)	1437-1254	1817-1572	1713-1434	(1200)

BSG = Borosilicate Glasses
IEB = Iron Enriched Basalts
TSG = Titanosilicate Glass
ASG = Aluminosilicate Glass
SLSG = Soda-Lime-Silica Glass, container glass composition, SRM 710 from NIST
Ash G = Alpha Waste Incinerator Ash Glass
(R_2O_3)

PNL

Corrosion of Glass-Contact Refractories in Various Glasses

Refractory	Static "C 621" Type Isothermal Testing (Corrosion* in mils/day)			
	BSG	TSG	SLSG	ASG
	1400 °C	1400°C	1400°C	1525°C
	Pa·s = 2	Pa.s =2.6	Pa.s =12.9	Pa.s=15.7
Deering, Dyko CR95WA	3.1	3.5	7.5	
Corhart C1215	3.5	4.3		5.9
Carborundum Monofrax E	3.9	5.5	13.0	5.5
Carborundum Monofrax K3	8.3	15.0		8.7
SEPR 2161	4.7	15.4	9.4	5.1
Dyson, Stannex	6.3	10.2	8.3	18.5
SEPR 1711	9.8	53.5	18.1	10.2
A.P. Green, Iso-Z-265	19.7	Failed		18.5
Didier, X13181	23.2	Failed		Failed
Dyson, Iso-alumina	37.8	Failed		26.8
SEPR Jurgal-M	Failed	Failed	44.1	44.9
Dyson, Iso-mullite	Failed	Failed		Failed

* Data from: Hayward, P.J., I.M. George, M.P. Woods, and T.S. Busby (1987).

PNL

Corrosion of Glass-Contact Refractories in Borosilicate Glass

Refractory	Test Type Corrosion in mils/day Average (Minimum - Maximum) Static(S) or Dynamic(D) "C 621" Type	Service Test (Melter)
Deering, Dyko CR95WA	2.4 (S)	
Corhart C1215	0.99(0.43-1.55) (S)	
	3.1 (S)	
Corhart 1780	0.78(0.54-1.03) (S)	
Carborundum Monofrax E	3.5 (S)	
Carborundum Monofrax K3	4.3 (S)	1.0
	6.1 (D)	0.92
	1.92(1.69-2.15) (S)	3.97(2.45-6.02)
	5.5 (S)	5.53(3.71-7.52)
	6.1 (s)	1.81(1.69-1.93)
XAU-30		(1.1 - 1.5)
SEPR 2161	2.00(1.85-2.15) (S)	
	3.5 (S)	
S216		(1.3 - 2.6)
Dyson, Stannex/SnO_2	3.5 (S)	(0.4 - 0.8)
SEPR 1711	11.4 (S)	
Bakor-33		(3.8-5.3)
Chamotte		7.6-9.4
A. P. Green, Iso-Z-265	12.6 (S)	
Didier, X13181	13.0 (S)	
Dyson, Iso-alumina	33.9 (S)	
SEPR Jurgal-M	45.3 (S)	
Dyson, Iso-mullite	55.9 (S)	

PNL

Results

Static Corrosion of Refractories in Conventional Glass
(LD6-5510, 1300°C)

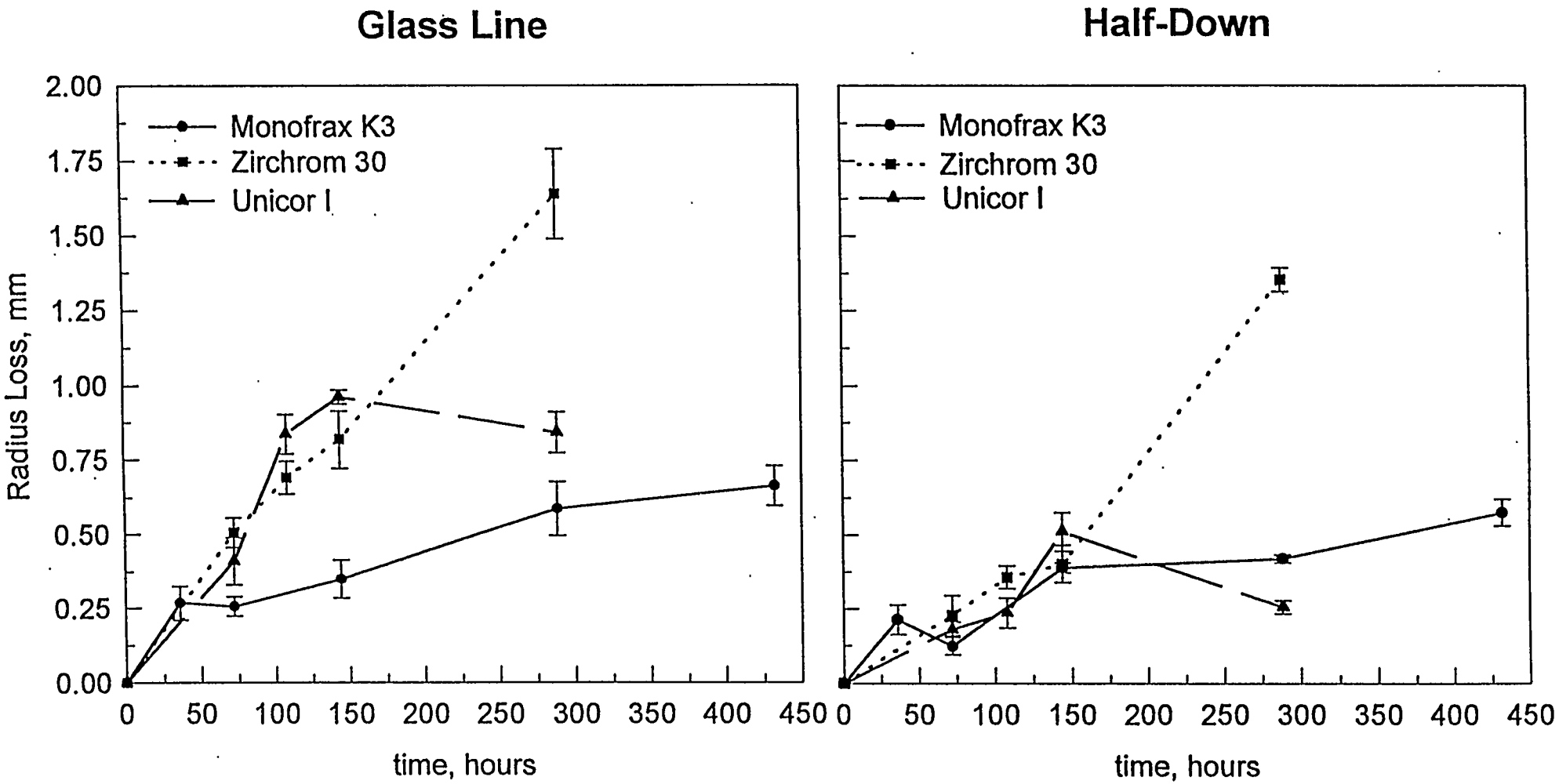

PNL

CORROSION MECHANISM OF MONOFRAX K3 IN LD6-5510 (CONVENTIONAL) MELT

Before testing

1300°C, 72 hours, Glass line

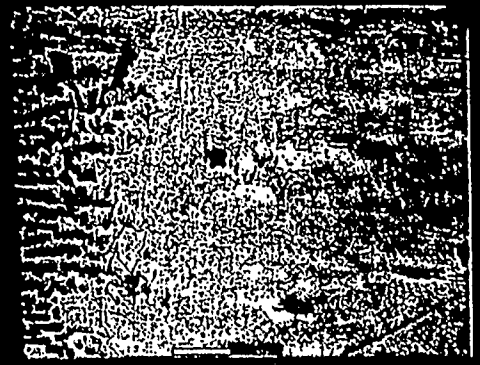

1300°C, 72 hours, Half-down

Observation:

- Cr-rich interfacial reaction layer (~50-200μm) confirmed by EDS.
- Corundum (present in the refractory) absent after corrosion. $MgCr_2O_4$ and Cr_2O_3 phases detected on the corroded refractory surface by XRD

Mechanism:

Preferential leaching of alumina and spinel phase out of the refractory into the melt leaving a Cr-rich interface which reduces further corrosion due to limited solubility.

CORROSION MECHANISM OF UNICOR 1 IN LD6-5510 (CONVENTIONAL) MELT

Before tasting

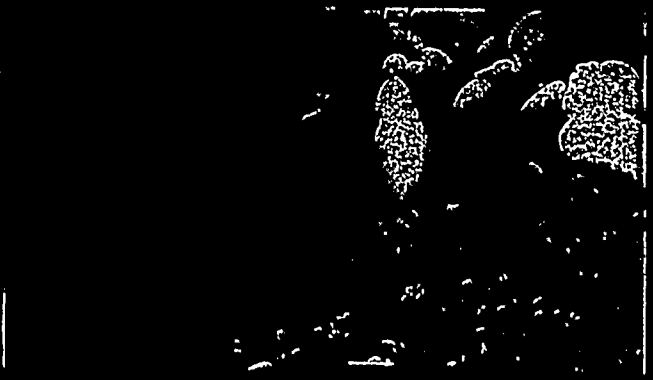

1300°C, 72 hours, Glass line

1300°C, 72 hours, Half-down

Observations:

- ZrO_2 grains along the glass-refractory interface confirmed by EDS.
- Only ZrO_2 phase detected on the corroded refractory surface by XRD.

Mechanism:

Preferential leaching of alumina and glassy phase out of the refractory into the melt leaving corrosion resistant (limited solubility) ZrO_2 grains at the interface.

CORROSION MECHANISM OF ZIRCHROM 30 IN LD6-5510 (CONVENTIONAL) MF

Before Testing

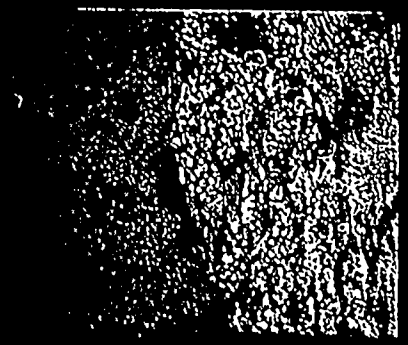

1300 C, 72 hours, Glass line

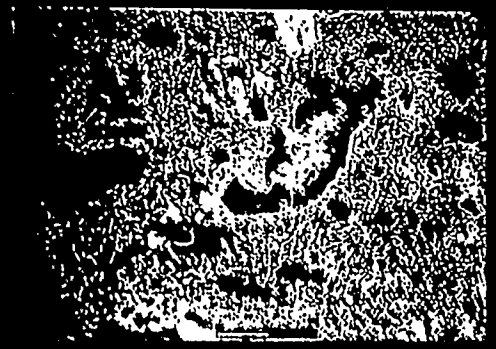

1300 C, 72 hours, Half-down

Observations:

- Cr-rich interfacial reaction layer (100-200 μm) confirmed by EDS.
- ZrO, spinel, and Mg-Al-Si-O phases (present in the refractory) absent after corrosion. Cr_2O_3 detected at the corroded surface by XRD

Mechanism:

Preferential leaching of ZrO, spinel and Mg-Al-Si-O phases out of the refractory into the melt leaving corrosion resistant (limited solubility) Cr_2O_3 grains at the interface.

Summary

- Corrosion rate is dependent on diffusion at the glass-refractory interface, both refractory and glass.
  - ◆ Interfacial temperature
  - ◆ Flow rate at interface
  - ◆ Surface tension, density gradients
  - ◆ Corrosion rate proportional to glass fluidity
  - ◆ Porosity of the refractory
- High chromia content refractories
  - ◆ Higher corrosion resistance
    - resistant to basic fluxing
    - low solubility in waste glasses
  - ◆ Lower thermal shock resistance
  - ◆ Lower electrical resistivity
- High salt levels increase corrosion rates.
  - ◆ Sulfates: S, P, As, Se, T
  - ◆ Chromates: V, Nb, W, Mo
  - ◆ Halides: Cl, F

Summary (contd.)

- Monofrax K3 most used glass-contact refractory for Joule-heated waste melters
  - Low refractory corrosion rate
  - High electrical resistivity (1100-1200°C)
  - Good thermal shock resistance
- Corrosion mechanisms of glass-contact refractories
  - Alkaline fluxing
  - Iron and nickel oxides content of melt
  - Spinel formation
  - Poor understanding/documentation
- Predicted design life of 2 years for current HLW Joule-heated melters
  - Monofrax K3 corrosion, 0.98-5.53 mils/day
  - Inconel 690 corrosion, 0.07-14.6 mils/day

Summary (contd.)

- In LD6-5510 glass at 1300°C, Monofrax K3 is the least corroded refractory followed by Unicor I and Zirchrom 30.
- Corrosion mechanisms
  - ◆ Monofrax K3: preferential leaching of spinel and alumina phases leaving Cr_2O_3-rich interfacial layer which reduces further corrosion due to limited solubility.
  - ◆ Unicor I: preferential leaching of alumina and silicate phases leaving ZrO_2 grains at the interfacial region which reduces further corrosion due to limited solubility.
  - ◆ Zirchrom 30: preferential leaching of spinel, alumina, and zirconia phases leaving a Cr_2O_3-rich interfacial layer, but does not reduce corrosion due to higher porosity.

Future Trend

- Inconel 690 will continue to be the choice of electrode material for melters operating at temperatures below 1200°C. New refractory metals and oxides are being researched for high temperature melters. Molybdenum, tin oxide, and Cr-Al_2O_3 cermet are promising candidate materials.

- Electrochemical corrosion and protection potential of Inconel 690 and other candidate materials in waste glass melts have to be identified.

- Monofrax K3 will be the choice of refractory for melters operating at below 1200°C and is a potential choice of refractory for high-level waste high temperature (1500°C) melters. High chromia containing refractories with improved corrosion resistance and thermal shock resistance and lower electrical conductivity at the temperature of operation are being researched. C1215Z and AZS are promising candidate materials.

- Mechanism of corrosion of Monofrax K3 needs to be established.

- Mechanisms of mixed salt corrosion of the electrodes and refractories need to be established to avoid any catastrophic failure .

- Study of the effects of glass composition, redox, and process parameters on corrosion of electrodes and refractories is crucial in the development of high temperature melting technology.

PNL

Suggested Reading

TEXTS:

Wolfgang Trier, ``Glass Furnaces: Design, Construction, and Operation'', Society of Glass Technology, Sheffield, UK, (1987).
Herbert H. Uhlig and R. W. Revie, ``Corrosion and Corrosion Control'', Third Edition, John Wiley & Sons, NY, USA, (1985).

REFERENCES:

Fay V. Tooley, The Handbook of Glass Manufacture'', Volumes I & II, Third Edition, Ashlee Publishing Co., Inc., NY, USA, (1984).
Metals Handbook, Volume 13, ``Corrosion'', Ninth Edition, ASM International, Metals Park, OH, USA, (1987).

PAPERS:

Refractory Corrosion:

1. A. R. Cooper, ``Kinetics of Refractory Corrosion'', Ceram. Eng. & Sci. Proc., 2(11-12), 1063-1089, (1981).
2. P. Hrma, ``Effects of Surface Forces in Glass Technology (a review)'', Glass Tech., 23(3), 151-155, (1982).
3. T. S. Busby, ``Progress in Refractory Usage in the Glass Industry'', Glass Tech., 28(1), 30-37, (1987).
4. F. E. Woolley, ``Predictions of Refractory Corrosion Rate form Glass Viscosity and Composition'', UNITCR'89 Proceedings, Editor: L. J. Trostel, Jr., American Ceramic Society, OH, 768-779, (1989).

Electrode Corrosion:

1. G. A. Pecoraro, H. Franz, and J. D. Mackenzie, ``Corrosion of Refractory Metals by Molten Oxides'', The Glass Ind., 51(10), 454-458, (1970).
2. G. B. Balazs and C. R. Russel, ``Electrochemical Studies of the Corrosion of Molybdenum Electrodes in Soda-Lime Glass Melts'', J. Non-Cryst. Sol., 105, 1-6, (1988).
3. J. K. Higgins, ``Studies of Platinum and Molybdenum Electrodes in Molten Silicates, Borates, and Phosphates'', J. Electrochem. Soc., 140(12), 3436-3448, (1993).
4. S. K. Sundaram, J-Y. Hsu, and R. F. Speyer, ``Molten Glass Corrosion Resistance of Immersed Combustion-Heating Tube Materials in Soda-Lime-Silicate Glass'', J. Am. Ceram. Soc., 77(6), 1613-23, (1994).